



Blain, Stuart (2010) *The effects of higher oxygenates on methanol synthesis*. PhD thesis.

<https://theses.gla.ac.uk/1601/>

Copyright and moral rights for this work are retained by the author

A copy can be downloaded for personal non-commercial research or study, without prior permission or charge

This work cannot be reproduced or quoted extensively from without first obtaining permission in writing from the author

The content must not be changed in any way or sold commercially in any format or medium without the formal permission of the author

When referring to this work, full bibliographic details including the author, title, awarding institution and date of the thesis must be given

Enlighten: Theses

<https://theses.gla.ac.uk/>
research-enlighten@glasgow.ac.uk

The Effects of Higher Oxygenates on Methanol Synthesis



Stuart Blain ©

A Thesis Presented to the University of Glasgow for the
Degree of Doctor of Philosophy

Abstract

BP are currently in the process of developing a process whereby methanol is synthesised and then further carbonylated to acetic acid, all in the gas phase and utilising the same synthesis gas feed throughout. However, it was envisaged that recycling of unreacted synthesis gas from the carbonylation stage could contain traces of acetic acid or methyl acetate, which would then be passed into the methanol synthesis reactor. The current project therefore examined the effect methyl acetate and acetic acid had on an industrial methanol synthesis catalyst. In the initial stages of the project the ability of precious metal catalysts to synthesise methanol were also examined.

Precious metal catalysts (Ir, Pd and Rh supported on SiO₂) were found to synthesise methanol in small yield from a CO/H₂ feed. Pd and Ir based catalysts were found to be selective, in agreement with the literature. The Rh based catalyst was found to catalyse a number of reactions, with methane being the primary product. As the yields of methanol produced were so low and therefore unrealistic for commercialisation, it was decided to focus on studying the effects of acetic acid and methyl acetate over the commercial catalyst, as it already displayed the selectivity and activity required.

The effects of acetic acid addition at low concentrations were investigated first. Under a CO/CO₂/H₂ feed, acetic acid underwent several reactions, namely (i) hydrogenation to ethanol, (ii) esterification between methanol and acetic acid to methyl acetate and (iii) decomposition to CO/CO₂. Complete conversion of the acid took place, with no carbon laydown on the surface of the catalyst.

Labelling studies were performed on the system, feeding in ¹³C labelled acetic acid, and following the responses of relevant masses using a mass spectrometer. Results showed migration of the carbon label to the aforementioned products, confirming the proposed routes. Methane formation was not detected by GC or MS throughout the acid addition and this was important as acetic acid has been postulated to decompose on metal surfaces via a simple decarboxylation to yield a surface methyl group and gas phase CO₂:



As no carbon laydown was detected during the acid addition, the methyl group was proposed to decompose further to adsorbed carbon and gaseous hydrogen, rather than abstracting a proton to form methane. Oxidation of the surface carbon was proposed to occur via reaction with adsorbed surface oxygen or by a reverse Boudouard type process. Hydrolysis of the acid was shown not to be the route towards CO/CO₂.

A decrease in methanol production was observed upon addition of the acid and was attributed to the adsorption of acetate groups on the surface of the catalyst, displacing reactants. Upon cessation of the acid feed methanol production returned to normal, indicating the acid had a transient effect on the catalyst. However, additions of higher concentrations resulted in severe degradation of the catalyst pellets and therefore permanent deactivation.

The behaviour of the acetic acid was found to vary by altering the feed gas and was attributed to morphological changes in the copper, induced by the feed gas.

Methyl acetate at low concentrations was found to decompose to CO/CO₂ under a CO/CO₂/H₂ feed, with hydrogenation to ethanol and methanol also taking place. Substantial carbon laydown however was observed, which could lead to permanent deactivation of the catalyst. As for acetic acid, the behaviour of the ester was found to vary by altering the gas feed composition, and was attributed to changes in the copper morphology.

Acknowledgements

First and foremost I would like to thank my supervisor, Professor S. David Jackson for all his guidance and support over the course of my PhD. He was never too busy to chat or to answer my questions (for which there were many!) and I thank him for that.

Secondly, I'd also like to thank my industrial supervisor, Evert Ditzel for all his help, support and encouragement throughout my PhD, especially during the early days of the project.

Thanks also go to my second supervisor Justin Hargreaves, for all his expertise in all things thermodynamic, and also in general for giving me ideas and for taking the time to help me.

The technical staff at Glasgow were also of great help throughout my project and there are a few people I'd like to thank in particular:

- Ron Spence for all his advice and help in fixing any rig based issues I had. Unfortunately as a struggling student, his bottle of 30yr old Macallan will have to wait!
- Andy Monaghan for running all the TGA and BET analysis throughout the project, and also for the many debates on the Glasow footballing divide.
- Jim Gallagher for assisting me with SEM

I'd also like to thank the catalysis group members past and present for all the chat and helping to make the last three years so enjoyable. Special mentions go to Mark, Davie and Graham for the good chat and even better nights out – many of which I can't fully remember!

I would also like to take the opportunity to thank my family for all their support and encouragement throughout the whole of my PhD, it would not have been possible to have done it without you. Special mention goes to my dad [1], for setting me out

into the world of chemistry and still having the record for publications within the Blain household!

Finally, special thanks go to Lynsey, for putting up with me throughout the writing of this thesis and for helping to keep me sane. Thank you!!

[1] J. Blain, J. C. Speakman, L. A. Stamp, L Goliž and I. LebanJ., Chem. Soc., Perkin Trans. 2, 1973, 706 – 710

Declaration

This work contained in this thesis, submitted for the degree of Doctor of Philosophy, is my own work except where due reference is made to other authors. No Material within this thesis has been previously submitted for a degree at this or any other university.

Stuart D. Blain

Contents

1	Introduction.....	17
1.1	Methanol	17
1.2	Methanol Synthesis	18
1.2.1	High Pressure Process	18
1.2.2	Low Pressure Process	18
1.2.3	Thermodynamics	19
1.2.4	Commercial Catalyst	22
1.2.5	Selectivity	23
1.2.6	Mechanism	25
1.2.7	Precious Metal Catalysts	34
1.3	Methanol Carbonylation	38
1.3.1	Homogenous Carbonylation	38
1.3.2	Heterogeneous Carbonylation	39
1.4	Reactions of Acetyls	41
1.4.1	Acetic Acid	41
1.4.2	Methyl Acetate	43
1.5	Project Background	44
1.6	Project Aims.....	45

2	Experimental	46
2.1	Catalyst Preparation	46
2.1.1	Support Impregnation	46
2.1.2	Support Properties	47
2.1.3	Preparation Procedure	47
2.2	Catalyst Characterisation	48
2.2.1	Surface Area Analysis	48
2.2.2	Thermo-gravimetric Analysis	48
2.2.3	X-Ray Diffraction	48
2.2.4	Scanning Electron Microscopy	49
2.3	Catalytic testing	49
2.3.1	Apparatus	49
2.3.2	Reaction Procedure	50
2.3.3	Gas chromatography	50
2.3.4	Soxhlet Extraction	53
2.3.5	Mass Spectroscopy	54
2.4	Materials	55
2.4.1	Calibrations & Reactions	55
2.4.2	Labelled Materials	56
2.4.3	TGA Studies	56
2.5	Calculations	57
2.5.1	Conversion	57
2.5.2	Mass Balances	57
2.5.3	Selectivity	58

3	Results	59
3.1	Precious Metal Catalytic testing	59
3.1.1	Characterisation	59
3.1.2	Catalytic Testing	73
3.2	Commercial Catalyst Testing.....	82
3.2.1	Characterisation	82
3.2.2	Catalytic Testing	84
3.3	Acetic Acid studies	93
3.3.1	Standard Addition	93
3.3.2	Labelling Studies.....	106
3.3.3	Conversion of Acid to CO/CO ₂	127
3.3.4	Acetate/Carbonate TGA Studies	136
3.3.5	Gas Composition Studies	140
3.3.6	High Concentration / Long Term Studies.....	163
3.4	Methyl Acetate Studies	180
3.4.1	Standard Addition.....	180
3.4.2	Gas Composition Studies.....	188
3.4.3	High Concentration Additions.....	198
4	Conclusions	199
5	Future Work.....	201
6	References	202

List of Figures

Figure 1-1 Methanol applications 2008[1]	17
Figure 1-2 Thermodynamics of formation for various compounds[10]	24
Figure 1-3 Specific radioactivities of carbon monoxide, carbon dioxide and methanol as a function of space velocity. Reaction feed gas 10%CO / 10% CO ₂ / 80% H ₂ containing ¹⁴ CO ₂ at 50bar, 523K[12].....	27
Figure 1-4 Methanol synthesis activity as a function of copper metal area [3]	28
Figure 1-5 Schematic model for wetting / non wetting of copper on zinc surface [57-59].....	30
Figure 1-6 Cativa process cycle[92].....	39
Figure 1-7 Mode of adsorption of methyl acetate on silica[103].....	43
Figure 2-1 Reactor Setup.....	50
Figure 2-2 GC Temperature ramp profile.....	51
Figure 2-3 Calibration graph 1	52
Figure 2-4 Calibration graph 2	53
Figure 2-5 Soxhlet Apparatus	54
Figure 3-1 TGA analysis of rhodium acetate supported on silica under 2%O ₂ /Ar feed.....	60
Figure 3-2 TGA analysis of iridium acetate supported on silica under 2%O ₂ /Ar feed	61
Figure 3-3 TGA analysis of palladium chloride supported on silica under 2%O ₂ /Ar feed.....	62
Figure 3-4 TGA analysis of calcium doped palladium chloride supported on silica under 2%O ₂ /Ar feed.....	63
Figure 3-5 TGA analysis of rhodium oxide supported on silica under 5%H ₂ /N ₂ feed	64
Figure 3-6 TGA analysis of iridium oxide supported on silica under 5%H ₂ /N ₂ feed	65
Figure 3-7 TGA analysis of palladium oxide supported on silica under 5%H ₂ /N ₂ feed.....	66
Figure 3-8 TGA analysis of calcium doped palladium oxide supported on silica under 5%H ₂ /N ₂ feed.....	67
Figure 3-9 XRD pattern from calcined silica support.....	68

Figure 3-10 XRD patterns from calcined and reduced rhodium supported on silica	69
Figure 3-11 XRD patterns from calcined and reduced iridium supported on silica	70
Figure 3-12 XRD patterns from calcined and reduced palladium supported on silica	71
Figure 3-13 XRD patterns from calcined and reduced calcium doped palladium supported on silica	72
Figure 3-14 Reaction profile from CO hydrogenation over Pd/SiO ₂ catalyst under CO/H ₂ feed	75
Figure 3-15 Reaction profile from CO hydrogenation over Pd/Ca/SiO ₂ catalyst under CO/H ₂ feed	77
Figure 3-16 Reaction profile from CO hydrogenation over Ir/SiO ₂ catalyst under CO/H ₂ feed	78
Figure 3-17 Reaction profile from CO hydrogenation over Rh/SiO ₂ catalyst under CO/H ₂ feed	80
Figure 3-18 TGA analysis of Katalco 51-8 catalyst under 5%H ₂ /N ₂ feed	82
Figure 3-19 XRD patterns of Katalco 51-8 catalyst at various temperatures under a 5%H ₂ /N ₂ feed	83
Figure 3-20 Reaction profile from methanol synthesis over Katalco 51-8 under a CO/H ₂ feed	86
Figure 3-21 Mass balance from methanol synthesis over Katalco 51-8 under a CO/H ₂ feed	87
Figure 3-22 Post reaction TPO of Katalco 51-8 catalyst after CO/H ₂ run	88
Figure 3-23 Reaction profile from methanol synthesis over Katalco 51-8 under a CO/CO ₂ /H ₂ feed	90
Figure 3-24 Mass balances from methanol synthesis over Katalco 51-8 under a CO/CO ₂ /H ₂ feed	91
Figure 3-25 Reaction profile from 1.0mol% acid addition into CO/CO ₂ /H ₂ system over Katalco 51-8 catalyst (acid fed in between 8 and 24hrs)	94
Figure 3-26 Acetate group bound to copper surface[125]	95
Figure 3-27 Reaction profile from 1.0mol% acid addition into CO/CO ₂ /H ₂ system over Katalco 51-8 catalyst (acid fed in between 8 and 24hrs)	95
Figure 3-28 Mass balances from 1.0mol% acid addition into CO/CO ₂ /H ₂ system over Katalco 51-8 catalyst (acid fed in between 8 and 24hrs)	98
Figure 3-29 Mechanism of acetate decomposition on Ag(110) surface	101
Figure 3-30 Mechanism of acetate decomposition on Ag(110) surface	101

Figure 3-31 Post reaction TPO of catalyst from 1.0mol% acid addition into CO/CO ₂ /H ₂ system over Katalco 51-8 catalyst	103
Figure 3-32 ¹³ C labelled acetic acid	106
Figure 3-33 Reaction profile from 1.0mol% labelled acid addition into CO/CO ₂ /H ₂ system over Katalco 51-8 catalyst (unlabelled acid fed in between 26 and 34hrs, labelled acid fed in between 50 and 54hrs).....	107
Figure 3-34 Reaction profile from 1.0mol% labelled acid addition into CO/CO ₂ /H ₂ system over Katalco 51-8 catalyst (unlabelled acid fed in between 26 and 34hrs, labelled acid fed in between 50 and 54hrs).....	108
Figure 3-35 Mass balances from 1.0mol% labelled acid addition into CO/CO ₂ /H ₂ system over Katalco 51-8 catalyst (unlabelled acid fed in between 26 and 34hrs, labelled acid fed in between 50 and 54hrs).....	109
Figure 3-36 Post reaction TPO from 1.0mol% labelled acid addition into CO/CO ₂ /H ₂ system over Katalco 51-8 catalyst	110
Figure 3-37 Mass spectra from 1.0mol% labelled acid addition into CO/CO ₂ /H ₂ system over Katalco 51-8 catalyst	111
Figure 3-38 GC Data from labelled addition.....	112
Figure 3-39 Mass spectrometry data from labelled addition	112
Figure 3-40 Mass spectra from 1.0mol% labelled acid addition into CO/CO ₂ /H ₂ system over Katalco 51-8 catalyst	114
Figure 3-41 Mass spectra from 1.0mol% labelled acid addition into CO/CO ₂ /H ₂ system over Katalco 51-8 catalyst	115
Figure 3-42 Reaction profile from 1.5mol% deuterated acid addition into CO/CO ₂ /H ₂ system over Katalco 51-8 catalyst (non-deuterated acid fed in between 12 and 32hrs, deuterated acid fed in between 54 and approximately 64hrs).....	117
Figure 3-43 Reaction profile from 1.5mol% deuterated acid addition into CO/CO ₂ /H ₂ system over Katalco 51-8 catalyst (non-deuterated acid fed in between 12 and 32hrs, deuterated acid fed in between 54 and approximately 64hrs).....	118
Figure 3-44 Mass balances from 1.5mol% deuterated acid addition into CO/CO ₂ /H ₂ system over Katalco 51-8 catalyst (non-deuterated acid fed in between 12 and 32hrs, deuterated acid fed in between 54 and approximately 64hrs).....	119
Figure 3-45 Post reaction TPO from 1.5mol% deuterated acid addition into CO/CO ₂ /H ₂ system over Katalco 51-8 catalyst	120
Figure 3-46 Mass spectra from 1.5mol% deuterated acid addition into CO/CO ₂ /H ₂ system over Katalco 51-8 catalyst	121

Figure 3-47 Mass spectra from 1.5mol% deuterated acid addition into CO/CO ₂ /H ₂ system over Katalco 51-8 catalyst	122
Figure 3-48 Mass spectra from 1.5mol% deuterated acid addition into CO/CO ₂ /H ₂ system over Katalco 51-8 catalyst	123
Figure 3-49 Mass spectra from 1.5mol% deuterated acid addition into CO/CO ₂ /H ₂ system over Katalco 51-8 catalyst	124
Figure 3-50 Mass spectra from 1.5mol% deuterated acid addition into CO/CO ₂ /H ₂ system over Katalco 51-8 catalyst	125
Figure 3-51 Reaction profile from acid / water addition into N ₂ /H ₂ system over Katalco 51-8 catalyst (acid fed in continuously after 2hrs)	129
Figure 3-52 Reaction profile from acid / water addition into N ₂ /H ₂ system over Katalco 51-8 catalyst (acid fed in continuously after 2hrs)	130
Figure 3-53 Mass balances from acid / water addition into N ₂ /H ₂ system over Katalco 51-8 catalyst (acid fed in continuously after 2hrs)	131
Figure 3-54 Schematic model for wetting / non wetting of copper on zinc surface[59]	132
Figure 3-55 The dimensionless surface area $A/V^{2/3}$ (y axis) of the different facets versus the contact surface free energy γ / γ_0 (x axis)[69]	132
Figure 3-56 TGA data from decomposition of metal acetates in O ₂ /Ar	137
Figure 3-57 TGA data from decomposition of metal carbonates in O ₂ /Ar	139
Figure 3-58 Reaction profile from 1.0mol% acid addition into N ₂ system over Katalco 51-8 catalyst (acid fed in continuously after 2hrs)	142
Figure 3-59 Mass balances from 1.0mol% acid addition into N ₂ system over Katalco 51-8 catalyst (acid fed in continuously after 2hrs)	143
Figure 3-60 Post reaction TPO from 1.0mol% acid addition into N ₂ system over Katalco 51-8 catalyst	144
Figure 3-61 Typical post reaction TPO profile	144
Figure 3-62 Reaction profile from 1.0mol% acid addition into N ₂ /H ₂ system over Katalco 51-8 catalyst (acid fed in continuously after 6hrs)	145
Figure 3-63 Reaction profile from 1.0mol% acid addition into N ₂ /H ₂ system over Katalco 51-8 catalyst (acid fed in continuously after 6hrs)	146
Figure 3-64 Mass balances from 1.0mol% acid addition into N ₂ /H ₂ system over Katalco 51-8 catalyst (acid fed in continuously after 6hrs)	147
Figure 3-65 Post reaction TPO from 1.0mol% acid addition into N ₂ /H ₂ system over Katalco 51-8 catalyst	148

Figure 3-66 Reaction profile from 1.0mol% acid addition into CO/H ₂ system over Katalco 51-8 catalyst (acid fed in from 20 to 28hrs)	149
Figure 3-67 Reaction profile from 1.0mol% acid addition into CO/H ₂ system over Katalco 51-8 catalyst (acid fed in from 20 to 28hrs)	150
Figure 3-68 Reaction profile from 1.0mol% acid addition into CO/H ₂ system over Katalco 51-8 catalyst (acid fed in from 20 to 28hrs)	151
Figure 3-69 Post reaction TPO from 1.0mol% acid addition into CO/H ₂ system over Katalco 51-8 catalyst.....	153
Figure 3-70 Reaction profile from 1.0mol% acid addition into CO ₂ /H ₂ system over Katalco 51-8 catalyst (acid fed in between 28 and 54hrs).....	154
Figure 3-71 Reaction profile from 1.0mol% acid addition into CO ₂ /H ₂ system over Katalco 51-8 catalyst (acid fed in between 28 and 54hrs).....	155
Figure 3-72 Reaction profile from 1.0mol% acid addition into CO ₂ /H ₂ system over Katalco 51-8 catalyst (acid fed in between 28 and 54hrs).....	156
Figure 3-73 Post reaction TPO from 1.0mol% acid addition into CO ₂ /H ₂ system over Katalco 51-8 catalyst.....	159
Figure 3-74 Acid balance of each system versus the feed gas composition of each system	160
Figure 3-75 Reaction profile from 1.0mol% acid addition into CO/CO ₂ /H ₂ system over Katalco 51-8 catalyst (acid fed in between 6 and 142hrs).....	164
Figure 3-76 Reaction profile from 1.0mol% acid addition into CO/CO ₂ /H ₂ system over Katalco 51-8 catalyst (acid fed in between 6 and 142hrs).....	165
Figure 3-77 Mass balances from 1.0mol% acid addition into CO/CO ₂ /H ₂ system over Katalco 51-8 catalyst (acid fed in between 6 and 142hrs).....	166
Figure 3-78 Acid balance from 1.0mol% acid addition into CO/CO ₂ /H ₂ system over Katalco 51-8 catalyst (long term addition).....	166
Figure 3-79 Reaction profile from 5.0mol% acid addition into CO/CO ₂ /H ₂ system over Katalco 51-8 catalyst (acid fed in between 4 and 24hrs).....	168
Figure 3-80 Reaction profile from 5.0mol% acid addition into CO/CO ₂ /H ₂ system over Katalco 51-8 catalyst (acid fed in between 4 and 24hrs).....	169
Figure 3-81 Mass balances from 5.0mol% acid addition into CO/CO ₂ /H ₂ system over Katalco 51-8 catalyst (acid fed in between 4 and 24hrs).....	170
Figure 3-82 SEM image of Katalco 51-8 pellet pre acid addition	171
Figure 3-83 SEM image of Katalco 51-8 catalyst pellet after exposure to 5.0mol% acetic acid feed	172

Figure 3-84 XRD patterns of a reduced Katalco catalyst and a Katalco catalyst exposed to 1.0mol% acetic acid under a CO/CO ₂ /H ₂ feed.....	173
Figure 3-85 XRD patterns of Katalco catalysts exposed to 1.0mol% and 5mol% acetic acid under a CO/CO ₂ /H ₂ feed.....	174
Figure 3-86 Post reaction TPO from 5.0mol% acid addition into CO/CO ₂ /H ₂ system over Katalco 51-8 catalyst.....	178
Figure 3-87 Reaction profile from 1.1mol% ester addition into CO/CO ₂ /H ₂ system over Katalco 51-8 catalyst (ester addition between 6 and 22hrs).....	181
Figure 3-88 Reaction profile from 1.1mol% ester addition into CO/CO ₂ /H ₂ system over Katalco 51-8 catalyst (ester addition between 6 and 22hrs).....	184
Figure 3-89 Mass balances from 1.1mol% ester addition into CO/CO ₂ /H ₂ system over Katalco 51-8 catalyst (ester addition between 6 and 22hrs).....	185
Figure 3-90 Ester balance from 1.1mol% ester addition into CO/CO ₂ /H ₂ system over Katalco 51-8 catalyst.....	186
Figure 3-91 Reaction profile from 1.1mol% ester addition into N ₂ system over Katalco 51-8 catalyst (ester fed in continuously from 2hrs).....	190
Figure 3-92 Mass balances from 1.1mol% ester addition into N ₂ system over Katalco 51-8 catalyst (ester fed in continuously from 2hrs).....	191
Figure 3-93 Post reaction TPO of catalyst from 1.1mol% ester addition into N ₂ system over Katalco 51-8 catalyst	192
Figure 3-94 Reaction profile from 1.1mol% ester addition into N ₂ /H ₂ system over Katalco 51-8 catalyst (ester fed in continuously from 6hrs).....	193
Figure 3-95 Mass balances from 1.1mol% ester addition into N ₂ /H ₂ system over Katalco 51-8 catalyst (ester fed in continuously from 6hrs).....	194
Figure 3-96 Ester balance from 1.1mol% ester addition into N ₂ /H ₂ system over Katalco 51-8 catalyst.....	194
Figure 3-97 Ester balance of each system versus the feed gas composition of each system.....	196

List of Tables

Table 1-1 Literature values for $K_{p(\text{meth})}$ [10]	21
Table 1-2 Typical weight % of each component in copper methanol synthesis catalysts[25]	22
Table 1-3 Product selectivity during acetic acid hydrogenation ($P_{\text{HOAc}} = 14\text{torr}$, $P_{\text{H}_2} = 700\text{torr}$)	42
Table 2-1 Metal precursors used for preparation of catalysts	46
Table 2-2 Support Properties of silica Cariact Q10	47
Table 2-3 Lab prepared catalysts.....	48
Table 2-4 GC temperature ramp profile	51
Table 2-5 Materials	56
Table 2-6 Labelled materials.....	56
Table 2-7 Materials used for TGA analysis	57
Table 3-1 Conditions for the calcination of supported metal acetates.....	62
Table 3-2 Conditions for the calcination of supported palladium catalysts.....	63
Table 3-3 Surface area analysis of lab prepared catalysts	73
Table 3-4 Surface area analysis of Katalco 51-8 catalyst	84
Table 3-5 Acid balance from 1.0mol% acid addition into CO/CO ₂ /H ₂ system over Katalco 51-8 catalyst.....	102
Table 3-6 Acid balance from 1.0mol% labelled acid addition into CO/CO ₂ /H ₂ system over Katalco 51-8 catalyst	109
Table 3-7 Acid additions into CO/CO ₂ /H ₂ system over Katalco 51-8 catalyst	111
Table 3-8 Acid balance from 1.5mol% deuterated acid addition into CO/CO ₂ /H ₂ system over Katalco 51-8 catalyst	119
Table 3-9 Acid additions into CO/CO ₂ /H ₂ system over Katalco 51-8 catalyst	121
Table 3-10 Acid balance from acid / water addition into N ₂ /H ₂ system over Katalco 51-8 catalyst.....	134
Table 3-11 Post reaction TPO from acid / water addition into N ₂ /H ₂ system over Katalco 51-8 catalyst.....	134
Table 3-12 Feed gas compositions	141
Table 3-13 Acid balance from 1.0mol% acid addition into N ₂ system over Katalco 51-8 catalyst.....	144
Table 3-14 Acid balance from 1.0mol% acid addition into N ₂ /H ₂ system over Katalco 51-8 catalyst.....	146

Table 3-15 Acid balance from 1.0mol% acid addition into CO/H ₂ system over Katalco 51-8 catalyst.....	152
Table 3-16 Mass balances from 1.0mol% acid addition into CO ₂ /H ₂ system over Katalco 51-8 catalyst (acid fed in between 28 and 54hrs).....	157
Table 3-17 Acid balance from 1.0mol% acid addition into CO ₂ /H ₂ system over Katalco 51-8 catalyst.....	158
Table 3-18 Surface area comparison of fresh Katalco catalyst and Katalco catalyst exposed to 5mol% AcOH.....	175
Table 3-19 Acid balance from 5.0mol% acid addition into CO/CO ₂ /H ₂ system over Katalco 51-8 catalyst.....	177
Table 3-20 Ester balance from 1.1mol% ester addition into CO/CO ₂ /H ₂ system over Katalco 51-8 catalyst.....	185
Table 3-21 Feed gas compositions	189
Table 3-22 Ester balance from 1.1mol% ester addition into N ₂ system over Katalco 51-8 catalyst.....	191

1 Introduction

1.1 Methanol

Methanol, also known as wood alcohol, is the simplest of alcohols with a chemical formula of CH_3OH . It is produced on a worldwide scale of 47million tonnes per annum[1] and is used as a common laboratory solvent amongst other things. However the largest use of methanol by far is as a feedstock for other products. The three largest derivatives of methanol are formaldehyde, methyl tertiary butyl ether (MTBE) and acetic acid. Formaldehyde is used mainly to make amino and phenolic resins that are employed in the manufacture of wood based products such as flooring, panels and furniture. MTBE is used as an octane booster and oxygenate in gasoline, while acetic acid is used mainly for vinyl acetate monomer (VAM) and purified terephthalic acid (TPA). Methanol is also seeing a growing demand in fuel applications such as dimethyl ether (DME), biodiesel and direct blending into gasoline[1].

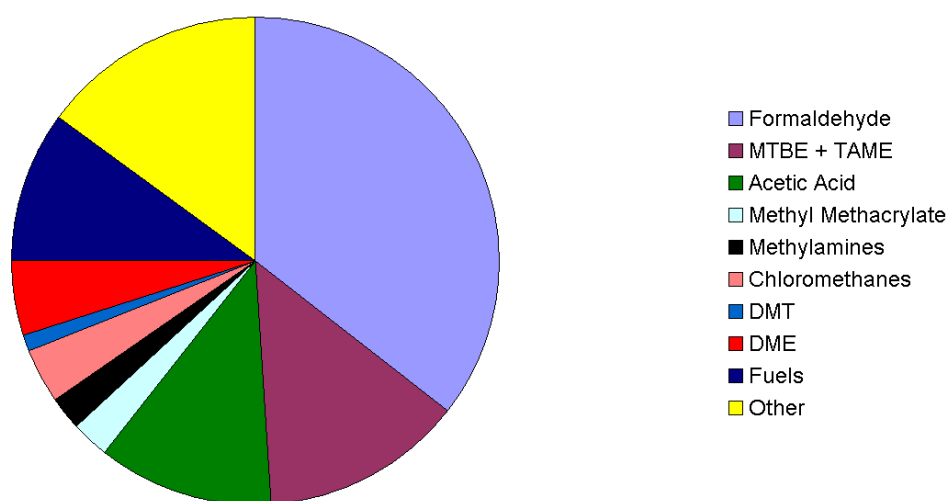


Figure 1-1 Methanol applications 2008[1]

Prior to 1923, methanol was derived from the distillation of wood. However there was a growing demand for an industrial process which could synthesise the chemical cheaply and efficiently.

1.2 Methanol Synthesis

1.2.1 High Pressure Process

In 1923, a German patent was granted to BASF[2] for a process to synthesize methanol from synthesis gas, CO and H₂, at 300-400°C and 100-250bar over a Zn/Cr₂O₃ catalyst[3]. The first commercial methanol synthesis plant was built by the same company in 1923. The process used a ZnO/Cr₂O₃ catalyst and operated at 300°C and 200bar. The catalyst was relatively poison resistant and could operate with a synthesis gas feed stream containing both chlorine and sulphur. Copper catalysts were also discovered shortly after, however were deemed to be of “only slight practical interest” due to their rapid deactivation[4]. This resulted from (i) the fact they were readily poisoned and (ii) were very unstable (sintering occurred easily). The ZnO/Cr₂O₃ catalyst remained virtually unchanged for the next 40 years, until ICI developed a much more active and stable catalyst. This catalyst could be used with lower temperatures and pressures, and this formed the basis of the modern “low pressure” process.

1.2.2 Low Pressure Process

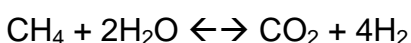
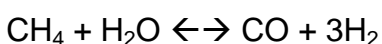
In 1966 ICI introduced patents for a Cu/ZnO/Al₂O₃ catalyst[5-7] with a much higher activity than the previous catalyst [8, 9]. This enabled methanol synthesis to be carried out at lower temperatures (<300°C) and much lower pressures (50-100bar). The process uses a synthesis gas feed of CO/CO₂/H₂, typically in a ratio of 1:1:8. The low pressure process is far more efficient, has a lower capital cost and is cheaper to run than the old process, which is now obsolete[9].

Since its introduction, the Cu/ZnO/Al₂O₃ has remained the catalyst of choice in industry for methanol synthesis, with only minor changes made to its original formulation. This is due to its excellent selectivity (+99%)[10], activity and lifespan (3-4years)[11].

1.2.3 Thermodynamics

1.2.3.1 Steam reforming

The synthesis gas used to produce methanol comes from the steam reforming of natural gas over nickel catalysts[12]. For example, the steam reforming of methane is shown below. The resulting gas is a mixture of carbon monoxide, carbon dioxide and hydrogen:



The gas mix is hydrogen rich, and this hydrogen can be utilised in the synthesis by the addition of more carbon dioxide, possibly from a nearby ammonia plant[9], which produces CO₂ as a by product.

1.2.3.2 Synthesis

The methanol synthesis reaction has always been expressed as the hydrogenation of CO:



Initially, this is how methanol synthesis was thought to proceed, with CO being the main carbon source of methanol and carbon dioxide present to prevent over reduction and therefore sintering [13-16]. However, recent studies have indicated that it is in fact CO₂ which is the primary source for methanol [17-19]:



Both reactions are reversible, as well as being exothermic. They are also thermodynamically unfavourable, showing positive Gibbs free energy changes at reaction temperatures. As both reactions are exothermic and proceed with a reduction in the number of moles, the highest yields of methanol are obtained at low temperatures and high pressures.

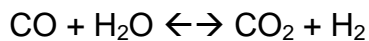
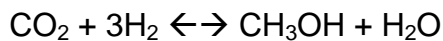
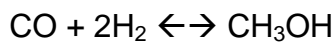
As well as the methanol synthesis there is also another reaction taking place in the system, the water gas shift (WGS). The reaction is shown below:



The reaction is believed to occur via a surface-redox mechanism. By this mechanism water is completely dissociated via hydroxy groups and adsorbed H species to gaseous H₂ and adsorbed O. The adsorbed O is removed by CO to produce gaseous CO₂[20, 21]. At reaction temperatures, the equilibrium is shifted to the right and therefore CO₂ and H₂ production is favourable.

1.2.3.3 Equilibrium

In summary, the three reactions relevant in methanol synthesis are:



These reactions define the equilibrium composition of the system. It has been customary to use the equilibrium constants for methanol synthesis from CO, $K_{p(\text{meth})}$, and the water gas shift reaction, $K_{p(\text{WGS})}$ [22].

$$K_{p(\text{meth})} = \frac{p_{\text{CH}_3\text{OH}}}{p_{\text{CO}} \cdot p_{\text{H}_2}^2} \quad K_{p(\text{WGS})} = \frac{p_{\text{CO}_2} \cdot p_{\text{H}_2}}{p_{\text{CO}} \cdot p_{\text{H}_2\text{O}}}$$

Corrections for non-ideality are significant in the calculation of the system equilibrium and the use of appropriate fugacity constants is required. Substantial research has been undertaken by investigators in assessing the two reactions and an example of a typical equation for the $K_{p(\text{meth})}$ value from CO hydrogenation comes from the work of Wade et al[23]. They defined the equilibrium constant as:

$$K_{p(\text{meth})} = 9.740 \times 10^{-5} \times \exp [21.225 + (9143.6 / T) - 7.492 \ln T + 4.076 \times 10^{-3} T - 7.161 \times 10^{-8} T^2]$$

An example of the equilibrium constant for the water gas shift reaction comes from the work of Bissett et al[24]. They defined the equation as:

$$K_{p(WGS)} = \exp [-13.148 + (5639.5 / T) + (1.077 \ln T) + (5.44 \times 10^{-4})T - (1.125 \times 10^{-7})T^2 - (49170 / T^2)]$$

Various different expressions for the equilibrium constants have appeared in the literature for both the water gas shift reaction and the hydrogenation of CO to methanol. Values of $K_{p(\text{meth})}$ derived from some of these equations are tabulated below:

Temperature (K)	Calculated value (bar^{-2}) K_5			
	Stull et al. [118]	Cherednichenko [116]	Thomas and Portalski [114]	Kotowski [117]
300	2.150×10^4	2.587×10^4	1.817×10^4	2.47×10^4
400	2.011	2.200	1.680	2.539
500	5.881×10^{-3}	6.384×10^{-3}	5.195×10^{-3}	9.029×10^{-3}
600	1.157×10^{-4}	1.153×10^{-4}	0.988×10^{-4}	2.022×10^{-4}
700	6.302×10^{-6}	6.134×10^{-6}	5.485×10^{-6}	13.49×10^{-6}

Table 1-1 Literature values for $K_{p(\text{meth})}$ [10]

The discrepancies between some of the calculated values are surprisingly large and there are a number of reasons for this (different fugacity constants, etc). It is likely that industrial companies have derived more accurate expressions for the composition mix in relation to plant design etc, however these studies remain confidential property.

1.2.4 Commercial Catalyst

In general the commercial Cu/ZnO/Al₂O₃ catalysts are usually made of the following composition:

Component	Weight %
CuO	40-80
ZnO	10-30
Al ₂ O ₃	5-10

Table 1-2 Typical weight % of each component in copper methanol synthesis catalysts[25]

Additives such as MgO may also be added to improve the performance of the catalyst by reducing copper sintering[25].

The Cu/ZnO/Al₂O₃ catalysts are prepared by co-precipitation. Co-precipitation is the technique whereby a solution of two metal salts (or more) is contacted with an aqueous alkali (usually a carbonate), to cause the precipitation of an insoluble metal carbonate[26]. This generates a homogeneous distribution of the catalyst components with a definite stoichiometry, which is difficult to achieve with other preparation methods. In this case, a solution containing Cu(NO₃)₂, Al(NO₃)₃ and Zn(NO₃)₂ is contacted with Na₂(CO₃) to produce a precipitate. The pH during the precipitation strongly influences the composition and particle size of the final catalyst. Ideal composition of the catalyst is achieved at a pH of ~7[27, 28]. The precipitate is then heated in air to transform the basic carbonates to oxides. This is known as calcination. Once this process is complete the catalyst is finished.

Each of the components in the catalyst has a specific role to play. Copper has long been acknowledged to be the active component for methanol synthesis [29-31]. The role of zinc oxide was initially thought to be as a “poison soak,” to absorb any poisons such as sulphur or chlorine from the feedstream[9]. However its role is not limited to this. It has been found to help disperse the copper particles[9], prevent sintering and has also been claimed to act as a promoter of the active sites through synergistic effects[32-35]. Studies have also shown that the zinc oxide can

be active for methanol synthesis itself. These claims will be discussed later on in the mechanism section. Finally the role of the alumina in the catalyst is to act as a stabiliser[9]. The alumina was found to minimise copper sintering more effectively than zinc oxide. The acidic sites on the alumina have been found to catalyse the production of dimethyl ether, however these sites are neutralised by the basic zinc oxide.

1.2.5 Selectivity

The Cu/ZnO/Al₂O₃ catalysts are very selective towards methanol. Under typical industrial conditions and a feed of CO/CO₂/H₂, the carbon selectivity can be in excess of 99%[10]. Trace amounts of other species - mainly higher oxygenates - are produced, including:

- Alcohols (ethanol, butanol, etc)
- Esters (methyl acetate, methyl formate)
- Aldehydes and ketones (acetaldehyde, acetone etc)
- Ethers (dimethyl ether)

The selectivity towards methanol is surprising as thermodynamically, methanol is not the most likely product derived from the reaction of CO and hydrogen.

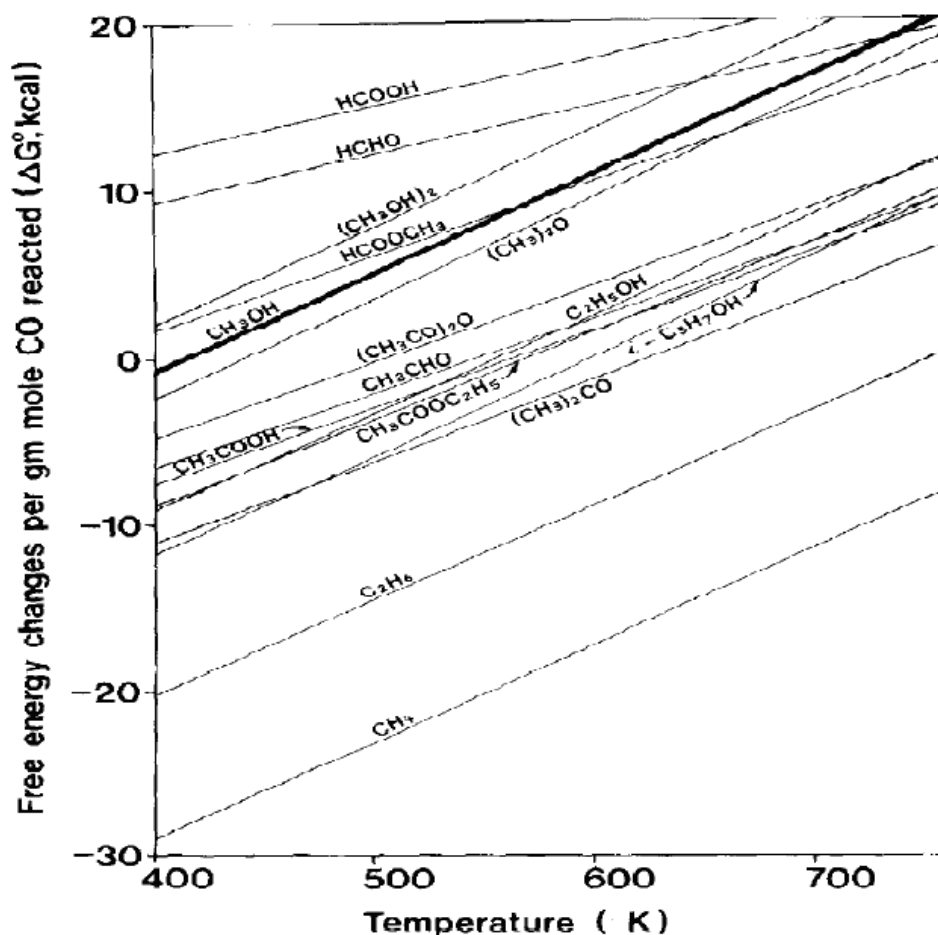


Figure 1-2 Thermodynamics of formation for various compounds[10]

Several other species such as methane and ethanol are much more favoured. This indicates that the system is kinetically controlled rather than thermodynamically. The contact times in methanol synthesis are long enough for methanol to be formed but too short for longer chain products such as ethanol to be produced. Fully hydrogenated species such as methane are not able to be formed due to copper's inability to fully dissociate CO.

By-product formation is influenced by any impurities present in the catalyst. For example if iron is present, methane can be produced. Alkaline impurities can result in the formation of higher alcohols whereas acidic impurities tend to lead to the formation of waxes.

As the selectivity of the catalyst is extremely high, consequently there has not been a major body of work in trying to improve this aspect of the catalyst. Work in this area has been limited to altering the composition of the methanol synthesis catalyst to produce higher oxygenates such as alcohols and carboxylic acids.

1.2.6 Mechanism

The methanol synthesis reaction has been studied widely by countless research groups since the process was first introduced. These studies have ranged from Cu based catalysts, ZnO based catalysts, combinations of these and finally the Cu/ZnO/Al₂O₃ catalyst itself. The studies have often thrown up conflicting data and postulated mechanisms, showing that the investigations into these types of catalyst are non – trivial. There are several reasons for this[9]:

- In the commercial copper based catalysts there are at least three phases present, the copper, the zinc oxide and the alumina. There may also be other phases added such as magnesium oxide. Each of these components could potentially play a role in the synthesis and therefore there could be many effects to take into account.
- Preparation of the catalysts also varies and the preparation method has been shown to be very important with regards to the final properties of the catalysts. One problem for example is that the amounts of copper, zinc oxide and alumina vary from catalyst to catalyst and even small changes could have an important effect on the final catalyst properties.
- The catalyst pre-treatment is also an issue, as there is a vast range of activation conditions used in the literature. The variation in pre-treatment will have an effect on each of the phases present in the catalyst and this effect should not be dismissed.
- The range of reaction conditions and gas feeds also makes it difficult for comparisons to be made.

Methanol synthesis is therefore still a topic of controversy even now, and there are still some crucial issues to be resolved. Chinchén *et al.* summarised the debates into five distinct questions[29]:

- 1) In synthesis gas mixtures of CO / CO₂ / H₂, which carbon oxide is the source of methanol – CO or CO₂?
- 2) What is the state of copper in the active catalyst?

- 3) What roles do the other components in the catalyst play?
- 4) What is the methanol synthesis mechanism?
- 5) What are the active sites for methanol synthesis?

Much work has gone in to answering these questions and some of the research performed is detailed below.

1.2.6.1 Role of CO and CO₂

The most controversial issue in methanol synthesis to date is when a feed of carbon monoxide / carbon dioxide and hydrogen is used, what carbon oxide is the source of methanol – carbon monoxide or carbon dioxide? Initially, it was assumed that carbon monoxide was the primary source of methanol[36, 37], as stoichiometrically this is possible and energetically it is more favourable than synthesis from carbon dioxide (requires breaking of C-O bond, a process requiring $\sim 485\text{kJ mol}^{-1}$). Carbon dioxide was assumed to play one of three roles[37]. It could (i) oxidize the catalyst and keep it in an active state, (ii) be converted to methanol (although this was discounted at the time) or (iii) prevent carbon deposition by oxidizing surface species. This view was generally accepted at the time but in the last 20 years there has been an increasing amount of evidence that it is in fact carbon dioxide which is the direct source for methanol.

1.2.6.1.1 CO₂

The earliest evidence for methanol synthesis from carbon dioxide came from the work of Kagan et al in 1975[18, 19]. In their investigations they used labelled carbon monoxide which produced methanol with the same specific activity as carbon dioxide and therefore showed that the carbon dioxide was the direct precursor to methanol. The findings have since been reproduced by other workers, notably Chinchin[17] who performed experiments feeding in labelled carbon dioxide in industrially relevant conditions (1:1:8 ratio of CO:CO₂:H₂, 50bar pressure, 250°C) over a Cu/ZnO/Al₂O₃ catalyst. The results obtained at different inlet flow rates are shown in figure 1-3. At high flow rates the specific activity of methanol is almost exactly the same as the activity of the inlet labelled carbon dioxide. At these flow rates, the WGS is not an issue as it is slower than the synthesis

reaction. This indicates that the source of methanol in the reaction is from the dioxide rather than the monoxide.

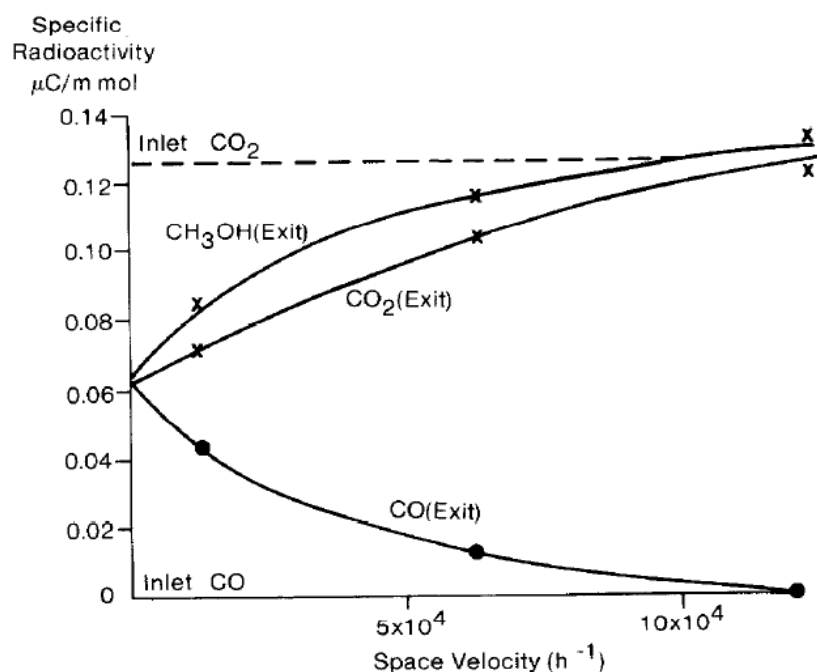
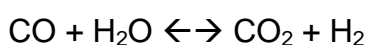


Figure 1-3 Specific radioactivities of carbon monoxide, carbon dioxide and methanol as a function of space velocity. Reaction feed gas 10%CO / 10% CO₂ / 80% H₂ containing ¹⁴CO₂ at 50bar, 523K[12]

The authors further suggest that the role of carbon monoxide in the system is to act as a source of carbon dioxide via the forward water gas shift reaction, which is favourable under the reaction conditions.



Although the hydrogenation of carbon dioxide is energetically less favourable than for carbon monoxide, it has been found to be kinetically faster[38]. This evidence alone would suggest that in feed gas mixtures containing both carbon monoxide and carbon dioxide, that the dioxide is the primary route towards methanol.

1.2.6.1.2 CO

The role of carbon monoxide as suggested in the previous section is to act as a source of carbon dioxide via the water gas shift. Conflicting arguments however have emerged as to whether this is the monoxides only role in the synthesis. It has been suggested by many researchers that over copper based catalysts, the hydrogenation of the monoxide does not occur. Rozovskii et al[19, 39, 40]

recorded no measurable methanol yield over the old USSR methanol synthesis catalyst SNM-1 (Cu/ZnO/Al₂O₃). They operated at 220°C and 50 bar pressure, with a feed gas of carbon monoxide / hydrogen. The result was attributed to the feed gas being carefully cleaned of all water and carbon dioxide. However many other workers have reported sizeable yields of methanol over similar Cu/ZnO/Al₂O₃ catalysts[41, 42] and therefore it is possible that the result could be due to the variable nature of the catalyst rather than the feed gas.

Perhaps the most popular view is that the presence of CO suppresses the formation of steam via the water gas shift, which can lead to sintering of the copper particles [43-46].

1.2.6.2 Role of Copper

The role of copper in the Cu/ZnO/Al₂O₃ catalysts has been widely studied. Copper metal (Cu⁰) has been proposed as the active component in the catalyst by a number of researchers. Waugh [29-31] performed a series of experiments under industrial conditions using a 1:1:8 CO/CO₂/H₂ feed. The copper metal area of each of the catalysts was determined by N₂O frontal chromatography. The results showed a straight line correlation between methanol synthesis activity and copper surface area, with the turnover number virtually identical for all the catalysts.

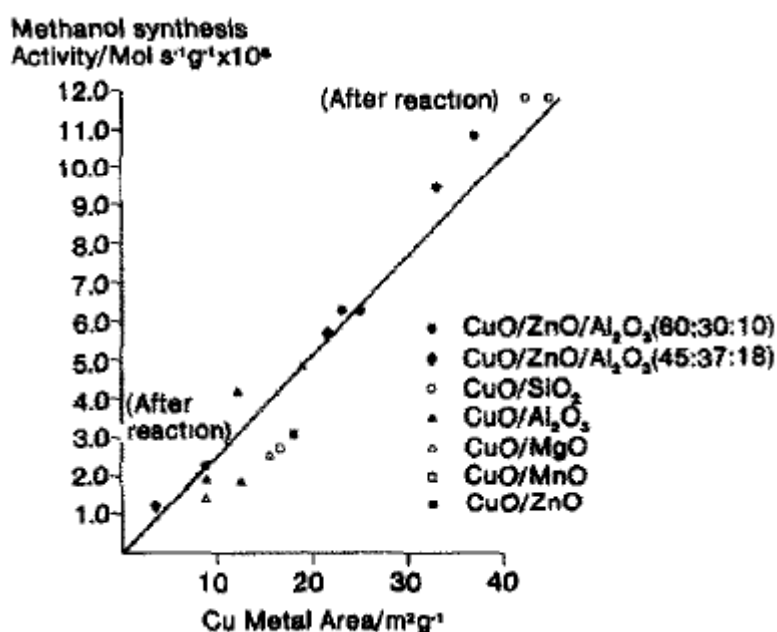


Figure 1-4 Methanol synthesis activity as a function of copper metal area [3]

From this they concluded that all of the copper is active and that the other components in the catalyst (zinc oxide and alumina) do not play a significant role. Other groups have also reported similar findings[47, 48].

However, contrasting results to these have also been published. Ponec[49] performed experiments on copper catalysts supported on pure silica, under CO/H₂ and CO/CO₂/H₂ feeds. Results showed when impurities are not present, the copper is not active for methanol synthesis. They concluded that the impurities or in the case of the commercial catalyst, ZnO, promote and stabilize Cu⁺ sites. It is these sites that the authors propose are active for methanol synthesis.

Further groups have also supported this view that the role of ZnO is crucial in creating the active sites in copper through synergistic effects [32-35].

What is known is that under industrial conditions the surface of the catalyst is in a dynamic state [50-52]. Initial studies by ICI indicated that ~30% of the copper surface area is covered by adsorbed oxygen under working conditions [8, 10, 30], and this coverage is a function of the CO/CO₂ ratio. This suggested that the role of CO in the system is to maintain the catalyst surface in a more reduced and hence active state than can be achieved by hydrogen alone. However recent studies using transient in situ techniques where CO was pulsed into a CO₂ / H₂ feed and vice versa have indicated otherwise[53]. Step change experiments were also performed where CO/H₂ or CO₂/H₂ feed mixtures were instantly changed to CO/CO₂/ H₂ mixtures. The results showed that the working surface on the catalyst is essentially oxygen free (less than 2%). These results are in accordance with surface science experiments [54, 55]. The ICI group later acknowledged that the initial oxygen coverage's reported were erroneous[56].

The dynamic nature of the copper surface can be significantly affected by the feed gas composition. Studies using X-ray adsorption fine structure (EXAFS) on Cu/ZnO have shown that the copper particles morphology changes depending on the reduction potential of the feed gas[57]. To explain this behaviour, the authors constructed a simple model based on the surface and interface free energies. Upon increasing oxidation potential of the syn gas, the copper particles form spheres with relatively high co-ordination numbers. When the reducing potential of

the feed gas is increased the copper particles form flat, disc like shapes, which have relatively low co-ordination numbers [57-59].

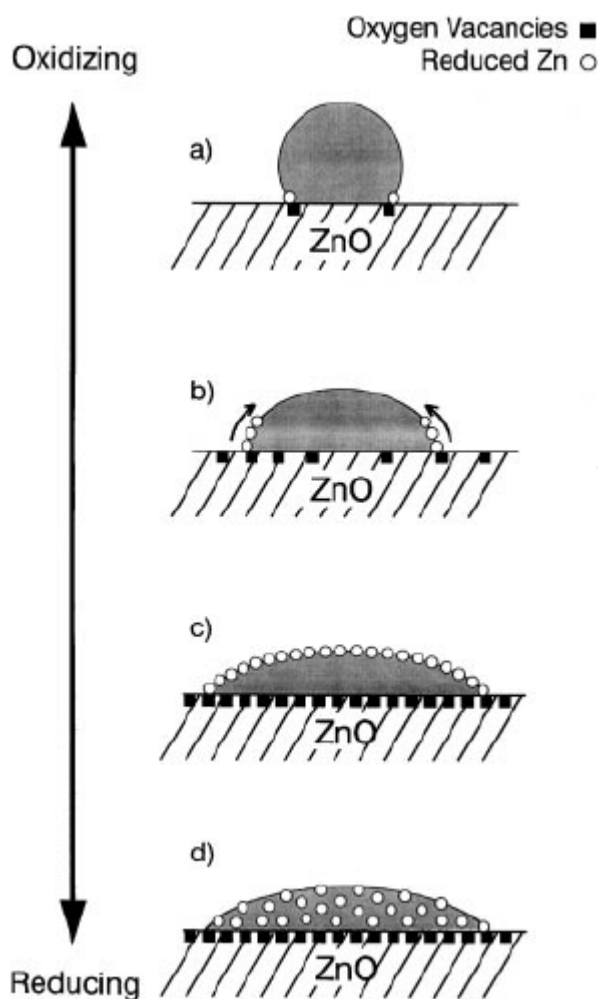


Figure 1-5 Schematic model for wetting / non wetting of copper on zinc surface [57-59]

Upon increasing the reducing potential of the synthesis gas, the driving forces for the morphological changes were deemed to be oxygen vacancies at the Cu – ZnO interface, resulting in increased interaction with the copper particles to form disc like shapes with higher surface areas [57-59]. The higher surface area, coupled with the formation of the catalytically active Cu (110) and Cu (100) planes explains the increasing methanol production rate as the reducing potential of the syn gas is increased.

1.2.6.3 Role of Zinc Oxide

Initially thought of as a dispersant for copper and as a ‘poison soak,’ the role of zinc oxide has turned into one of the most controversial topics in methanol synthesis to date. The argument can be separated into two contrasting views (i)

that the zinc oxide plays no obvious part in the synthesis and (ii) that the zinc oxide is crucial in creating the active sites for the synthesis.

The observed linear relationship between methanol synthesis rate and the copper metal area was shown to apply to copper catalysts supported on not only zinc oxide, but alumina, silica, magnesium oxide and manganese oxide as well[29-31]. This suggested that the role of the zinc oxide was as a support for the active copper phase, and that the oxide played no part in the synthesis. Earlier reports of enhanced activity induced by modifying the composition of the catalyst were deemed to be attributable to changes in dispersion or morphology of the copper particles[10].

Other groups however have proposed that the zinc oxide can play a promotional role in the synthesis. Campbell et al[46], Ovesen et al[57] and Waugh et al[60] claim that the zinc oxide support changes the morphology of the copper particles depending on the reaction atmosphere and that during the synthesis the copper surface particles form catalytically active planes such as (110). They did not however propose any other active phase other than the copper. Other groups have gone further however and claim a synergistic effect between the copper and the zinc oxide. Klier et al[13, 14] using x-ray diffraction showed that post reduction, copper could be incorporated into the zinc oxide lattice. The copper was in the form of Cu^+ , which is isoelectronic with Zn^{2+} . They concluded that the Cu^+ sites were the catalytically active centres upon which CO hydrogenation occurred, due to its ability to back donate to the carbon monoxide from the d orbital's. However, evidence that CO_2 was the primary precursor to methanol and the discovery of a linear relationship between methanol synthesis activity and copper surface area led to this view being largely discredited.

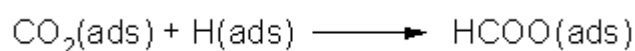
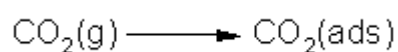
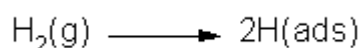
Other evidence that zinc oxide is crucial to the synthesis came from the work of Fujitani et al[61]. In their studies using a physical mixture of Cu/SiO_2 and ZnO/SiO_2 , they showed that catalytic activity increased upon migration of ZnO_x species from the ZnO particles to the surface of the copper particles. Therefore promotion of the catalytic activity of the copper by a tiny amount of Zn was observed without the use of the ZnO as a support. The authors suggested that the formation of a Cu-Zn alloy was key in enhancing the methanol synthesis activity.

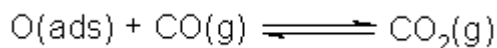
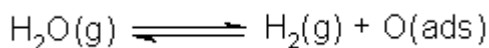
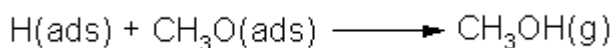
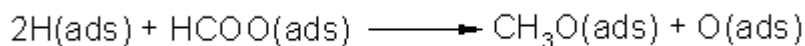
Finally, it has also been claimed that the active sites for methanol synthesis are actually based on the zinc oxide rather than the copper particles. Frost et al[62] presented results which demonstrated that high methanol synthesis activity can be obtained in the absence of copper by using oxides promoted by metals such as silver or gold, not normally considered active for methanol synthesis. From these results they concluded that the active sites were contained on the surface of the metal oxide and that the role of the metal was to adjust the electronic properties of the oxide, creating the active sites (oxygen-ion vacancies). Although zinc oxide itself has been widely acknowledged to be active for methanol synthesis, the view that it is the primary active component for the synthesis has been largely discounted amongst the research community.

1.2.6.4 Mechanism

The mechanisms for both CO hydrogenation and CO₂ hydrogenation over Cu/ZnO/Al₂O₃ have been investigated using a variety of techniques, mainly a combination of TPD and TPR experiments [8, 29, 63, 64]. No intermediate has ever been identified by temperature programmed desorption for the CO/H₂ interaction to form methanol. This suggests that the intermediate, probably a formyl species is weakly bound to the surface[8].

The mechanism for the hydrogenation of CO₂ to methanol is understood a lot clearer. The carbon dioxide adsorbs onto copper to form a symmetric carbonate[8]. The carbonate is then hydrogenated to a bidentate formate which is the longest lived intermediate in methanol synthesis[8]. The rate determining step in the reaction is the hydrogenation of this species to methoxy species, which is then hydrogenated once more to give the product methanol[8]. The remaining O_(ads) is picked up by either CO to give CO₂ or by H₂ to produce H₂O. The elementary reaction steps are listed below:





1.2.6.5 Active Sites

Copper has been shown to be the likely active phase for methanol synthesis.

Studies have shown that under a CO_2/H_2 feed, methanol can be synthesised on clean Cu(100) and Cu(110) surfaces, as well as on copper foil[46, 65-67].

Recently, studies performed on zinc deposited copper single crystals revealed that when the Zn coverage is ~ 0.2 , the zinc deposited Cu(111) is highly reactive and promotes methanol synthesis by an order of magnitude[68]. The authors suggested that in a working methanol synthesis catalyst, Cu-Zn was the active site.

Another factor that affect the copper particles and hence, the active sites is the synthesis gas feed. Recent studies have shown that under reducing conditions, the Cu(100) and Cu(110) planes are predominant[69]. These planes are highly active for methanol synthesis. As the reducing potential of the feed gas is decreased, the Cu(111) plane becomes more dominant. The Cu(111) plane is less active and therefore the methanol synthesis activity is decreased upon increasing the oxidation potential of the feed.

1.2.7 Precious Metal Catalysts

Although the conventional Cu/ZnO/Al₂O₃ catalysts perform very well, a significant amount of research has gone in to investigating precious metals as catalysts for methanol synthesis. Initially the research was borne out of the need to create a poison tolerant catalyst, an application that precious metals showed promise for [70, 71]. However, recent research has been more out of general scientific interest.

Precious metal catalysts have been used extensively for various synthesis gas reactions (Fischer- Tropsch, higher alcohol synthesis) and have shown promise for the production of alcohols including methanol.

1.2.7.1 Palladium based catalysts

Palladium based catalysts have shown significant promise for alcohol production from a feed gas of carbon monoxide and hydrogen. They have extremely high selectivity (>99%) towards methanol and have been shown to be active for methanol synthesis[72]. However, the catalysts suffer from a very low rate of reaction.

Initially thought to be inactive and only useful for methanation, Poutsma provided the first evidence that Pd could be used to produce methanol selectively[72]. Operating within the temperature - pressure range for methanol synthesis they reported that over Pd/SiO₂ catalysts, selectivities of ~98-99% were observed, with methyl formate the only side product of note (typically ~1-2%). The authors suggested that the ability of the palladium to synthesise methanol at elevated temperatures and pressures resulted from its excellent hydrogenation ability coupled with its tendency to adsorb carbon monoxide non-dissociatively[72]. However, in comparison with the commercial copper catalysts, the rate of reaction was significantly slower.

Since the discovery, substantial research has been undertaken into the development of Pd based catalysts for methanol synthesis. However the high cost of Pd and the relatively slow rate of reaction have so far prevented the commercialisation of any such catalyst.

Several approaches have been undertaken to try and improve and understand the performance of Pd based catalysts. It is understood now that the catalytic properties of the catalysts are dependant on the nature of the support, the palladium particle size, the presence of promoters and the palladium precursor used[73].

CO hydrogenation on various supports has been investigated comprehensively. Ali and Goodwin studied the hydrogenation over SiO_2 , Al_2O_3 and $\text{SiO}_2\cdot\text{Al}_2\text{O}_3$ using Steady State Isotopic Transient Kinetic Analysis (SSITKA)[74]. They found that the nature of the support had a dramatic effect on the selectivity and activity of the catalyst. On the neutral support SiO_2 , methanol was the only product observed. On the $\text{SiO}_2\cdot\text{Al}_2\text{O}_3$ support, dimethyl ether formation was observed as the support is slightly acidic. On the Al_2O_3 support, methane was the major product. The activities of the catalysts increased with rising acidity, with the Al_2O_3 supported catalyst being the most active.

Results similar to these have appeared in the literature and so it is apparent that the acid-base properties of the support play a pivotal role in determining the selectivity and activity of the catalyst.

The SSITKA studies also performed by Ali and Goodwin showed that the number of surface intermediates leading to methanol and methane were affected dramatically by the support[74]. The authors concluded that the impact of the support on the reaction rate was to increase / decrease the number of intermediates present on the palladium.

Jackson et al suggested another possibility[75]. In their investigations, they studied the hydrogenation of CO over Pd supported on tungsten and molybdenum trioxides. A substantial increase in activity was observed when the trioxides replaced silica as a support. The effect was attributed by the authors to be hydrogen spill over from the support to the metal, which increased the hydrogen available to the reaction intermediates to form methanol.

Another popular theory is that the support interacts with the palladium electronically. Poels et al[76] proposed that the support could create ionic Pd sites

through strong metal support interactions (SMSI) and it was on these sites that methanol synthesis occurred.

Promoters are also deemed to enhance the methanol synthesis activity in a similar way. Gotti and Prins prepared Pd catalysts on ultrapure SiO₂ supports, and further doped the catalysts with various metals[77]. They found that presence of basic metals in particular such as calcium and sodium depressed CO dissociation and had a strong promoting effect on the methanol synthesis activity. In contrast, they found that Pd supported on pure SiO₂ had very little methanol synthesis activity, indicating that impurities in the support could play a role. Similar work by Nonneman et al showed that the presence of impurities in the support could promote the palladium metal and therefore increase the rate of methanol synthesis[49, 78].

The prevalent theory amongst researchers is that a basic metal situated on or next to the noble metal is required to promote the metal and therefore enhance the methanol synthesis activity [49, 77, 78].

The particle size and dispersion of the particles can have a dramatic effect on the methanol synthesis activity. If the surface area can be increased then the activity can also increase. An example of this comes from the work of Kim et al, who produced Pd / ZrO₂ catalysts using a novel water in oil micro emulsion technique [79, 80]. Using this technique they produced catalysts with average particle sizes much smaller than wet impregnated catalysts. The dispersion was also increased in comparison with the wet impregnated catalysts. The effect on the hydrogenation of CO was remarkable, with a 3-fold increase in activity. Selectivity towards methanol remained high.

Finally, the metal precursor can have an effect on the catalytic properties. The types of anions in the Pd salt used in the catalyst preparation may alter the reaction properties of the resulting catalyst. It has been reported that catalysts prepared using a PdCl₂ precursor exhibited a higher methane and methanol production rate than those prepared from a Pd (NO₃)₂ precursor, although the type of precursor did not affect the selectivity[77],. Studies by Shen et al[81] indicated that the anions had an effect on the final palladium particles, and therefore

affected the support – metal interaction which the authors believe to be crucial in promoting methanol synthesis on these types of catalyst.

1.2.7.2 Other metals

Non – dissociative adsorption of CO is crucial in the synthesis of methanol. If the C-O bond is cleaved upon adsorption (dissociative) methane is formed rather than an oxygenate. Of the remaining group VIII metals only Rh, Ir and Pt are considered to adsorb CO non-dissociatively.

Rhodium has been studied extensively in the literature as it has a unique ability to adsorb CO dissociatively and non-dissociatively. It is known to catalyse the production of various oxygen containing compounds such as alcohols, aldehydes and acetic acid[82-86]. The selectivity towards each product is governed by the support oxide used. For example, supports and promoters including V_2O_3 , La_2O_3 , CeO_2 , TiO_2 and ZrO_2 have been used to maximise ethanol production. Selectivity's as high as 70% have been reported[87, 88].

Methanol formation can also be achieved by the selection of an appropriate support. Katzer et al demonstrated that the selectivity towards alcohols varies with the basicity of the support[88]. Rhodium supported on magnesium oxide, the most basic of the supports tested, could selectively catalyse the production of methanol (~90%), whereas on less basic supports ethanol was the alcohol selectively produced. Ichikawa et al came to similar conclusions, in that the more basic the support, the more selective the catalyst was towards methanol[87].

Although methanol can be synthesised over rhodium based catalysts, the problems associated with the low selectivity and low activity coupled with the expensive rhodium metal at the moment means that these catalysts are not commercially viable at present.

Platinum and iridium have also been studied for use in CO/H₂ reactions. Poutsma et al studied the metals supported on silica in CO/H₂ reactions in 1978[72]. In the temperature-pressure domain for methanol synthesis to be thermodynamically favourable, methanol was produced selectively on both catalysts. However, both catalysts showed lower activity compared with the Pd/SiO₂ catalyst also studied, which in itself was low in activity. The addition of promoters such as transition

metals have been found to increase activity but can be at the expense of selectivity[89]. Due to the low activity issue, these metals have not been extensively studied for methanol synthesis properties.

1.3 Methanol Carbonylation

One of the primary uses of methanol is as a feedstock to produce acetic acid. Acetic acid is used for a variety of applications such as vinyl acetate monomer synthesis, acetic anhydride synthesis and as a solvent for terephthalic acid production. It is produced annually on the scale of ~7.8million tonnes per annum[90]. There are various different industrial processes for the synthesis of acetic acid, including ethylene oxidation, hydrocarbon oxidation and methanol carbonylation. Currently methanol carbonylation accounts for ~60% of the world production capacity for acetic acid[90].

1.3.1 Homogeneous Carbonylation

The first homogeneous methanol carbonylation process was commercialised by BASF in 1960. The process used a $\text{CoH}(\text{CO})_4$ catalyst and methyl iodide co-catalyst[91]. The selectivity of the process was 90% based on methanol. In 1966, Monsanto discovered that a rhodium based catalyst could achieve greater selectivity (>99%) and could operate under milder conditions (150-200°C, 30-60bar) than the BASF process (250°C, 680 bar)[92]. The most recent advancement in the methanol carbonylation technology was made in 1996, when BP commercialised their Cativa process. The process uses an iridium catalyst, a Ruthenium promoter and a hydrogen iodide co-catalyst. The Cativa process has several advantages over the Monsanto process, including (i) improved selectivity with reduced formation of side products such as propionic acid, (ii) at low water concentrations the stability of the iridium catalyst is greater than the rhodium catalyst and (iii) the low water concentrations suppresses CO_2 formation via the WGS. The Cativa process is now operated commercially a simplified reaction cycle is shown below:

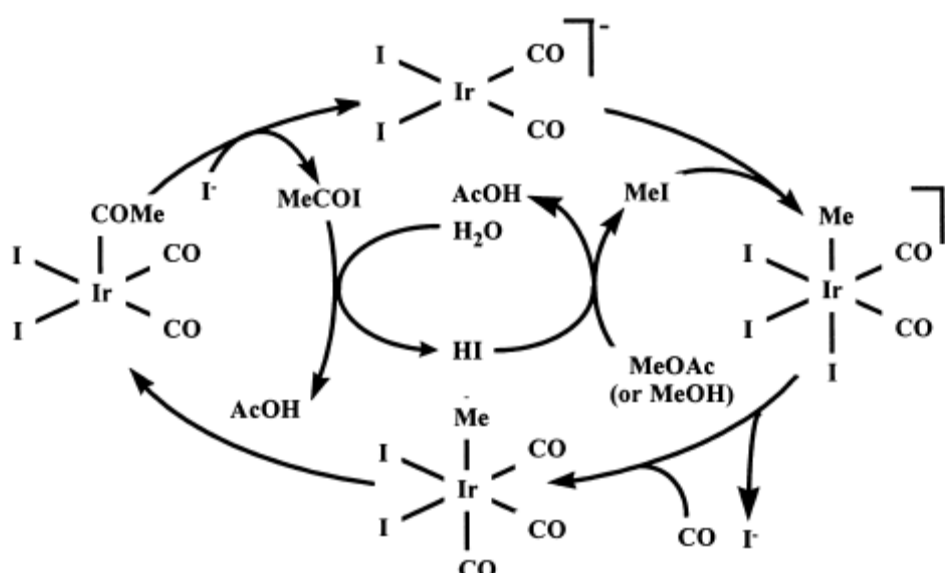


Figure 1-6 Cativa process cycle[92]

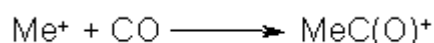
The rate determining step of the Cativa process is believed to be the dissociation of ionic iodide and the co-ordination of CO. Although there is a lower concentration of methyl iodide required to achieve high reaction rates in the Cativa process compared with the Monsanto, it is still very corrosive and may also poison downstream processes, such as vinyl acetate monomer synthesis. It would therefore be of significant commercial interest if a process for methanol carbonylation without the need for promoters could be developed.

1.3.2 Heterogeneous Carbonylation

A heterogeneous process that does not require the presence of a halide promoter would have several advantages over the liquid phase carbonylation. Apart from the obvious lack of corrosive promoter, separation of the products from the catalyst would be far easier and cleaner, resulting in little loss of expensive metal catalyst.

At the present time, there is no selective heterogeneous process for the carbonylation of methanol to acetic acid that exists that doesn't require the use of an organic halide promoter. There are, however various reports in the literature for the selective vapour phase carbonylation of methanol to acetyls (methyl acetate and acetic acid) that do not require the use of promoters.

Wegman at Union Carbide studied the possibility of vapour phase carbonylation of methanol using exchanged hetero-poly acid catalysts (HPA's)[93]. The basis for the work was in the possibility of creating and carbonylating carbonium ions using the HPA. The mechanism was envisaged to be similar to the liquid phase Koch reaction:



Reactions were carried out at atmospheric pressure with varying temperature. Several different HPA's were tested. The most effective catalyst found in the study was $\text{IrW}_{12}\text{PO}_{40}$ which at 225°C gave a product yield of 40% methyl acetate. The authors found that increasing the temperature above this resulted in the formation of hydrocarbons.

Peng et al studied the vapour phase carbonylation of methanol over various metallic chlorides supported on activated carbon without the addition of any promoter in the feed[94]. The prepared NiCl_2/C showed high conversion of methanol, whereas CuCl_2/C exhibited a much higher selectivity towards methyl acetate. Bimetallic catalysts were prepared using CuCl_2 and NiCl_2 , and the optimum composition was found to be 5% NiCl_2 and 15% CuCl_2 . This catalyst exhibited high activity and selectivity towards methyl acetate. The reaction conditions were also investigated and it was observed that as temperature increased, conversion of methanol increased however carbonylation activity decreased, agreeing with Wegmans results[93]. After thorough investigation of the reaction parameters, the optimum conditions and catalyst exhibited a 97.4mol% selectivity towards carbonylation.

Direct carbonylation of methanol to acetic acid in the vapour phase clearly yields methyl acetate as the main acetyl formed. Acetic acid so far is only produced selectively in the vapour phase when methyl iodide is present as a promoter.

The production of acetyls is industrially significant, and it is of interest as to how these compounds would react on the surface of a catalyst.

1.4 Reactions of Acetyls

1.4.1 Acetic Acid

Adsorption studies of acetic acid on various precious metals such as Rh and Pd have been studied comprehensively by Bowker et al[95-97].

Bowker et al studied the adsorption and decomposition of acetic acid on Pd (110) using temperature programmed desorption[97]. On a clean surface they found that the acid dissociates to form a stable acetate and hydrogen gas at ~300K. The acetate decomposed via decarboxylation into CO₂ and H₂ at 350 and 375K. The evolution of the CO₂ was accompanied by the deposition of the methyl group on the catalyst surface. The methyl group then further decomposed to yield H₂.

Subsequent adsorptions of acetic acid followed by decomposition led to a build up of carbon on the surface and it was found that this stabilised the acetate species on the surface, as the desorption temperature of CO₂ was increased by as much as 100K.

The effect of pre-dosing the surface of the Pd with oxygen was also investigated and it was found that the oxidised surface initially stabilised the acetate group. This was then followed by a type of autocatalytic decomposition, which occurred rapidly and converted the acetate to CO₂, H₂O and H₂. Although some carbon was left on the surface, further oxygen dosing could remove the carbon in the form of CO₂.

Similar results were obtained by the same authors, this time on a Rh(110) surface[95, 96]. On an oxygen pre-dosed surface, adsorption of ethanol yielded an acetate group via insertion of oxygen into the molecule. Temperature programmed desorption showed the autocatalytic decomposition of acetate that was observed on the Pd(110), with CO₂ and H₂ evolved and carbon left on the surface.

However, decarboxylation is only one of several different decomposition routes that have been shown to proceed over transition metals. For example, on copper surfaces acetate groups decompose to yield CO₂, CH₄, CH₃COOH, C₂H₂O₂ and

other carbon fragments. The decomposition was believed to proceed via an acetic anhydride intermediate. The decomposition temperature of adsorbed acetates and the decomposition products are dependant on the metal, the coverage of the acetate and the presence of co-adsorbates such as oxygen.

As well as adsorption studies, the hydrogenation of carboxylic acids has also been investigated as a cheap and renewable source for the production of aldehydes, esters and alcohols. Acetic acid has often been used as a probe molecule for these studies because of its molecular simplicity as well as the desire to produce acetaldehyde selectively[98].

Patent literature reveals that most of the studies performed have used group VIII metals supported on metal oxides[99, 100]. Selectivity has been reported to vary markedly. For example a Ru / TiO₂ catalyst was found to be highly selective to ethyl acetate (98% ethyl acetate, 2% ethanol)[101] whereas a Pd-Re / C catalyst reversed the selectivity and gave 93% ethanol[100]. From this it is obvious that the nature of the metal and the support could both influence the reaction mechanism and therefore the selectivity.

Vannice et al studied the hydrogenation of acetic acid over a series of platinum catalysts on various supports (TiO₂, SiO₂, η -Al₂O₃ and Fe₂O₃)[98]. The results showed that the product selectivity was strongly dependant on the oxide support as shown below:

Catalysts	Temp. (K)	Conversion (%)	Selectivity (mol%)						
			Acetaldehyde	Ethanol	Ethane	Ester	CO ₂	CO	CH ₄
0.69% Pt/TiO ₂ (HTR)	447	5.9	0	59	14	27	0	0	0
0.69% Pt/TiO ₂ (LTR)	443	5.6	0	51	20	29	0	0	0
2.01% Pt/TiO ₂ (LTR)	420	5.0	0	70	16	14	0	0	0
0.78% Pt/ η -Al ₂ O ₃	523	4.7	0	8	10	4	5	33	40
0.49% Pt/SiO ₂	511	2	0	0	0	0	0	50	50
1.91% Pt/Fe ₂ O ₃	523	4	80	20	0	0	0	0	0
Pt powder	588	4.7	0	0	0	0	32	21	47
Fe ₂ O ₃	500	4	79	21	0	0	0	0	0

Table 1-3 Product selectivity during acetic acid hydrogenation ($P_{\text{HOAc}} = 14\text{torr}$, $P_{\text{H}_2} = 700\text{torr}$)

The authors concluded that the catalytic behaviour of the catalysts resulted from either the interaction between the platinum crystallites and the oxide support to

create new sites at the support-metal interface or that more than one site is required for hydrogenation i.e. both the support and the metal are active phases and the behaviour is dictated by the adsorbed species on each site. An example would be that hydrogen spill over could occur from the metal onto the support, where the acetate group is bound.

In contrast, Cressely et al also performed studies on the hydrogenation of the acid and investigated the effect that various metals (Cu, Fe, Co) supported on silica had on the product selectivity[102]. Cu/SiO₂ was active for the formation of ethanol, acetaldehyde and ethyl acetate whereas the reaction over Fe/SiO₂ resulted in the production of acetone. Only decomposition products were observed over the Co/SiO₂ catalyst. The author suggested that hydrogenation to ethanol or acetaldehyde took place via a surface acetate intermediate, and the difference in selectivity between the three catalysts was associated with the presence or absence of these groups and their relative stability.

1.4.2 Methyl Acetate

Very little studies on the reactions and adsorption of methyl acetate were found in the literature. The adsorption of methyl acetate has been studied on silica surfaces and was found to proceed via formation of hydrogen bonds between the carbonyl oxygen and hydroxyl groups on the oxide surface[103]:

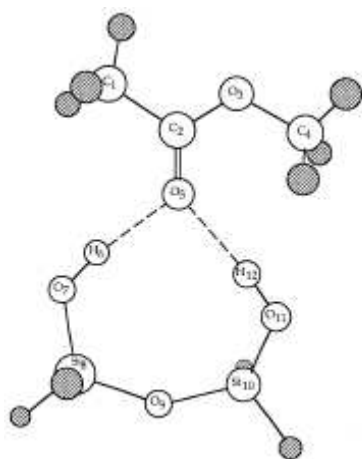
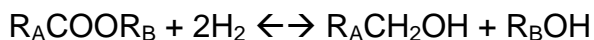


Figure 1-7 Mode of adsorption of methyl acetate on silica[103]

The catalytic reduction of esters to alcohols encompasses reactions in which the C-O bond adjacent to the carbonyl group is cleaved according to the following stoichiometry[104, 105]:

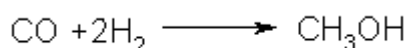


Where R_A represents an alkyl group and R_B represents another alkyl group or hydrogen. For example the reduction of ethyl acetate over copper catalysts proceeds via the dissociative adsorption of the reagent into $\text{CH}_3\text{C}^*\text{O}$ and $\text{C}_2\text{H}_5\text{O}^*$ species in which * represents a surface site. Subsequent hydrogenation of these species yields the desired alcohols.

1.5 Project Background

One of the processes currently under development by BP involves the conversion of synthesis gas into methanol followed by the carbonylation of this methanol over a hydrogen tolerant catalyst towards acetic acid. The process is summarised by the following equations

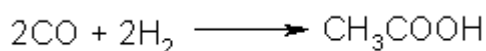
Methanol Synthesis



Carbonylation



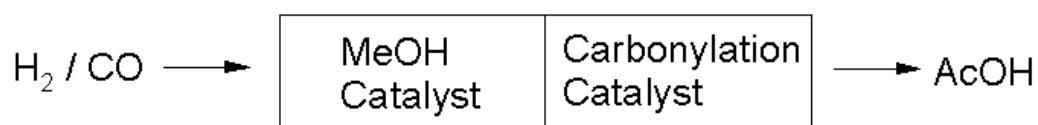
Overall



The current methanol synthesis process and catalyst have been refined over the years so that nearly 100% selectivity to methanol is obtained and high conversions are achieved. Typically the process is run with a feed gas containing $\text{CO}/\text{CO}_2/\text{H}_2$ in a 1:1:8 ratio at 250°C and 85 barg pressure. For the acetic acid process described above it is possible that the feed to the methanol reactor may be CO rich and / or contain much larger amounts of CO_2 . It is not clear whether the commercial methanol catalyst will continue to work well under these conditions.

At the start of the project BP envisaged two processes:

1) A stacked or mixed bed system where one catalyst is used to make the methanol and the other is used to carbonylate the methanol in the gas phase in the presence of H_2



2) A separate reactor system, where one reactor is used to make methanol and the other is used for the gas phase carbonylation



Whichever system is chosen, it is likely that the process will involve recycle streams and it is possible that the recycle streams may contain traces of acetic acid or methyl acetate into the feed for the methanol catalyst.

Hence it would be of interest to learn how acetic acid and methyl acetate affect a methanol synthesis catalyst when passed over it. The need for an acid tolerant methanol synthesis catalyst is required.

1.6 Project Aims

The aim of the project was to:

- 1) Investigate the use of precious metal catalysts for methanol synthesis and if so, investigate their tolerance towards acetic acid / methyl acetate
- 2) Investigate the effect acetic acid has on a commercial methanol synthesis catalyst
- 3) Investigate the effect methyl acetate has on a commercial methanol synthesis catalyst

2 Experimental

For catalytic testing, a series of precious metal catalysts were prepared using materials supplied from BP. These include two Pd catalysts, one of which was doped with calcium, a Rh catalyst and an Ir catalyst. These catalysts were all supported on silica. An industrial methanol synthesis catalyst, JM's Katalco 51-8 of formulation CuO/ZnO/Al₂O₃/MgO (64/24/10/2wt%) was also used for catalytic testing and again, this was supplied by BP.

2.1 Catalyst Preparation

2.1.1 Support Impregnation

The catalysts were prepared by impregnating the support to incipient wetness with an aqueous solution containing the precursor salt. The wet catalyst was then oven dried prior to calcination. The metal precursors of the catalysts are listed in table 2-1:

Catalyst	Precursor
Rh	Rh(OAc) ₃
Pd	PdCl ₂
Ir	Ir (OAc) ₂

Table 2-1 Metal precursors used for preparation of catalysts

To ensure uniform and maximum metal dispersion throughout the support the precursor was dissolved in a volume of water equal to the pore volume of the support.

2.1.2 Support Properties

The support chosen for the catalysts was silica Cariat Q10 produced by Fuji Silysia. Support properties are shown below:

Average Pore diameter (nm)	10
Pore Volume (ml / g)	1.0
Surface Area (m ² / g)	300

Table 2-2 Support Properties of silica Cariat Q10

2.1.3 Preparation Procedure

15g of each catalyst were prepared at a 5wt% metal loading level. The catalyst precursor was dissolved in H₂O and made up to 14.5ml in a round bottomed flask (In the case of the Ca doped palladium catalyst, an appropriate amount of Ca nitrate was dissolved in solution along with the metallic precursor). 14.25g of the silica support was added in. The flask was then placed on the rotary evaporator and heated until excess solution was evaporated off. The catalyst was transferred to an oven and dried overnight at 100°C.

After drying, the catalyst was transferred to a glass calcination tube and inserted into the centre of the calcination furnace. Flowing air was passed over the catalyst as the furnace temperature was raised at a rate of 3°C min⁻¹ to a final temperature of 350°C. This temperature was held for 4hrs before cooling to room temperature.

A table of prepared catalysts is shown below:

Catalyst
5% Rh / SiO ₂
5% Pd / SiO ₂
5% Pd - 0.5% Ca / SiO ₂
5% Ir / SiO ₂

Table 2-3 Lab prepared catalysts

2.2 Catalyst Characterisation

2.2.1 Surface Area Analysis

The total surface area of the catalyst was determined by Brunauer, Emmett, Teller (BET) analysis. It was determined using a Micromeritics Gemini III 2375 Surface Area Analyser. Approximately 0.04g of the catalyst was weighed into a glass tube and purged in a flow of N₂ overnight at 383K before the measurement was carried out.

2.2.2 Thermo-gravimetric analysis

Thermo-gravimetric analysis was performed on post reaction catalysts using a combined TGA/DSC SDT Q600 thermal analyser coupled to an ESS mass spectrometer for evolved gas analysis. Samples were heated from 30°C to 1000°C using a heating ramp of 10°Cmin⁻¹. This temperature profile was employed using O₂/Ar at a flow rate of 100ml min⁻¹. For mass spectrometric analysis, various relevant mass fragments were followed such as 28 (CO) and 44 (CO₂). The sample loading was typically 10-15mg.

2.2.3 X – Ray Diffraction (XRD)

Diffraction patterns were measured using a Siemens D5000 x-ray diffractometer (40kV, 40mA, monochromatised) using a CuK alpha source (1.5418Å). The

scanning range was $5 - 85^{\circ} 2\theta$ with a scanning rate of 1 second / step and a step size of 0.02° .

2.2.4 Scanning Electron Microscopy (SEM)

A Philips XL30 SEM-FEG was used, operating at 20 KV in high vacuum mode with a working distance of 10 mm. An Oxford instruments EDX was attached to the side giving elemental analysis capability, of elements as light as carbon. This microscope was only used in high vacuum work though it did have environmental mode capabilities. A standard SED was used to detect the electrons.

2.3 Catalytic Testing

2.3.1 Apparatus

Catalytic tests were carried out in a 300ml Berty reactor fitted with a magnedrive 075-mkII impeller for agitation. The rig was constructed of 316 stainless steel and is depicted in Fig.2. Gases could be fed into the reactor via mass flow controllers and pressures of up to 50 bar were achieved by use of a gas booster. Liquid feeds could be introduced into the system prior to the reactor via the use of an HPLC pump. The feeds were vaporised using inlet trace heating at a temperature of 423K. All tubing after the reactor was heated to 463K to prevent condensation of products before reaching the GC. The GC valves were also heated to the same temperature in a purpose built oven.

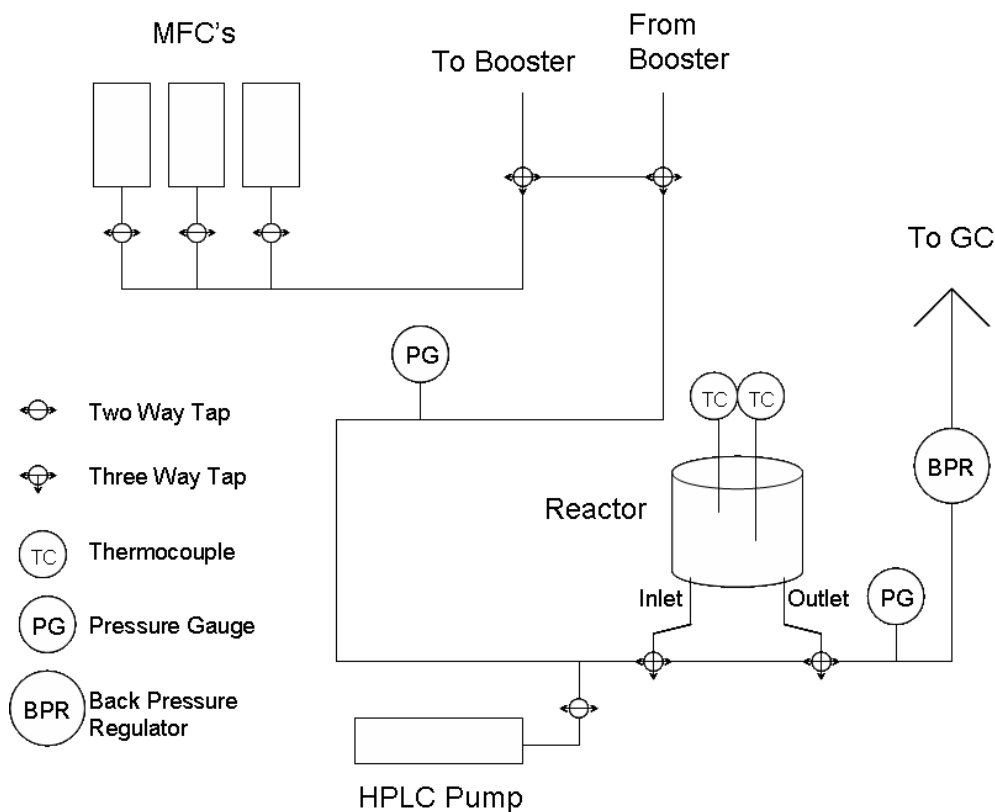


Figure 2-1 Reactor Setup

2.3.2 Reaction Procedure

Catalyst pellets (1.36ml) were placed in the reaction basket and the reactor lid bolted down. Prior to reaction the catalyst was reduced *in-situ* at 523 K for 3h in a flow of 50 ml min⁻¹ hydrogen. The catalyst was then introduced to a flow of the desired reaction gas mix. The pressure was built up in the reactor using the booster and backpressure regulator to that required for the reaction. Once all the desired reaction parameters had been reached the analysis began.

2.3.3 Gas Chromatography (GC)

Product analysis was carried out by online GC (Thermofinnigan Trace GC) fitted with two columns and two TCD detectors. The two columns were; a 50 m molsieve 5A used for methane, CO, nitrogen and ethane separation and a 30 m HP PLOT Q column for all other products. The sample loop volume was 1ml. Prior to analysis the GC had been calibrated for CO, CO₂, nitrogen, methane, ethane, water, methanol, ethanol, methyl acetate, acetaldehyde, acetone, ethyl acetate and acetic acid. All calibration curves gave good linear responses. Throughout the

reaction samples were taken every 60 minutes. This allowed for complete elution of all products and a 15 minute equilibrium time.

2.3.3.1 Column Conditions

Injector Temperature – 473K

Carrier Gas - Helium

The column heating profile is shown below:

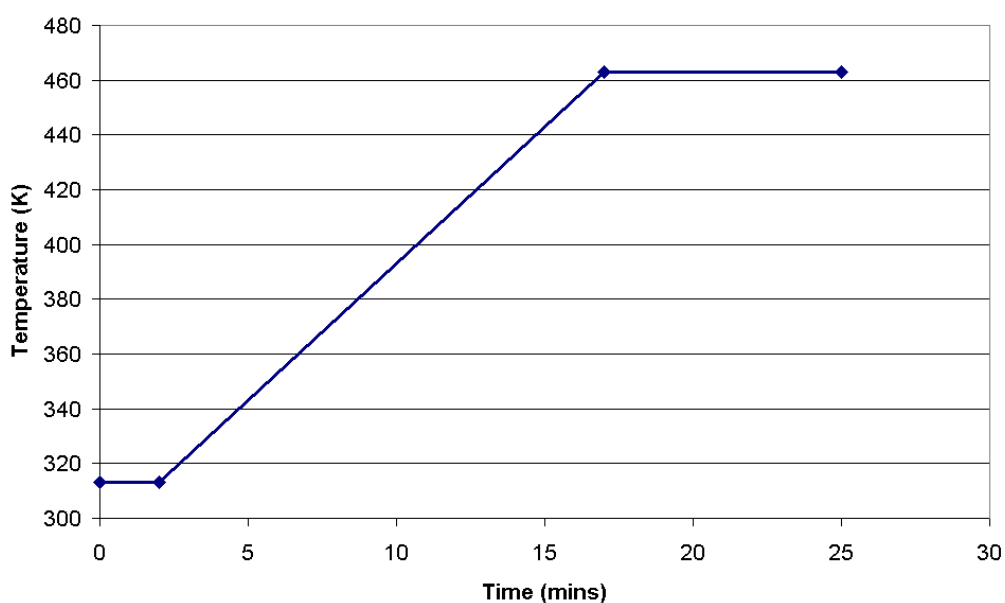


Figure 2-2 GC Temperature ramp profile

Time (mins)	Temperature (K)
0 – 2	313
2 – 17	313 - 463
17 – 25	463

Table 2-4 GC temperature ramp profile

2.3.3.2 Calibrations

The GC responses to carbon monoxide, carbon dioxide, methane, DME, ethane and nitrogen were calibrated by connecting the appropriate gas cylinder to the MFC. The partial pressure of each gas in the sample loop was varied using H₂ as a diluent.

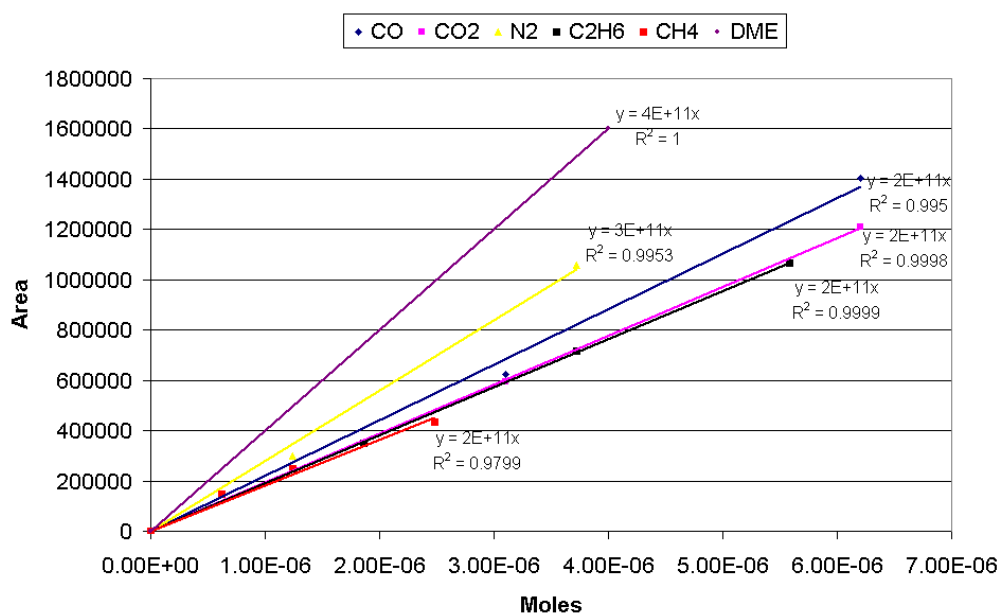


Figure 2-3 Calibration graph 1

Calibration standards for methanol, ethanol, water, methyl acetate, ethyl acetate, acetic acid, acetaldehyde and acetone were prepared in varying concentrations in 50ml volumetric flasks, using an appropriate diluent. A 1 μ l sample from the flask was injected into the GC using a 10 μ l syringe. From the peak area responses, linear calibration plots were obtained.

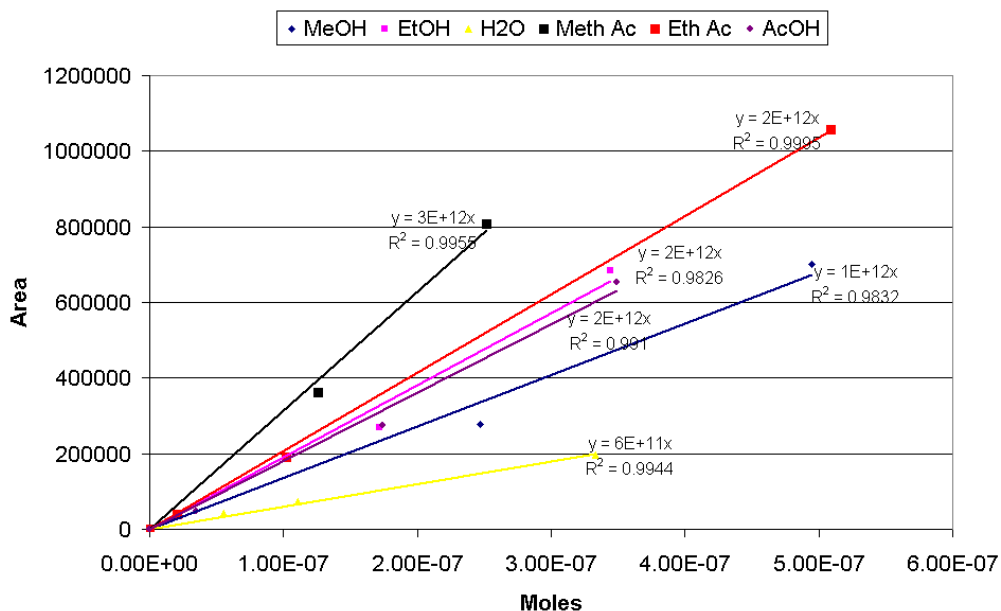


Figure 2-4 Calibration graph 2

The gradients for acetaldehyde and acetone were 1×10^{12} and 2×10^{12} respectively.

2.3.4 Soxhlet Extractions

Soxhlet equipment was used to extract soluble species from the catalyst surface post-reaction. The catalyst was crushed using mortar and pestle into a fine powder and a portion (typically ~0.3g) was placed in the glass thimble. The thimble was placed in the soxhlet chamber and the equipment set up as shown:

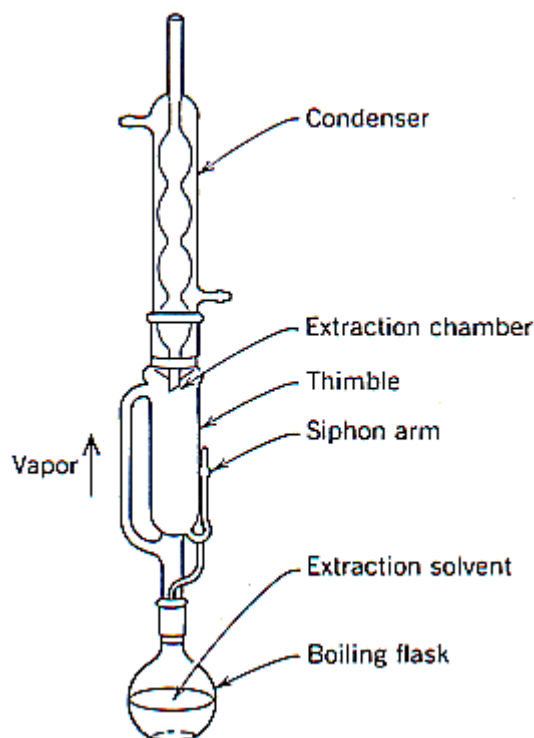


Figure 2-5 Soxhlet Apparatus

The solvent, iso-propyl alcohol (IPA) was poured into the still pot along with boiling chips.

The solvent was heated to reflux using an oil bath. Solvent vapour travelled up the distillation arm, reached the condenser and dripped back down into the soxhlet chamber. The thimble filled with the solvent and any soluble material was extracted. When the chamber was nearly full, the chamber automatically emptied via the siphon side arm and the solvent drained back down into the still pot.

The process was left to repeat itself overnight to ensure all soluble material was extracted from the catalyst sample. Post extraction a sample was injected into the GC for analysis.

2.3.5 Mass Spectrometry

For the isotopic studies, a quadrupole mass spectrometer (QMS) was connected to the effluent line post GC analysis. The mass spectrometer was used in MID mode. This mode allowed the analysis of up to 20 mass to charge ratios (m/e) over time to be followed.

2.4 Materials

2.4.1 Calibrations & Reactions

The following materials were used for reactions and also calibration of the GC. Methyl acetate and acetic acid were also used as liquid feeds during the addition studies:

Material	Purity	Supplier
Helium	99.997%	BOC
Air	99%	BOC
Nitrogen	99.998%	BOC
Hydrogen	99.995%	BOC
Methane	99%	BOC
Carbon Monoxide	99.99%	BOC
Carbon Dioxide	99.999%	BOC
Carbon Monoxide / Carbon Dioxide	99%	BOC
Ethane	>99%	BOC
Methanol	99.99%	Fisher Scientific
Ethanol	99.99%	Fisher Scientific
Methyl Acetate	99%	Alfa Aesar
Acetic Acid	100%	VWR
Acetone	99.5%	VWR

Dimethyl ether (DME)	99+%	Sigma Aldrich
Ethyl Acetate	99%	Sigma Aldrich
Acetaldehyde	99%	Alfa Aesar

Table 2-5 Materials

2.4.2 Labelled Materials

The following labelled materials were used:

Material	Purity	Supplier
Acetic acid d ₄	99.5atom% D	Sigma Aldrich
Acetic acid-1- ¹³ C	99atom% ¹³ C	Sigma Aldrich
Acetic acid-2- ¹³ C	99atom% ¹³ C	Sigma Aldrich

Table 2-6 Labelled materials

2.4.3 TGA Studies

Thermogravimetric analysis (TGA) was performed on the following materials:

Material	Purity	Supplier
Zinc acetate dihydrate	98%	Alfa Aesar
Zinc carbonate, basic	>58% zinc basis	Sigma Aldrich
Copper acetate hydrate	98%	Sigma Aldrich
Copper Carbonate	>95%	Sigma Aldrich

Magnesium acetate tetrahydrate	98%	Alfa Aesar
Magnesium carbonate, basic	>40% ZnO basis	Sigma Aldrich
Aluminium acetate basic hydrate	98%	Alfa Aesar

Table 2-7 Materials used for TGA analysis

2.5 Calculations

As the production of methanol from CO and H₂ or CO₂ and H₂ involves a reduction in the number of moles of gas, the apparent concentration of reactants and products measured by the GC would not be accurate. Therefore a tracer gas (N₂) was fed in to each experiment to allow easy calculation of the true concentration.

For example, a reduction in the number of moles of gas (due to methanol synthesis) resulted in a reduction of the flowrate exiting the reactor. This made the tracer gas (and every other species present) appear more concentrated than they actually were. To correct for this effect and to calculate the true concentrations, the concentrations for every species were multiplied by [N₂in]/[N₂out].

2.5.1 Conversion

$$\text{Conversion} = \left[\frac{(\text{moles CO/CO}_2 \text{ in}) - (\text{moles CO/CO}_2 \text{ out})}{\text{moles CO/CO}_2 \text{ in}} \right] \times 100$$

2.5.2 Mass Balances

$$\text{Carbon Balance} = (\text{moles carbon out} / \text{moles carbon in}) \times 100$$

$$\text{Oxygen Balance} = (\text{moles oxygen out} / \text{moles oxygen in}) \times 100$$

$$\text{Acid Balance} = (\text{moles of carbon from acid in products} / \text{moles of carbon in acid}) \times 100$$

2.5.3 Selectivity

MeOH selectivity = moles MeOH / total moles of products (including MeOH)

3 Results

3.1 Precious Metal Catalyst Testing

Initially, four precious metal catalysts were prepared according to the procedure laid out in section. The prepared catalysts were as follows:

- Pd/SiO₂
- Pd/Ca/SiO₂
- Ir/SiO₂
- Rh/SiO₂

As outlined in section 1.6, the aim of the project was to develop a catalyst that exhibited tolerance towards acetic acid / methyl acetate. Initial studies by BP indicated that precious metal catalysts might be suitable candidates for this application, due to their ability to withstand conventional poisons such as chlorine and sulphur [70, 71]. However as well as exhibiting tolerance, the catalysts were also required to be active for methanol synthesis. Therefore, prior to acid / ester tolerance studies, the catalysts were tested for their ability to synthesise methanol.

3.1.1 Characterisation

All catalysts were characterised using thermogravimetric analysis (TGA), X-ray diffraction (XRD) and Brunauer, Emmett, Teller (BET) analysis prior to catalytic testing.

3.1.1.1 Thermo-gravimetric Analysis (TGA)

The initial step was to determine the temperatures at which to calcine and activate the catalysts. Calcination is the process whereby the catalyst precursor is converted to the oxide by heating in air[26]. This was desirable as the ultimate goal was to reduce the precious metal precursor to the metallic phase.

Calcination

The rhodium acetate supported on silica catalyst was examined first. The graph showed that a small weight loss occurred around 58°C and a large sharp weight loss occurred at 276°C.

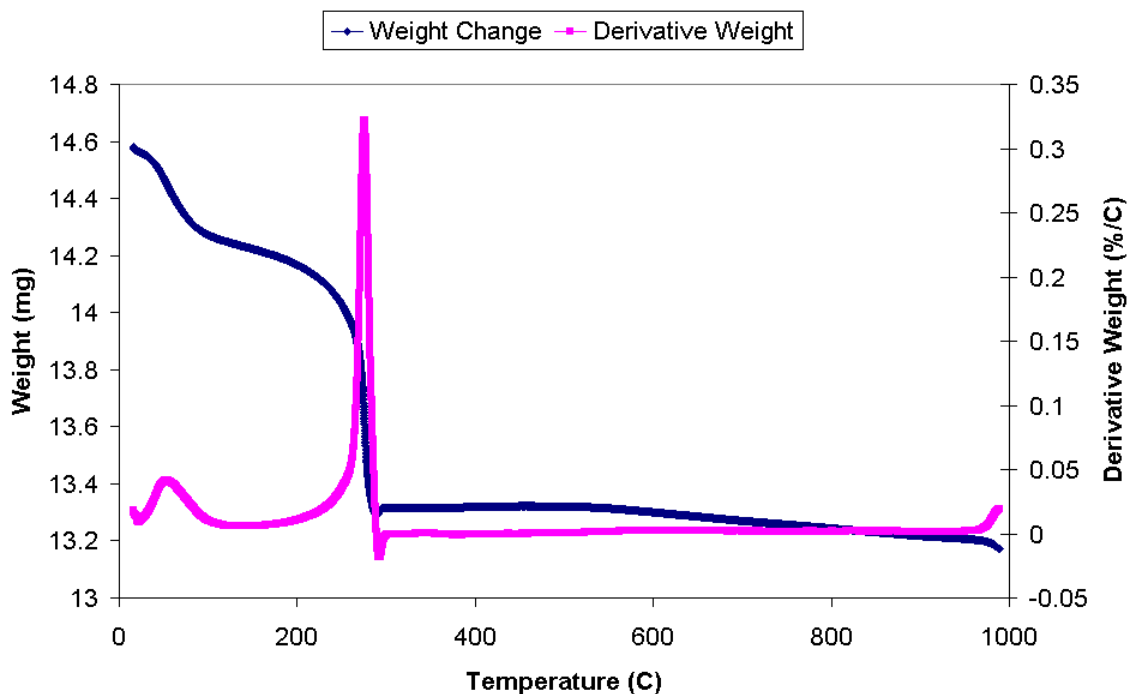


Figure 3-1 TGA analysis of rhodium acetate supported on silica under 2%O₂/Ar feed

Mass spectrometer results showed that the species evolved at 58°C corresponded to water, most likely physisorbed water on the catalyst surface. At 276°C there was a sharp evolution of CO₂, water and hydrogen. A DSC trace showed that the evolution was exothermic which suggested that the acetate precursor was breaking down to form the oxide. The decomposition of acetates is well known in the literature and studies by Bowker et al have shown that on oxidised surfaces, acetate groups break down auto-catalytically [95-97]. In their work investigating acetate species on Pd(110) and Rh(110) crystals, they observed a sharp decomposition similar to that observed here[95-97].

The iridium acetate supported on silica showed a similar profile to the rhodium catalyst, and was perhaps not surprising as iridium is in the same group as rhodium in the periodic table.

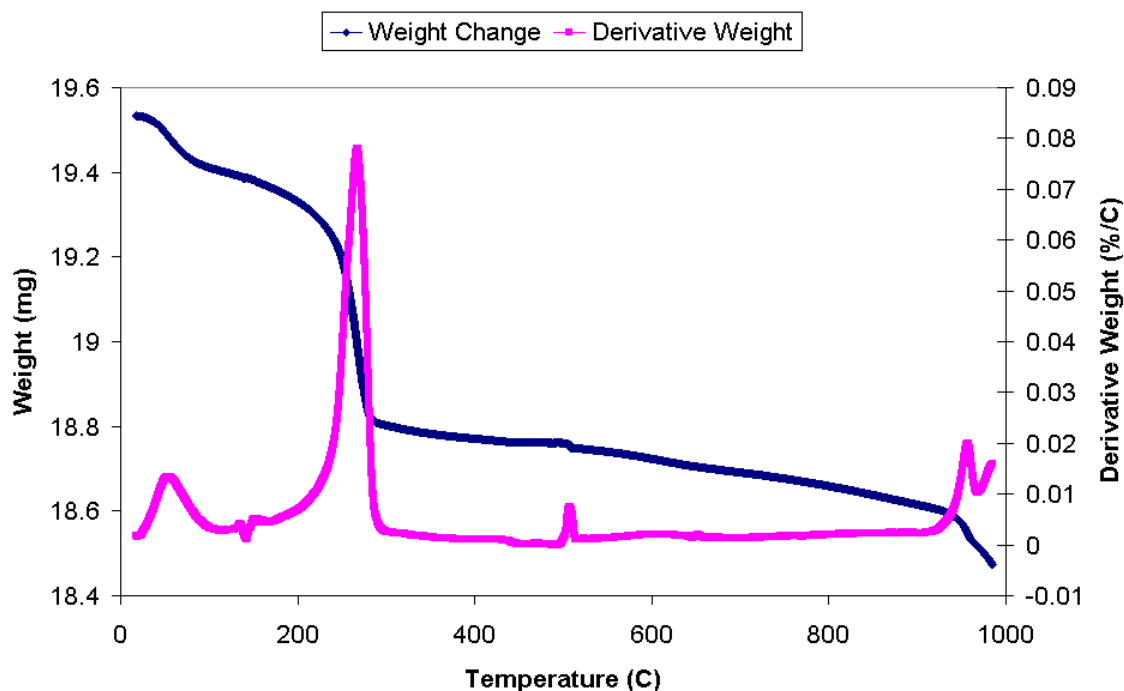


Figure 3-2 TGA analysis of iridium acetate supported on silica under 2%O₂/Ar feed

Two distinct weight loss events were observed, the first at 56°C which corresponded to the loss of physisorbed water. The second weight loss occurred at 268°C and corresponded to the evolution of CO₂, water and hydrogen. Like the previous catalyst, the evolution was exothermic and could therefore be attributed to the breakdown of the precursor acetate to form the metal oxide.

From the TGA studies, the conversion of the metal acetates to the metal oxides was shown to occur before 300°C. It was decided to calcine the catalysts at a slightly higher temperature to ensure complete conversion of the metal acetates to the metal oxide.

Calcinations of each catalyst took place inside a glass tube with glass wool plugs at both ends to prevent spillage of the catalyst. The tube was placed inside the calcination furnace and a peristaltic pump attached to the tube to push air through. The heating ramp was then started. Calcination conditions are tabulated below:

Ramp Rate ($^{\circ}\text{C min}^{-1}$)	Temperature ($^{\circ}\text{C}$)	Hold (mins)
3.0	350	180

Table 3-1 Conditions for the calcination of supported metal acetates

The calcination of the unpromoted palladium catalyst (fig 3-3) showed several features. The large evolution at $\sim 43^{\circ}\text{C}$ corresponded to water, most likely physisorbed on the catalyst surface. Several other evolutions took place at elevated temperatures, and it was unclear from the weight change profile if PdO was formed.

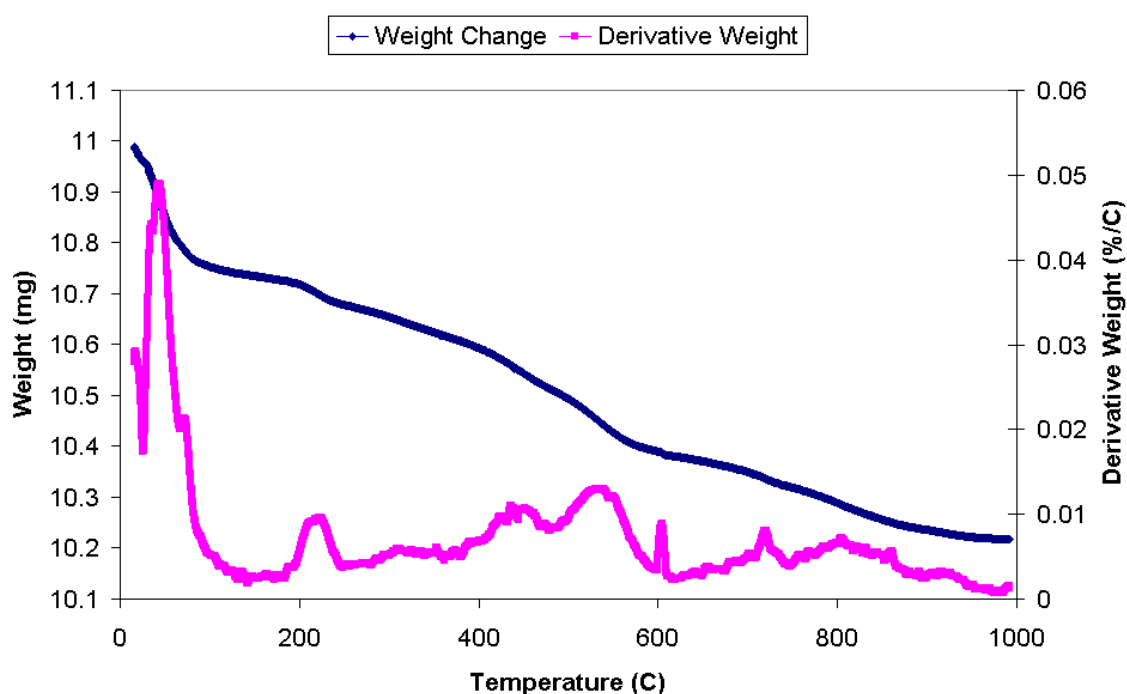


Figure 3-3 TGA analysis of palladium chloride supported on silica under 2%O₂/Ar feed

The Ca promoted Pd catalyst showed a similar profile, with physisorbed water being driven from the catalyst at a temperature of $\sim 49^{\circ}\text{C}$. Again it was unclear from the weight change profile if PdO was formed.

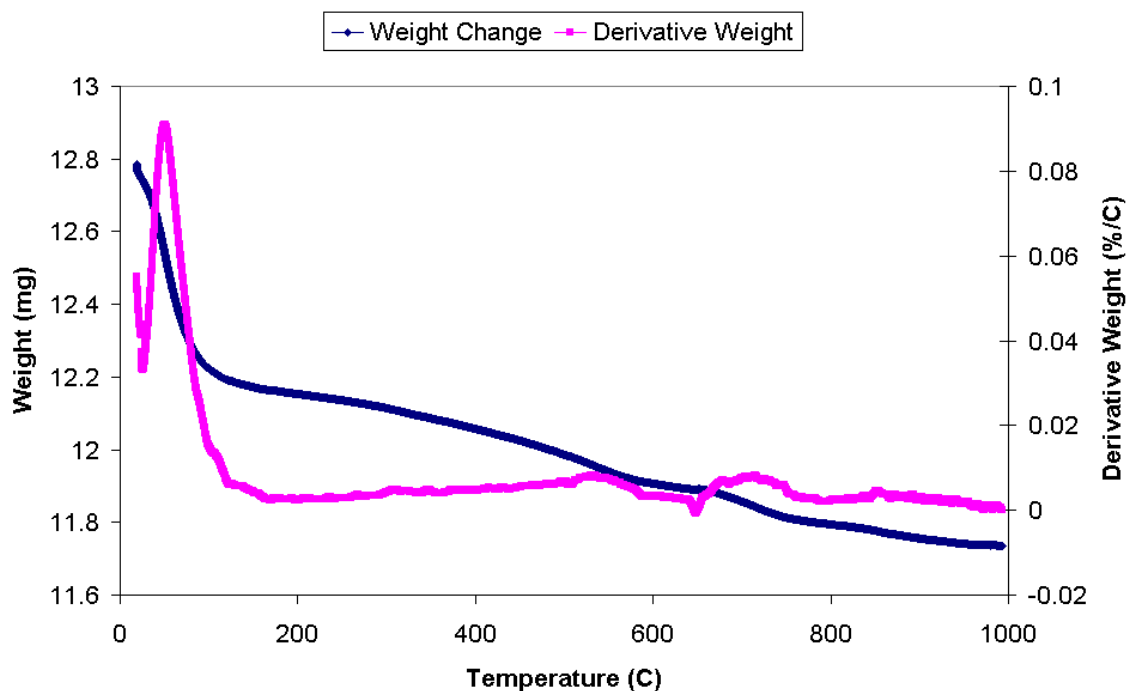


Figure 3-4 TGA analysis of calcium doped palladium chloride supported on silica under 2%O₂/Ar feed

As it was unclear from the TGA studies as to whether PdO was formed it was decided to calcine the Pd catalysts at a higher temperature than for the previous catalysts. The calcination procedure used for both Pd catalysts is shown below:

Ramp Rate (°C min ⁻¹)	Temperature (°C)	Hold (mins)
3.0	400	180

Table 3-2 Conditions for the calcination of supported palladium catalysts

Reduction

Once the catalysts were calcined, the next stage was to determine the temperature at which to activate the catalysts. This is the process whereby the metal oxide is reduced to the metal, which is considered the active phase[26].

The Rh₂O₃/SiO₂ catalyst was examined first. The results showed two weight loss events, and these occurred at 57°C and 195°C.

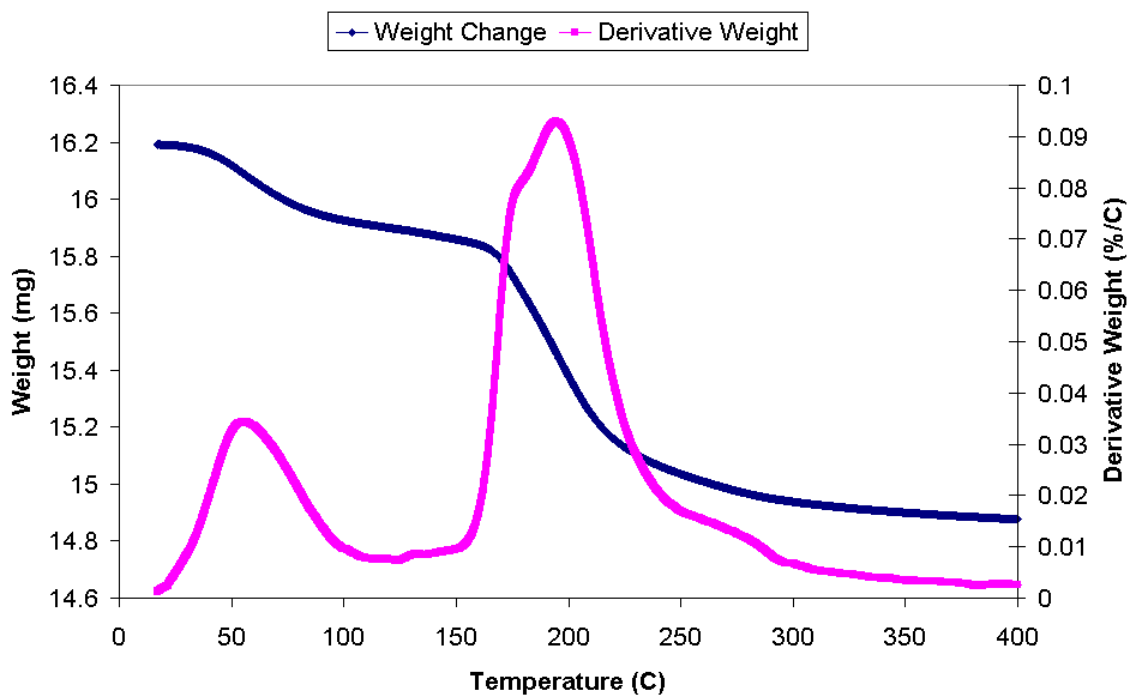
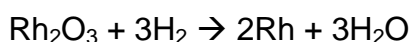


Figure 3-5 TGA analysis of rhodium oxide supported on silica under 5% H_2/N_2 feed

Mass spectrometry data showed that the weight loss at 57°C corresponded to the loss of water, most likely physisorbed on the catalyst surface. The weight loss at 195°C proceeded with the uptake of hydrogen and the loss of water. A small amount of CO_2 was also evolved, indicating that not all of the precursor acetate had been converted to the oxide during the calcination stage. The uptake of H_2 and release of H_2O however was most likely due to the reduction of the rhodium oxide to metallic rhodium:



The IrO_2/SiO_2 catalyst showed a similar trend to the rhodium catalyst, with two weight loss events taking place at 54°C and 191°C (fig 3-6).

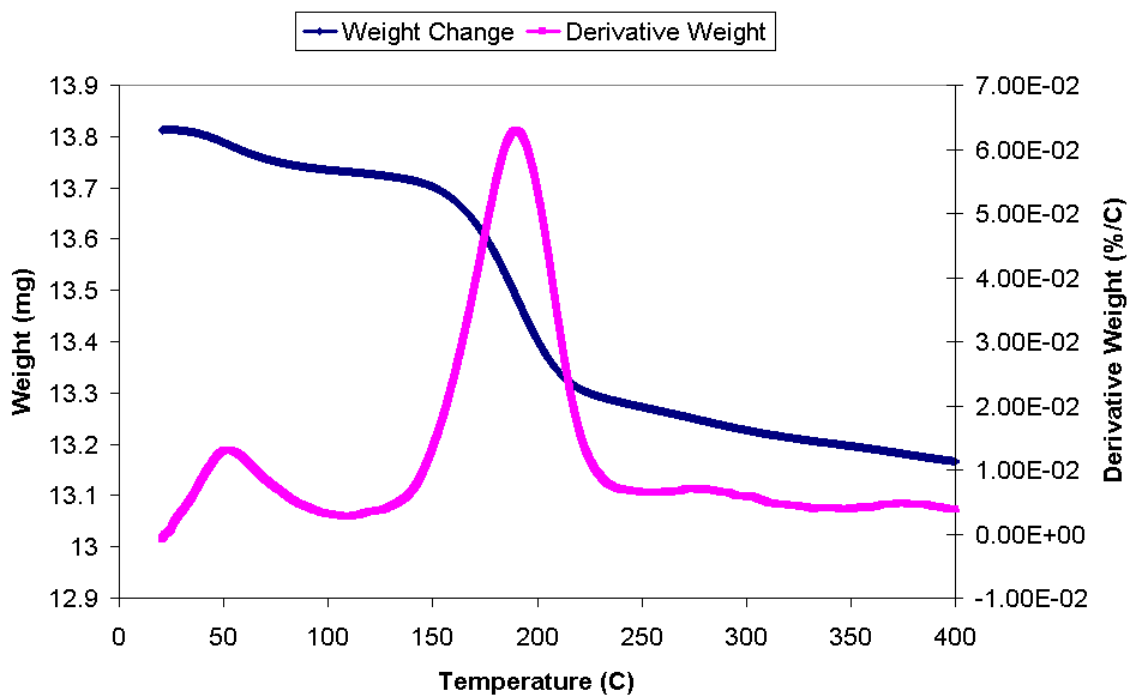


Figure 3-6 TGA analysis of iridium oxide supported on silica under 5% H_2/N_2 feed

Like the rhodium catalyst, the weight loss at 54°C corresponded to physisorbed water being evolved from the surface, while the weight loss at 191°C related to the uptake of H_2 and the evolution of H_2O and CO_2 . Again this suggested that not all the precursor acetate was converted to the metal oxide during the calcination.

The unpromoted palladium catalyst exhibited two distinct evolutions upon reduction:

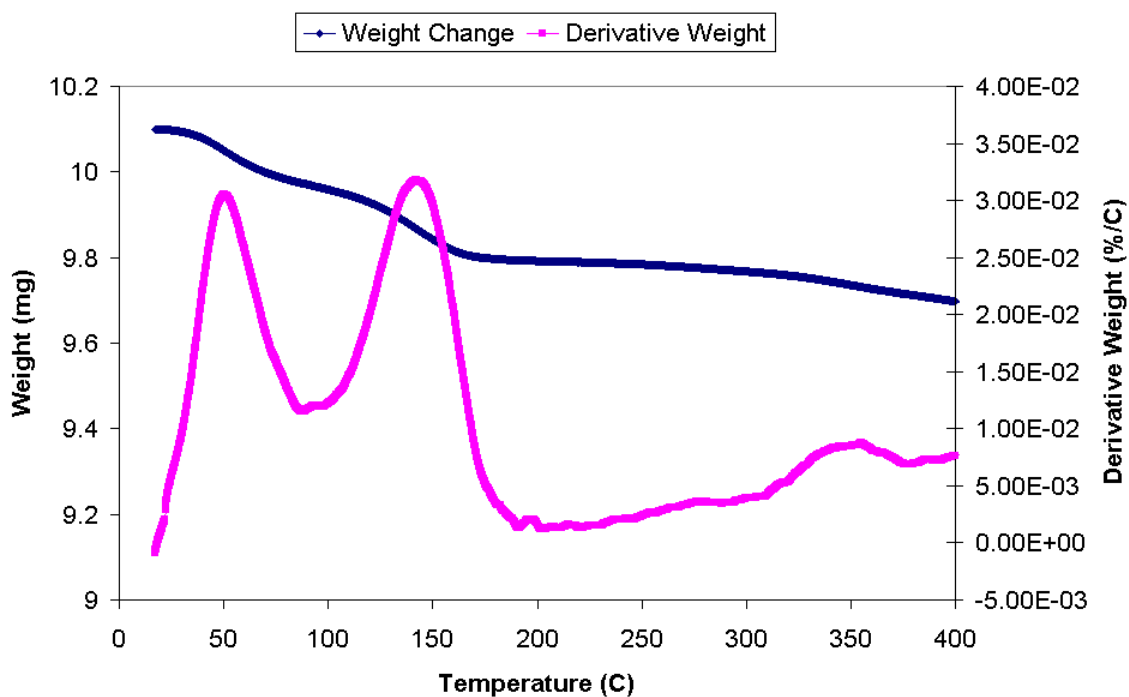


Figure 3-7 TGA analysis of palladium oxide supported on silica under 5% H_2/N_2 feed

The first evolution at 51°C corresponded to physically adsorbed water being driven from the catalyst. The second evolution, which occurred at 143°C was also attributed to water, but proceeded with the uptake of hydrogen. This suggested that it was possibly the reduction of PdO to Pd metal that was taking place.

Finally, the promoted palladium catalyst showed a similar trend to the unpromoted catalyst, with two evolutions of water detected.

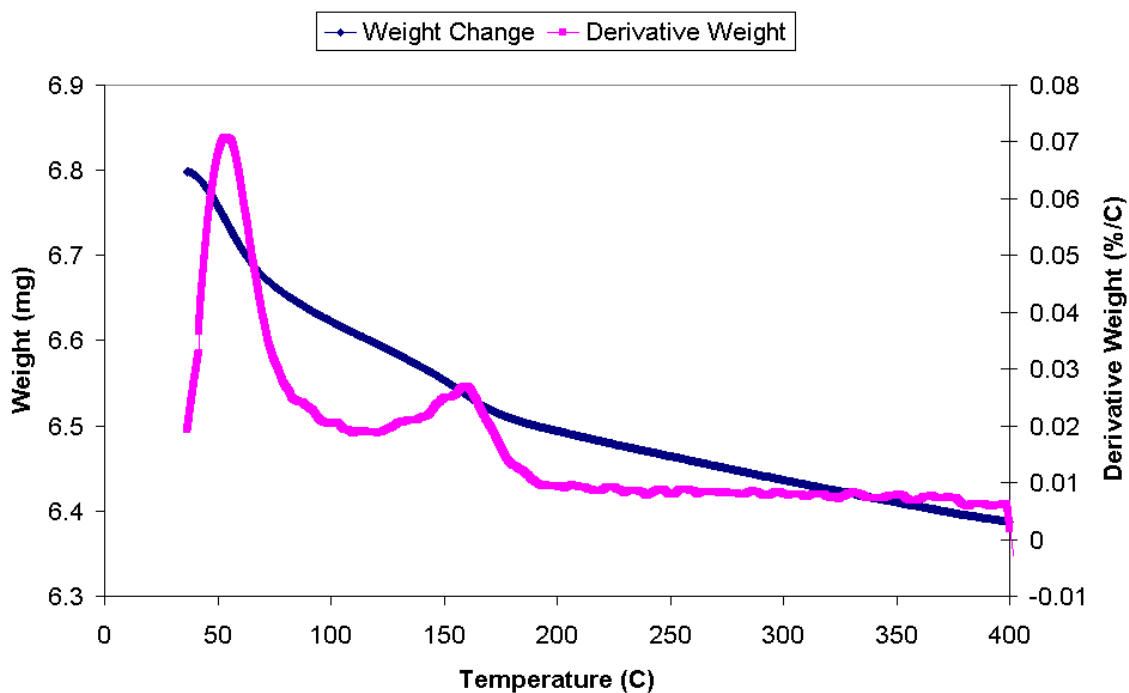


Figure 3-8 TGA analysis of calcium doped palladium oxide supported on silica under 5% H_2/N_2 feed

However, some differences were apparent. Firstly, there was approximately three times the amount of physisorbed water evolved from the promoted catalyst than for the unpromoted. Secondly, the reduction of the PdO to Pd metal was shifted to a higher temperature (161°C) compared with the unpromoted system (151°C). This indicated that the calcium promoter had exhibited a stabilising effect on the PdO. This was in agreement with research that indicated Pd⁺ is stabilised by the presence of an alkaline promoter[106].

After studying the data collected from the TGA analysis, it was decided that the catalysts would be reduced at a temperature of 250°C for 3hrs in the catalyst reactor under 50ml min⁻¹ flowing H₂. It was thought that the conditions would be suitable for the conversion of the metal oxides to the metallic species.

3.1.1.2 X-Ray Diffraction (XRD)

X-ray diffraction can provide information regarding a materials crystal structure, degree of crystallinity and crystallite size. Although unable to determine the complete active phase of a catalyst, XRD can be used to gain information about materials with long range order. It is particularly useful for characterising materials with well ordered structures such as zeolites[107, 108]. Although materials such as silica (the support for the catalysts) are amorphous, XRD can still be used to gain

information regarding the active species on the support if it exists in a crystalline phase.

Powder XRD was used to examine calcined and reduced catalysts to determine if any phase changes occurred upon reduction. Identification of the species present on the support was made by comparison with the Powder Diffraction Database[109]. The reduction of the samples took place inside the catalyst reactor using the conditions defined in the previous section.

Silica

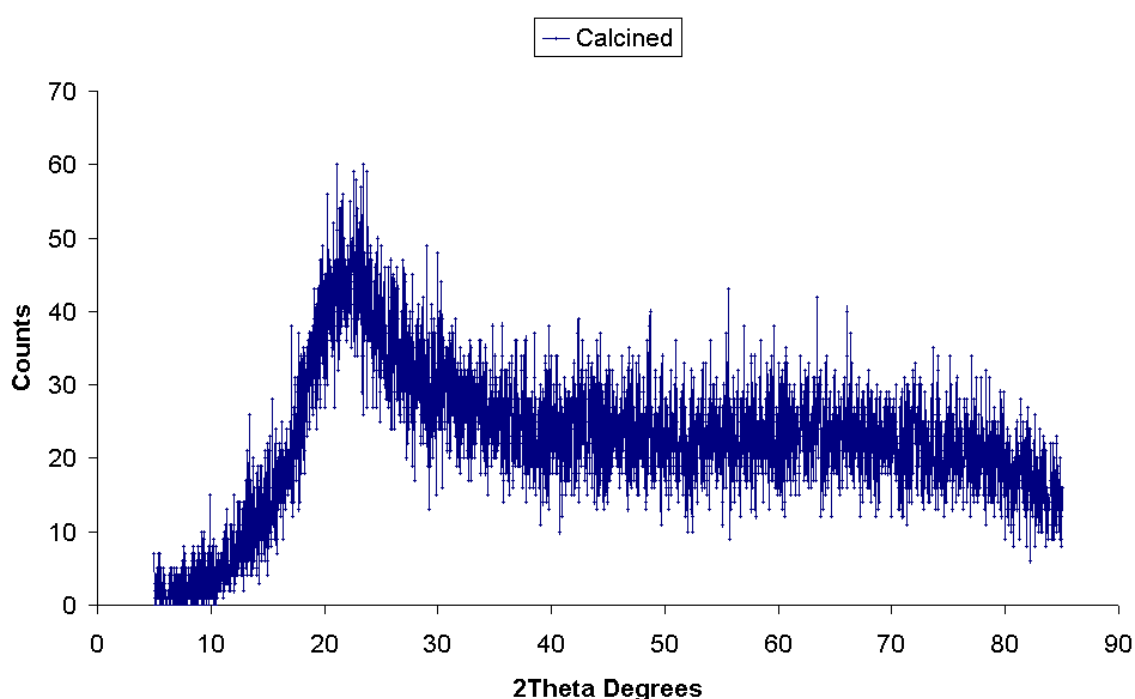


Figure 3-9 XRD pattern from calcined silica support

A sample of the silica support used in the preparation of the catalysts was also examined using XRD, so that any features due to metal species in the prepared catalysts could be easily identified. Prior to performing the XRD, the silica was calcined under the same conditions as used for the catalysts. The resulting XRD pattern showed only one feature, a broad band due to the amorphous nature of the silica.

Rhodium supported on silica

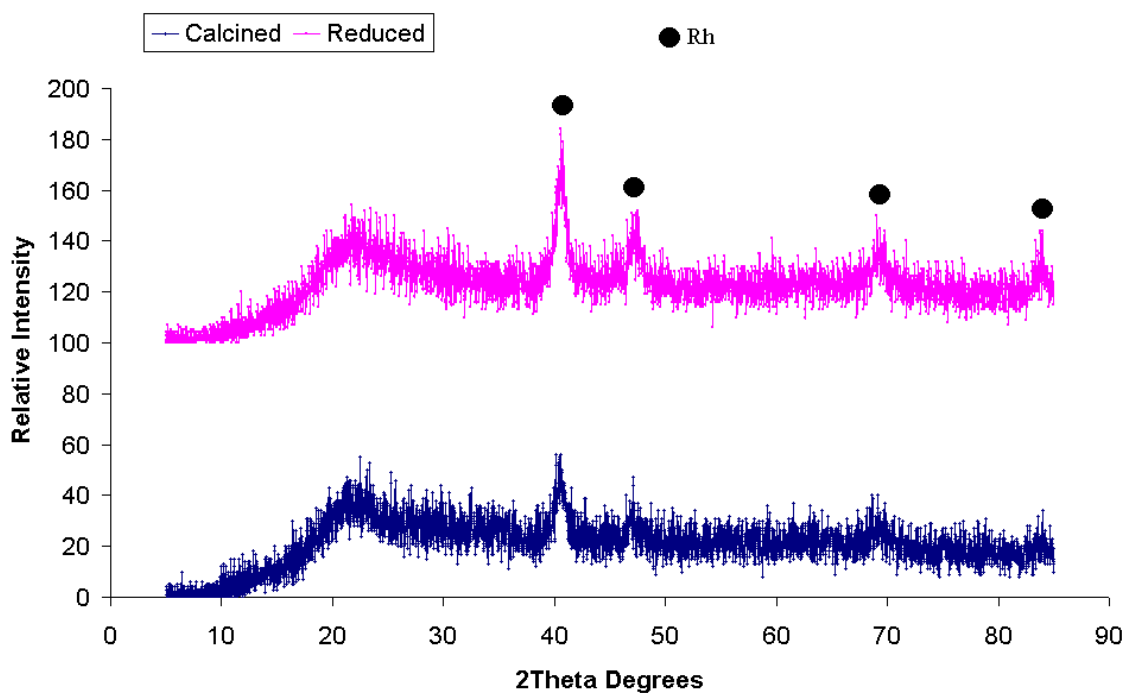


Figure 3-10 XRD patterns from calcined and reduced rhodium supported on silica

The XRD data showed several features for the calcined and the reduced samples. The features in both samples corresponded to rhodium metal, which was unusual for the calcined catalyst as the Rh_2O_3 spinel was expected to be formed during the calcination process. The XRD for the reduced sample showed sharper, more defined peaks than in the calcined sample, indicating an increase in crystallinity upon reduction, possibly due to sintering.

Iridium supported on silica

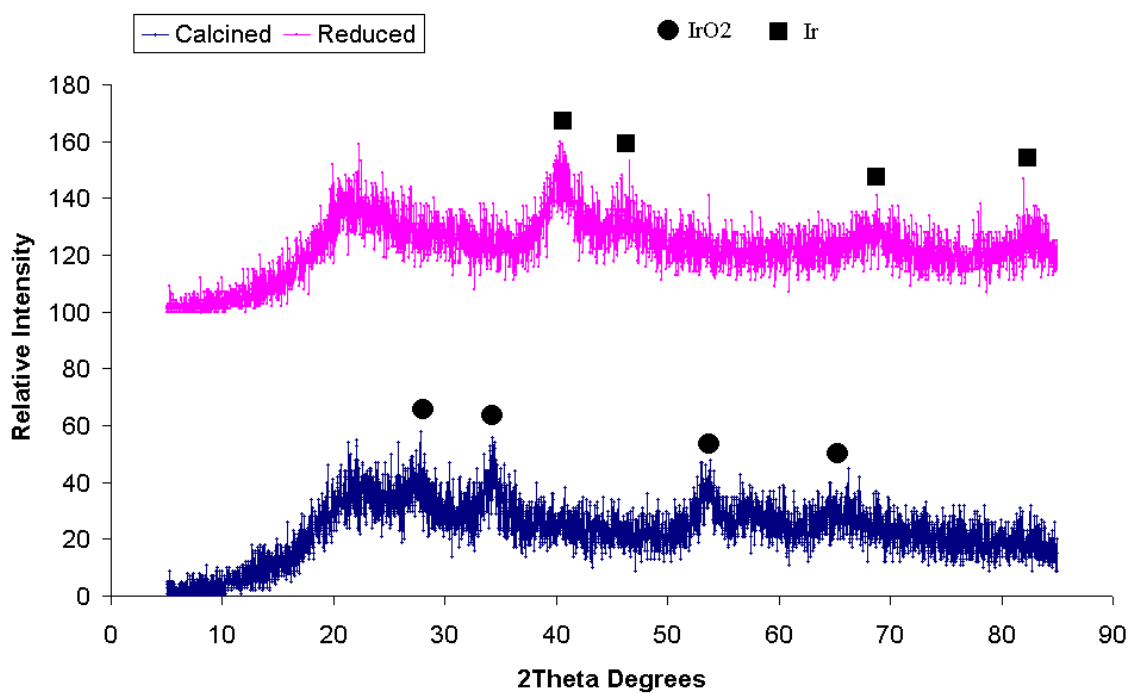


Figure 3-11 XRD patterns from calcined and reduced iridium supported on silica

The XRD pattern for the calcined catalyst was as expected, showing several features relating to the presence of oxidised iridium (IrO₂). Post reduction, these features disappeared, and new peaks relating to metallic iridium became apparent. No oxidised iridium features remained post reduction, indicating complete conversion of the oxidised iridium to the metallic form.

Palladium supported on silica

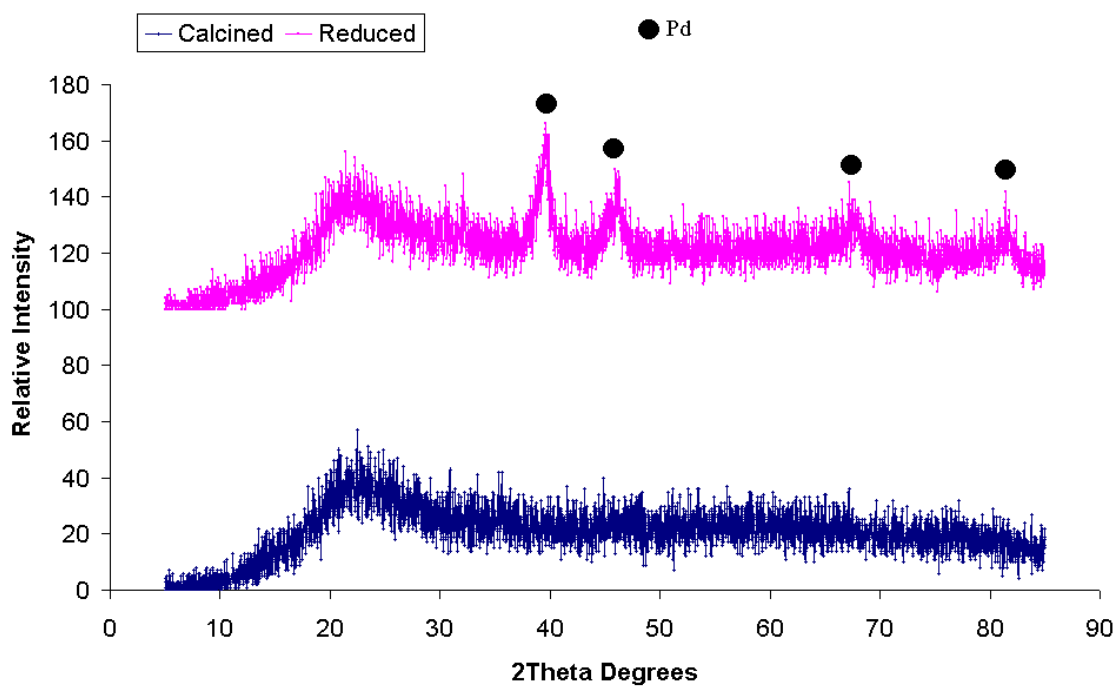


Figure 3-12 XRD patterns from calcined and reduced palladium supported on silica

Prior to reduction the XRD data showed no features due to the presence of palladium on the silica. The material was completely amorphous, with only a broad band due to the presence of silica apparent. Unlike for the iridium catalyst no features due to oxidised metal were visible, indicating that it was present in an amorphous state. Post reduction, several sharp features emerged which were attributed to the growth of palladium metal particles during the reduction.

Palladium doped with calcium supported on silica

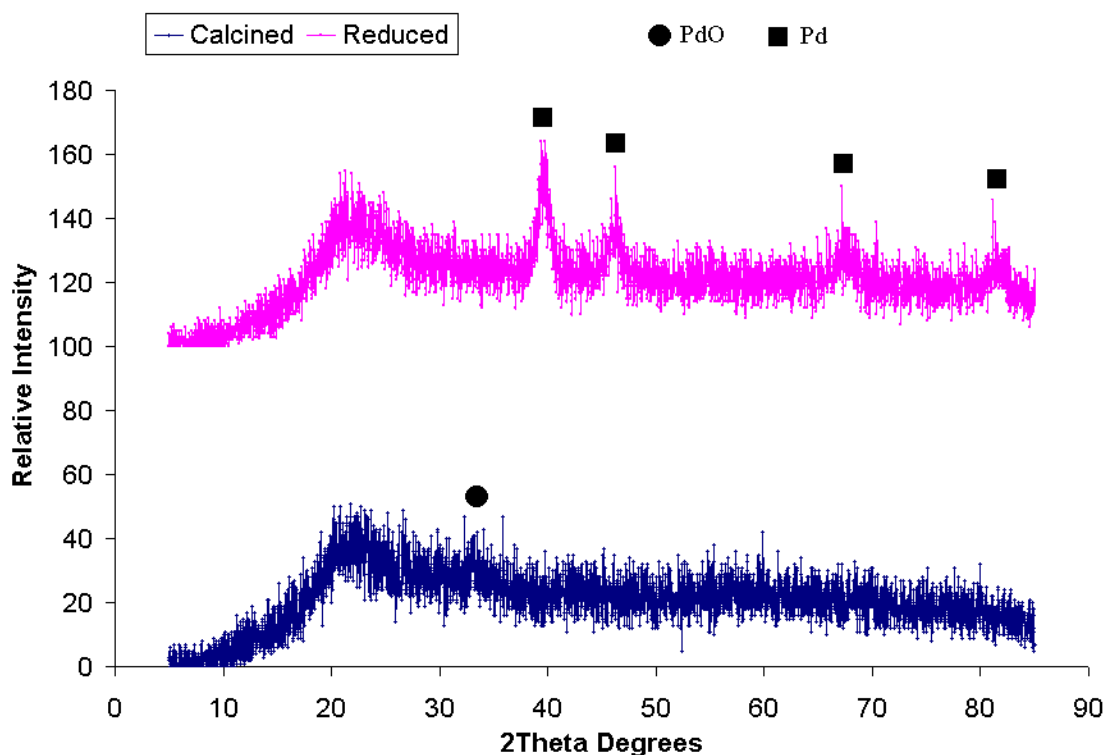


Figure 3-13 XRD patterns from calcined and reduced calcium doped palladium supported on silica

The XRD pattern of the calcined sample indicated an amorphous surface, similar to the pattern obtained for the previous Pd catalyst. However, a small feature was visible, and this was matched to PdO. Post reduction, this feature disappeared as peaks relating to Pd metal became visible. No features in either the calcined or reduced sample could be attributed to Ca species, indicating it was present in an amorphous state.

3.1.1.3 BET Analysis

Surface area analysis was performed on the catalysts after calcination but prior to activation (reduction). A sample of the silica support was also examined for comparison. The results are tabulated below:

Catalyst	Surface Area (m ² / g)	Pore Diameter (Å)
Rh ₂ O ₃ /SiO ₂	264	48
Ir ₂ O ₃ /SiO ₂	253	48
PdO/SiO ₂	268	63
PdO/CaO/SiO ₂	268	48
SiO ₂	282	123

Table 3-3 Surface area analysis of lab prepared catalysts

Results showed that generally upon addition of the metal oxide to the silica support both the surface area and the pore diameter decreased significantly.

3.1.2 Catalytic Testing

Although the primary aim of the project was to develop an acid tolerant catalyst, the catalyst also had to show reasonable activity for methanol production. To this end, the methanol synthesis activities of the catalysts were investigated using the following conditions:

- Reaction Temperature (K) 523
- Pressure (barg) 50
- Gas Flow (ml min⁻¹) 250
- Catalyst Volume (ml) 1.36
- GHSV (hr⁻¹) ~11,000

The feed gas composition employed was 10ml N₂/80ml CO/160ml H₂. This equated to a molar ratio of 1:2 CO:H₂. The nitrogen present in the feed was used as a reference for calculating conversion.

Prior to reaction, the catalysts were reduced *in situ* in the reactor under 50ml min⁻¹ flowing hydrogen at a temperature of 523K. The catalysts were held at this temperature for 3hrs.

3.1.2.1 Pd/SiO₂

Pd based catalysts have long been investigated as potential methanol synthesis catalysts. Since the early discovery by Poutsma et al in 1978 that Pd supported on silica could selectively produce methanol[72], substantial research has been undertaken to understand and improve the catalytic properties[70, 73, 76, 77, 81, 110]. In the present investigation, two Pd based catalysts were produced, both supported on silica. One of the catalysts was doped with a level of Ca, which has been reported to act as a promoter on these types of catalysts[77]. Both catalysts were tested catalytically, to determine how active the Pd metal was for the production of methanol and also to determine the effects of the promoter.

The un-promoted palladium based catalyst was investigated first for methanol synthesis activity.

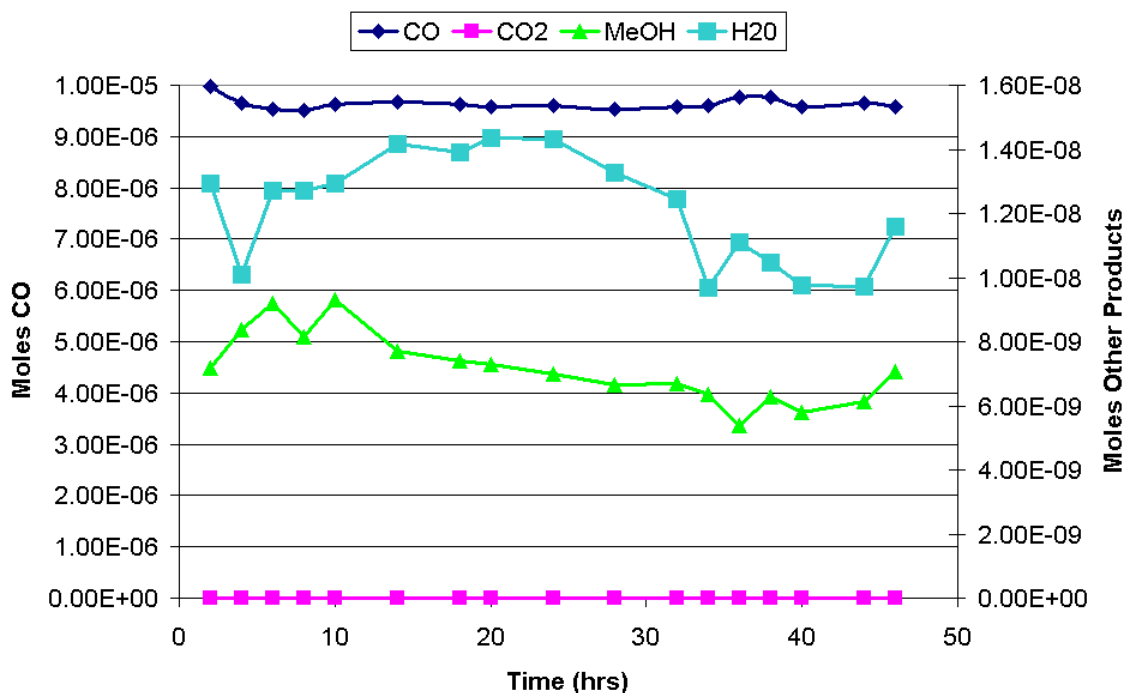
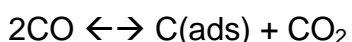


Figure 3-14 Reaction profile from CO hydrogenation over Pd/SiO₂ catalyst under CO/H₂ feed

Figure 3-14 showed that only two carbon based products were observed from the reaction – methanol and carbon dioxide. Methane was not observed as Pd is unable to adsorb CO dissociatively[77]. The carbon dioxide formed was most likely to be the result of water gas shift, as all the other components from the reaction were present (water, carbon monoxide and hydrogen) and the production of the dioxide was favourable at the reaction temperature employed. A Boudouard type reaction was also a possibility:



The reaction would produce surface carbon and CO₂. The carbon balance for the system remained reasonably high throughout the run (~97%), however the concentration of CO₂ produced was very small, and so a tiny amount of carbon laydown was possible. As only a small concentration of CO₂ was produced, consequently carbon selectivity towards methanol was very high (~95%). This was expected as various other researchers have reported that supported Pd can be very selective towards methanol [72, 74, 75, 79]

A reasonable concentration of water was observed in the system (larger than methanol) and was unexpected as stoichiometrically and mechanistically,

methanol is synthesised over precious metal catalysts without the production of water. Methanol is formed by stepwise hydrogenation of the CO[111]. This indicated that another reaction was possibly occurring in the system, however no other products were observed by the GC.

Although the catalyst was selective towards methanol, it was also required to be active. The yield of methanol produced was only 0.06%, therefore the activity of the catalyst was very low.

Low rate of reaction has become a characteristic of Pd based catalysts and has been reported many times in the literature [74, 80, 89]. Various methods for increasing the activity of the catalysts have been employed such as changing the support [76, 77] and increasing the dispersion of the palladium by altering the preparation method[79, 80]. Another technique used for increasing the activity is to add basic promoters such as calcium[77].

3.1.2.2 Pd/Ca/SiO₂

A Ca promoted Pd catalyst was tested next, to determine if the rate of reaction over the catalyst could be increased by the presence of a basic promoter. This technique has been demonstrated to be successful by several research groups [49, 77, 78]. It is thought that the basic metal is required to be next to, or on the Pd metal to be able to enhance the methanol synthesis activity[49, 78].

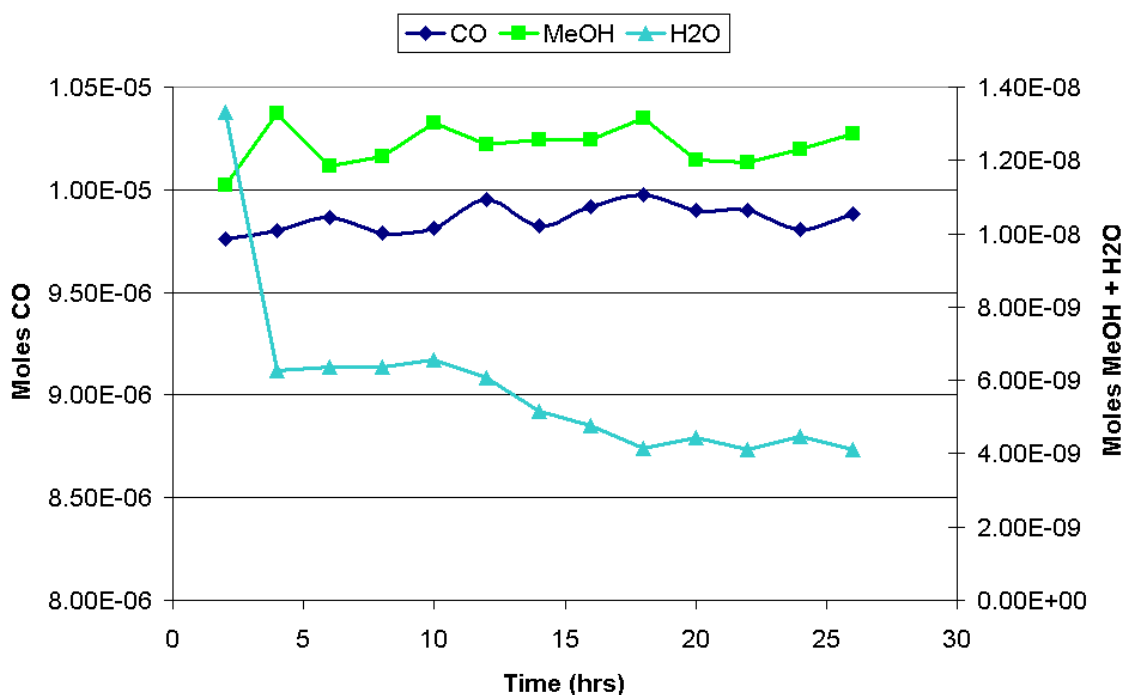


Figure 3-15 Reaction profile from CO hydrogenation over Pd/Ca/SiO₂ catalyst under CO/H₂ feed

Unlike the previous experiment, no CO₂ was detected in the system. Methanol was the only carbon based product, with some water also detected. Therefore the carbon selectivity towards methanol was extremely high (~99%), similar to the selectivity observed in the unpromoted system. Methanol production increased, with the yield almost double that of the previous system (~0.12%). The calcium promoter had the effect of doubling the activity of the catalyst without compromising on the selectivity towards methanol. However the activity of the catalyst was still very low.

As the methanol yields obtained from the catalytic testing of the Pd based catalysts were very low, it was unlikely that the catalysts activity could be enhanced enough to make them viable replacements for the commercial copper based methanol synthesis catalysts. To date, no Pd based catalyst has been commercialised for this application and the low rate of reaction is almost certainly the reason why. It was decided at this point to no longer investigate Pd based catalysts as potential replacements.

3.1.2.3 Ir/SiO₂

Iridium based catalysts, although deemed to be less active than Pd based catalysts, have not been extensively studied in the literature for methanol

synthesis. Poutsma et al first investigated iridium supported on silica in 1978 and their studies revealed that iridium was selective towards methanol[72]. However the metal was much less active than palladium. Very few studies have been performed using the metal since. To this end, an Ir/SiO₂ catalyst was investigated for its ability to synthesise methanol.

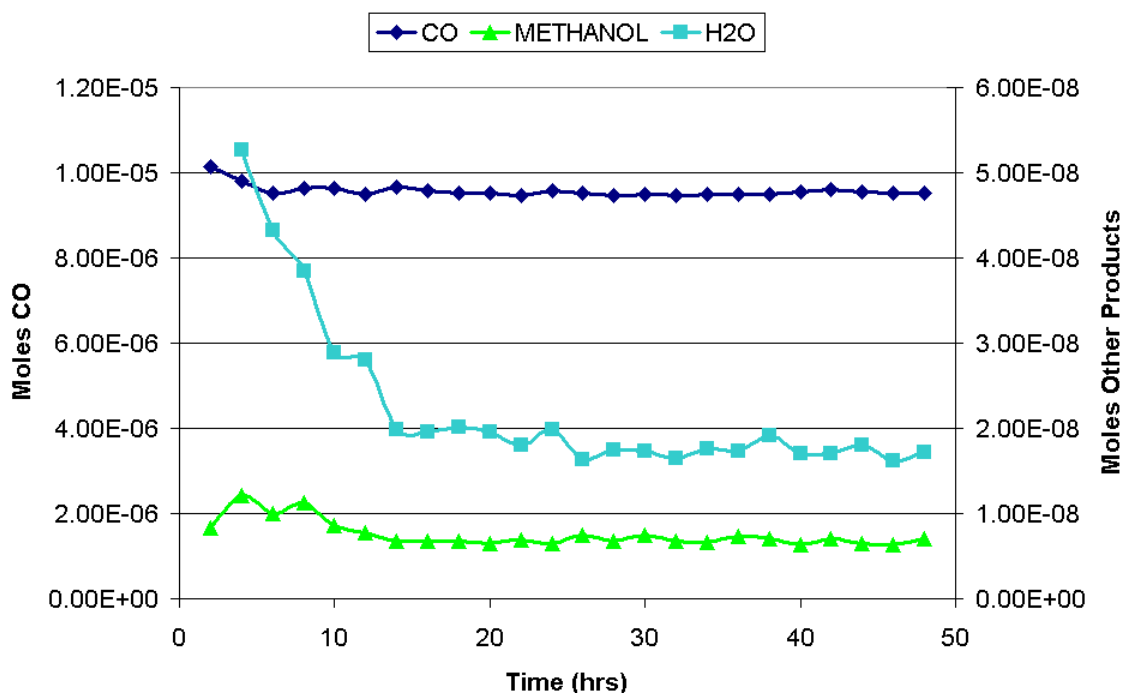


Figure 3-16 Reaction profile from CO hydrogenation over Ir/SiO₂ catalyst under CO/H₂ feed

Experimental results (fig 3-16) revealed that the catalyst was very selective towards methanol (~99%) with tiny traces of methane observed. Like the palladium systems, a reasonable amount of water was present, indicating that another reaction was possibly occurring. However no other products were detected by the GC.

The activity of the iridium catalyst was similar to the activity of the unpromoted palladium catalyst, with a methanol yield of ~0.07%. This result suggested that the iridium catalyst was more active than the Pd catalyst (based on no of moles of metal present on the catalyst), a result which was in direct conflict with Poutsma's results[72]. However, as the yields of methanol detected were so low, the experimental error in the system was consequently reasonably high.

Like the Pd based catalysts, the activity of the Ir catalyst was very low. It was therefore decided that an Ir based catalyst would also be unviable as a replacement methanol synthesis catalyst, and hence research into this application would not be pursued.

3.1.2.4 Rh/SiO₂

Rhodium has been shown to be a versatile metal for the hydrogenation of CO, having a weak ability to dissociate CO but nevertheless being able to synthesise higher alcohols, aldehydes and acids [82-86]. Its ability to catalyse the production of a wide range of products is related to its position in the periodic table, where it is located between metals which clearly dissociate CO (Fe, Co) and metals which do not (Pd).

The product distribution is dependant on the exact form of rhodium, and can be affected by factors such as the support used and promoters present[82, 85].

Therefore the catalyst can be “tuned” to produce the desired product. However one major disadvantage for industrial use is that impurities in the feed, poisons and sintering could dramatically affect the product distribution.

Although rhodium deposited on supports such as MgO have been shown to be active for methanol synthesis[88], it was decided to investigate Rh supported on a neutral support such as SiO₂ first, as a base experiment.

During the run, methane was the major product observed, with other carbon based products such as methanol and ethanol also obtained. This was consistent with the literature which suggested that rhodium supported on silica was active for methanation[86]. Over the course of the experiment the levels of each product dissipated.

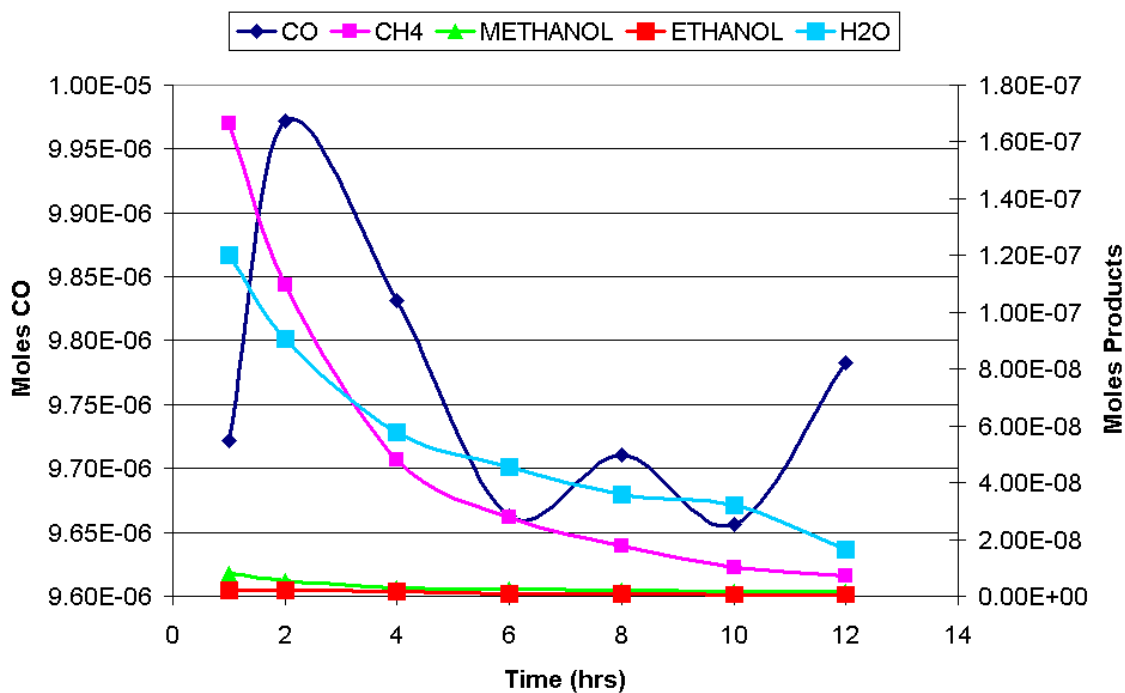


Figure 3-17 Reaction profile from CO hydrogenation over Rh/SiO₂ catalyst under CO/H₂ feed

The CO conversion over the catalyst was very low, around 2%. With methane and ethanol both produced, the carbon selectivity towards methanol was very low compared with the other precious metal catalysts investigated. Selectivity is a major problem with rhodium catalysts as small impurities, changes in morphology etc can change the product distribution markedly [82, 83, 86, 112].

Due to the problems with selectivity and activity, it was decided not to pursue rhodium based catalysts as a potential methanol synthesis catalyst.

3.1.2.5 Summary

It was clear from the results that Pd and Ir supported on silica could be very selective towards methanol, in agreement with the literature. However, the activity of the catalysts was very low and even in the presence of a promoter the methanol yield that was produced was only 0.12%. Although there was scope to improve the performance of the catalysts by varying the support, preparation technique, precursors etc it was decided instead to focus on studying the effects of acid / ester addition on the commercial catalyst instead, as it already displayed the necessary activity and selectivity required.

3.2 Commercial Catalyst Testing

The commercial methanol synthesis catalyst selected was Katalco 51-8, which is manufactured by Johnson Matthey and has the formulation Cu/ZnO/Al₂O₃/MgO. Prior to catalytic testing, the catalyst was characterised using TGA, X-ray diffraction (XRD) and BET.

3.2.1 Characterisation

3.2.1.1 Thermo-gravimetric Analysis

As the commercial catalyst was sold pre-calcined, all that remained was to activate the catalyst. To investigate the temperature that this should occur at, a temperature programmed reduction was performed using the TGA-DSC connected to a mass spectrometer.

The results showed three major weight loss events at 286°C, 367°C and 921°C. The first two evolutions consisted of water and carbon dioxide.

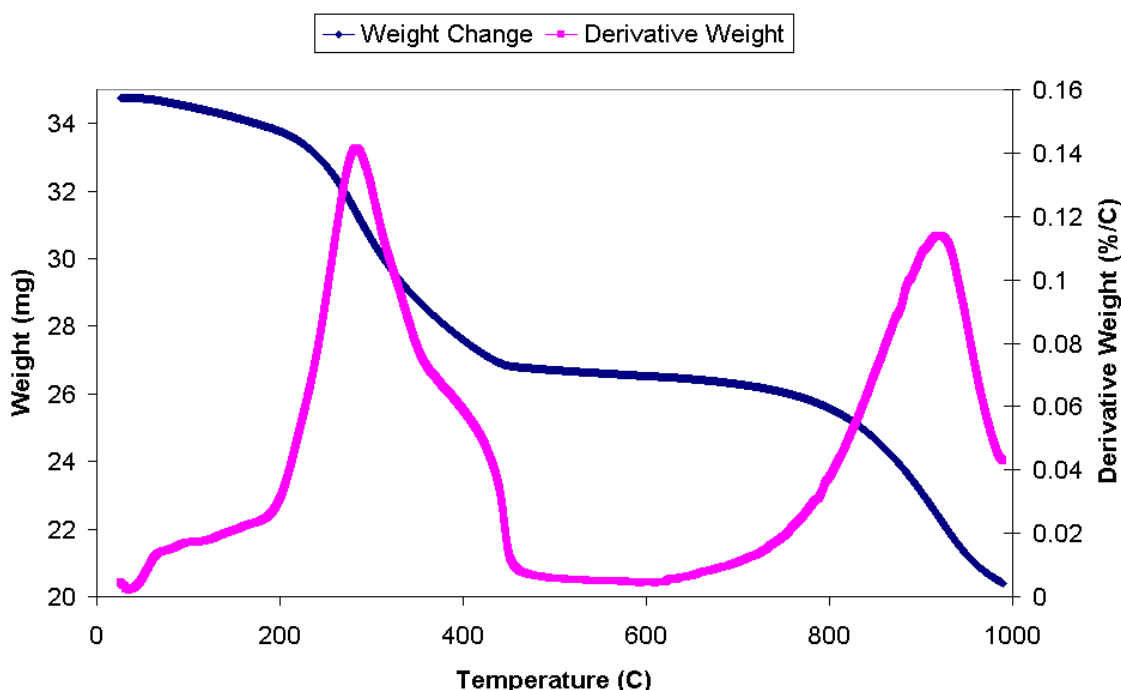


Figure 3-18 TGA analysis of Katalco 51-8 catalyst under 5%H₂/N₂ feed

As the catalyst was pre-calcined, it was likely that the overlapping evolutions corresponded to the reduction of CuO to copper metal, and also the evolution of adsorbed CO₂ from the catalyst. As zinc oxide is amphoteric, it would be likely that any CO₂ adsorbed from the atmosphere would be held there. The reduction of all

the CuO present to copper metal alone would result in the sample weight dropping to 29.92mg. The copper metal produced is the active phase of the catalyst.

The high temperature weight loss could be ignored as the catalyst would only be operated at 250°C.

It was decided from the TGA studies that the catalyst would be reduced at a temperature of 250°C for 3hrs, to ensure the reduction of copper oxide to copper metal.

3.2.1.2 X-Ray Diffraction (XRD)

The Katalco 51-8 catalyst was examined using hot stage XRD operating with a feed gas of 5% H₂/N₂, to determine the phases present.

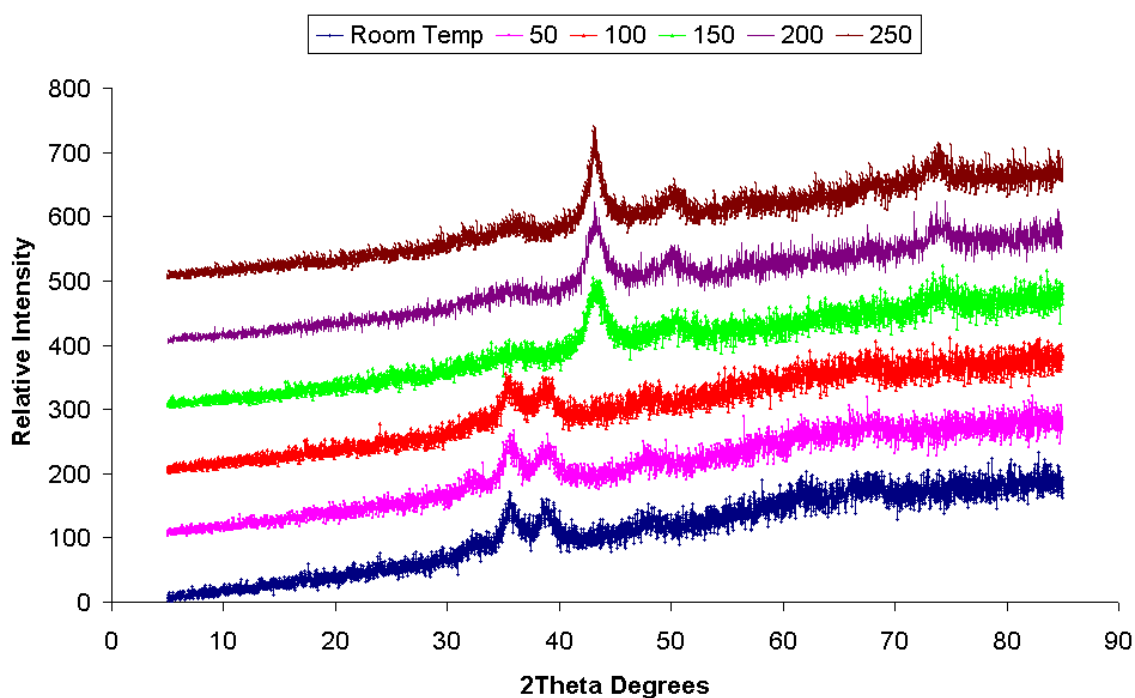


Figure 3-19 XRD patterns of Katalco 51-8 catalyst at various temperatures under a 5%H₂/N₂ feed

At room temperature the XRD pattern showed features relating to the presence of copper oxide (CuO). No peaks were apparent for the presence of the other components of the catalyst, such as ZnO, MgO or Al₂O₃. This indicated that these components were amorphous in nature. At 150°C the pattern shifted and the new

phase that was present was copper metal, with small peaks relating to copper oxide still remaining. Although at 250°C the copper oxide phase was still present, in the hot stage XRD the partial pressure of hydrogen was 5%, whereas in the *in situ* reduction prior to catalytic testing, the partial pressure was 100%. It was therefore probable that the copper oxide phase would not be present after the reduction prior to catalytic testing.

3.2.1.3 BET Analysis

Catalyst	Surface Area (m ² / g)	Pore Diameter (Å)
Katalco 51-8	89	37

Table 3-4 Surface area analysis of Katalco 51-8 catalyst

The surface area and pore diameter of the Katalco catalyst was significantly lower than for the lab prepared catalysts.

3.2.2 Catalytic Testing

Although the Katalco 51-8 catalyst is used industrially under a CO/CO₂/H₂ feed (1:1:8 molar ratio), studies have shown that the copper based catalysts can also synthesise methanol from a gas feed of CO/H₂. It was therefore decided to investigate both systems for their methanol synthesis activity.

Prior to reaction, the catalyst was reduced *in situ* in the reactor under 50ml min⁻¹ flowing hydrogen at a temperature of 523K. The catalyst was held at this temperature for 3hrs.

For the catalytic testing, the following conditions were used:

- Reaction Temperature (K) 523
- Pressure (barg) 50
- Gas Flow (ml min⁻¹) 250
- Catalyst Volume (ml) 1.36

- GHSV (hr^{-1}) $\sim 11,000$

The feed gas composition employed for the CO/H_2 reaction was 10ml N_2 / 80ml CO / 160ml H_2 . This equated to a molar ratio of 1:2 $\text{CO}:\text{H}_2$. For the $\text{CO}/\text{CO}_2/\text{H}_2$ reaction, a gas feed of 10ml N_2 / 25ml CO / 25ml CO_2 / 160ml H_2 was employed. This equated to a 1:1:8 molar ratio of $\text{CO}:\text{CO}_2:\text{H}_2$, which is the gas mix used industrially for methanol synthesis. The nitrogen present in the feed was used as a reference for calculating conversion.

3.2.2.1 CO/H_2 Feedstream

The synthesis of methanol from CO/H_2 over Cu based catalysts has long been a subject of controversy. It was unclear from the literature as to whether methanol could be synthesised from CO when there was no CO_2 present in the feed. For example Kagans work on SNM-1 (a soviet $\text{Cu}/\text{ZnO}/\text{Al}_2\text{O}_3$ catalyst) yielded no methanol from a feed of CO/H_2 and this result was attributed to the feed gases being carefully scrubbed of water (which would produce CO_2 via water gas shift)[18, 19]. However other researchers have obtained sizeable yields of methanol when CO is the only carbon oxide in the feed [13, 42, 113]. The variation in the literature is probably due to the variable nature of the catalysts. Often slight variations in catalyst preparation can result in an altering of the catalytic properties. For this reason it was therefore unclear prior to the experiment how the Katalco 51-8 would react under a CO/H_2 feed.

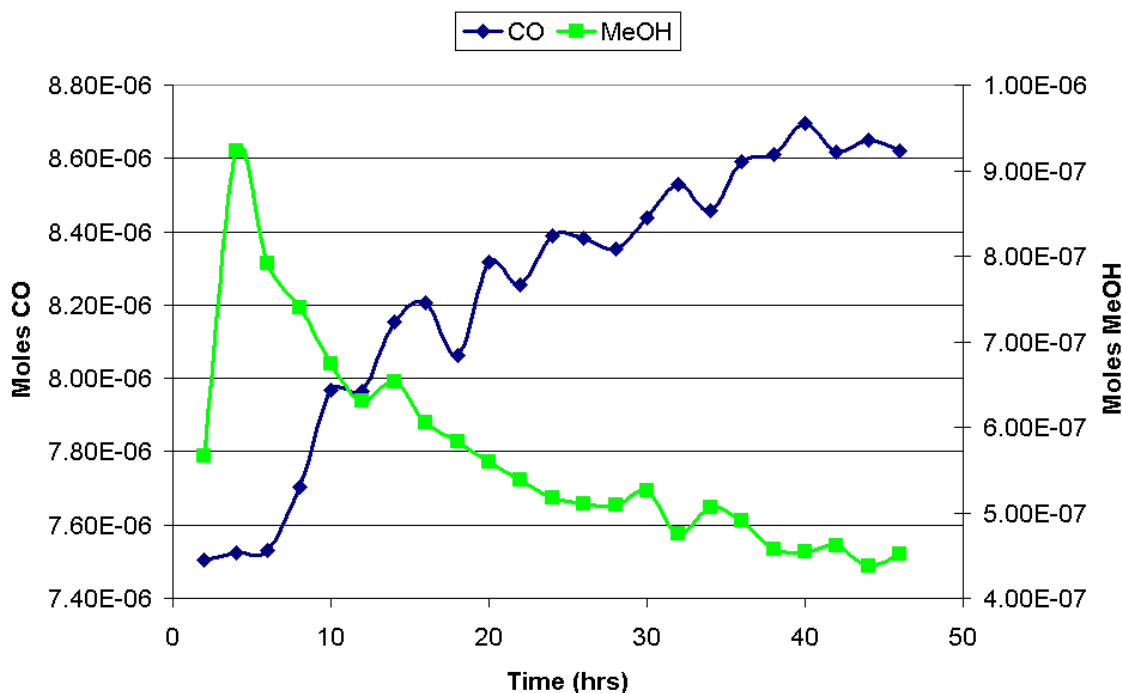


Figure 3-20 Reaction profile from methanol synthesis over Katalco 51-8 under a CO/H₂ feed

The results showed that methanol could be produced over a Katalco 51-8 catalyst under a CO/H₂ feed. The catalyst was selective towards methanol (99%), with minor traces of water, ethanol and dimethyl ether (DME) present. The production of DME was a result of a condensation reaction between two methanol molecules, most likely catalysed by the acidic Al₂O₃.

Although the yield of methanol initially was reasonable (~9%), the levels decayed over time and after 40hrs the yield had decreased by half to ~4.5%. The CO levels followed the opposite trend, as less methanol was produced the CO levels increased. This deactivation behaviour has been observed by other researchers [37, 112, 114]. Irreversible deactivation was observed when a Cu/ZnO catalyst was operated in a CO/H₂ feed without CO₂ or H₂O and was interpreted to be due to reduction of Cu⁺¹ from the ZnO matrix[37, 115]. Other explanations that have been suggested were the evaporation of Zn or the formation of brass (Cu_nZn). Rapid formation of brass has been observed in methanol synthesis catalysts using CO/H₂ mixtures above 570K, leading to rapid deactivation[114]. In all cases, the deactivation of the catalyst was attributed to the highly reducing nature of the feed gas.

Another possibility for the decreasing methanol yield could also be due to the methanol synthesis mechanism. Many researchers believe that over copper catalysts the hydrogenation of CO does not occur, due to the inability to isolate intermediates species for the reaction. The hydrogenation of CO₂ however over copper surfaces has been well documented [17-19, 116]. It has therefore been postulated that under CO/H₂ feeds, the mechanism taking place is that a CO picks up surface oxygen to form CO₂ before hydrogenation occurs. If the predicted mechanism is correct, then a level of adsorbed oxygen is required on the catalyst surface for the production of methanol to proceed. Under the highly reducing atmosphere of CO/H₂ it was possible that the surface oxygen concentration was slowly being depleted and therefore preventing methanol synthesis. Like the previous possibilities for deactivation, the reducing nature of the feed gas could be the cause.

The carbon and oxygen balances of the system (fig 3-21) showed an increase as the reaction proceeded, indicating that initially, surface saturation of CO and/or carbon laydown occurred.

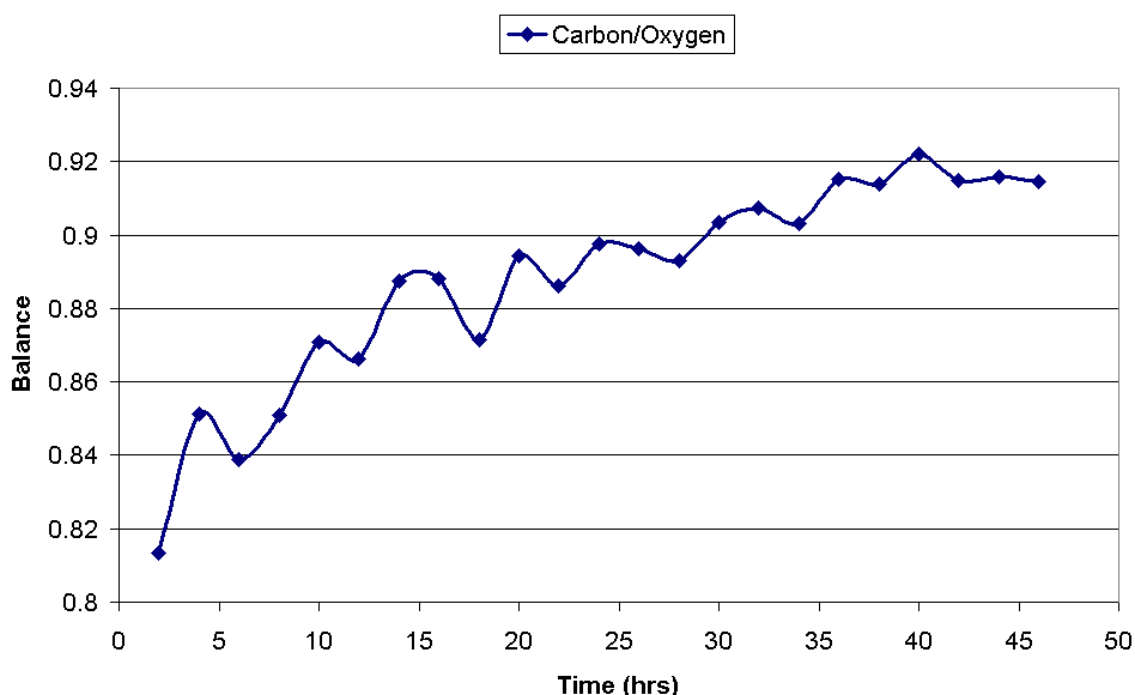


Figure 3-21 Mass balance from methanol synthesis over Katalco 51-8 under a CO/H₂ feed

To determine as to whether carbon laydown had occurred on the surface of the catalyst, a temperature programmed oxidation (TPO) was performed on a sample

of the post reaction catalyst. Any carbonaceous species deposited on the surface of the catalyst would be removed in the form of CO_2 .

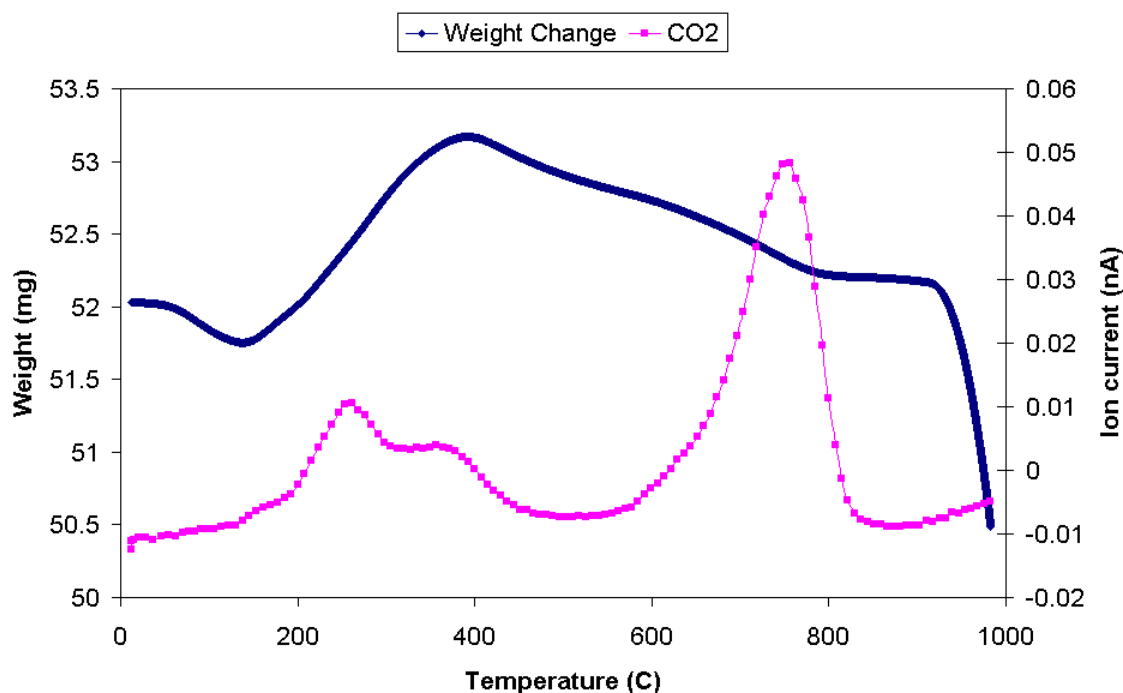


Figure 3-22 Post reaction TPO of Katalco 51-8 catalyst after CO/H_2 run

The graph shows that carbon was present on the catalyst surface in three distinct deposits. Two low temperature evolutions of CO_2 were observed at 261°C and 356°C, and a high temperature evolution at 755°C. It was probable that the low temperature deposits could be due to formate groups on the surface of the catalyst (formate being the longest lived methanol intermediate) or other methanol precursor species, although carbon laydown was also a possibility. A DSC trace showed that the evolutions were exothermic, confirming that burn off of carbonaceous species was likely. The high temperature evolution was most likely to be the decomposition of metal carbonates formed during the reaction. The formation of carbonates on oxide supported metal catalysts upon exposure to CO or CO_2 is a well known effect that can be monitored by infrared spectroscopy or temperature programmed methods[117]. The carbonate species are characterised by their relatively high decomposition temperatures.

An unusual feature of the temperature programmed oxidation was that there was a significant weight increase upon exposure to the 2% O_2/Ar gas. This was most likely due to the high levels of copper oxide that were present in the catalyst prior

to reaction. Upon reduction of the catalyst and under the CO/H₂ feed employed during the experiment, the copper oxide will have been reduced to metallic copper. Upon performing the TPO the copper in the catalyst re-oxidised to copper oxide. The weight increase in the sample indicates that only ~15% of the copper was re-oxidised. However prior to the TPO being performed the catalyst was exposed to air upon opening of the reactor lid and therefore its probable that the majority of the copper had been oxidised during this instance.

3.2.2.2 CO/CO₂/H₂ Atmosphere

Industrially methanol synthesis is not performed using a stoichiometric amount of CO and H₂, but rather a mixture of CO, CO₂ and H₂. Although a mixture of CO and H₂ would produce the highest equilibrium yield in principle, there are a number of reasons why the presence of CO₂ in the feed is beneficial for methanol synthesis. Kinetically CO₂ hydrogenation to methanol is much faster than CO hydrogenation so therefore a concentration of CO₂ in the feed is desirable[113]. Another reason is that it is possible that CO hydrogenation over copper catalysts actually does not occur, only CO₂ hydrogenation [18, 19, 116]. Finally, under a CO/H₂ feed, slow deactivation has been shown to take place, both in the literature and in the previous experiment. However, CO₂ can not be used solely as the carbon feed as this would result in a high concentration of water in the system, produced through the water gas shift. Water has been shown by various researchers to be detrimental to the methanol synthesis activity of the copper catalysts, both by competitive adsorption and by sintering the catalyst[38]. Therefore the presence of CO in the system helps to minimise water formation through the water gas shift reaction by suppressing the reverse reaction.

Using a classic methanol synthesis gas feed of CO/CO₂/H₂ in a 1:1:8 molar ratio, the catalyst performed very well as expected. Fig

Figure 3-23 revealed a steady level of methanol was produced (~10% yield), with no sign of the methanol decay that was observed in the CO/H₂ system. This suggested that the oxidation provided by the presence of CO₂ was enough to prevent deactivation of the catalyst.

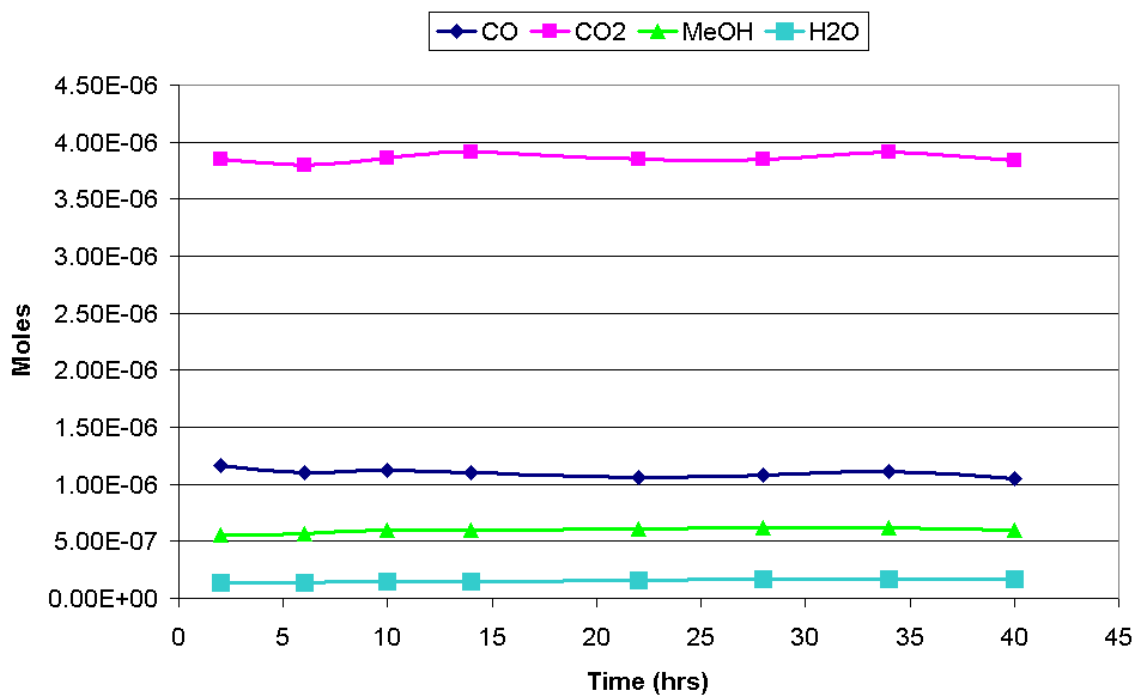


Figure 3-23 Reaction profile from methanol synthesis over Katalco 51-8 under a CO/CO₂/H₂ feed

As mentioned earlier, the presence of CO₂ in the feed also results in the formation of water through the water gas shift reaction, and this was observed during the experiment. Water was the only other product apart from methanol, with only tiny traces of ethanol detected as well. All the components in the system were observed at steady levels over the course of the reaction, indicating that the system had attained equilibrium.

Both the carbon and oxygen balances throughout the reaction showed consistent levels, with the carbon balance showing around 90% of the carbon in the system accounted for.

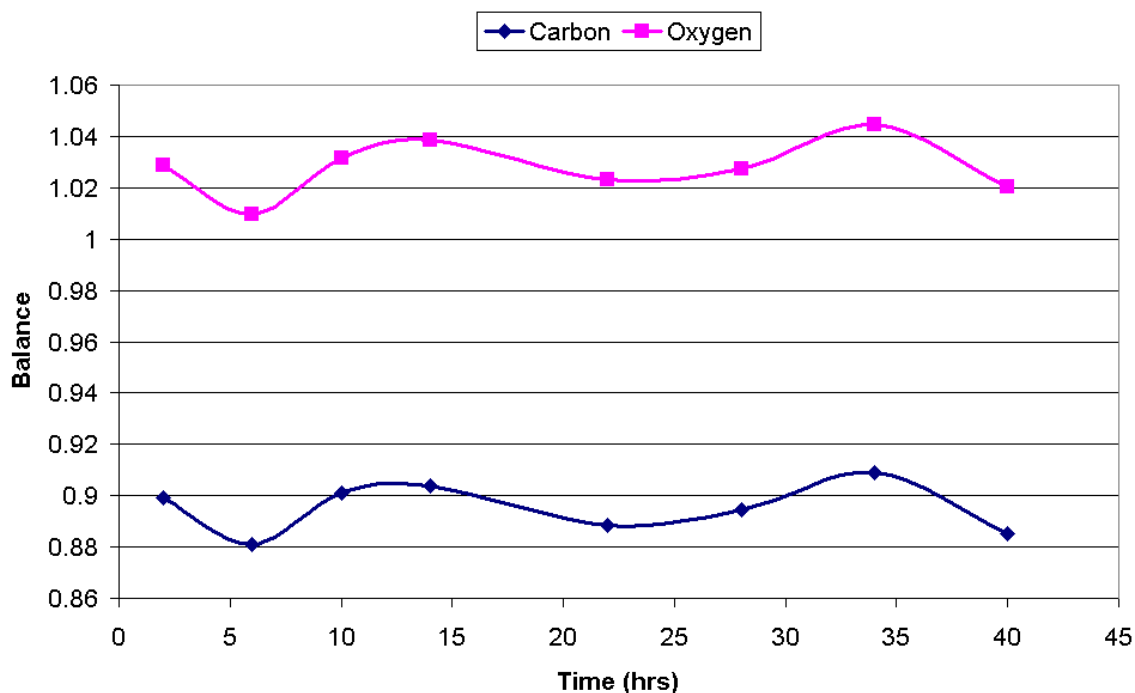


Figure 3-24 Mass balances from methanol synthesis over Katalco 51-8 under a CO/CO₂/H₂ feed

This was in complete contrast to the CO/H₂ system, where the carbon balance was initially low and increased over time. As in both reactions the same volume of catalyst had been used, this suggested that in the CO/H₂ system it was carbon laydown that occurred initially, rather than surface saturation.

A post reaction TPO of the catalyst showed a very similar profile to the one observed for the CO/H₂ run, with low temperature evolutions of CO₂ observed. Like for the previous CO/H₂ run, the evolutions were exothermic in nature and suggested that burn off of carbonaceous species was likely. A high temperature evolution was present as well and was thought to be the decomposition of metal carbonates formed during the run.

3.2.2.3 Summary

The commercial catalyst Katalco 51-8 was able to selectively synthesise methanol from CO/H₂ and CO/CO₂/H₂ gas feeds. Under the CO/H₂ feed, methanol production decreased as the reaction proceeded, and this effect was attributed to be due to the highly reducing nature of the feed gas deactivating the catalyst. Possibilities included the formation of brass, reduction of Cu⁺ species, and over reduction leading to sintering. In contrast, under a CO/CO₂/H₂ feed, methanol was produced in reasonable yields and at a constant rate, which was expected as CO₂

is the carbon oxide precursor to methanol. The presence of CO_2 in the feed had the effect of lowering the reducing potential of the gas and preventing the over reduction phenomenon observed prior.

The steady baseline of methanol production obtained in the $\text{CO}/\text{CO}_2/\text{H}_2$ system was ideal for observing the effects of acetic acid addition over the catalysts and it was decided to proceed with the acetic acid studies.

3.3 Acetic Acid Studies

Acetic acid has been studied widely in the literature as a product (from methanol carbonylation, syngas etc)[91, 98, 118-120] and also as a reactant (synthesis of aldehydes, alcohols and esters)[98, 121, 122]. In the proposed system by BP, it was thought that the acid could have a number of effects on the methanol synthesis system. Firstly, initial studies by BP indicated that the presence of acetic acid in the synthesis gas feed could deactivate the commercial methanol synthesis catalyst. Secondly, it was also found that the acetic acid could further react to produce ethanol. The effects of acid addition over the commercial catalyst (Katalco 51-8) were therefore investigated.

3.3.1 Standard Addition

In section 3.2.2.2 the reaction profile of methanol synthesis over the Katalco 51-8 catalyst using a CO/CO₂/H₂ feed was established. The catalyst performed very well, with steady levels of both products and reactants observed, and no deactivation apparent. As an initial experiment it was decided to introduce acetic acid at a low concentration into a classic methanol synthesis system, to observe the effects of the acid on the catalyst. It was of interest to determine if the acid deactivated the catalyst, and if so, if the deactivation was transient or permanent. It was of further interest to determine if the acid would react to produce other species such as acetaldehyde and ethanol.

3.3.1.1 Experimental

Prior to reaction, the Katalco 51-8 catalyst was reduced *in situ* in the reactor under 50ml min⁻¹ flowing hydrogen at a temperature of 523K. The catalyst was held at this temperature for 3hrs.

The experiment was performed using a classic methanol synthesis gas feed of CO/CO₂/H₂ in a 1:1:8 molar ratio. A small concentration of nitrogen was also fed in as a reference gas, for the calculation of conversion. The exact gas mix composition used was 10ml N₂ / 25ml CO / 25ml CO₂ / 190 ml H₂.

- Reaction Temperature (K) 523
- Pressure (barg) 50

- Gas Flow (ml min^{-1}) 250
- Catalyst Volume (ml) 1.36
- GHSV (hr^{-1}) $\sim 11,000$

The acetic acid was fed in at a molar feed rate of 1.0mol% (3.1×10^{-7} moles min^{-1})

3.3.1.2 Reaction Data

For the first 8hrs of the run, no acid was introduced. The catalyst performed exactly as previously shown, with a methanol yield of $\sim 10\%$ obtained. Steady levels of all the components were observed, indicating that the system was at equilibrium.

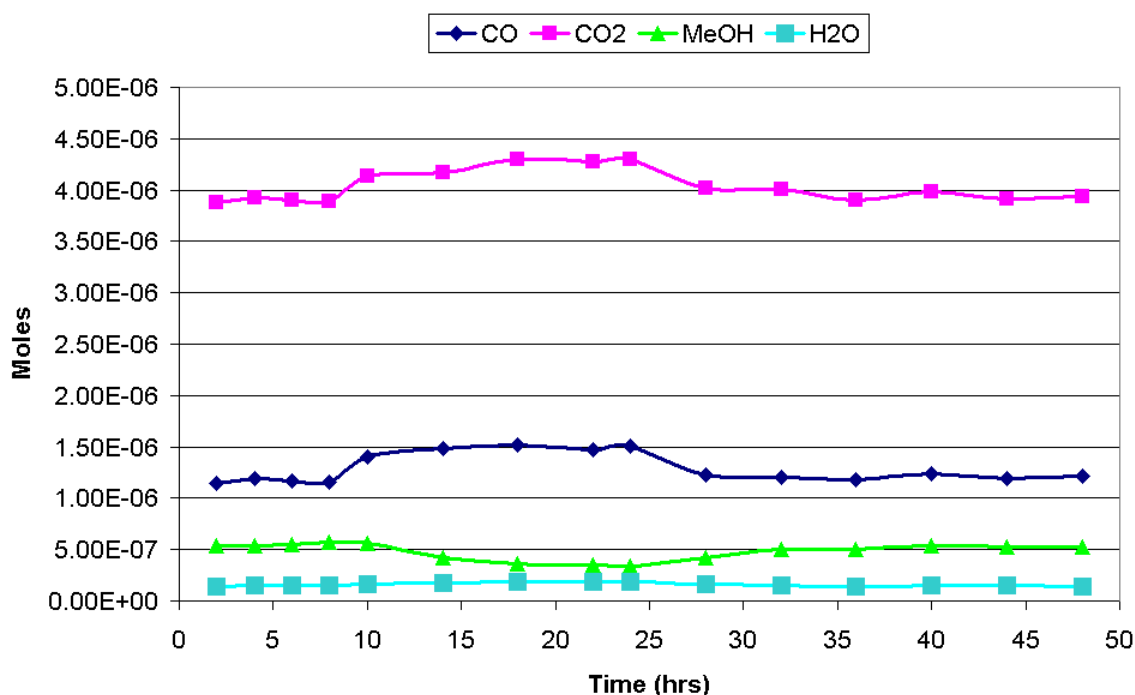


Figure 3-25 Reaction profile from 1.0mol% acid addition into CO/CO₂/H₂ system over Katalco 51-8 catalyst (acid fed in between 8 and 24hrs)

After 8hrs, acetic acid was fed into the system via an HPLC pump at a molar feed rate of 1.0mol% (3.1×10^{-7} moles min^{-1}). Initially when the acid was fed in there was a brief increase in methanol levels. This was thought to be acetic acid adsorbing dissociatively onto the catalyst surface to form acetate groups, and displacing methoxy groups ($-\text{OCH}_3$) which are the direct precursors to methanol. The adsorption of acetic acid on copper surfaces has been studied previously [123-

125]. It was found that on Cu(100) planes the acetate was bound to the surface via the oxygen atoms, in a bidentate fashion [123-125]. It was thought that the acetate was bound to the surface via the whole COO group (through delocalization) rather than to individual oxygen atoms (as shown below)[125].

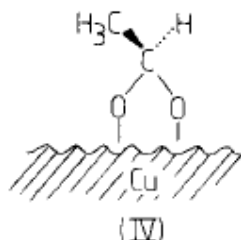


Figure 3-26 Acetate group bound to copper surface[125]

When the acetate groups were bound to the surface, methanol production then began to diminish, due to the acetate groups inhibiting the methanol synthesis either through steric hindrance or stronger binding than one of the reactants.

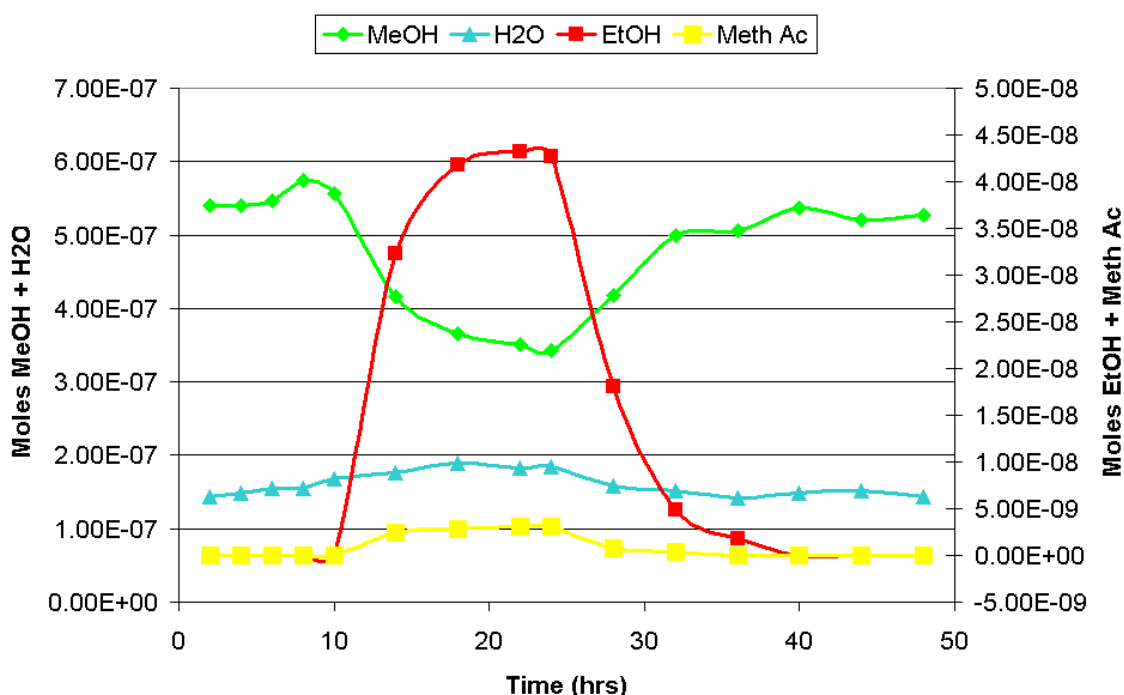
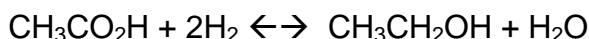


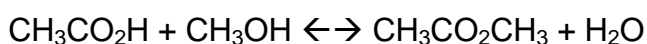
Figure 3-27 Reaction profile from 1.0mol% acid addition into CO/CO₂/H₂ system over Katalco 51-8 catalyst (acid fed in between 8 and 24hrs)

As well as inhibiting the methanol synthesis, the acetate groups on the surface of the catalyst were also found to be reactive. Ethanol and methyl acetate were detected and increased in yield, plateauing at just before the acetic acid feed was

discontinued. The ethanol produced was due to the hydrogenation of the acetic acid:



The hydrogenation of acetic acid over copper catalysts has been studied previously in the literature [102, 105]. Cressely et al studied the hydrogenation over Cu/SiO₂ catalysts and the results showed ethanol in high yield, along with other products such as acetaldehyde and ethyl acetate[102]. Although neither acetaldehyde nor ethyl acetate were observed in the current study, methyl acetate was detected in a small concentration. In Cressely's work, the production of ethyl acetate was linked to ethanol reacting with acetic acid to form the ester[102]. However in the reaction shown here, methanol was the most abundant alcohol (8:1 ratio of methanol:ethanol). The production of methyl acetate was therefore attributed to be the reaction of the methanol in the system with the acetic acid:



Both the hydrogenation of the acid and the esterification reaction involved the production of water as a by product. An increase in water concentration was observed when the acid was introduced, as expected.

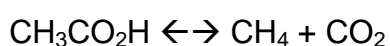
The kinetics of the hydrogenation and esterification reactions were briefly examined by comparing the ratios of reactants to products. In the system there was a molar ratio of 14:1 of ethanol to methyl acetate formed.

Reactants	Products
2H ₂ : CH ₃ OH	Ethanol : Methyl Acetate
19 : 1	14 : 1

In comparison, there was a ratio of 19:1 of 2H₂ to methanol. If both of the products were favoured equally, then a molar ratio of 19:1 of ethanol to methyl acetate would have been observed. This suggested that the formation of methyl acetate was slightly more favourable than the production of the ethanol, but was perhaps limited by the relatively low concentration of methanol.

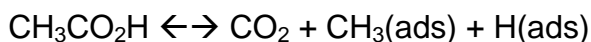
As well as the production of ethanol and methyl acetate, the introduction of the acid into the system also resulted in the increase of both CO and CO₂ concentrations. Although, the decrease in methanol production would account for some of the carbon oxide increase, it would not account for it all. The only other potential carbon source in the system for the CO/CO₂ was the acetic acid itself. Conversion of acetic acid to CO/CO₂ was not expected as the system was reasonably reducing and it was thought that the formation of methane or possibly ethane was more likely. A literature search revealed that a possible route for the production of CO₂ from acetic acid was through the decomposition of surface acetates [95-97, 125, 126]. Studies performed on copper crystals have shown that the decomposition of surface acetates resulted in evolutions of CO₂, CH₃CO₂H, CH₄, H₂C₂O (ketene) and the deposition of carbon fragments on the surface. The desorption rates for the fragments were identical, indicating a common intermediate[125]. The common intermediate was postulated to be acetic anhydride, formed on the surface of the catalyst from two acetate groups reacting together[125]. However, the decomposition profile for acetate has been shown to vary markedly depending on the metal, the metal particle morphology and the presence of different adsorbates [97, 123, 124, 127]. For example, the decomposition of acetate groups present on a Ni/Cu alloy yielded CO₂, surface carbon and gaseous hydrogen[128]. The presence of oxygen on the metal was also shown to have a pronounced effect on the decomposition of acetates [95-97]. On group 9-10 metals, its presence has been shown to initially stabilise the acetate, beyond the decomposition temperature on clean surfaces. Adsorbed oxygen has the effect of ordering the acetate, generating small islands whereby the attractive forces between the molecules stabilise them [97, 129, 130]. When acetate does decompose it happens auto-catalytically, to yield CO₂, H₂ and adsorbed carbon [95-97, 130].

Overall, the most common route for acetate decomposition on metal surfaces was via decarboxylation, to yield CO₂ and CH₄ [95-98, 125]:



However in our tests methane was not detected by the GC analysis. On closer inspection of the decomposition mechanism, the acetate group is proposed to

“fragment” on the metal surface to yield gas phase CO₂ and an adsorbed methyl group and adsorbed H [95-97, 125, 126]:



The methyl group then further decomposes to yield adsorbed carbon and gas phase hydrogen [95-97, 129, 130]. Density Functional Theory (DFT) has shown that this occurs by the tilting of the acetate group such that the methyl group can interact with the surface leading to C-H bond cleavage[131, 132], followed by C-C bond scission. On Pd(110) surfaces this was shown to occur explosively, on both carbon covered and oxygen covered surfaces [126, 131-133].

However, the carbon balance for the system showed that there was no loss of carbon during the period where the acid was introduced to the system (Fig 3-28). (Experimental error of +/- 5% was assumed for all mass balances due to inherent areas in calibrating, subsequent mole calculations and the variability of atmospheric pressure in the sample loop)

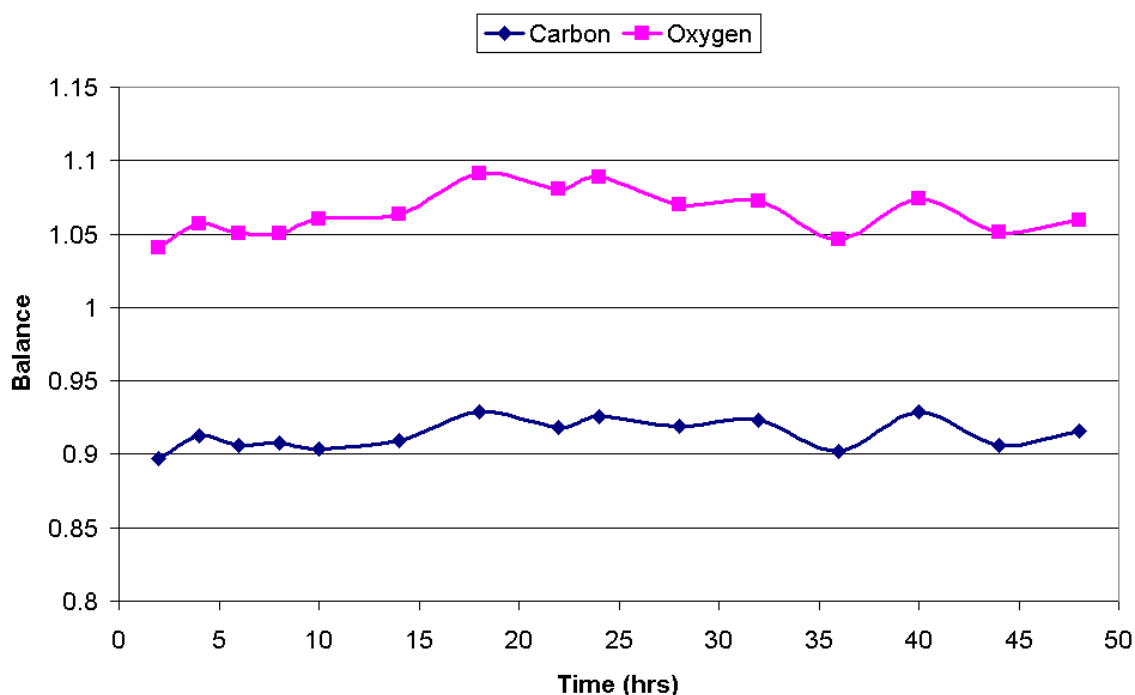
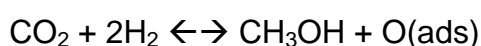


Figure 3-28 Mass balances from 1.0mol% acid addition into CO/CO₂/H₂ system over Katalco 51-8 catalyst (acid fed in between 8 and 24hrs)

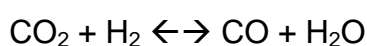
If decomposition of the acetate was taking place on the surface, and decarboxylation was the route, then re-oxidation of the surface carbon would need to take place on the catalyst surface.

To consider how oxidation of the surface carbon might proceed in the methanol synthesis system, the surface of the catalyst has to be considered. Under working conditions the surface is in a dynamic state, with a small percentage of the surface covered with adsorbed atomic oxygen [53-55]. Adsorbed oxygen is derived from the hydrogenation of CO₂ to yield methanol:



Under normal conditions, adsorbed oxygen is picked up by either CO or H₂ to form CO₂ or H₂O. However, with acetate groups on the surface, the decomposition of the acetate could yield CO₂, H₂ and surface carbon. If adsorbed oxygen was to react with the surface carbon instead of CO or H₂ then no carbon laydown would occur.

If this process were to proceed, decomposition of the acetic acid would yield 2CO₂ and 2H₂ (assuming the adsorbed carbon was fully oxidised to CO₂). Conversion of CO₂ to CO could take place via the WGS reaction:



The proposed model explains both the CO and the CO₂ increases observed in the system. However, the oxidation of the surface carbon could equally have taken place via a reverse Boudouard mechanism, which involved the presence of CO₂:



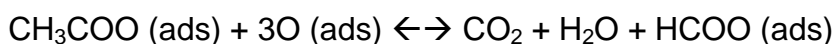
Or by oxidation due to the presence of water in the system:



Rather than surface oxidation of the catalyst being important, the presence of CO₂ or water in the system would be crucial in preventing carbon laydown. However, the thermodynamics of both reactions were calculated (+80 and +60 kJ mol⁻¹

(assuming adsorbed carbon was present as graphite)) and suggested that the mechanisms were not very favourable.

On certain metals, acetates have been shown to decompose completely, without the loss of carbon to the catalyst surface[134, 135]. On a clean Ag (1 1 0) surface, acetate decomposed above 600K to yield CH₄, CO₂, CH₃COOH, H₂C₂O and adsorbed carbon[134]. However, with atomic oxygen present on the surface, acetate decomposed at temperatures as low as 400K, and was attributed to destabilisation of the acetates due to the presence of oxygen atoms. The acetate reacted with the oxygen to yield H₂O, CO₂ and formate, which further decomposed to yield CO₂ and H₂.



Labelling experiments performed using ¹³C labelled acetic acid revealed that the methyl carbon of the acetic acid was incorporated into the formate. Oxygen labelling experiments showed that oxygen from the acetate was present in the CO₂, while oxygen atoms in the water and the formate came from oxygen present on the catalyst surface.

The results of the labelling studies led to a postulated mechanism of decomposition. Carboxylate species such as acetate have been shown previously using DFT calculations, to decompose via decarboxylation by tilting the methyl group towards the metal surface [131, 132]. It was postulated that if the methyl group was tilted towards the surface, abstraction of a hydrogen atom by a surface oxygen atom (or hydroxyl group) could occur to make a surface hydroxyl (or water) and CH₂OO (ads). Abstraction of methyl protons has been observed for acetonitrile on a Ag(110) surface previously[136]. As the pK_a of the acetonitrile ion was similar to that of acetate, it was thought that they may react similarly. Once the hydrogen was abstracted, the CH₂OO (ads) group could react with surface oxygen to form a glycolate intermediate (fig 3-29):

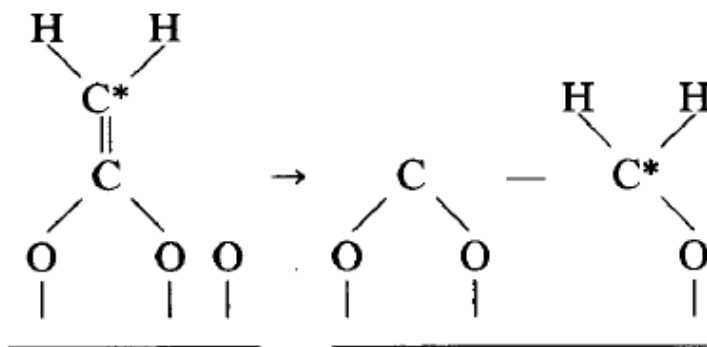


Figure 3-29 Mechanism of acetate decomposition on Ag(110) surface

Nucleophilic attack on C* by a surface oxygen atom would take place, followed by C-C bond scission to form CO_2 and CH_2CO_2 (ads) (fig 3-30). The CH_2CO_2 (ads) could then decompose to yield formate:

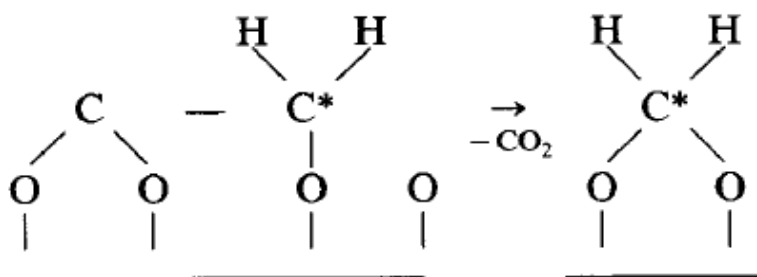
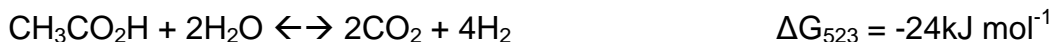


Figure 3-30 Mechanism of acetate decomposition on Ag(110) surface

Formate would decompose further to CO_2 and H_2 .

Overall, the decomposition of acetates on a Ag(110) surface with oxygen present yielded CO_2 , H_2 and H_2O [134]. It was entirely possible that the oxygen present on the surface of the Katalco catalyst under methanol synthesis conditions could play a similar role in preventing carbon deposition on the surface of the catalyst. However, it must also be noted that formate is a key intermediate in the synthesis of methanol [56, 116, 137], and therefore under the reaction conditions it would be expected to become hydrogenated towards methanol rather than decompose.

Another possible route towards the formation of CO/CO_2 from acetic acid was simply through the hydrolysis of the acid. As a reasonable concentration of water was present in the system it was thought that at the reaction temperature it might be able to breakdown the acid into CO_2 and H_2 :



The thermodynamics suggested that it was a feasible route towards CO/CO₂. Hydrothermal studies of the liquid phase decomposition of acetic acid can be found in the literature, and the reaction products were CO₂, CO, CH₄ and H₂ (a combination of hydrolysis and decarboxylation)[138]. However, no studies on the vapour phase hydrolysis could be found.

Finally, when the acid addition was stopped at 27hrs, the system returned to normal. Ethanol and methyl acetate production dropped to zero, whilst CO₂, CO, methanol and water concentrations returned to their original levels. This suggested that the effects of acetic acid addition were transient and that the acid did not intrinsically affect the catalyst.

3.3.1.3 Acid Balance

Acid to Ethanol (%)	14.0
Acid to Methyl Acetate (%)	1.0
Acid to CO / CO ₂ (%)	84.5
Total (%)	99.5

Table 3-5 Acid balance from 1.0mol% acid addition into CO/CO₂/H₂ system over Katalco 51-8 catalyst

A balance of the acid introduced to the system revealed that all the acid could be accounted for in the form of ethanol, methyl acetate and CO/CO₂. The acid balance was in complete agreement with the mass balances for the reaction, and confirmed that little to no carbon deposition of the acid occurred during the run.

As the acid balance was almost 100%, it was unlikely that any of the acid had been converted to methanol.

3.3.1.4 Temperature Programmed Oxidation (TPO)

Post reaction, a TPO was performed on the catalyst as a final check to determine if any carbon laydown had occurred during the run.

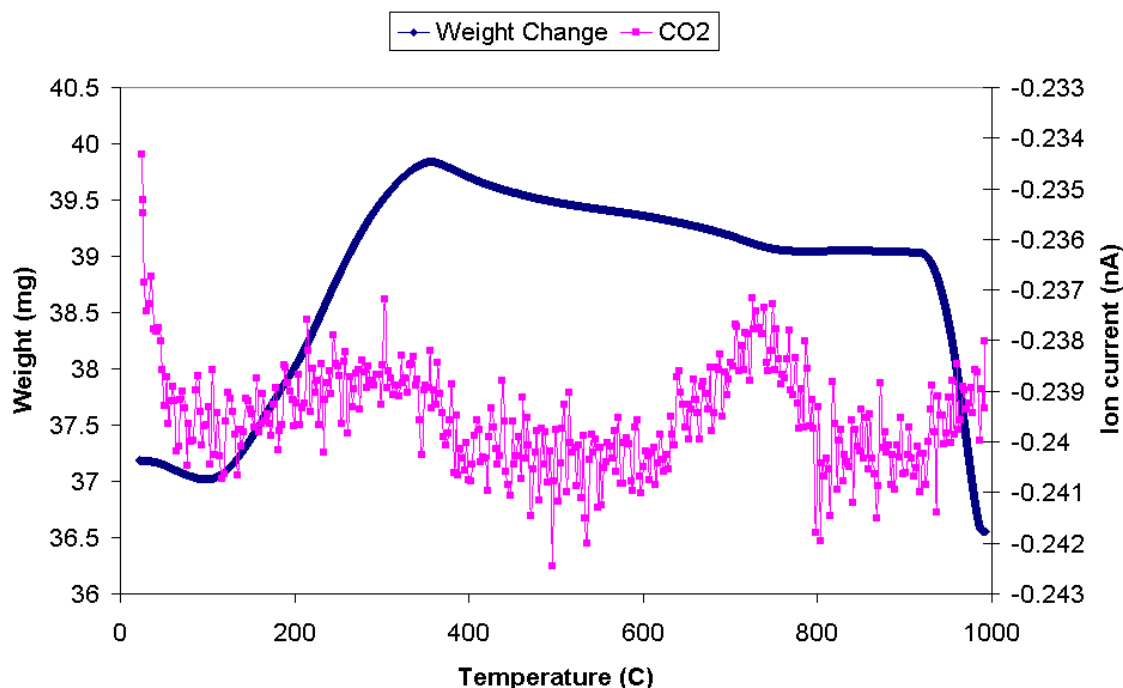


Figure 3-31 Post reaction TPO of catalyst from 1.0mol% acid addition into CO/CO₂/H₂ system over Katalco 51-8 catalyst

Upon performing the TPO, the sample weight increased significantly. As explained previously, this can be attributed to the reduced copper metal re-oxidising.

The graph shows that there was very little deposition of carbon on the catalyst surface. A broad amorphous evolution of CO₂ was evolved at a temperature of ~277°C. This was possibly a mixture of surface form ate groups and other methanol precursor species. Carbon laydown was also a possibility. As the acid balance suggested that all the acid introduced to the system could be accounted for as products, it was not thought that the evolutions were due to adsorbed acid or acetate groups on the surface. The high temperature evolution was thought to be the thermal breakdown of metal carbonates, formed during the run. The mechanism of decomposition of metal carbonates is shown below:



Where M represents any metal.

3.3.1.5 Summary

From the initial experiment it was observed that the acetic acid had a number of effects on the system upon its introduction. Firstly and most importantly, the

methanol production decreased dramatically. A possibility was that the introduction of acetic acid resulted in strongly bound acetate groups on the catalyst surface. As these groups would displace reactants, then methanol synthesis would be hindered. Another possibility was that the surface oxidation of the catalyst was affected. Studies have shown that the methanol synthesis activity of copper based catalysts is directly related to the CO/CO₂ ratio[8]. As the acid was shown to be converted to CO/CO₂, it was a possibility that the ratio had been changed, resulting in the decrease in methanol production. However, the ratio was found to remain the same upon introduction of the acid.

Without Acid (CO₂:CO)

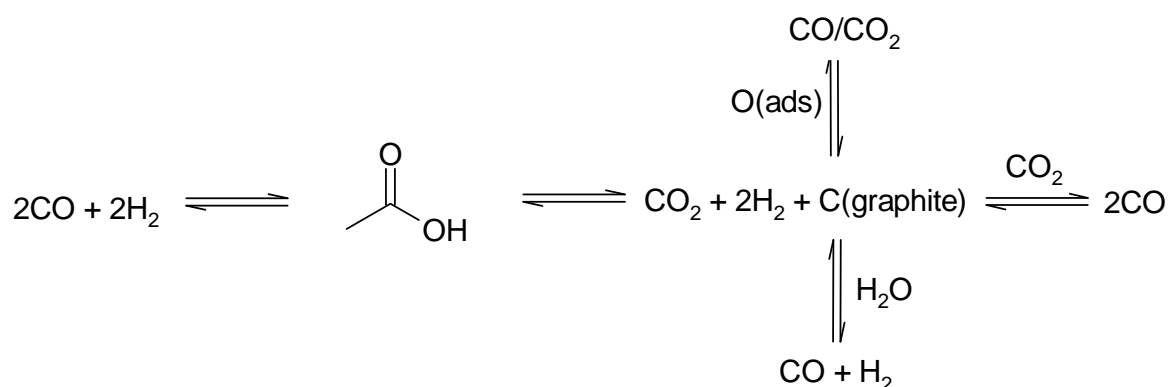
1 : 0.30

With Acid (CO₂:CO)

1 : 0.31

The acetic acid itself was found to react in several different ways. Hydrogenation of acetic acid to ethanol was found to proceed, along with an esterification reaction with methanol to form methyl acetate [98, 102]. These reactions were well documented in the literature and were not unexpected in the current system considering the concentrations of hydrogen and methanol present. However the conversion of acetic acid to CO/CO₂ was not expected. Possible routes to CO/CO₂ are shown below:

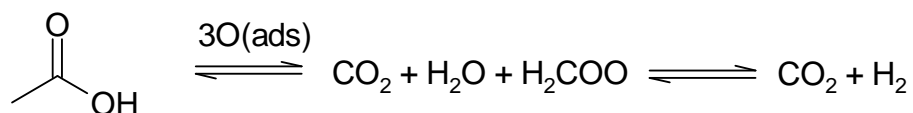
Decomposition / Oxidation of Surface Carbon



Decomposition of the acetate groups on various transition metal surfaces were shown to occur via a simple decarboxylation route to yield gas phase CO₂ and H₂, with carbon deposited on the surface [95-97, 129, 130]. Oxidation of the surface carbon under the working conditions of the methanol synthesis catalyst was

envisaged to possibly occur via three distinct routes. Firstly, it was thought that the leftover adsorbed oxygen from CO₂ hydrogenation could oxidise the carbon to CO₂. Secondly, a reverse Boudouard type reaction was possible, as CO₂ could lift off the carbon in the form of CO. Finally, the water present in the system could also potentially re-oxidise the carbon.

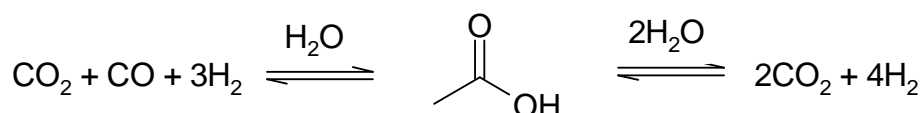
Decomposition / Formate Decomposition



Similar to the previous system in that CO₂ is evolved via decarboxylation, in this case the methyl fragment reacts with the oxidised surface of the catalyst to form a surface formate group. The formate could then further decompose to yield CO₂ and H₂[134].

However, under methanol synthesis conditions, it would be more likely that the formate would be hydrogenated to methanol. The acid balance indicated that the conversion of acid to methanol was unlikely.

Hydrolysis



Hydrolysis of the acid was thermodynamically possible, although there was no precedent in the literature.

All three systems were thought to be possible due to the structure sensitivity of acetate surface reactions, although conversion of acetic acid to methanol was thought to be the least likely. As the formation of CO/CO₂ from acetic acid was unexpected, it was decided to perform a series of experiments to determine as to whether the conversion of acid to CO/CO₂ could be followed.

3.3.2 Labelling Studies

As the conversion of acetic acid to CO/CO₂ was unexpected, it was decided to perform labelling studies using ¹³C labelled acetic acid, to determine if carbon from the acid could be detected in CO/CO₂. Two labelled samples of acetic acid were purchased, each with a different carbon labelled. The samples are shown below:

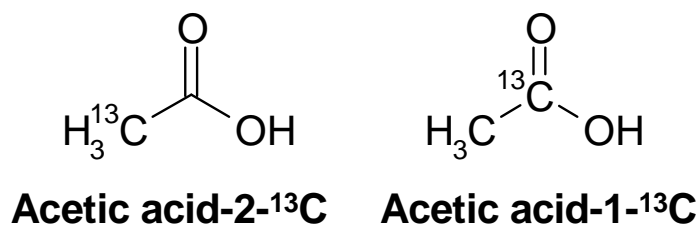


Figure 3-32 ¹³C labelled acetic acid

Two experiments were performed, and in each experiment there were two acetic acid additions; one unlabelled and one labelled. The unlabelled acid was added in as a reference, so that identification of labelled carbon during the labelled addition would be easier. Mass spectrometry was used as well as the usual GC data to analyse the run. As a final experiment to complete the labelling studies, a run with an addition of deuterated acid was performed, to determine if a kinetic isotope effect (KIE) was observed.

3.3.2.1 Experimental

Prior to reaction, the Katalco 51-8 catalyst was reduced *in situ* in the reactor under 50ml min⁻¹ flowing hydrogen at a temperature of 523K. The catalyst was held at this temperature for 3hrs.

The experiments were performed using a classic methanol synthesis gas feed of CO/CO₂/H₂ in a 1:1:8 molar ratio. A small concentration of nitrogen was also fed in as a reference gas, for the calculation of conversion. The exact gas mix composition used was 10ml N₂ / 25ml CO / 25ml CO₂ / 190 ml H₂.

- Reaction Temperature (K) 523
- Pressure (barg) 50
- Gas Flow (ml min⁻¹) 250

- Catalyst Volume (ml) 1.36
- GHSV (hr^{-1}) $\sim 11,000$

In the ^{13}C labelled experiments the acid additions were performed at a molar feed rate of 1.0mol% ($3.1 \times 10^{-7} \text{ moles min}^{-1}$). In the run where deuterated acid was fed in, the additions were performed at a molar feed rate of 1.5mol% ($4.65 \times 10^{-7} \text{ moles min}^{-1}$).

3.3.2.2 [$2\text{-}^{13}\text{C}$] Acetic Acid Addition

For the first 26hrs of the run, no acetic acid was fed into the system. The system was in equilibrium, with a steady level of methanol production observed ($\sim 10\%$ yield).

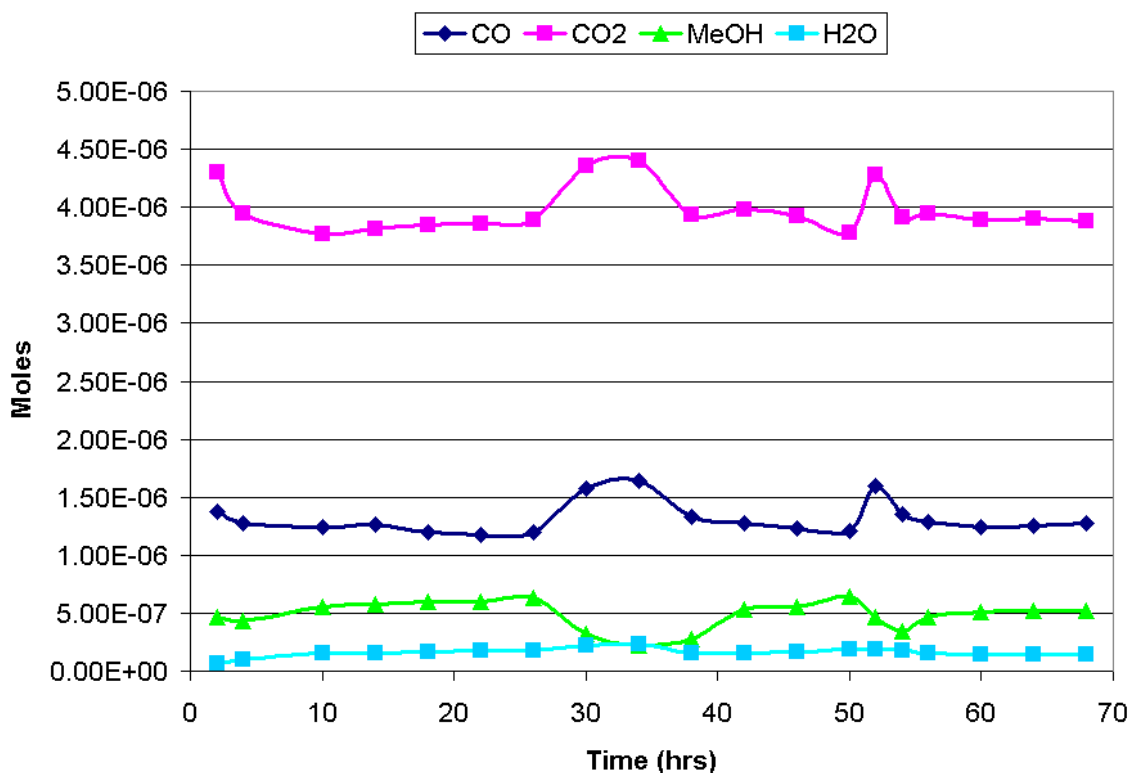


Figure 3-33 Reaction profile from 1.0mol% labelled acid addition into CO/CO₂/H₂ system over Katalco 51-8 catalyst (unlabelled acid fed in between 26 and 34hrs, labelled acid fed in between 50 and 54hrs)

After 26hrs, unlabelled acetic acid was fed in to the system at a molar feed rate of 1.0mol% ($\sim 3.1 \times 10^{-7} \text{ moles min}^{-1}$). The system behaved exactly as previously shown, with a decrease in methanol production and increases in CO, CO₂ and H₂O concentrations. Production of ethanol and methyl acetate were also

observed (fig 3-34). Upon cessation of the acid feed at 34hrs, the system returned back to normal, with the levels of ethanol and methyl acetate dissipating to zero.

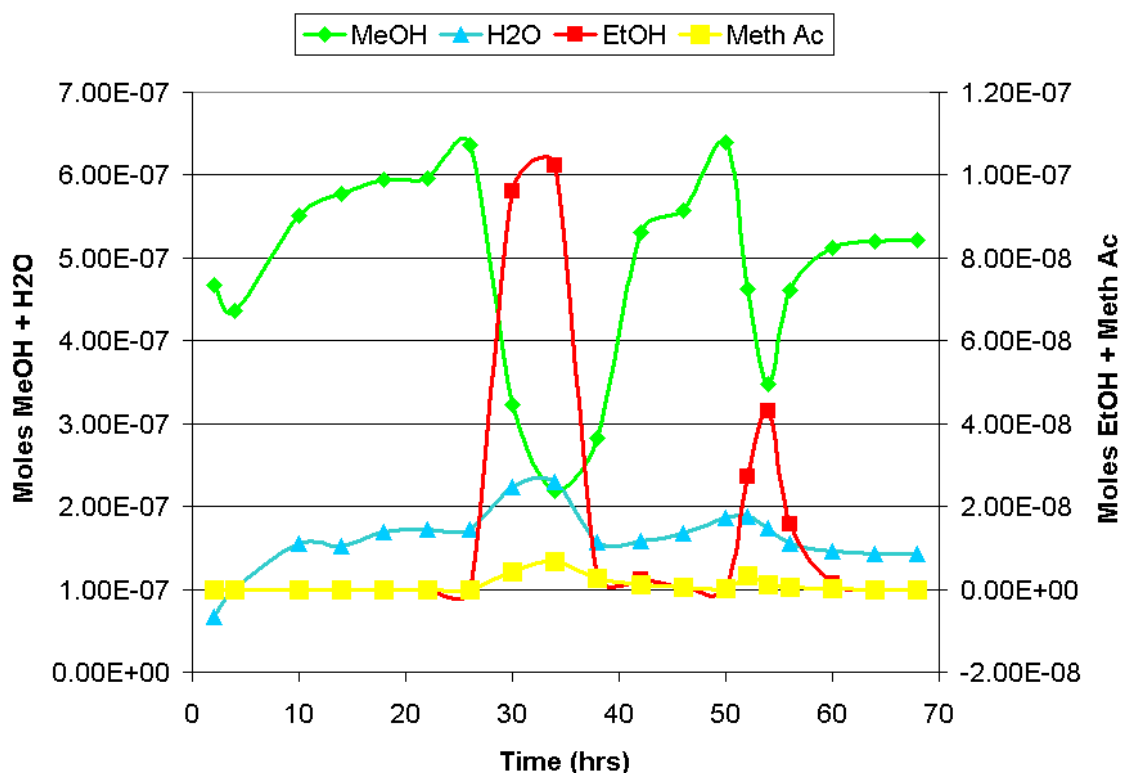


Figure 3-34 Reaction profile from 1.0mol% labelled acid addition into CO/CO₂/H₂ system over Katalco 51-8 catalyst (unlabelled acid fed in between 26 and 34hrs, labelled acid fed in between 50 and 54hrs)

The system was allowed to reach equilibrium again before the labelled addition. The system behaved in exactly the same manner for the labelled acid addition as it did for the unlabelled, although the levels of ethanol and methyl acetate produced were not quite as high and the decrease in methanol production was not as dramatic (due to shorter duration of acid addition). Again, upon cessation of the acid the system returned back to normal, suggesting that the effect of the acid on the methanol production was transient.

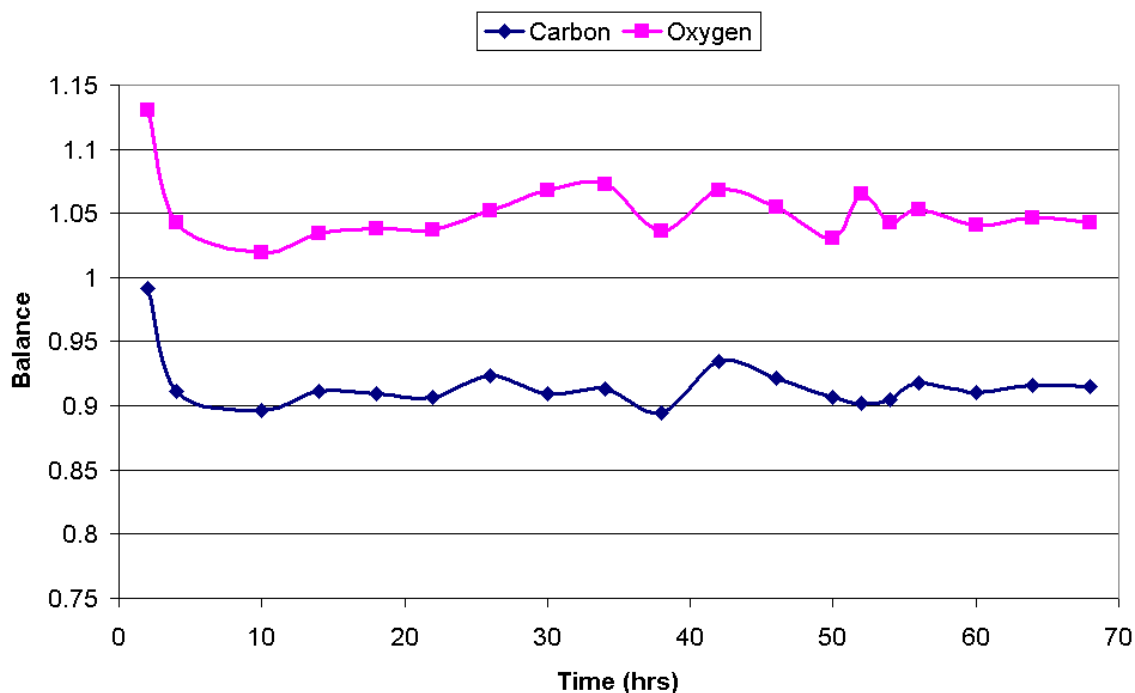


Figure 3-35 Mass balances from 1.0mol% labelled acid addition into CO/CO₂/H₂ system over Katalco 51-8 catalyst (unlabelled acid fed in between 26 and 34hrs, labelled acid fed in between 50 and 54hrs)

The carbon and oxygen balances of the system remained constant throughout the run, indicating that little to no carbon was deposited on the catalyst during the additions of acetic acid (Fig 3-35).

3.3.2.3 Acid Balance

Acid to Ethanol (%)	13.9
Acid to Methyl Acetate (%)	1.0
Acid to CO / CO ₂ (%)	89.0
Total (%)	103.9

Table 3-6 Acid balance from 1.0mol% labelled acid addition into CO/CO₂/H₂ system over Katalco 51-8 catalyst

The acid balance (Table 3-7) showed that the majority of the acid was converted to CO/CO₂, with ethanol and methyl acetate also produced as expected. In comparison with the standard run shown previously, almost identical levels of

ethanol and methyl acetate were observed, with only a slight increase in CO/CO₂ apparent. However the differences were well within experimental error.

3.3.2.4 Temperature Programmed Oxidation (TPO)

A TPO was performed on the catalyst post reaction (Fig 3-36). The usual mass increase of the catalyst sample upon exposure to the oxidising gas was observed. This was due to the copper metal re-oxidising to copper oxide.

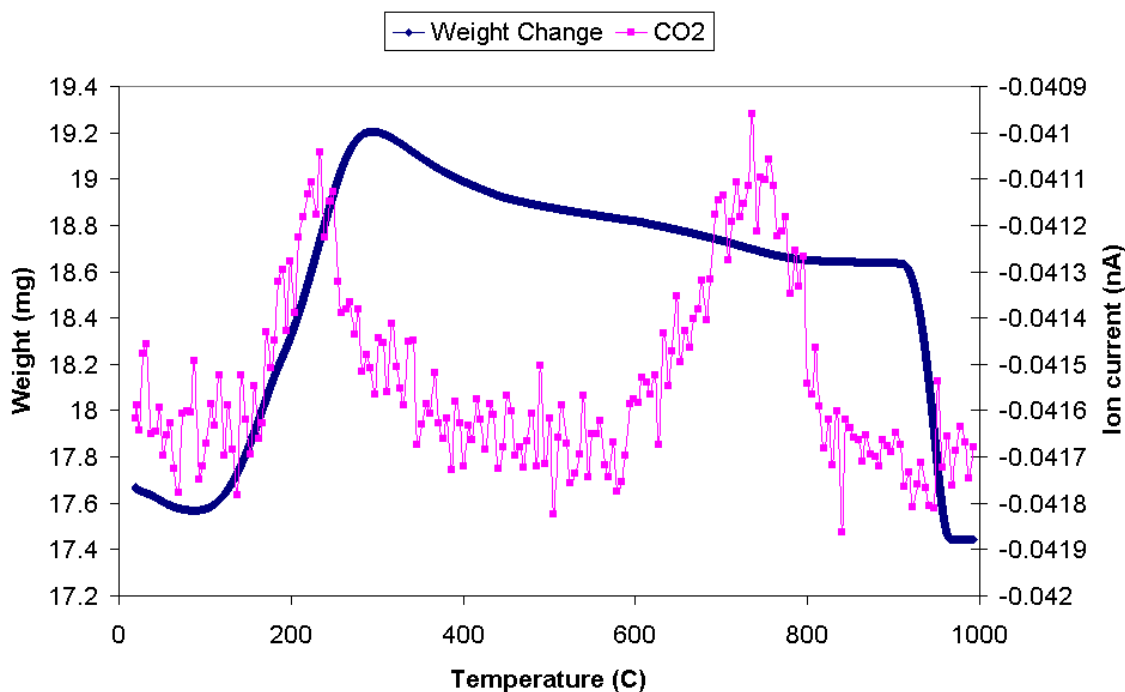


Figure 3-36 Post reaction TPO from 1.0mol% labelled acid addition into CO/CO₂/H₂ system over Katalco 51-8 catalyst

Evolutions of CO₂ were observed at 234°C and at 735°C. ¹³CO₂ was also followed using mass spectrometry, and no evolutions were observed, indicating that deposition of labelled carbon did not occur. As postulated earlier, the low temperature evolution was possibly due to formate groups or other methanol precursor species. The high temperature evolution was postulated to be due to the decomposition of metal carbonates.

3.3.2.5 Mass Spectrometry Data

Mass spectrometry data for relevant masses were recorded throughout the experiment. The acid additions were made at the following cycles:

Addition	Added (cycles)	Stopped (cycles)
CH ₃ CO ₂ H	3729	5211
¹³ CH ₃ CO ₂ H	7531	8369

Table 3-7 Acid additions into CO/CO₂/H₂ system over Katalco 51-8 catalyst

Ethanol/CO₂

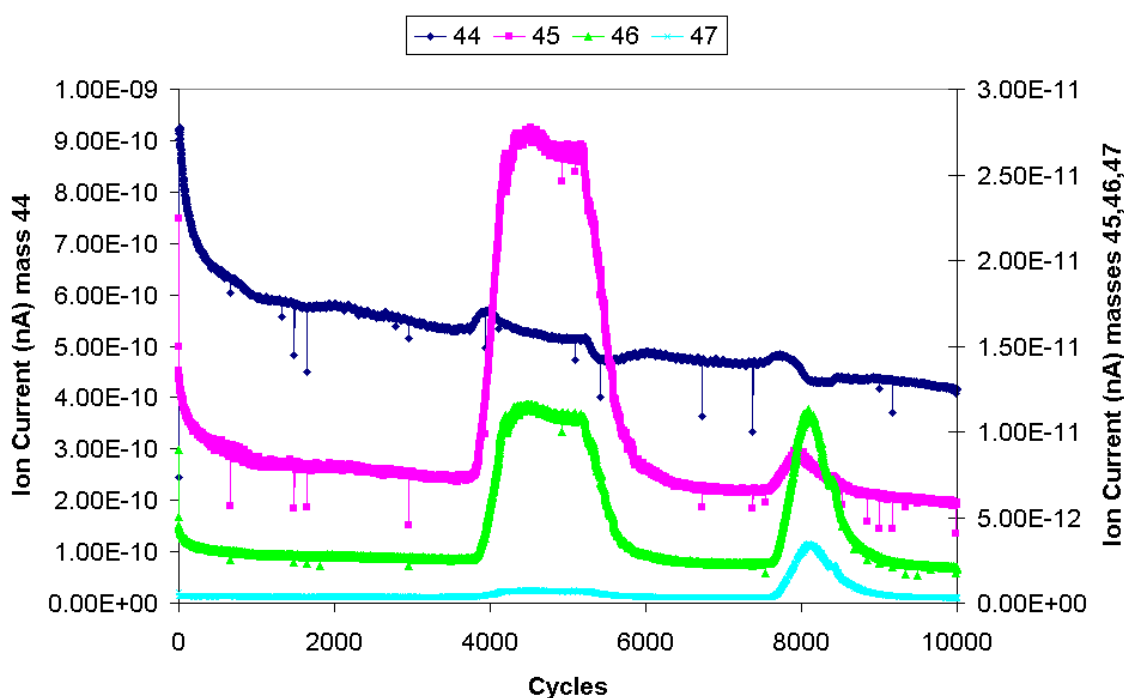


Figure 3-37 Mass spectra from 1.0mol% labelled acid addition into CO/CO₂/H₂ system over Katalco 51-8 catalyst

When the unlabelled addition was made there were responses observed in the mass 44, mass 45 and mass 46 signals. Mass 44 related to unlabelled CO₂ and the increase in the signal was consistent with the increase observed in the GC analysis. Masses 45 and 46 were both fragments for ethanol and the ratio of the relative signals matched exactly the relative abundances of the fragments. Again,

the mass spectra data matched the GC trace for ethanol production perfectly, and therefore both masses 45 and 46 were assigned to be unlabelled ethanol.

Mass 47 showed no response during the unlabelled addition.

When labelled acid was introduced to the system, responses were observed for masses 44 – 47. The response in mass 44 could only be due to CO₂, and therefore suggested that the unlabelled carbon in the acid had been converted to CO₂.

The response of mass 45 was more difficult to interpret, as the response could have been due to ¹³CO₂ or unlabelled ethanol. The increase was attributed to being due to the formation of ¹³CO₂ for several reasons. Firstly, if the mechanism for ethanol formation in the system was through the hydrogenation of the acid, then unlabelled ethanol could not be formed from introduction of labelled acid. Secondly, the peak maxima of the mass 45 signal did not match up with peak maxima for mass 47, which could only be labelled ethanol. This suggested that the responses were due to two separate species entirely. The GC data for the run also supported this theory, as the GC responses for CO₂ and EtOH matched the proposed responses for ¹³CO₂ and ¹³EtOH exactly (figs 3-38 and 3-39) .

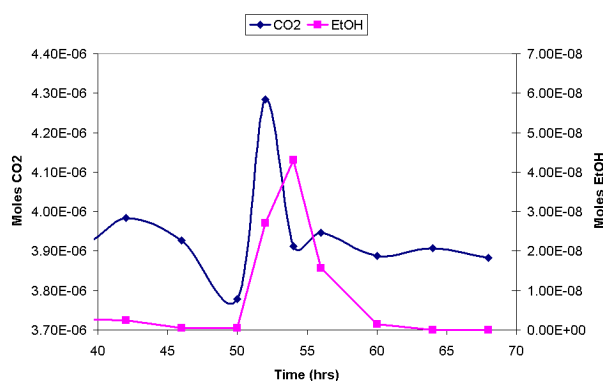


Figure 3-38 GC Data from labelled addition

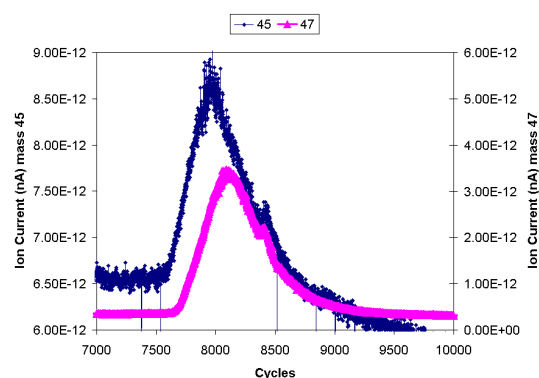


Figure 3-39 Mass spectrometry data from labelled addition

The mass spectra data confirmed that ¹³CO₂ was produced from the addition of labelled acetic acid.

The response for mass 46 was attributed to the production of labelled ethanol. Unlabelled ethanol was ruled out on the basis that for ethanol production, the carbon chain in the acid would remain intact.

Finally, mass 47 related to the production of labelled ethanol, and a reasonable signal increase was observed indicating its formation upon addition of the labelled acid.

Methyl Acetate

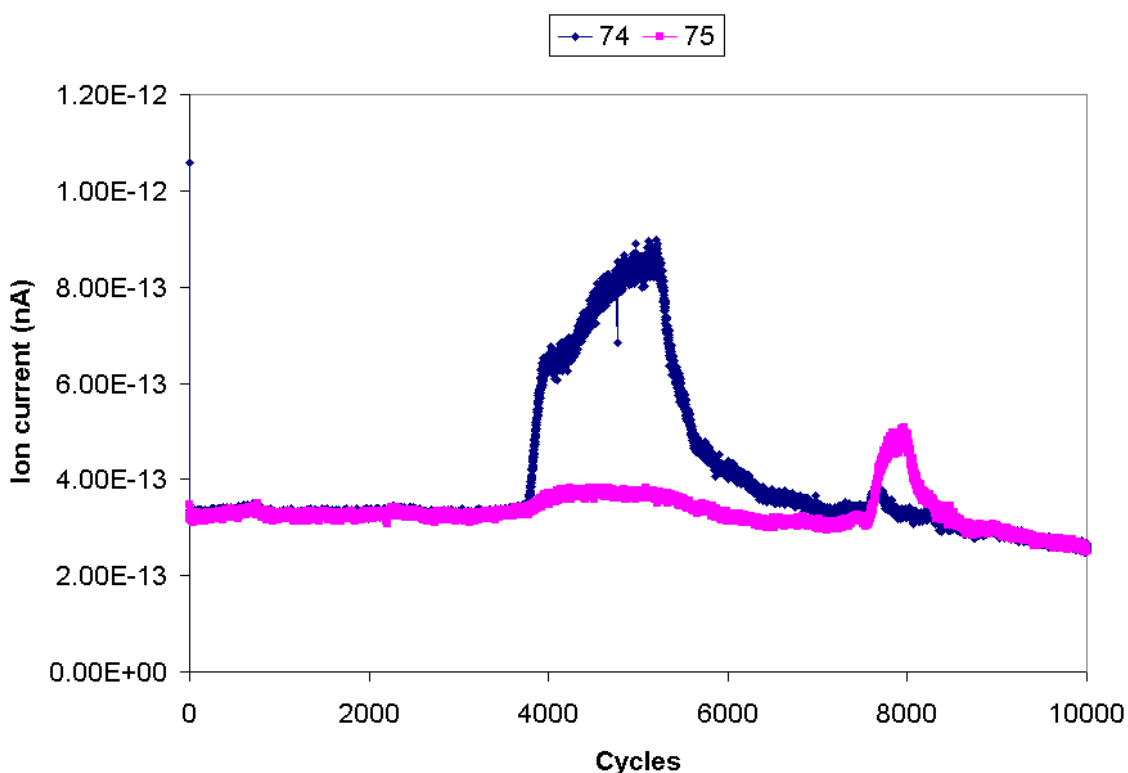


Figure 3-40 Mass spectra from 1.0mol% labelled acid addition into CO/CO₂/H₂ system over Katalco 51-8 catalyst

GC analysis showed that for both the labelled and unlabelled acetic acid additions, methyl acetate was produced. Prior to the acid addition there was no methyl acetate in the system. When the unlabelled addition was made, there was a response in the mass 74 signal (unlabelled methyl acetate) and no response in the mass 75 signal (labelled methyl acetate). This was expected as no label had been introduced at this point. However upon addition of the labelled acid the opposite occurred. There was a response in the mass 75 signal but no response in the mass 74 signal. The label was incorporated into the methyl acetate. This confirmed that acetic acid reacted with methanol in the system to produce the ester.

Methanol

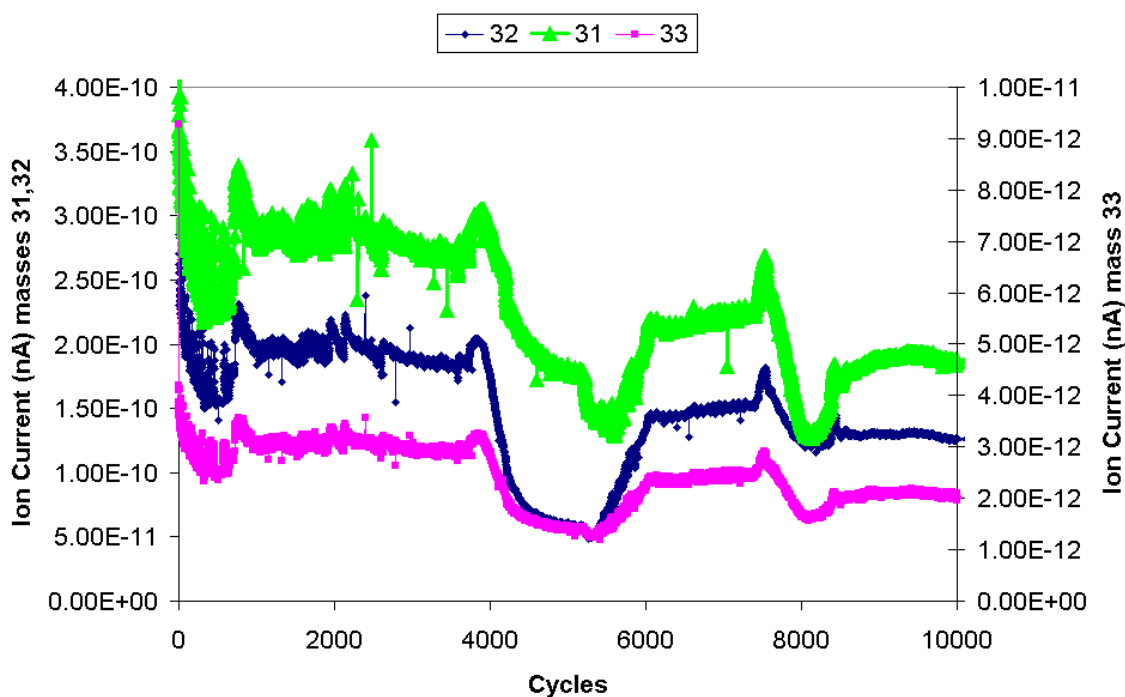


Figure 3-41 Mass spectra from 1.0mol% labelled acid addition into CO/CO₂/H₂ system over Katalco 51-8 catalyst

The graph showed that prior to the unlabelled acid addition a steady level of methanol production was present. When the unlabelled acid was fed in, there was an initial rise in methanol levels. This could be attributed to the acid displacing methoxy groups (-OCH₃) from the surface of the catalyst. The methanol levels then steadily decreased until a steady state was reached. This was in complete agreement with the GC data. It was expected that the mass 33 signal (labelled methanol) would show a flat baseline throughout as it was an unlabelled addition. However the mass 33 signal showed the same trend as for mass 32. This was entirely due to the natural abundance of ¹³C which is ~1.1%. Upon cessation of the acid the system returned back to normal, as expected.

When the labelled acid was fed in, the system behaved in the same way (for both masses 32 and 33) as for when the unlabelled acid was added, indicating that the labelled carbon did not migrate into the methanol. This ruled out the decomposition of acetic acid via formate as a potential route, as the label would be expected to appear in the methanol (methanol being the hydrogenation product of formate). However, the labelled acid was only fed in for a short period of time. As the label was shown to appear in CO₂ (and therefore CO via the WGS) it would be

expected that eventually the label would be incorporated into the methanol. This would possibly have been observed if the labelled acid was fed in for a longer period of time.

Other Masses

The mass fragment for CO labelled (29) was also a mass fragment for methanol. Therefore there was overlapping of the signals so was impossible to observe the ^{13}C label in the CO. However because of the WGS reaction, it can be assumed that because the label was observed in the CO_2 , it would also be present in the CO. Mass fragments for methane were also followed even though methane was not detected by the GC. The mass spectra also confirmed that no methane was formed during the labelled or unlabelled addition.

3.3.2.6 [1- ^{13}C] Acetic Acid Addition

For the C1 labelled acetic acid experiment, the exact same mass spectrometry and GC results were obtained. Combined with the data gathered from the C2 labelled run, the results indicated that for ethanol and methyl acetate formation, the carbon structure of the acetic acid remained intact in agreement with the postulated mechanisms of acid hydrogenation to ethanol and esterification of acid with methanol to form methyl acetate.

The results also showed that both carbons of the acetic acid could be converted to CO_2 . This was important as the decomposition of acetic acid has been shown previously to occur over metal surfaces via decarboxylation [95-97, 129, 130]. This would yield CO_2 and an adsorbed methyl group on the surface of the catalyst, in a 1:1 ratio. If the postulated route for acetic acid to CO/ CO_2 was correct, then instead of picking up a proton to form methane, the methyl group must be converted to CO or CO_2 . A potential route would be for the methyl group to further decompose (as discussed previously) to yield adsorbed carbon and gaseous hydrogen. The carbon could then be oxidised by whatever means to yield CO or CO_2 . Decomposition of the acid via an adsorbed formate[134], without the deposition of carbon was ruled out as a possibility as the label was not observed in the methanol (methanol being the hydrogenation product of formate). However, as the label was found in CO_2 , and CO_2 is the direct precursor to methanol, it was

probable that if the labelled addition was run for longer the label would eventually be incorporated.

Hydrolysis of the acid remained a distinct possibility and would be investigated later.

3.3.2.7 Deuterated Acetic Acid ($\text{CD}_3\text{CO}_2\text{D}$) Addition

To complete the labelling studies, it was decided to run an experiment with addition of fully deuterated acetic acid ($\text{CD}_3\text{CO}_2\text{D}$), to determine if there were any kinetic isotope effects (KIE). To this end an experiment was performed with two additions of acid; one unlabelled addition followed by an addition of the deuterated acid. This was done to allow comparison of the two additions in the same experiment, so that any effects could be easily observed.

The GC data for the run showed the usual features that were observed in the previous experiments upon introduction of the acid. The unlabelled acid was fed in first at a molar feed rate of 1.5mol% (4.6×10^{-7} moles min^{-1}) after 12hrs. Increases in CO , CO_2 and water were observed, along with production of ethanol and methyl acetate. In contrast the methanol production decreased dramatically.

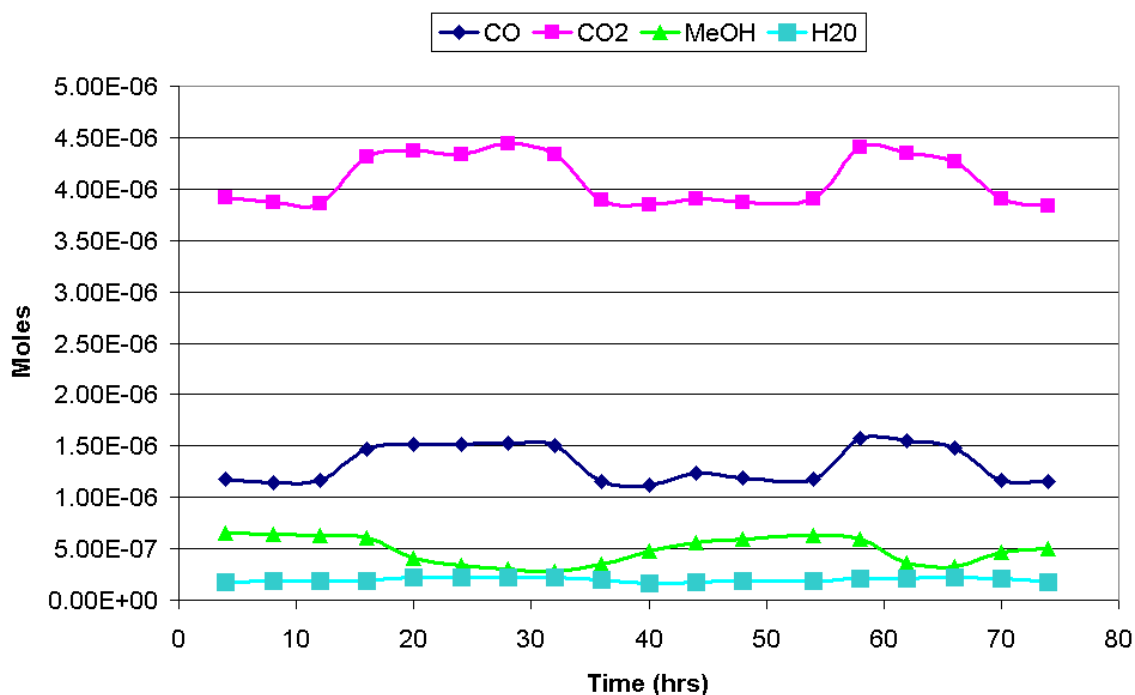


Figure 3-42 Reaction profile from 1.5mol% deuterated acid addition into $\text{CO}/\text{CO}_2/\text{H}_2$ system over Katalco 51-8 catalyst (non-deuterated acid fed in between 12 and 32hrs, deuterated acid fed in between 54 and approximately 64hrs)

The acid was stopped at 32hrs and the system was allowed to return to equilibrium prior to the 2nd acid addition. At 54hrs, fully deuterated acid was fed into the system, at the same molar feed rate as for the 1st addition. Like previously increases in CO, CO₂ and water concentrations were observed along with production of ethanol and methyl acetate.

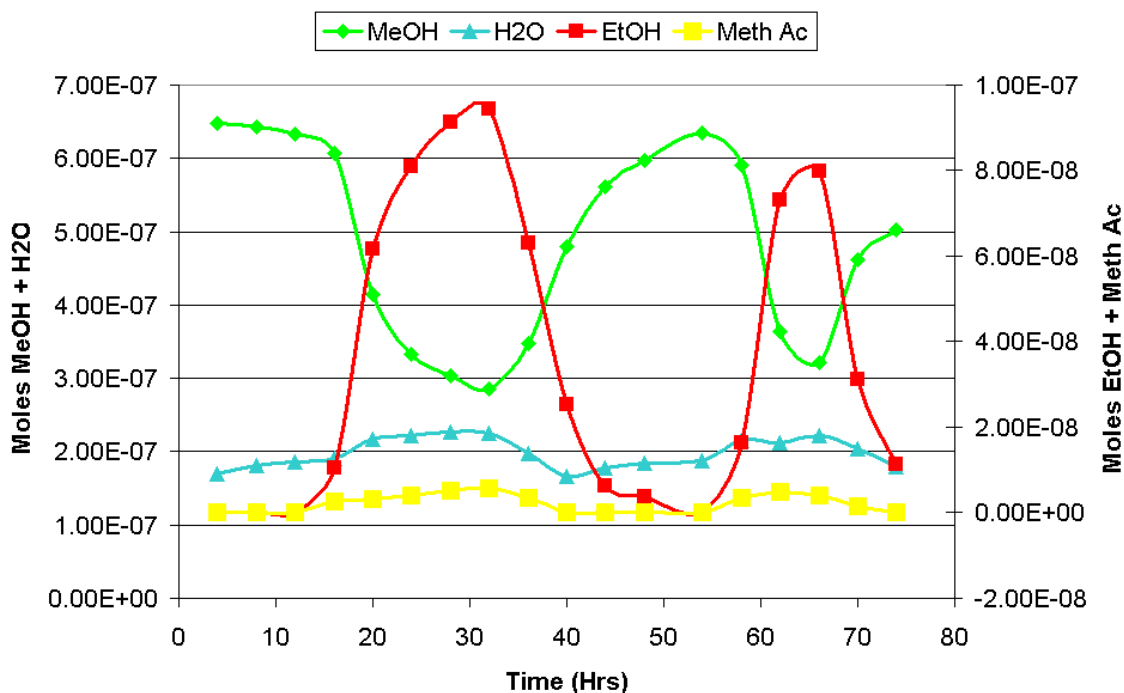


Figure 3-43 Reaction profile from 1.5mol% deuterated acid addition into CO/CO₂/H₂ system over Katalco 51-8 catalyst (non-deuterated acid fed in between 12 and 32hrs, deuterated acid fed in between 54 and approximately 64hrs)

Methanol production again decreased dramatically. As the deuterated acid was fed in for a shorter period of time (12hrs) than for the unlabelled addition (20hrs), the production of ethanol and methyl acetate did not reach the same levels. However if the additions were compared after 12hrs, both additions were similar and therefore the differences in the additions were most likely due to the length of time the acid was added in for, and not any kinetic isotope effect.

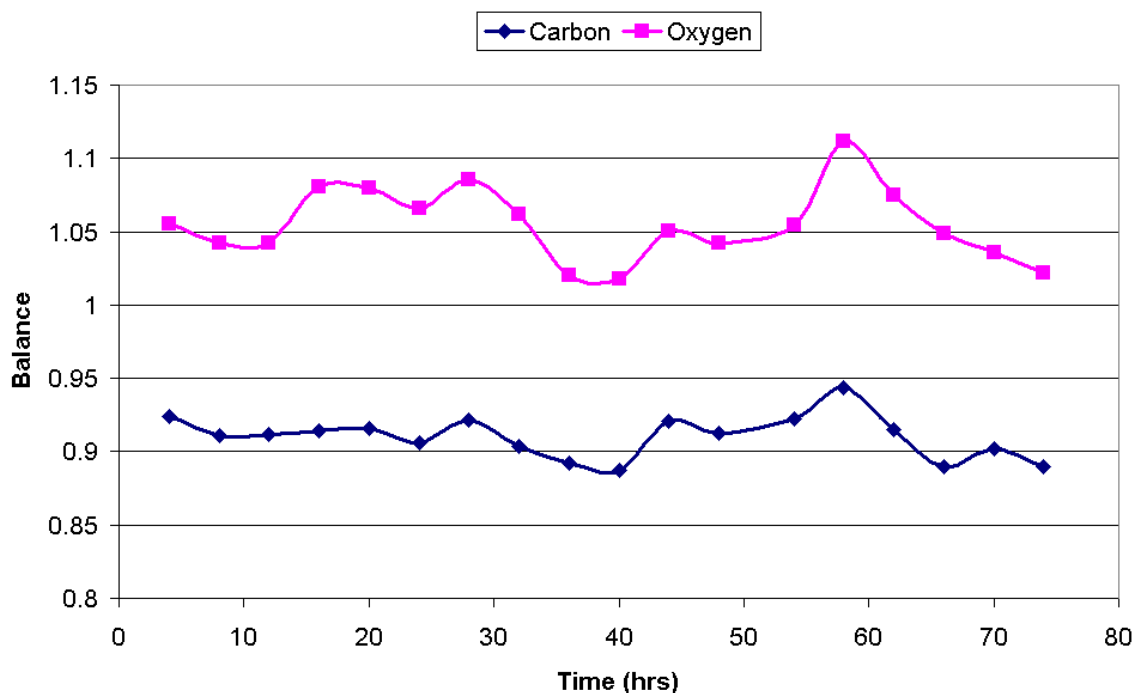


Figure 3-44 Mass balances from 1.5mol% deuterated acid addition into CO/CO₂/H₂ system over Katalco 51-8 catalyst (non-deuterated acid fed in between 12 and 32hrs, deuterated acid fed in between 54 and approximately 64hrs)

After the second addition it was observed that the methanol production did not return to its original level. However, further GC sampling was prevented by the loss of the carrier gas overnight. It was anticipated that had that not occurred, the methanol concentration would have been observed returning to normal.

Throughout both additions the carbon and oxygen balances remained reasonably steady, indicating that like the previous experiments, little carbon was deposited on the catalyst surface.

3.3.2.8 Acid Balance

Acid to Ethanol (%)	20.9
Acid to Methyl Acetate (%)	1.2
Acid to CO / CO ₂ (%)	84.2
Total (%)	106.3

Table 3-8 Acid balance from 1.5mol% deuterated acid addition into CO/CO₂/H₂ system over Katalco 51-8 catalyst

The acid balance of the system showed that all the acid that was fed into the system could be accounted for. The additions performed in the experiment were of the 1.5mol% level whereas in the previous systems the additions were of the 1.0mol% level. The increase in acid concentration resulted in an increase in the ethanol:methyl acetate ratio. In the 1mol% systems the ratio was 14:1 whereas in the 1.5mol% system the ratio was 17.4:1. This indicated that at higher concentrations of acid, ethanol was the favoured product.

3.3.2.9 Temperature Programmed Oxidation (TPO)

The TPO of the catalyst post reaction showed a similar profile to the TPO performed in the previous experiment, although a slightly larger evolution of CO₂ at low temperatures was observed. It was unclear as to why however, as the acid balance shows that all the acid fed in to the system was accounted for and was therefore not present on the catalyst surface.

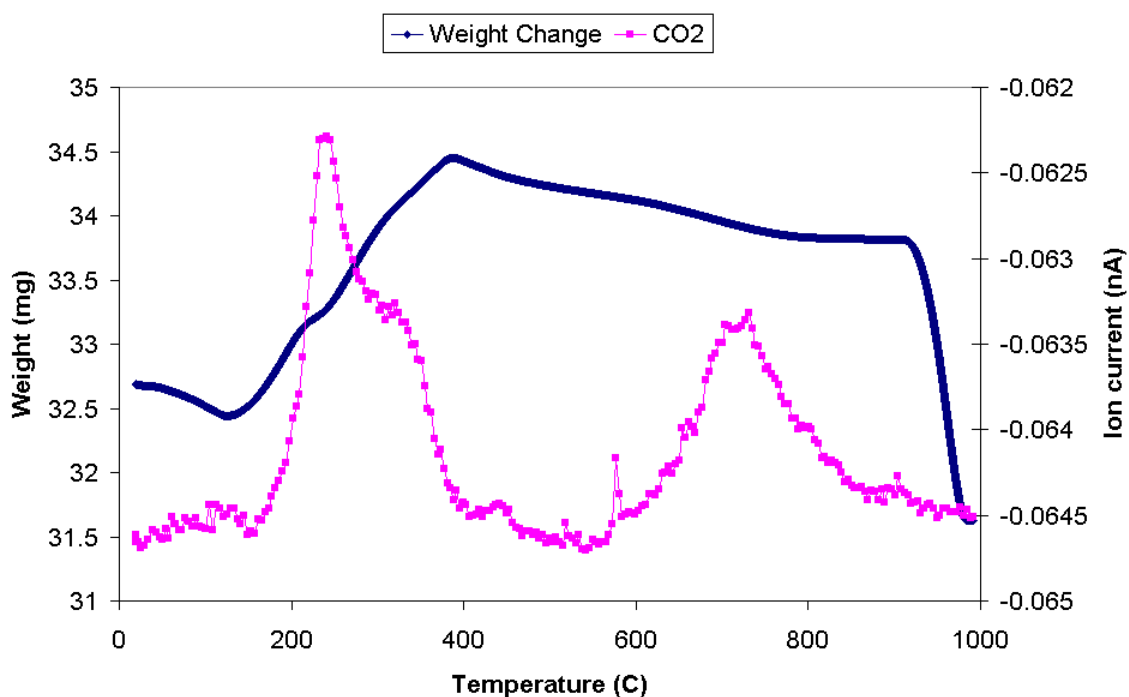


Figure 3-45 Post reaction TPO from 1.5mol% deuterated acid addition into CO/CO₂/H₂ system over Katalco 51-8 catalyst

In total, three evolutions of CO₂ were observed, two at low temperature (probably relating to methanol precursor species) and one at high temperature (probably relating to metal carbonate decomposition). Broad low temperature evolutions of

HDO and D₂O were observed as well, confirming the presence of deuterium on the catalyst surface.

3.3.2.10 Mass Spectrometry

The acid was fed in to the system at the following cycles:

Addition	Added (cycles)	Stopped (cycles)
CH ₃ CO ₂ H	1247	2916
CD ₃ CO ₂ D	5635	unknown

Table 3-9 Acid additions into CO/CO₂/H₂ system over Katalco 51-8 catalyst

(The exact cycle that the deuterated acid addition was unknown as the deuterated acid ran out overnight.)

Hydrogen

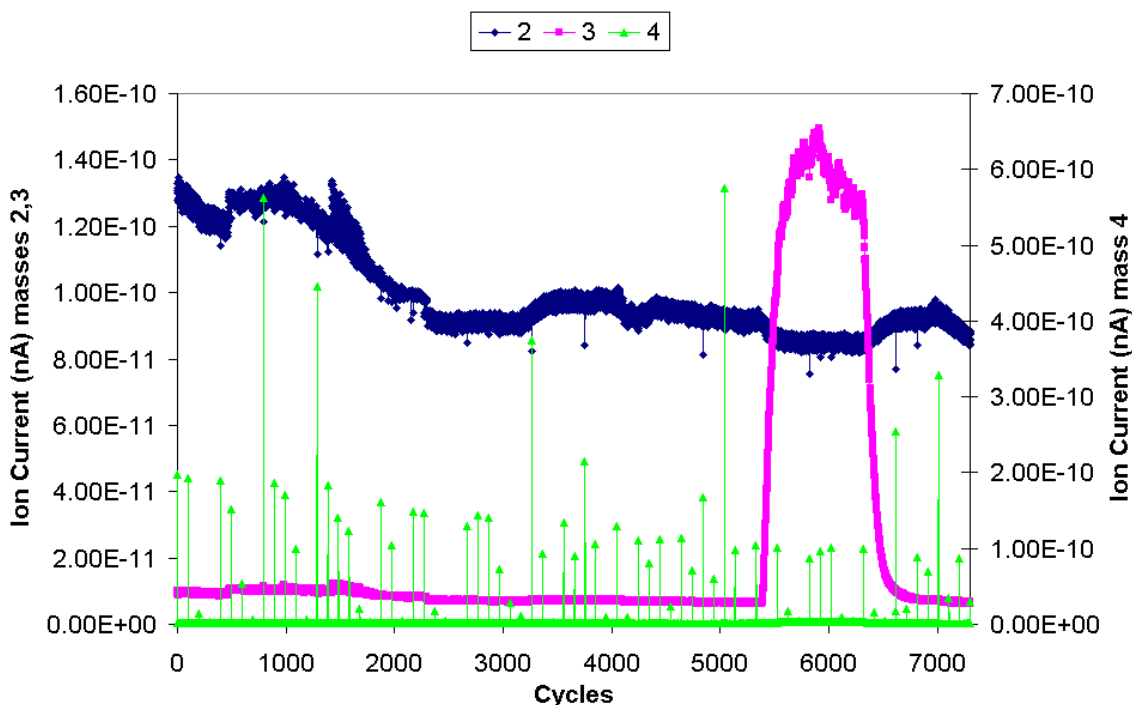


Figure 3-46 Mass spectra from 1.5mol% deuterated acid addition into CO/CO₂/H₂ system over Katalco 51-8 catalyst

The mass spectrometry results showed that for both acid additions, the levels of H_2 (mass 2) decreased. This was due to the increased hydrogenation activity, as the acid was readily hydrogenated to ethanol, a process requiring two moles of H_2 .

Mass 3 related to the presence of H-D. As expected there was no formation of HD during the undeuterated addition. However, when the deuterated acid was fed in, formation of H-D took place. This indicated that rapid exchange of the deuterium present on the surface acetate took place with adsorbed surface H_2 .

Mass 4 related to the formation of deuterium (D_2). However, no D_2 was formed as the concentration of hydrogen in the system was so high the chances of two D atoms combining to form D_2 were minimal. The ratio of hydrogen (H_2) in the system to deuterium in the acid (D_2) was 30:1

Water

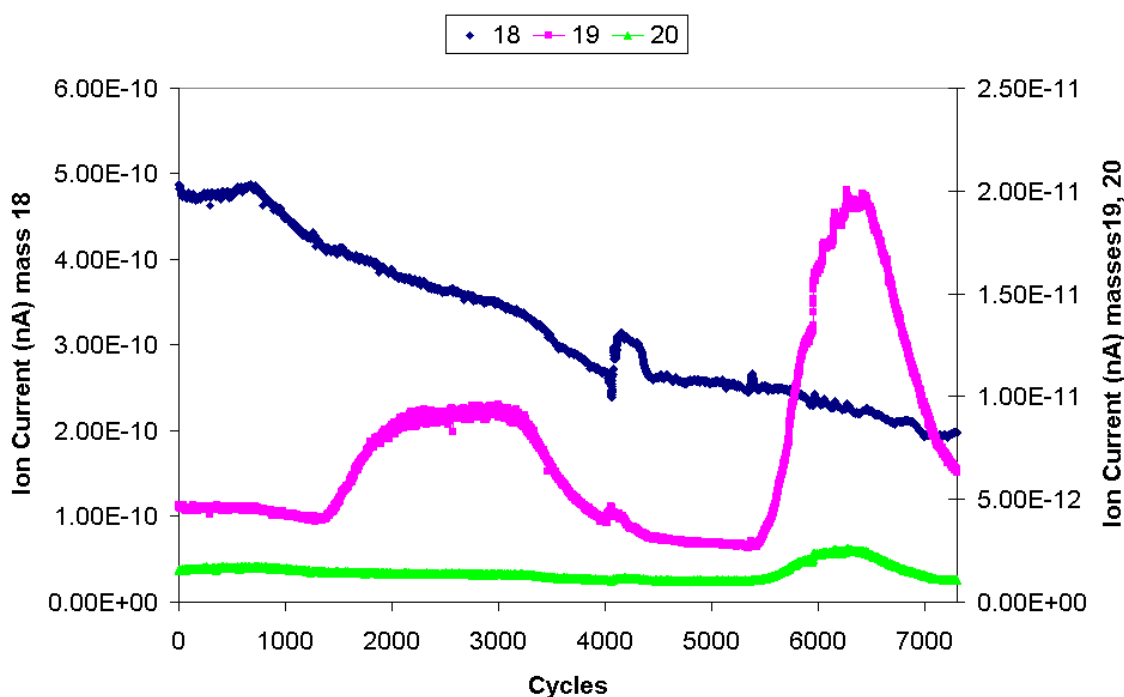


Figure 3-47 Mass spectra from 1.5mol% deuterated acid addition into $CO/CO_2/H_2$ system over Katalco 51-8 catalyst

The baseline for water (mass 18) was constantly decreasing throughout the course of the run, making observations difficult. However, a slight increase was evident upon the addition of the unlabelled acid, which was supported by the GC data. The GC data also showed an increase in water levels when the deuterated

acid was fed in, however no increase was observed in the mass 18 signal at this point. As explained previously the increase in water when the acid was introduced to the system was most likely derived from the hydrogenation of the acid to form ethanol and the condensation reaction between the acid and methanol to form methyl acetate. However, when the deuterated acid was fed in, water would not be produced, but rather HDO or D₂O. This was reflected by the increases in the mass 19 signal (HDO) and mass 20 signal (D₂O) when the deuterated acid was present.

The increase in mass 19 for the non-deuterated addition was at first suspected to be simply due to the isotopic abundance of H₂¹⁸O. However the increase was far too large in size and it was unclear as to why. The response could still be used for comparison for the deuterated addition. The increase in mass 19 for the deuterated addition was much larger and was attributed to the production of HDO.

Methanol

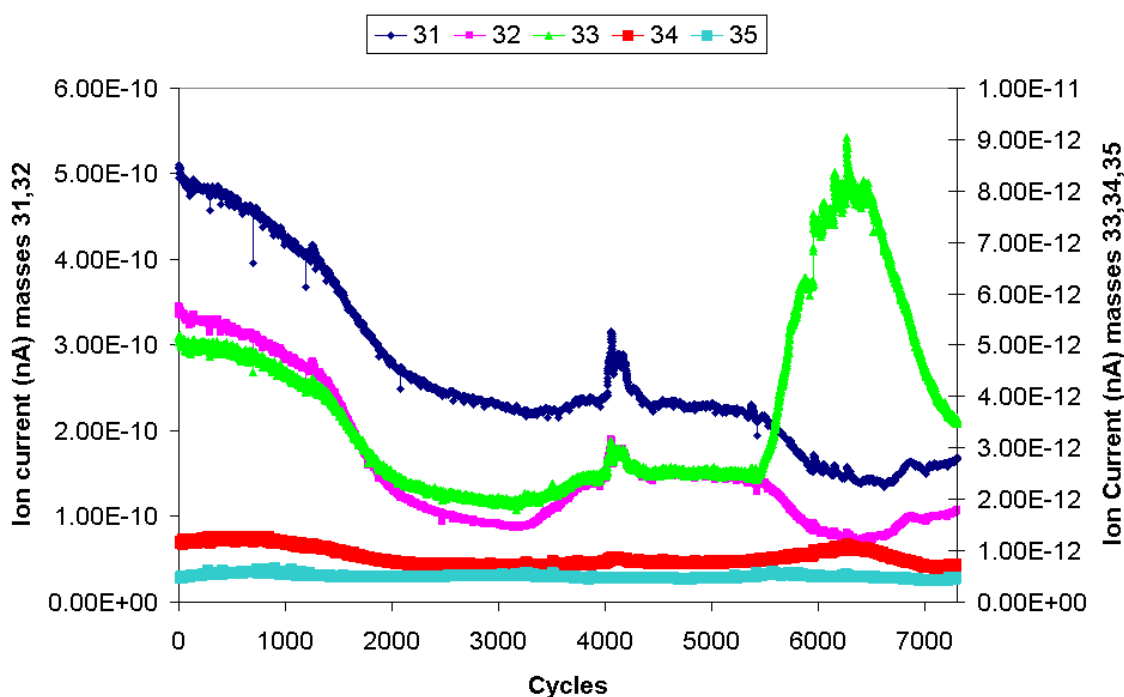


Figure 3-48 Mass spectra from 1.5mol% deuterated acid addition into CO/CO₂/H₂ system over Katalco 51-8 catalyst

The mass spectrometer data for the run showed that the mass fragments for methanol (masses 31 and 32) correlated very well with the GC data, with obvious decreases upon introduction of both the deuterated and the undeuterated acid.

Interestingly, masses 33 and 34 both showed an increase upon addition of the deuterated acid, indicating that deuterium was present in the methanol. Only two pathways could have led to the presence of deuterium. Firstly if the deuterated acid was converted to methanol, and secondly if exchange from HD or surface deuterium took place. The conversion of acetic acid to methanol was ruled out, as the previous ^{13}C labelling studies showed no incorporation of the label into methanol. Therefore the presence of deuterium in the methanol could only have occurred through exchange with deuterium either on the catalyst surface or from the gas phase HD.

Masses 33 and 34 were attributed to be mono-deuterated methanol and di-deuterated methanol respectively. Mass 35 showed no response throughout the run for both the undeuterated and the deuterated additions.

Ethanol

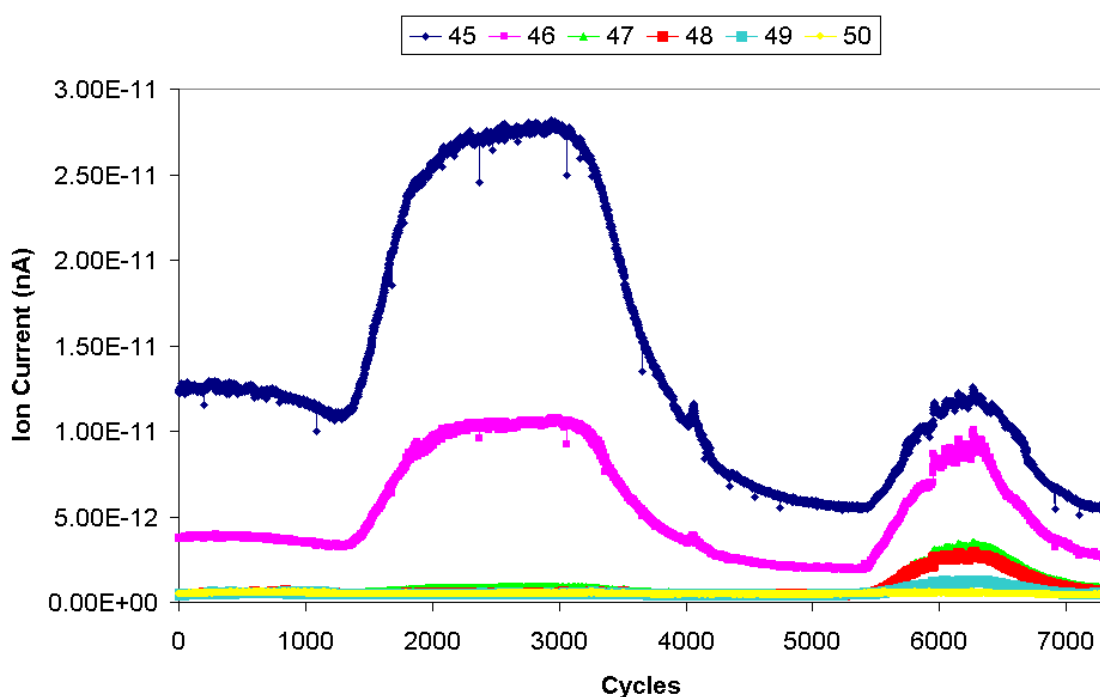


Figure 3-49 Mass spectra from 1.5mol% deuterated acid addition into $\text{CO}/\text{CO}_2/\text{H}_2$ system over Katalco 51-8 catalyst

For the undeuterated addition, responses were observed in masses 45 and 46. These masses corresponded to the production of ethanol. The ratio of the ion currents of the masses respective to each other matched exactly with the relative abundance of each mass. This ratio was used to aid identification of the mass

fragments in the deuterated addition. Mass 45 represented undeuterated ethanol and a reasonable increase was observed. Mass 46 was assigned to being mono deuterated ethanol, as was mass 47. Mass 48 and mass 49 were assigned to be doubly deuterated ethanol and tri deuterated ethanol respectively. No response was observed in the mass 50 signal for both the deuterated and undeuterated addition.

The results showed clearly that deuterium was present in the ethanol to varying degrees. As the production of ethanol was due to the hydrogenation of the deuterated acid, it was expected that some deuterium would still be present. Up to 3 deuterium atoms were detected present in the ethanol, indicating that possibly a whole deuterated methyl group remained. The increase in mass 45 upon addition of the deuterated acid indicated that the deuterium was fully exchanged with hydrogen for a portion of the ethanol.

Methyl Acetate

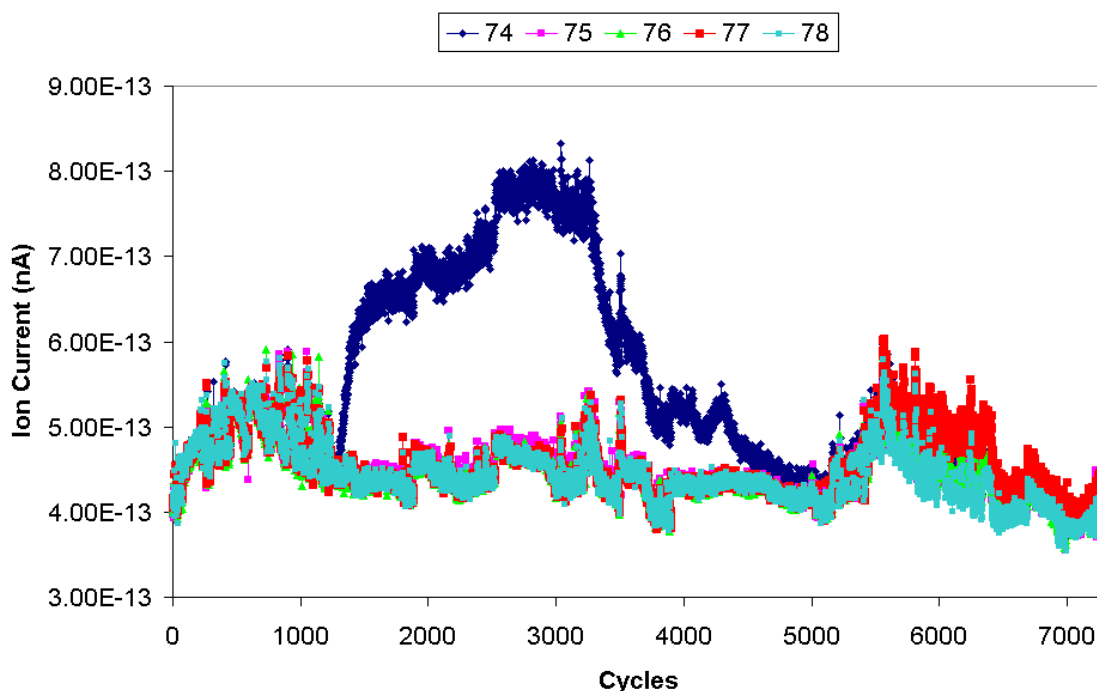


Figure 3-50 Mass spectra from 1.5mol% deuterated acid addition into CO/CO₂/H₂ system over Katalco 51-8 catalyst

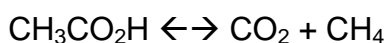
The mass spectrometry data showed only an increase in the mass 74 signal for the undeuterated acid addition. Mass 74 was the mass fragment corresponding to undeuterated methyl acetate. For the deuterated addition, responses were

observed for masses 74-78, indicating that deuterium was present in the methyl acetate to varying degrees.

3.3.2.11 Summary

The results from the ^{13}C labelling studies confirmed that acetic acid was a precursor to both ethanol and methyl acetate as the label showed up in both compounds. The mechanisms would be the hydrogenation of the acetic acid to form the ethanol and an esterification reaction involving the acid and methanol to produce methyl acetate. The ^{13}C label was also found to be incorporated into the CO_2 , confirming that a route for acetic acid to be converted to CO/CO_2 existed. Although the label was not able to be observed in the CO due to overlapping with a methanol fragment, it can be assumed that the label will be present at least through the WGS, if not directly.

The label was not detected in methanol, ruling out decomposition of the acid via a surface formate. No methane formation was observed throughout both the labelled and unlabelled additions. This was important as one of the proposed routes for acetic acid conversion to CO/CO_2 was through decomposition. Acetic acid has been shown to decompose on metal surfaces via a simple decarboxylation to yield methane and CO_2 [95-97].



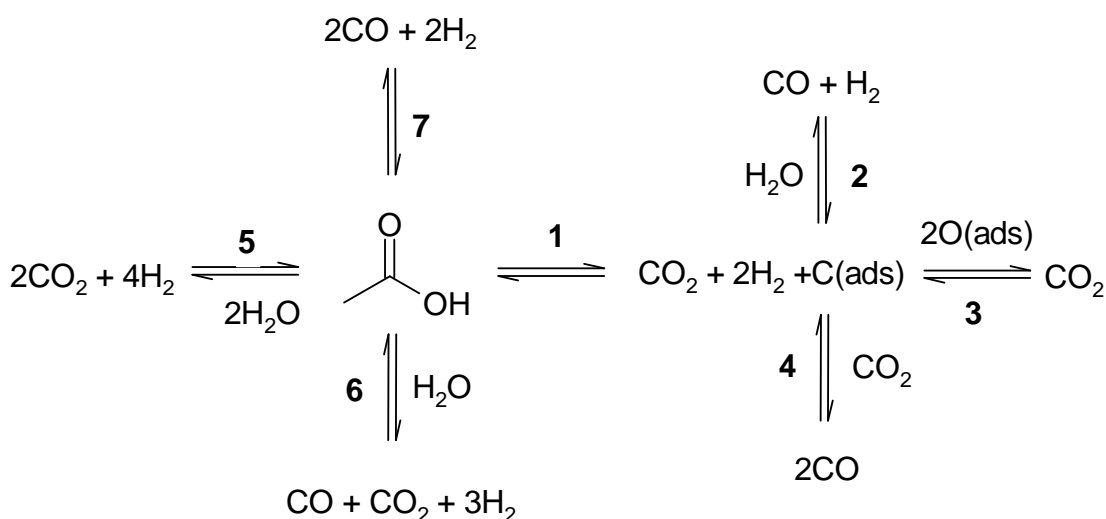
However, if decomposition occurred in the current system the methyl group of the acetic acid must decompose further, rather than pick up a proton to form methane. Oxidation of the surface carbon could then take place to yield CO/CO_2 .

The deuterated acid studies revealed that there was no kinetic isotope effect when deuterium was present in the acid. The deuterium was found to be incorporated in hydrogen, water, ethanol, methyl acetate and methanol. Incorporation into the methanol was through deuterium on the surface of the catalyst being utilised during the hydrogenation of CO_2 . Post reaction TPO confirmed the presence of deuterium on the catalyst surface.

3.3.3 Conversion of Acid to CO/CO₂

Although the labelling studies identified that a route for converting acetic acid to CO/CO₂ existed, they revealed little as to the mechanism. Initially it was considered that decomposition of the acetate to a surface formate could be occurring, this mechanism was ruled out on the basis that carbon labelling did not show migration of acetic acid carbon to methanol (methanol being the hydrogenation product of formate).

Other possibilities remained such as hydrolysis, and also decomposition of the acid via decarboxylation followed by reoxidation of surface carbon. Several different routes for the conversion of acid to CO/CO₂ along with the associated ΔG values are shown below:



- | | |
|--|--|
| 1) $\Delta G_{523} = -64.55\text{kJ mol}^{-1}$ | 5) $\Delta G_{523} = -23.71\text{kJ mol}^{-1}$ |
| 2) $\Delta G_{523} = +60.44\text{kJ mol}^{-1}$ | 6) $\Delta G_{523} = -4.11\text{kJ mol}^{-1}$ |
| 3) $\Delta G_{523} = \text{unknown}^*$ | 7) $\Delta G_{523} = +15.49\text{kJ mol}^{-1}$ |
| 4) $\Delta G_{523} = +80.04\text{kJ mol}^{-1}$ | |

*A ΔG value was unable to be obtained for route three, as thermodynamic data on adsorbed oxygen was unavailable

Routes **5** and **6** show the possible hydrolysis routes, and the associated ΔG values suggested that both mechanisms were plausible. Routes **1** and **7** were both possible decomposition pathways to CO and CO₂, although the associated ΔG

values suggested that route **7** was not as favourable. Routes **2**, **3** and **4** were possible ways that the surface carbon could be re-oxidised.

Overall, the most likely route towards CO₂ was through decomposition. Although two routes for the decomposition were included for completeness, thermogravimetric studies have previously shown that surface acetate groups decompose via route **1** on transition metal surfaces [95-97, 125, 126]. The oxidation of the surface carbon however could proceed through three routes and it was unclear as to what route (if any) was occurring.

It was of interest to determine if hydrolysis of the acetic acid on the surface of the catalyst was a route towards CO/CO₂. Although energetically favourable, the hydrolysis of acetic acid, or indeed any carboxylic acid in the gas phase had not been observed in the literature previously. It was decided to investigate as to whether these processes were occurring over the Katalco catalyst.

3.3.3.1 Experimental

Prior to reaction, the Katalco 51-8 catalyst was reduced *in situ* in the reactor under 50ml min⁻¹ flowing hydrogen at a temperature of 523K. The catalyst was held at this temperature for 3hrs.

To investigate the effects of water on the acid, an experiment was designed whereby instead of concentrated acid being fed in to the system, a mix of water and acetic acid (2:1 molar mix) was fed in. As the presence of water would affect the water gas shift reaction, it was decided to remove CO and CO₂ from the feed and replace with nitrogen. This would also allow any CO/CO₂ evolved from the acid to be easily detected. The exact gas mix composition used was 60ml N₂ / 190 ml H₂.

- Reaction Temperature (K) 523
- Pressure (barg) 50
- Gas Flow (ml min⁻¹) 250
- Catalyst Volume (ml) 1.36

- GHSV (hr^{-1}) $\sim 11,000$

The acid was fed in at a molar feed rate of $4.51 \times 10^{-7} \text{ moles min}^{-1}$ and the water was fed in at a molar feed rate of $9.01 \times 10^{-7} \text{ moles min}^{-1}$.

3.3.3.2 Acetic Acid / Water Addition

The acetic acid/water mix was fed in to the system from the beginning. Sampling began after 2hrs. Ethanol was the main carbon based product formed, and was expected due to the reducing nature of the feed gas.

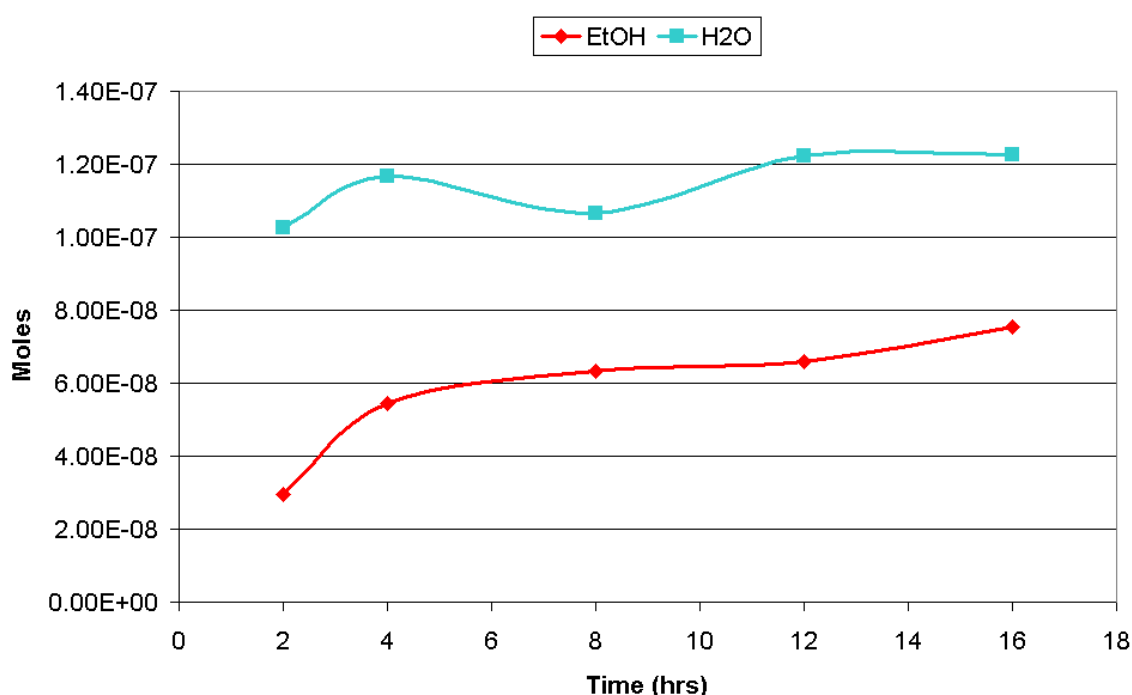


Figure 3-51 Reaction profile from acid / water addition into N_2/H_2 system over Katalco 51-8 catalyst (acid fed in continuously after 2hrs)

Other carbon based species observed included ethyl acetate, acetic acid and methanol. The ethyl acetate observed was simply a condensation reaction between the acetic acid and the ethanol produced through the hydrogenation of the acid. In the classic methanol synthesis system methyl acetate was formed as methanol was the abundant alcohol. In the absence of CO and CO_2 in the feed, the ethanol became the abundant alcohol. Although methanol was detected in the system, its presence was attributed to being an artefact from a previous run rather than as a product from the addition of acetic acid.

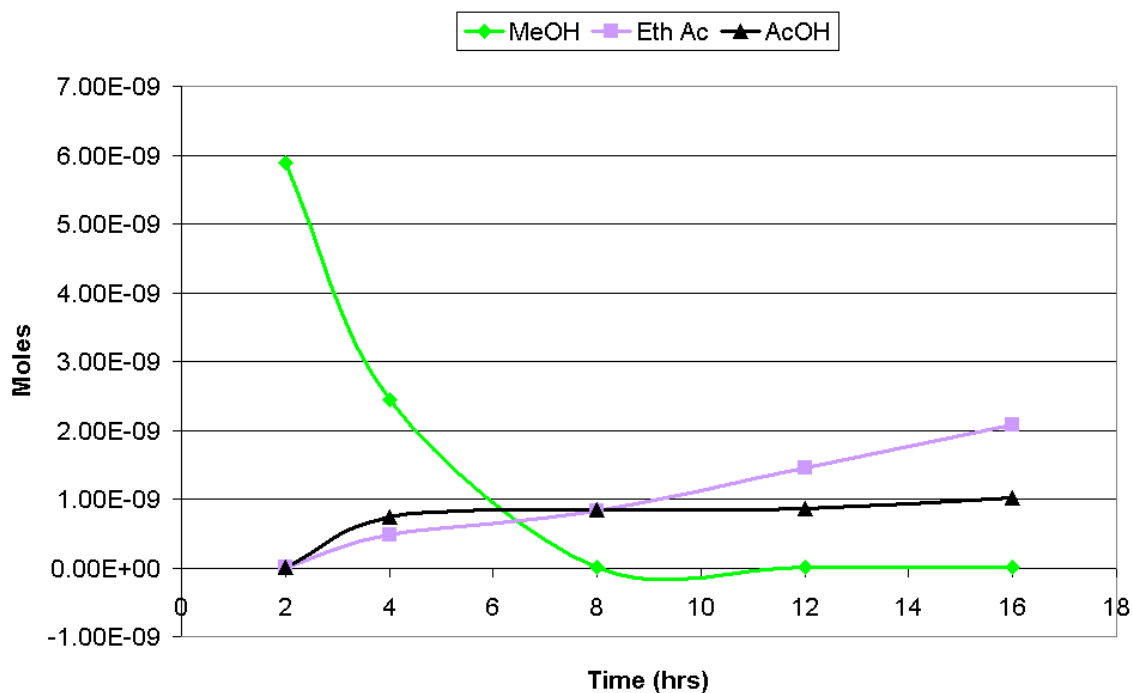


Figure 3-52 Reaction profile from acid / water addition into N_2/H_2 system over Katalco 51-8 catalyst (acid fed in continuously after 2hrs)

A small concentration of acetic acid was also observed emerging through the system unreacted.

Although a reasonable concentration of water was detected throughout the experiment (from the liquid feed and also the hydrogenation / condensation reactions of acetic acid) neither CO nor CO_2 were detected by the GC analysis. This suggested that hydrolysis was not involved in the process whereby the acid was converted to CO/ CO_2 . Both the carbon balance and the oxygen balances of the system showed that substantial amounts of carbon and oxygen were missing

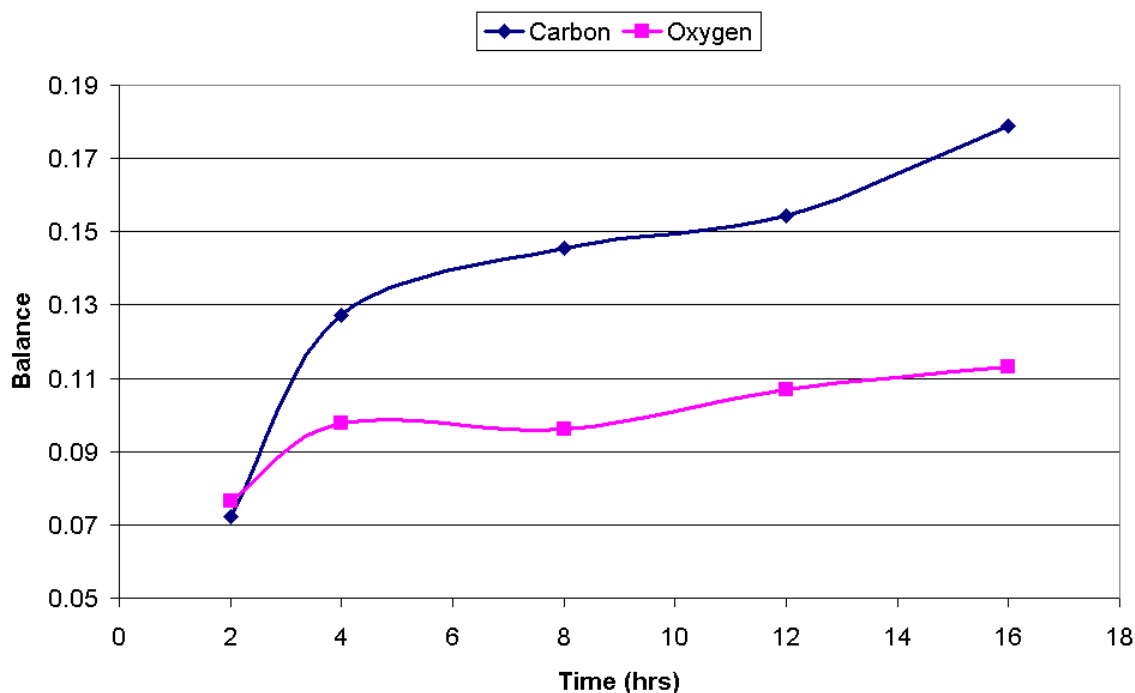


Figure 3-53 Mass balances from acid / water addition into N_2/H_2 system over Katalco 51-8 catalyst (acid fed in continuously after 2hrs)

This indicated that the missing carbon and oxygen were deposited on the catalyst surface. Although the result ruled out the possibility of acid hydrolysis, it also suggested that both the postulated decomposition of acetic acid and the subsequent oxidation of surface carbon mechanisms were also possibly incorrect.

3.3.3.3 Decomposition

Firstly, the postulated decomposition mechanism of the acid on the surface of the catalyst would yield gas phase CO_2 as well as an adsorbed methyl group. No CO_2 was detected by GC analysis. However the possibility of a different decomposition pathway under the reducing conditions was a distinct possibility. In the original paper on decomposition, Bowker acknowledged that reconstruction of the crystal surfaces could be a factor in the decomposition of the acetate[97]. This opened up to the possibility that the breakdown of the acid was structure sensitive. Further literature search revealed that the copper particles of methanol synthesis catalysts were directly affected by the nature of the feed gas surrounding them [58, 59, 69]. Under reducing conditions the formation of oxygen vacancies at the Cu-ZnO interface resulted in an increased interaction with the copper particles and the formation of disc like particles with higher surface areas. Under more oxidising conditions this effect did not occur and more spherical particles were present. The

dynamic morphology of the copper particles was attributed to gas-induced changes in the Cu/ZnO interface energy.

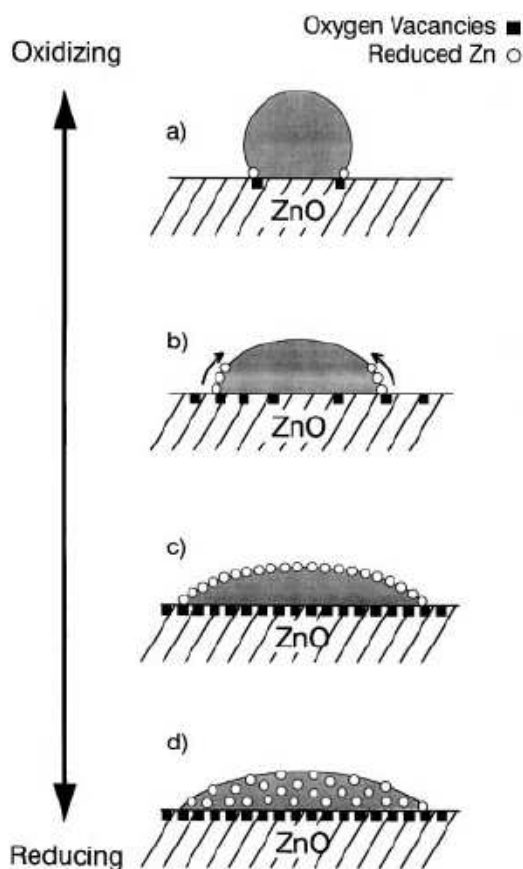


Figure 3-54 Schematic model for wetting / non wetting of copper on zinc surface[59]

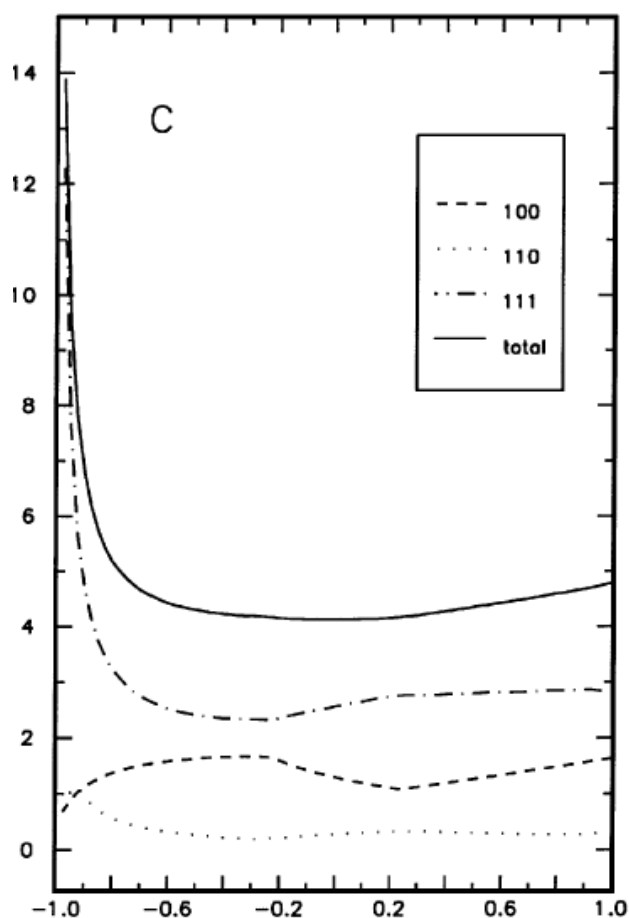


Figure 3-55 The dimensionless surface area $A/V^{2/3}$ (y axis) of the different facets versus the contact surface free energy γ / γ_0 (x axis)[69]

Changes in the morphology of the copper particles also resulted in a change of the relative abundances of different crystal planes. Under reducing conditions there was an increase in Cu(110) and Cu(100) planes, which were more active than Cu(111) for methanol synthesis[58, 59, 69].

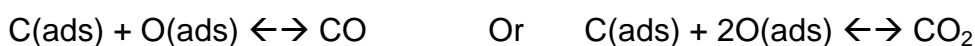
The studies indicated that the morphology of the copper particles varied under different gas environments. The shifts in morphology could explain why acid conversion to CO/CO₂ was observed under the classic methanol synthesis feed, but not under the N₂/H₂ feed. It was possible that the route was structure sensitive, and that under the N₂/H₂ feed, the morphology of the copper was not able to catalyse the conversion of acid to CO/CO₂ via decarboxylation. Instead, complete

decomposition of the acetate on the catalyst was postulated to proceed, with carbon fragments deposited on the surface.

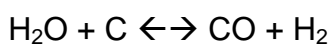
3.3.3.4 Oxidation of Surface Carbon

The result also suggested that the postulated oxidation of deposited carbon was incorrect. As shown by the mass balances throughout the reaction, a significant amount of both oxygen and carbon were missing, and presumably deposited on the surface of the catalyst. If this were the case then oxidation of the surface carbon would have been able to take place, as a significant amount of oxygen was present. The fact that CO/CO₂ was not observed suggested that the mechanism (route 5 in the earlier schematic) was incorrect.

However it was envisaged that for the oxidation of the surface carbon to proceed, adsorbed atomic oxygen was required on the catalyst surface.



With water in the feed, it was possible that the adsorbed water on the surface of the catalyst could have oxidised the surface carbon via the following mechanism:

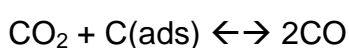


However, in the literature it has been observed that water does not adsorb molecularly on the surface of the catalyst at the reaction temperature, but rather dissociates on the catalyst surface to form surface hydroxide groups and gas phase hydrogen[139]:



As the oxygen was not present on the surface of the catalyst in atomic form, but rather as hydroxyl groups, it was possible that the hydroxyl groups may not have been able to oxidise the surface carbon.

Another route of oxidising the surface carbon similar to oxidation by surface water would be a reverse Boudouard reaction involving CO₂.



As CO₂ was not present in the current system, the conversion of surface carbon to CO could not take place. Under classic methanol synthesis feeds where CO₂ was present, the process could proceed. Investigation of the gas feed composition was required to ascertain as to whether this process could take place.

3.3.3.5 Acid Balance

Acid to Ethanol (%)	16.3
Acid to Ethyl Acetate (%)	0.9
Unreacted Acid (%)	0.2
Total (%)	17.4

Table 3-10 Acid balance from acid / water addition into N₂/H₂ system over Katalco 51-8 catalyst

The acid balance confirmed that a substantial amount of the acid was missing, and had been laid down on the catalyst surface.

3.3.3.6 Temperature Programmed Oxidation (TPO)

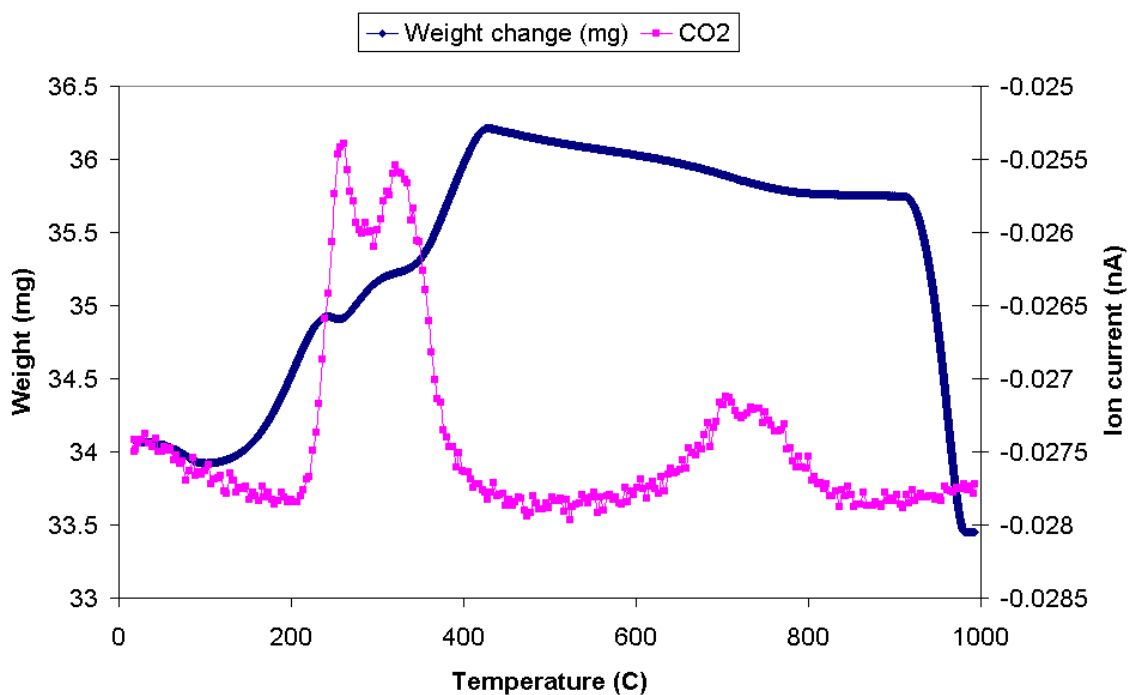


Table 3-11 Post reaction TPO from acid / water addition into N₂/H₂ system over Katalco 51-8 catalyst

The TPO of the catalyst post reaction showed the usual weight increase upon exposure to the oxidising feed, converting the reduced copper metal to copper oxide. The weight increase profile however was perturbed twice, at 271°C and 321°C. These perturbations corresponded to separate evolutions of CO₂ from the catalyst surface. A DSC trace indicated that the evolutions were exothermic, and suggested that surface carbon was being burned off. A substantial amount of carbon was removed from the catalyst, enough to disrupt the weight increase of the sample due to copper oxidation.

Previously these low temperature deposits were thought to be formate groups on the surface of the catalyst, or other methanol precursor species. Carbon laydown was also a possibility. As methanol synthesis was not carried out, the presence of formate groups on the surface of the catalyst was ruled out. Further investigations into the species deposited on the catalyst were required.

The usual high temperature evolution was also observed, and was thought to be metal carbonate decomposition.

3.3.3.7 Summary

Overall, the experiment showed that no CO/CO₂ was produced upon introduction of an acid/water mix over the Katalco catalyst. This confirmed that the acid was not being hydrolysed in the system, but most probably decomposing on the surface of the catalyst.

However, the decomposition profile of the acetate on the surface of the catalyst was different to that proposed in the literature. Several studies have shown that on transition metal surfaces the acetate decomposed to yield gas phase CO₂ and H₂, with adsorbed carbon left on the surface [95-97, 125]. However, no CO₂ was detected upon the introduction of the acid. This suggested that the mechanism of decomposition under the N₂/H₂ feed was not a decarboxylation.

One possibility was that the decomposition of the acid was structure sensitive. The literature revealed that the morphology of copper particles in methanol synthesis catalysts were directly related to the atmosphere surrounding them [58, 59, 69]. The morphology was sensitive to the gas feed composition. It was therefore

possible that under the N_2/H_2 system the decomposition route was different to that under a $CO/CO_2/H_2$ feed.

The mass balances of the system showed a substantial amount of carbon and oxygen missing, with both deposited on the catalyst surface. The TPO of the catalyst post reaction confirmed that substantial deposits of carbon were present. The presence of both deposited carbon and oxygen on the surface of the catalyst would have presumably led to oxidation of the surface carbon, however as mentioned, no CO or CO_2 was detected in the system.

As no CO or CO_2 production was observed, it was apparent that oxidation of the surface carbon via water did not take place, possibly due to the water dissociating to surface hydroxyl groups rather than remaining in a molecular form. Oxidation via CO_2 in a reverse Boudouard type reaction was still possible, as the feed gas did not contain CO_2 .

3.3.4 Acetate/Carbonate TGA Studies

The identity of the carbonaceous species present on the surface of the catalyst could not be identified from simply running post reaction TPOs of the catalyst, as all the carbon evolved came off in the form of CO_2 . Thermogravimetric analysis of the post reaction catalysts under inert feed also did not aid in the identification of the species present.

As metal carbonates and metal acetates were previously suggested as possible species on the catalyst, it was decided to investigate the breakdown of these species under the same conditions used for the post reaction TPO'S.

3.3.4.1 Experimental

The chemical composition of the Katalco 51-8 catalyst contained principally four metals: Cu , Zn , Mg and Al . If carbonates or acetates were present on the surface of the catalyst then in principle they could be present on any or all of the metals. It was therefore decided to test a series of metal acetates and metal carbonates using the same TPO heating profile as used for the analysis of post reaction catalysts.

The exact compounds and purities used are listed in the Experimental section.

3.3.4.2 Acetates

Several studies in the literature have been performed on the thermal decomposition behaviour of metal acetates [140-142]. The importance of metal acetates arises from their use for the preparation of metal and metal oxide catalysts. On decomposition, metal acetates often yield acetone and acetic acid and there may be incomplete melting and some hydrolysis of hydrated salts[140, 142].

Copper acetate was found to decompose to yield CO_2 at $\sim 280^\circ\text{C}$, with a slight shoulder peak apparent at $\sim 293^\circ\text{C}$. In the literature the thermal decomposition of hydrated copper acetate was believed to yield CO_2 , H_2 , CH_4 , ketene fragments and surface carbon. However in the present system as the studies were performed in an oxidising environment, CO_2 was the only carbon based product. The decomposition of zinc acetate took place at a higher temperature with an evolution of CO_2 observed at 322°C .

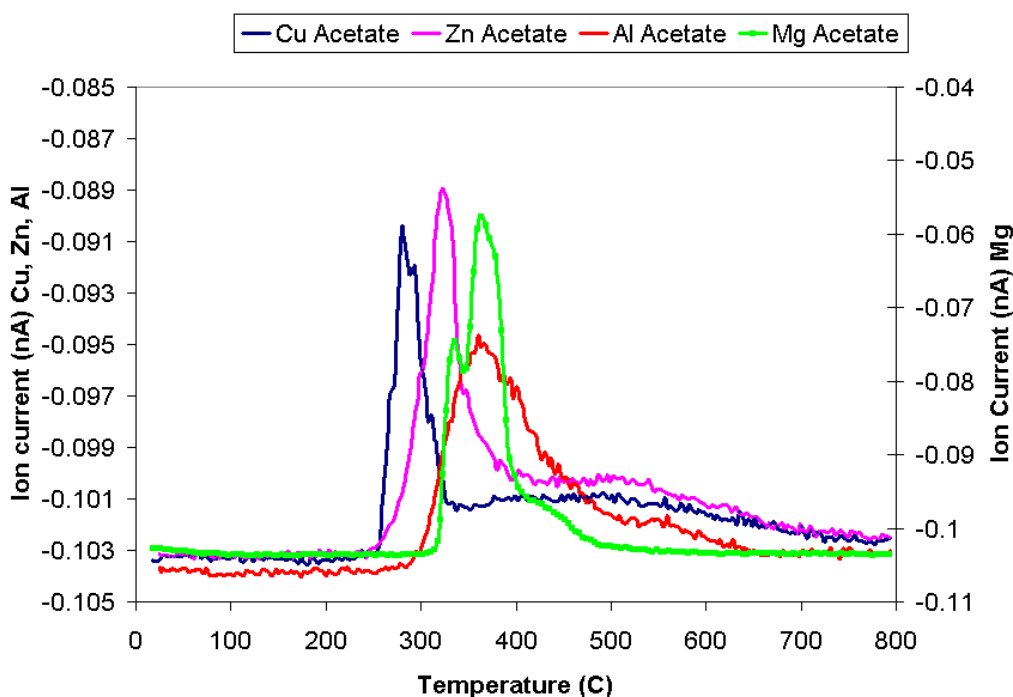


Figure 3-56 TGA data from decomposition of metal acetates in O_2/Ar

If the decomposition temperatures of copper and zinc acetate, 275°C and 322°C respectively, were compared with the low temperature CO_2 evolutions from the TPO of the previous experiment, the evolutions matched exactly. This indicated that it was possible that the carbonaceous species observed on the surface of the

catalyst post reaction were surface acetate groups of copper and zinc. As copper and zinc were the main metallic constituents of the Katalco catalyst, it was likely that the largest concentrations of acetate would be present on these metals.

Evolutions of CO₂ were observed from the breakdown of aluminium acetate and magnesium acetate at temperatures of 360°C and 363° C respectively. Although the decomposition of the acetates were at higher temperatures than observed for the copper and zinc, aluminium and magnesium were present in the catalyst to a much smaller degree. It was therefore possible that aluminium and magnesium acetates were formed as well during the acid addition, but were not observed in the post reaction TPO's due to overlapping with zinc and copper acetate decomposition.

3.3.4.3 Carbonates

The formation of carbonates over metal catalysts during reactions involving CO/CO₂ has been observed previously by several research groups. The mechanism is proposed to proceed via the reaction of CO₂ with support O²⁻ and OH⁻ groups to form CO₃²⁻ or HCO₃⁻ [110, 143]. Formation of carbonates has been shown to occur on basic supports such as MgO previously [144].

The thermal decomposition of metal carbonates is well known in the literature. The general equation is shown below, where M = any metal:



The TGA studies of the three metal carbonates (aluminium carbonate could not be obtained) revealed that the decomposition of the carbonates all took place below 600°C. Zinc carbonate decomposed first, at a temperature of 265°C, whereas copper carbonate decomposed at 333°C. The temperature of the evolutions suggested that the breakdown of these metal carbonates could be at least partly responsible for the low temperature evolutions of CO₂ observed in the post reaction TPO's.

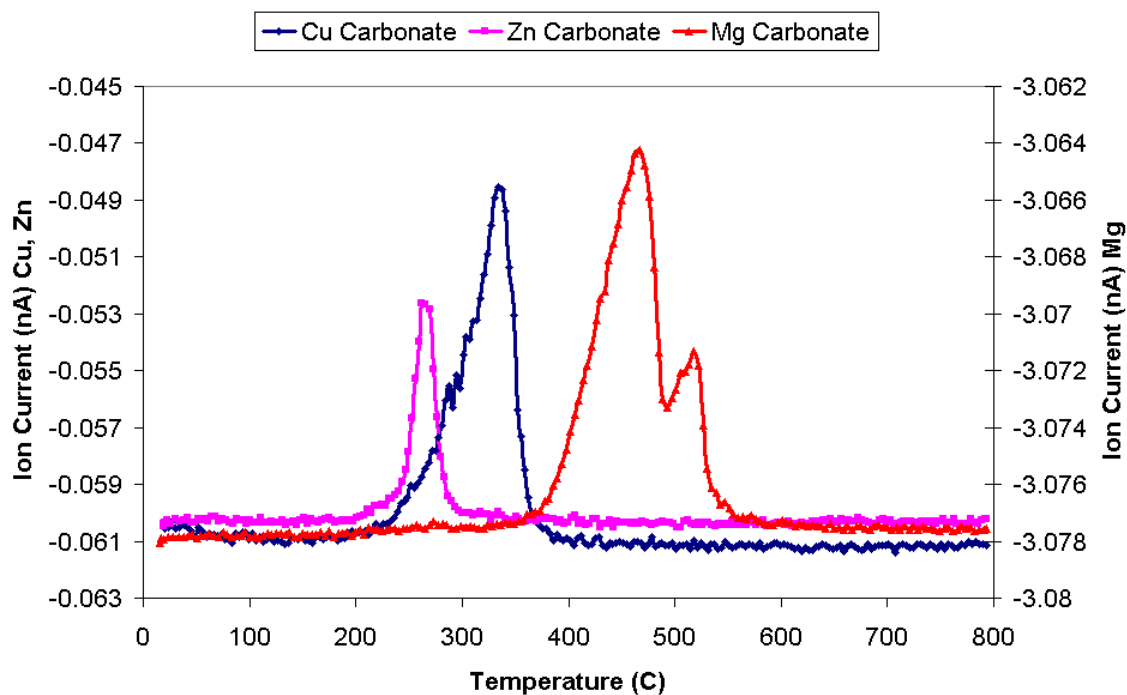


Figure 3-57 TGA data from decomposition of metal carbonates in O₂/Ar

Magnesium carbonate decomposed later in a two step decomposition, at temperatures of 467°C and 517°C.

The results indicated that metal carbonate decomposition was not responsible for the high temperature evolution of CO₂ that was observed in the post reaction catalyst TPO's, as the evolutions were at much lower temperatures.

3.3.4.4 Summary

The results from the TGA studies suggested that the low temperature evolutions from the post reaction catalyst TPO's were possibly due to a mixture of copper and zinc acetates and carbonates. This was not unexpected as copper and zinc are the main metallic components of the Katalco catalyst.

Under a methanol synthesis feed, it's likely that formate species or other methanol precursor species would still be present on the catalyst, and could therefore contribute to the low temperature evolutions. Further TGA studies on metal formates, the closest stable intermediate to methanol would be required to investigate this possibility. In the literature copper formate has been shown to decompose at ~200°C[145], although studies adsorbing methanol and formic acid onto CuO have shown that the decomposition of formate occurs at ~277°C[146].

At that temperature, the decomposition of surface formates are a possibility for the evolutions of CO₂ observed in the systems with and without acid additions.

The TGA studies however did not yield any information as to the nature of the high temperature species. The metal carbonates decomposed at much lower temperatures, ruling them out. Therefore it was thought that the evolution could actually be due to the breakdown of the catalyst binder. As the binder used by the manufacturers of the Katalco catalyst remains confidential, studies into this possibility are prevented.

3.3.5 Gas Composition Studies

Although hydrolysis of the acetic acid was shown not to take place, altering the feed gas composition from CO/CO₂/H₂ to the N₂/H₂ atmosphere resulted in a change in the behaviour of the acid. Decomposition via decarboxylation did not proceed (as suggested by the literature) and no CO/CO₂ was produced. Several possibilities were suggested as to why, such as morphological changes of the copper particles leading to a structure sensitive decomposition and also the possibility that water could not oxidise the surface carbon.

As the morphology of the copper particles had been previously shown in the literature to change depending on the feed gas environment surrounding them [57-59, 69], it was decided to carry out a programme of work investigating the effects of altering the feed gas composition on the behaviour of the acid. It was also of interest as to whether CO₂ present in the feed would lift off surface carbon, in a reverse Boudouard mechanism.

3.3.5.1 Reaction Conditions

Prior to reaction, the catalyst was reduced *in situ* in the reactor under 50ml min⁻¹ flowing hydrogen at a temperature of 523K. The catalyst was held at this temperature for 3hrs.

The following reaction conditions were used:

- Reaction Temperature (K) 523
- Pressure (barg) 50

- Gas Flow (ml min^{-1}) 250
- Catalyst Volume (ml) 1.36
- GHSV (hr^{-1}) $\sim 11,000$

The feed gas was varied for each experiment, to allow the effect of each gas component on the behaviour of the acid to be observed. The gas feeds used are listed below:

Gas Composition	MI min^{-1}
N_2	250
N_2 / H_2	60 / 190
$\text{N}_2 / \text{CO} / \text{H}_2$	10 / 80 / 160
$\text{N}_2 / \text{CO}_2 / \text{H}_2$	10 / 60 / 180
$\text{N}_2 / \text{CO} / \text{CO}_2 / \text{H}_2$	10 / 25 / 25 / 190

Table 3-12 Feed gas compositions

In all experiments N_2 was used as a reference gas, for the calculation of conversion. Acetic acid was fed in to each system at a molar feed rate of 1.0mol% (3.1×10^{-7} moles min^{-1}).

3.3.5.2 Nitrogen Atmosphere (N₂)

Under a N₂ atmosphere there was very little conversion of the acid to other products, with only small traces of ethanol and methanol observed.

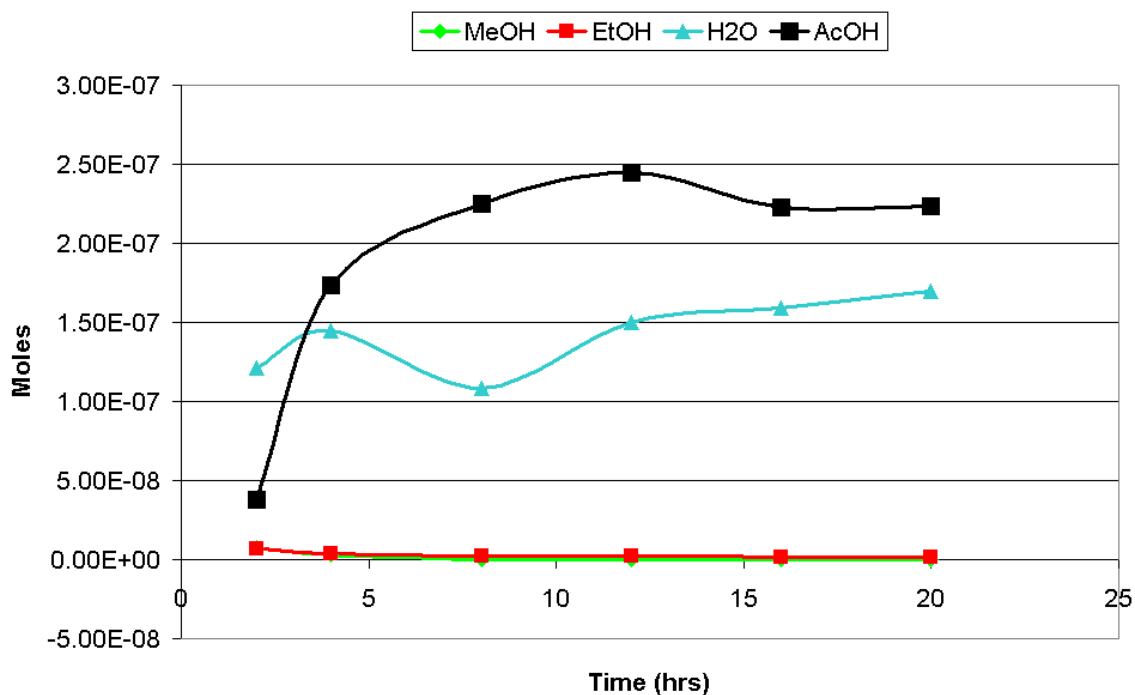


Figure 3-58 Reaction profile from 1.0mol% acid addition into N₂ system over Katalco 51-8 catalyst (acid fed in continuously after 2hrs)

The ethanol present was most likely formed from the hydrogenation of the acid. Although the experiment was conducted in an inert atmosphere, the catalyst was activated in flowing H₂ prior to the introduction of the acid. It was likely that some residual H₂ from the reduction was still present in the system and reacted with the acid to produce the alcohol. The methanol that was observed was most likely an artefact from a previous run.

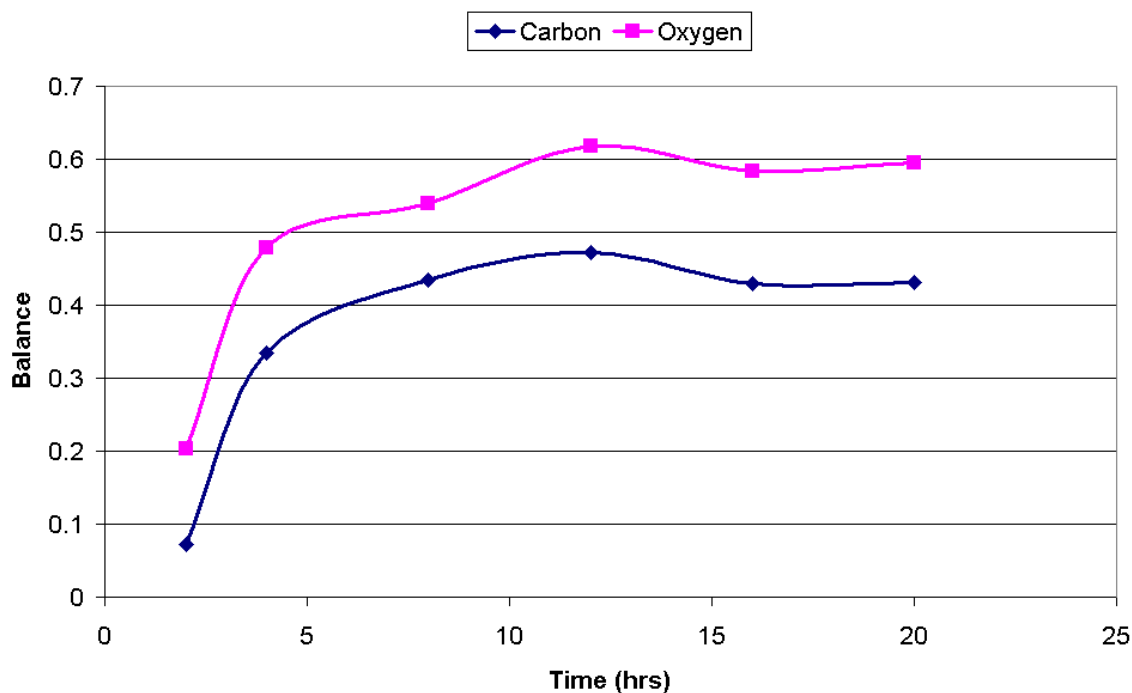
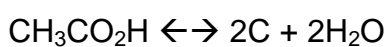


Figure 3-59 Mass balances from 1.0mol% acid addition into N₂ system over Katalco 51-8 catalyst (acid fed in continuously after 2hrs)

Although no other products were observed, only 43% of the acetic acid that was introduced to the system was accounted for. The levels of water produced in the system were reasonably high and suggested possibly that another reaction was occurring. However the GC traces showed no unexplained peaks and the traces were ran for long enough to ensure the elution of all products. This did not rule out the possibility of a surface reaction on the catalyst, possibly decomposition to form water and surface carbon.



$$\Delta G_{523} = -105.39 \text{ kJ mol}^{-1}$$

However, the water levels observed could only account for another 15% of the acid, and therefore a significant amount still remained unaccounted for.

Acid to Ethanol (%)	0.1
Unreacted Acid (%)	43.2
Total (%)	43.3

Table 3-13 Acid balance from 1.0mol% acid addition into N₂ system over Katalco 51-8 catalyst

Post reaction, a temperature programmed oxidation (TPO) was performed to determine if carbon had been deposited on the surface of the catalyst. Although carbon dioxide was evolved, the weight change profile of the TPO was unusual when compared with the previous TPO's. An example of both is shown below:

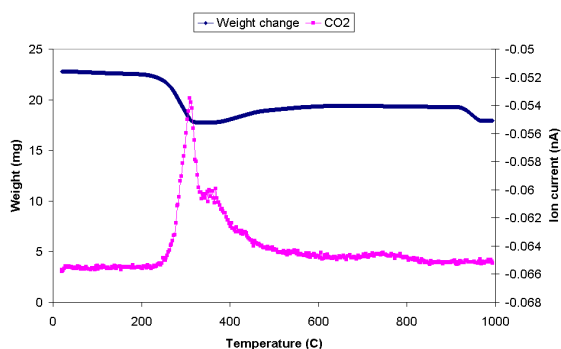


Figure 3-60 Post reaction TPO from 1.0mol% acid addition into N₂ system over Katalco 51-8 catalyst

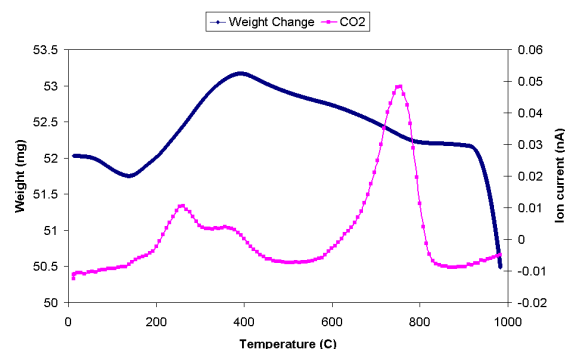
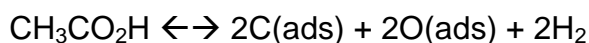


Figure 3-61 Typical post reaction TPO profile

Under a classic methanol synthesis feed (CO/CO₂/H₂), the copper in the catalyst was present in a reduced state i.e. copper metal. Upon performing the TPO a weight gain was observed as the copper re-oxidised to copper oxide. However it appeared that under the inert conditions used in the N₂ experiment, the acetic acid had already re-oxidised the copper prior to the TPO, as only a weight loss was exhibited for the evolution of surface carbon species. A possible route could be the complete decomposition of the acid on the catalyst surface to yield two surface oxygen atoms:



This would result in the oxidation of the surface copper, without an evolution of water. If the re-oxidation of the surface carbon took place via a reverse Boudouard

type mechanism involving CO_2 , rather than adsorbed surface oxygen's as proposed earlier, then this would explain why no CO was evolved from the catalyst.

3.3.5.3 Nitrogen / Hydrogen Atmosphere (N_2/H_2)

When the same experiment was conducted under a reducing atmosphere, significant hydrogenation of the acid (~25%) to ethanol was observed along with minor traces of ethyl acetate and unreacted acetic acid.

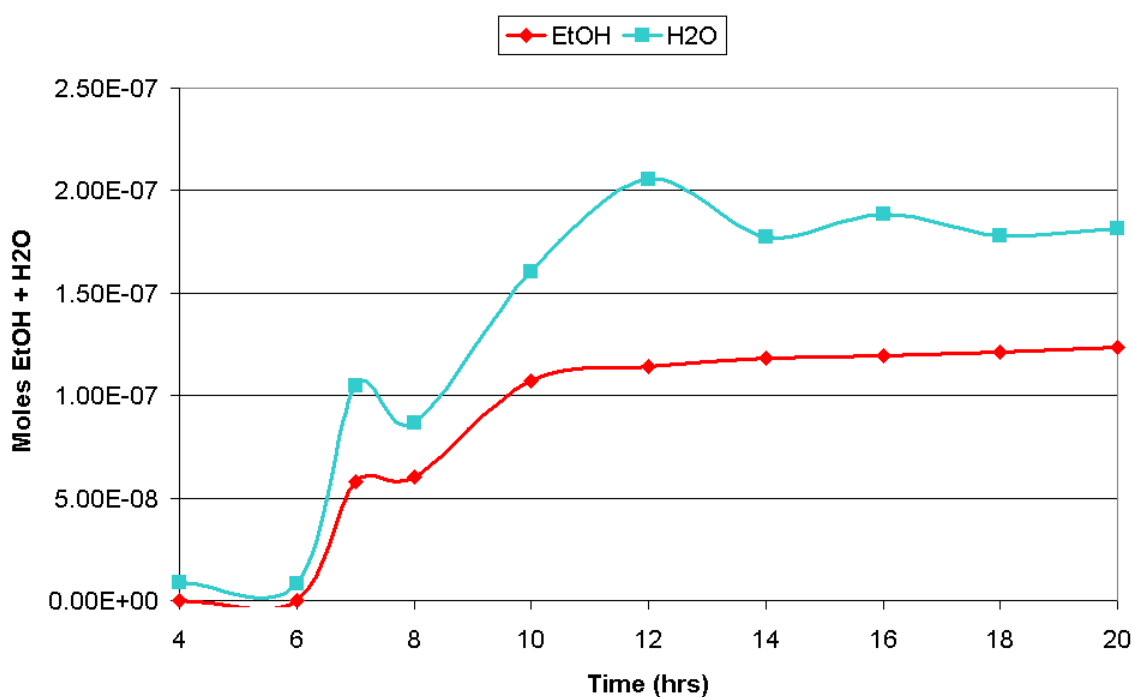


Figure 3-62 Reaction profile from 1.0mol% acid addition into N_2/H_2 system over Katalco 51-8 catalyst (acid fed in continuously after 6hrs)

The ethyl acetate was the product of a condensation reaction between the ethanol and the acid. It was only when a significant concentration of ethanol was observed in the system that production of ethyl acetate began.

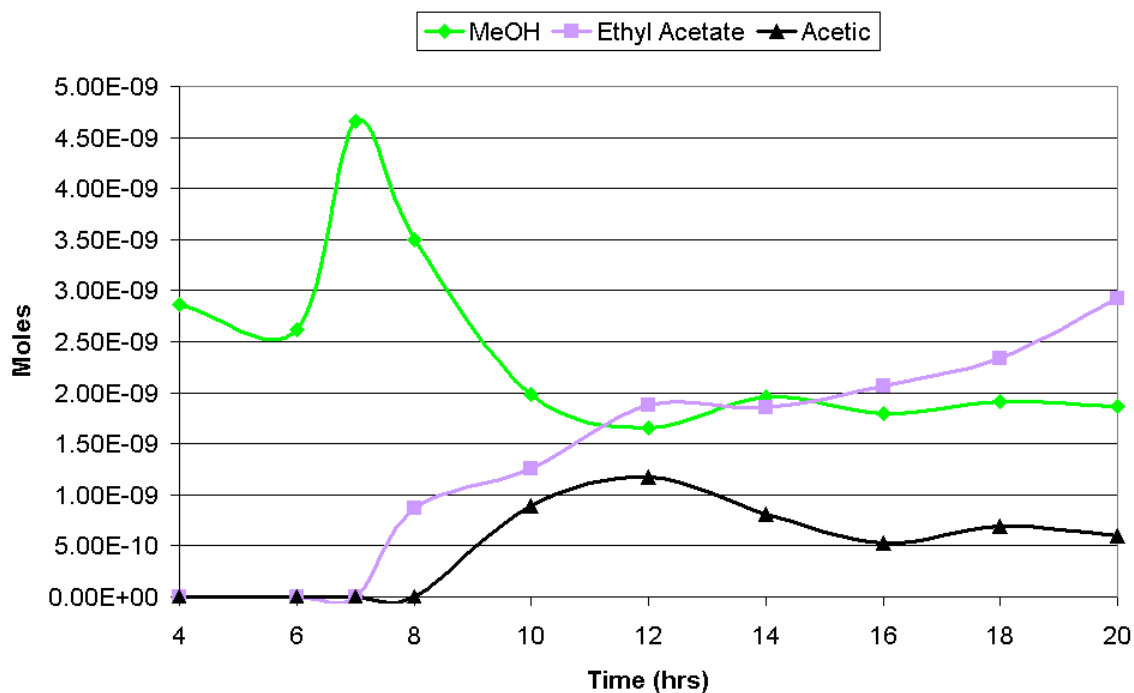


Figure 3-63 Reaction profile from 1.0mol% acid addition into N₂/H₂ system over Katalco 51-8 catalyst (acid fed in continuously after 6hrs)

Like the previous system, a significant concentration of water was produced. Both the production of ethanol and ethyl acetate involved the formation of water, however the production did not account for the concentration present. This suggested that another reaction was occurring although no other products were observed by the GC.

Acid to Ethanol (%)	24.7
Acid to Ethyl Acetate (%)	1.0
Unreacted Acid (%)	0.1
Total (%)	25.8

Table 3-14 Acid balance from 1.0mol% acid addition into N₂/H₂ system over Katalco 51-8 catalyst

Again, like the previous system this did not rule out the possibility of acid decomposition on the catalyst surface to yield carbon and water.

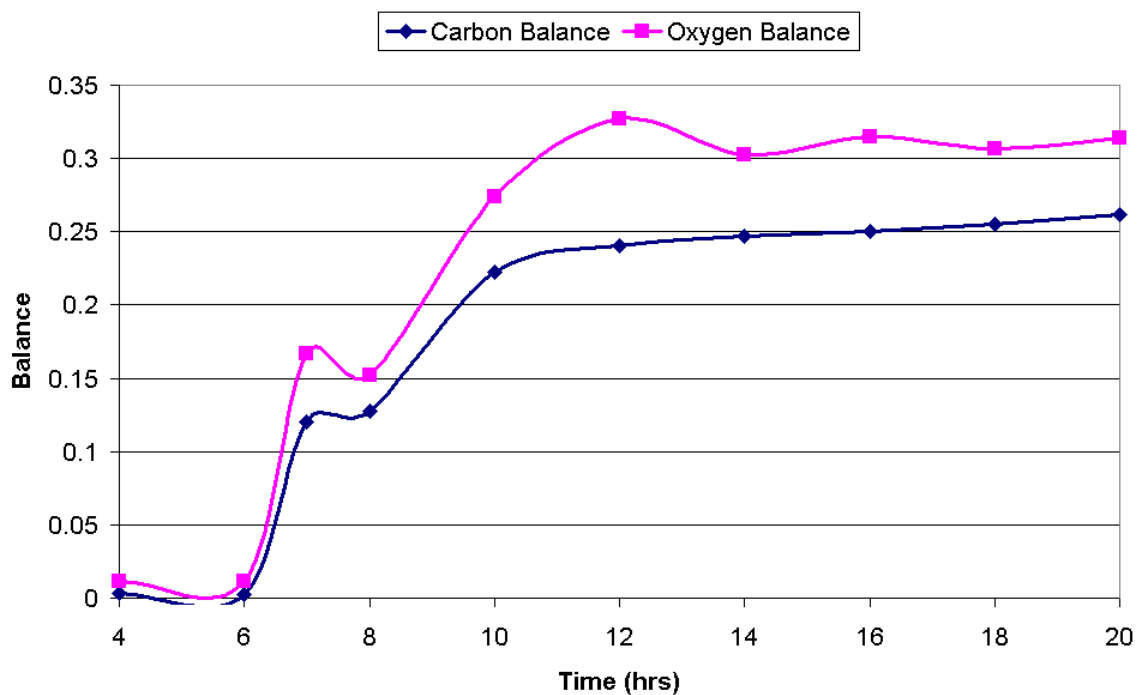


Figure 3-64 Mass balances from 1.0mol% acid addition into N₂/H₂ system over Katalco 51-8 catalyst (acid fed in continuously after 6hrs)

The mass balance of the system confirmed that a substantial amount of both carbon and oxygen were missing, and presumably deposited on the catalyst surface.

A TPO was performed on the catalyst post reaction, and the usual weight gain profile was observed, indicating that the catalyst was still in a reduced state after the acid addition.

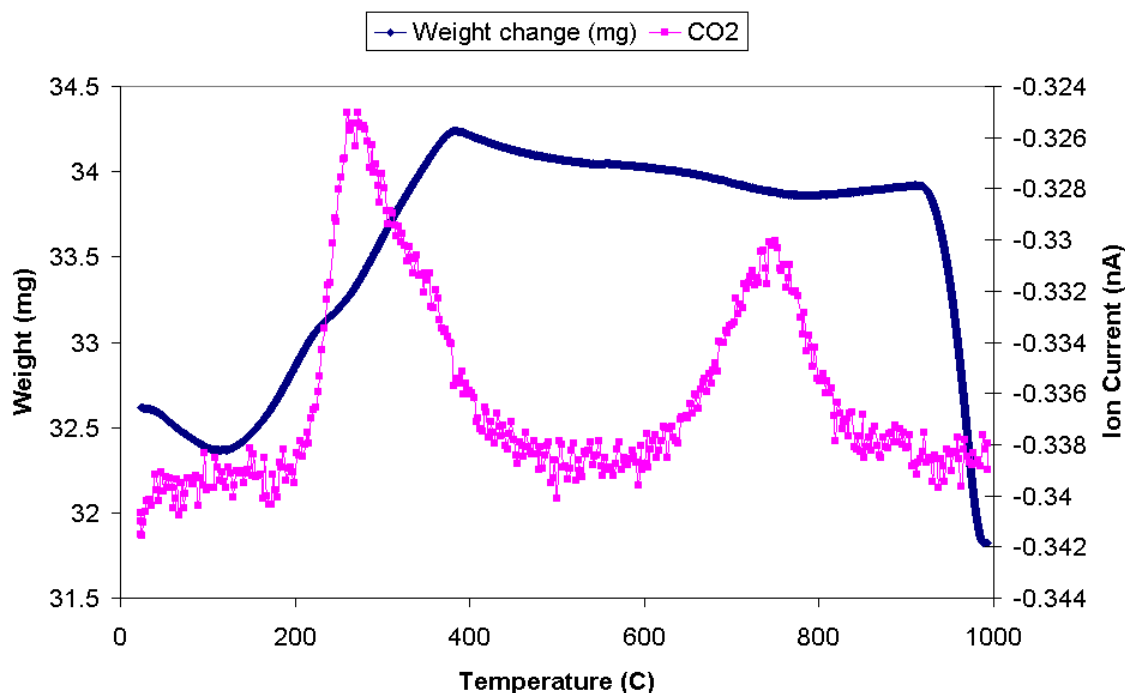


Figure 3-65 Post reaction TPO from 1.0mol% acid addition into N_2/H_2 system over Katalco 51-8 catalyst

This suggested that the decomposition pathway for the acid in the reducing atmosphere was different than the decomposition pathway observed previously under the inert feed. It was probable that the presence of hydrogen maintained the catalyst in a reduced state.

A significant amount of CO_2 was evolved from the catalyst during the TPO, confirming that laydown of the acetic acid on the catalyst surface had taken place.

3.3.5.4 Carbon Monoxide / Hydrogen (CO/H_2)

Under a syngas feed of $CO:H_2$ (molar ratio 1:2), methanol was produced selectively (~99%) over the Katalco catalyst. The same reaction profile was observed as in the baseline experiment performed in section 3.2.2.1. Deactivation in the methanol production was apparent, and was attributed to being due to the highly reducing nature of the feed gas.

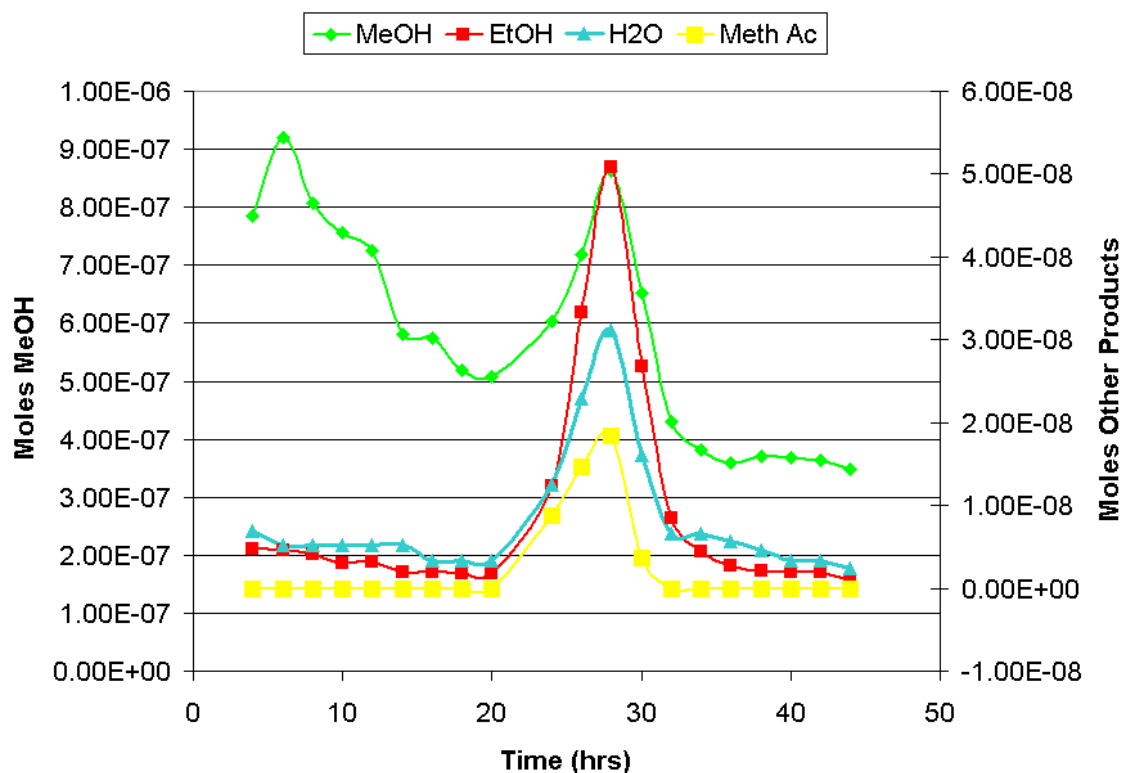


Figure 3-66 Reaction profile from 1.0mol% acid addition into CO/H₂ system over Katalco 51-8 catalyst (acid fed in from 20 to 28hrs)

Upon introduction of the acid into the system after 20hrs, increases in CO₂, methanol and water were observed along with production of ethanol and methyl acetate.

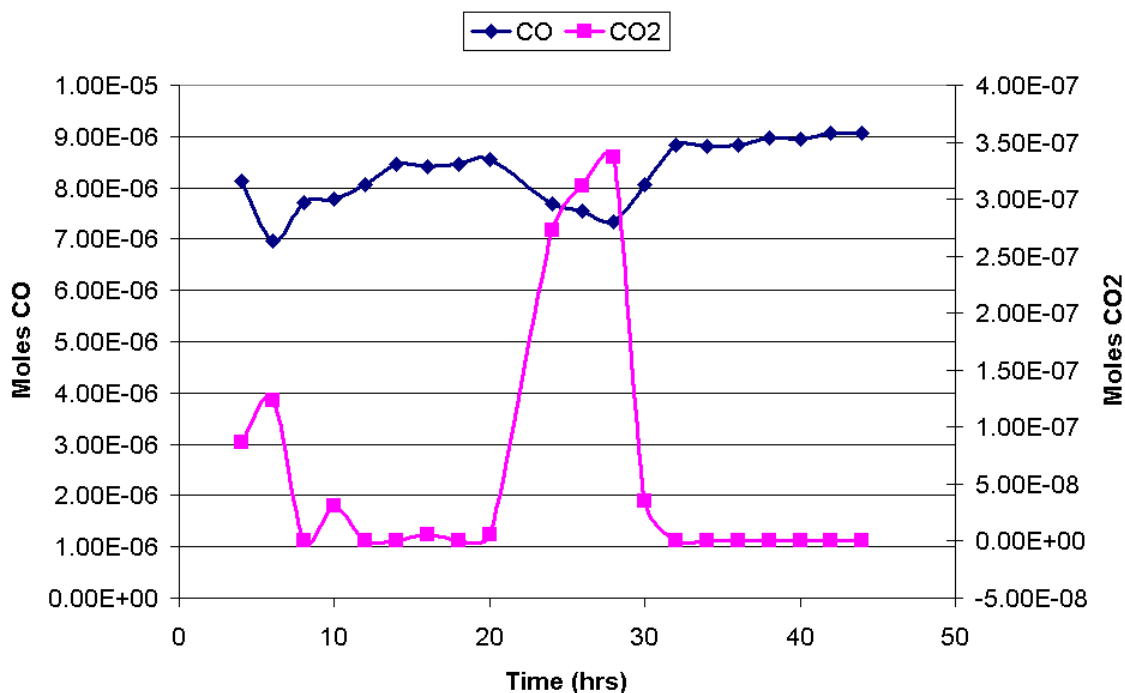
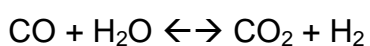


Figure 3-67 Reaction profile from 1.0mol% acid addition into CO/H₂ system over Katalco 51-8 catalyst (acid fed in from 20 to 28hrs)

The production of ethanol and methyl acetate were expected, along with the associated increase in water concentration. The increase in CO₂ was initially thought to be from water gas shift activity, as a decrease in CO levels was observed.



$$\Delta G_{523} = -19.6 \text{ kJ mol}^{-1}$$

Under the reaction conditions of temperature and pressure the conversion of CO to CO₂ was favourable.

However, there was not enough water produced from the ethanol and methyl acetate production to create the levels of CO₂ observed. Therefore the acetic acid was deemed to be the source of the CO₂ in the system, similar to that observed under the classic methanol synthesis feed. No methane was detected upon introduction of the acid, indicating that a straightforward decarboxylation whereby the methyl group further decomposed to surface carbon and gaseous hydrogen could be occurring.



However, unlike for the classic methanol synthesis feed result, not all of the acid carbon was accounted for in the products. Only ~60% was accounted for, indicating that a substantial amount was deposited on the catalyst surface.

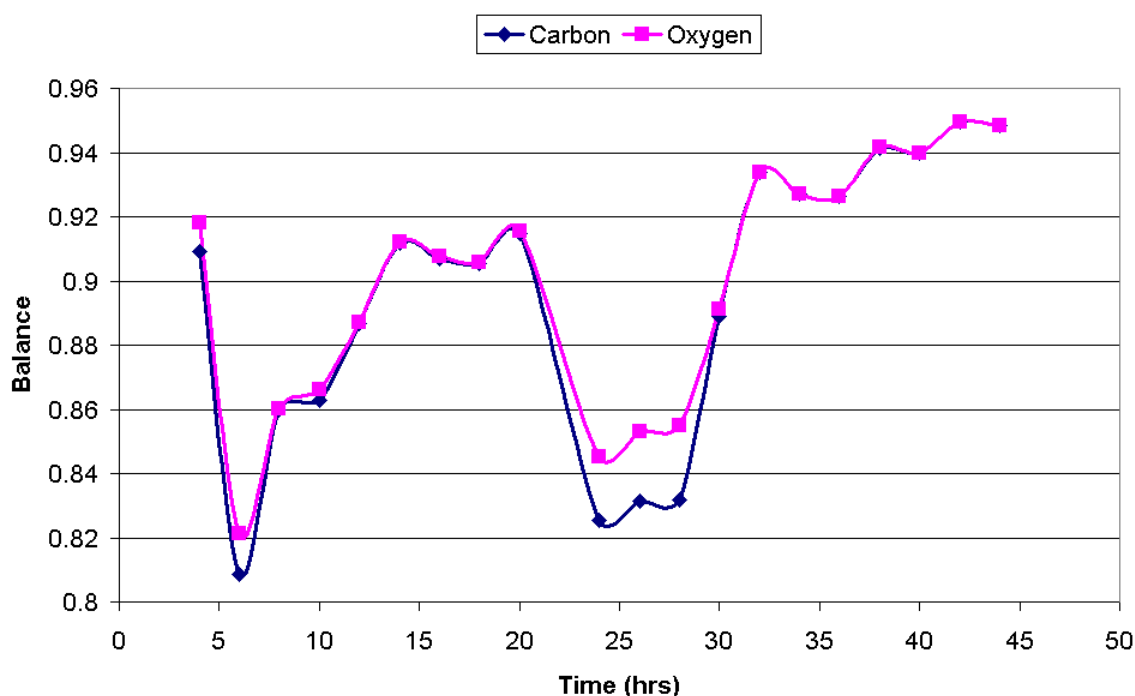


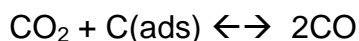
Figure 3-68 Reaction profile from 1.0mol% acid addition into CO/H₂ system over Katalco 51-8 catalyst (acid fed in from 20 to 28hrs)

The mass balances for the system during the acid addition also confirmed that some of the acid could not be accounted for, as a significant decrease was observed. The possible explanation for the deposition of carbon lay in the postulated mechanism of re-oxidation of the surface carbon.

Under a CO/H₂ feed there are a number of reasons as to why the re-oxidation of the surface carbon might not proceed:

- No CO₂ was present in the feed. CO₂ was postulated previously to be crucial in preventing carbon laydown, either through a reverse Boudouard process or through depositing oxygen onto the catalyst surface (via methanol synthesis). As no CO₂ was present in the feed, the re-oxidation could not proceed.
- Feed gas of CO/H₂ was highly reducing. It was possible that surface oxygen concentrations were being slowly depleted.

Interestingly if the decarboxylation route was correct and it was assumed for every mole of CO₂ that was produced one mole of carbon was laid down, the resulting acid balance would add up to 99%. Therefore it is possible that CO₂ was required in the feed to re-oxidise the surface carbon in a reverse Boudouard type reaction:



In summary, the product distribution obtained from the introduction of acetic acid was as follows:

Acid to Ethanol (%)	14.0
Acid to Methyl Acetate (%)	5.0
Acid to CO/CO ₂ (%)	40.0
Total (%)	59.0

Table 3-15 Acid balance from 1.0mol% acid addition into CO/H₂ system over Katalco 51-8 catalyst

Another point of interest was that the methanol production increased upon the introduction of the acid, unlike for CO/CO₂/H₂ system where the production decreased. This was most likely due to the conversion of some of the acid to CO₂. Kinetically hydrogenation of CO₂ is faster than the hydrogenation of CO and therefore explains the rise in methanol production. Increasing the partial pressure of CO₂ in a CO/H₂ feed has been shown to result in increases in methanol production by several research groups [113, 147, 148].

Finally, once the acid feed was switched off, the system returned back to normal, suggesting that the effect of the acid on methanol synthesis was transient.

To ensure that carbon from the acid had been deposited on the catalyst, a TPO was performed.

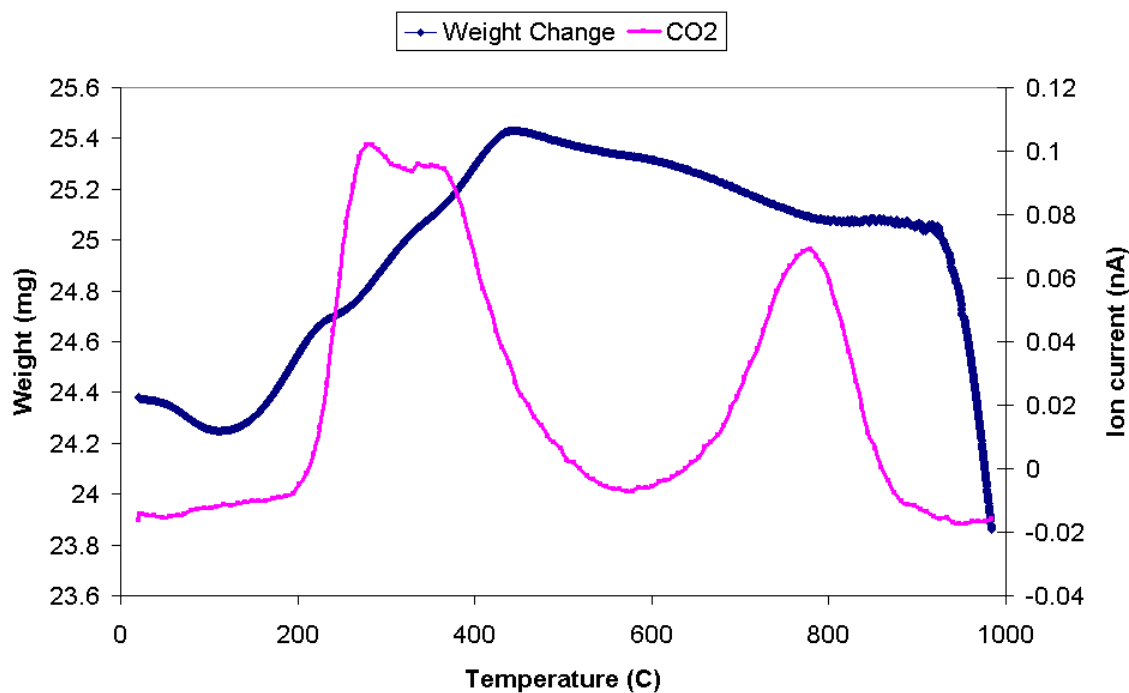
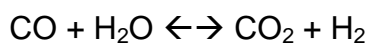


Figure 3-69 Post reaction TPO from 1.0mol% acid addition into CO/H₂ system over Katalco 51-8 catalyst

Three distinct evolutions of CO₂ were detected, with the evolutions resulting in a perturbation of the expected sample weight increase. This indicated that a substantial amount of carbon had been laid down.

3.3.5.5 Carbon Dioxide / Hydrogen (CO₂/H₂)

Under the reaction feed gas of CO₂/H₂ (molar ratio 1:3) methanol was produced at a yield of ~3.2%. Water was produced as a side product, and also through the water gas shift mechanism:



As CO₂ and H₂ were the starting components, CO and H₂O were produced as the system reached equilibrium.

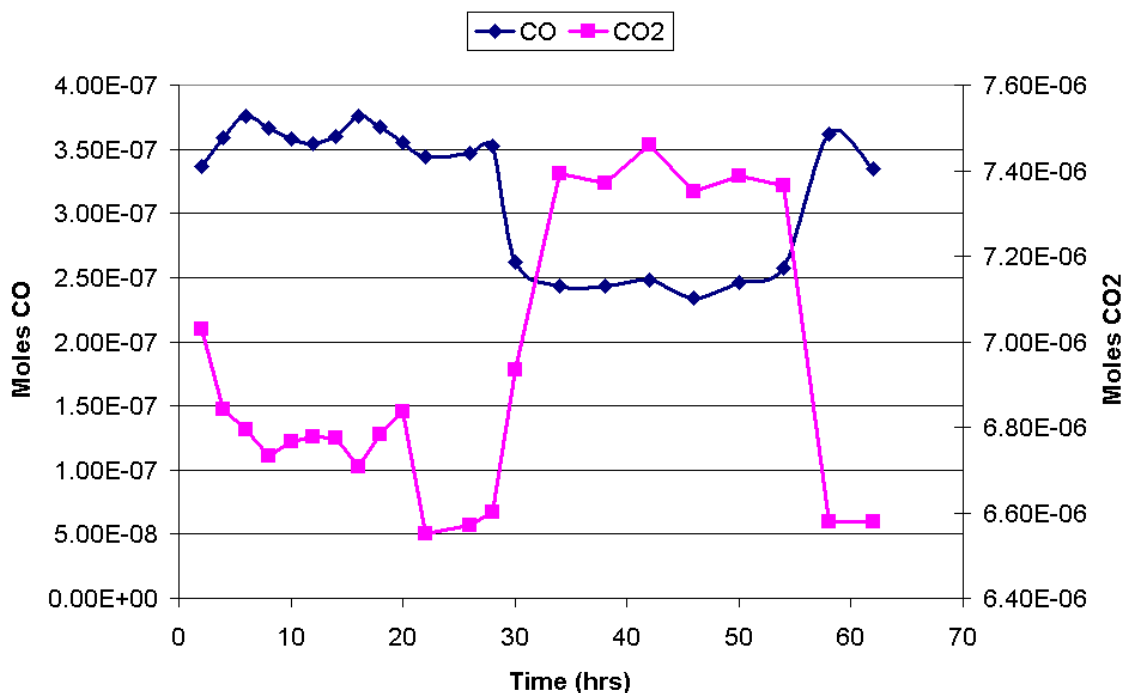


Figure 3-70 Reaction profile from 1.0mol% acid addition into CO₂/H₂ system over Katalco 51-8 catalyst (acid fed in between 28 and 54hrs)

Upon introduction of the acid after 28hrs the methanol production yield dropped from ~3.2% to ~1.2%. This was in complete contrast to the previous system where the methanol production increased. However in that system the CO₂ evolved from the introduction of the acid aided the methanol synthesis, as CO₂ hydrogenation was kinetically faster than CO hydrogenation. In the current system CO₂ was already present. The decrease in methanol production was therefore attributed to acetate groups blocking methanol synthesis on the catalyst surface.

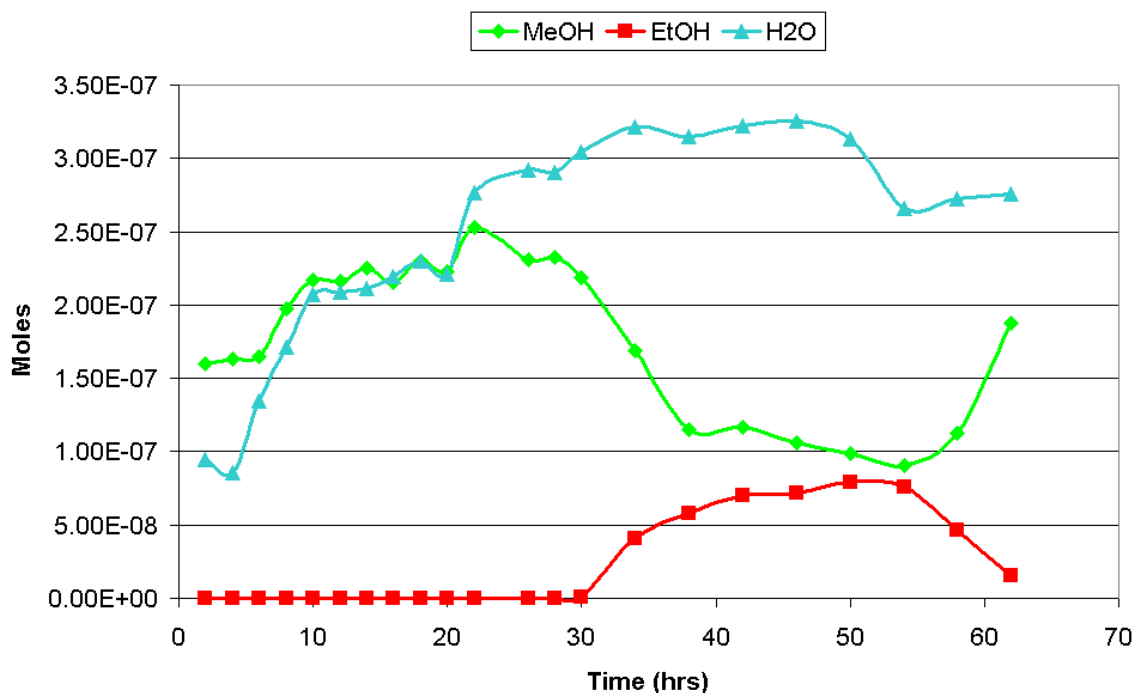
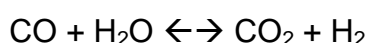


Figure 3-71 Reaction profile from 1.0mol% acid addition into CO₂/H₂ system over Katalco 51-8 catalyst (acid fed in between 28 and 54hrs)

As well as a decrease in methanol production, ethanol and methyl acetate production began as expected. Ethyl acetate production was observed, as the levels of ethanol and methanol in the system during the introduction of the acid were similar, i.e. the acid could react with both alcohols. Interestingly, an increase in water and CO₂ concentrations were observed along with a decrease in CO levels. This was unusual, as through the water gas shift mechanism it would be expected that the CO and H₂ levels would increase slightly as well, to equilibrate:



This indicated that the water gas shift mechanism was affected by the introduction of the acid.

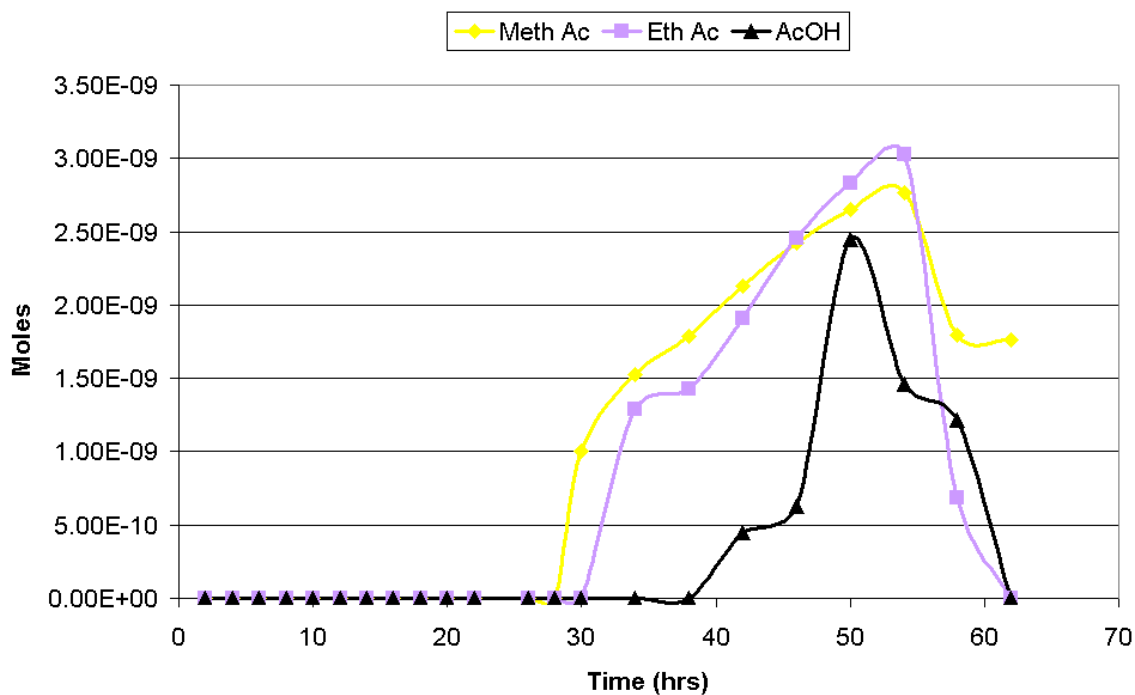


Figure 3-72 Reaction profile from 1.0mol% acid addition into CO₂/H₂ system over Katalco 51-8 catalyst (acid fed in between 28 and 54hrs)

Unlike for the previous system, the carbon balance remained reasonably steady throughout the run, indicating little to no loss of the acetic acid as carbon laydown. The oxygen balance increased slightly during the addition, possibly indicating that oxygen from the surface of the catalyst was being removed by reaction.

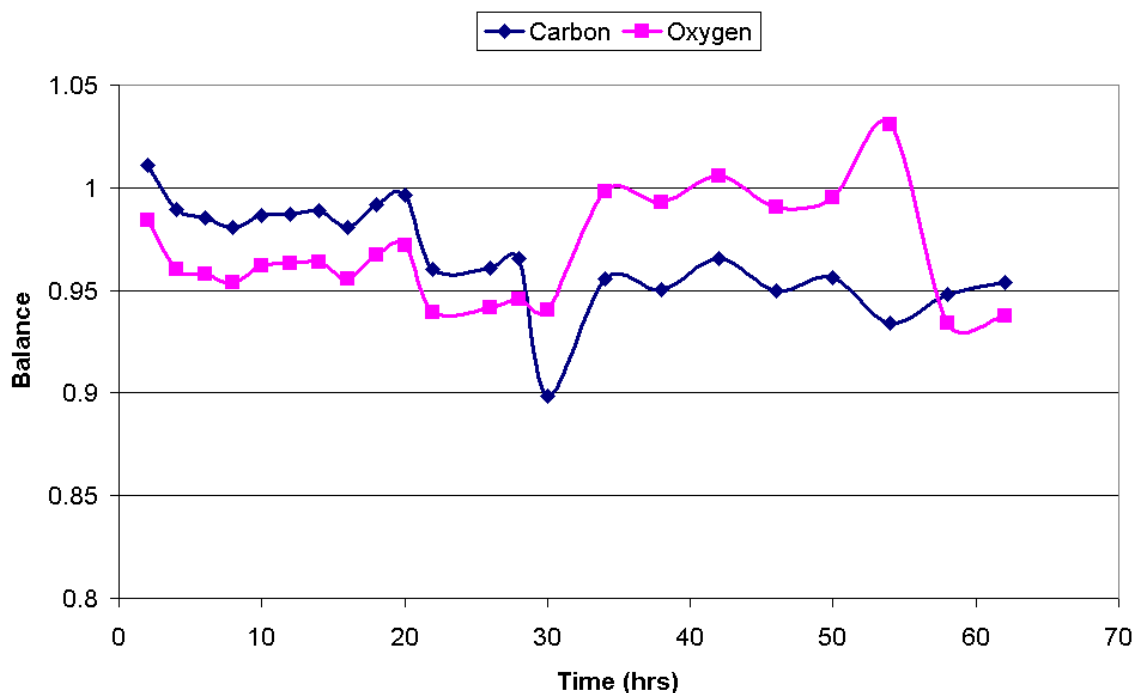


Table 3-16 Mass balances from 1.0mol% acid addition into CO₂/H₂ system over Katalco 51-8 catalyst (acid fed in between 28 and 54hrs)

If surface carbon could react with atomic oxygen on the catalyst surface to form CO or CO₂, then this could explain the rise. It would also explain why a decrease in the carbon balance was not observed.

Once the acid addition was stopped at 54hrs the system began to return to normal, with methanol production rising. However, longer analysis was prevented by the loss of the carrier gas in the GC. It was anticipated that as the system showed signs of recovery, the effect of the acid on the catalyst would be transient and not permanent.

Overall, the addition of acetic acid yielded in the production of the following species:

Acid to Ethanol (%)	17.0
Acid to Methyl Acetate (%)	0.5
Acid to Ethyl Acetate (%)	1.2
Unreacted Acid (%)	0.5
Acid to CO/CO ₂ (%)	67.5
Total (%)	86.7

Table 3-17 Acid balance from 1.0mol% acid addition into CO₂/H₂ system over Katalco 51-8 catalyst

In total approximately 86.7% of the acid that was added could be accounted for as products. As the presence of CO₂ in the feed had been postulated previously to prevent carbon laydown of the acid, it would have been expected that all of the acid would be accounted for as products. As all of the acid carbon could not be accounted for, this suggested that oxidation potential of the system was not the only factor involved in preventing carbon laydown.

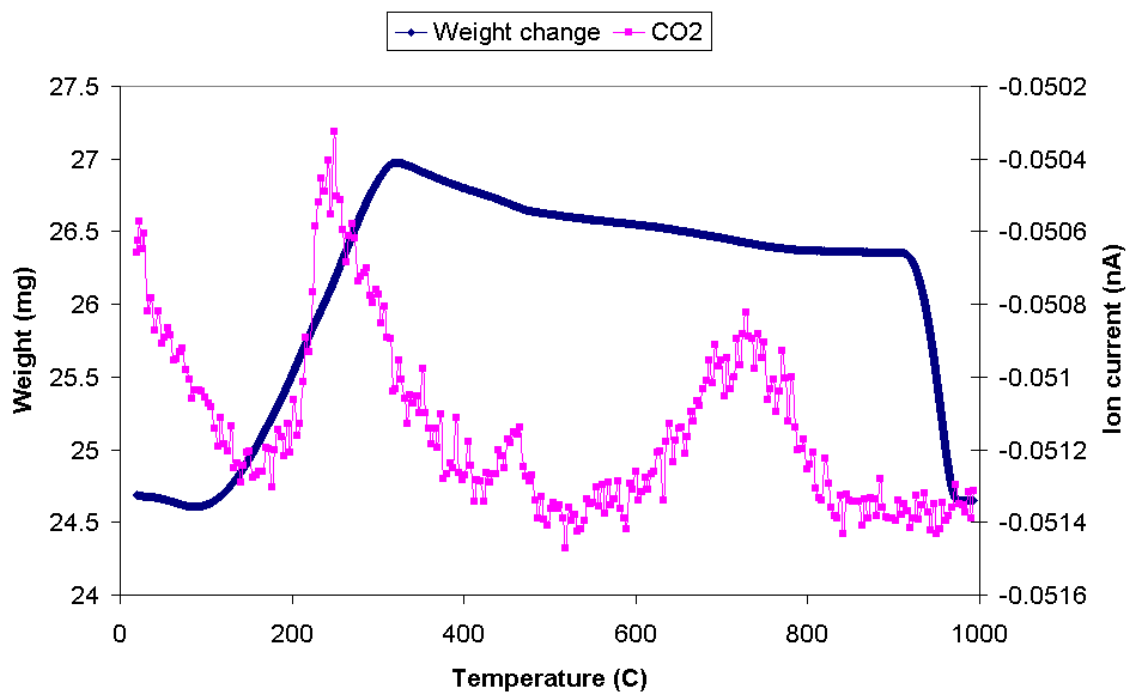


Figure 3-73 Post reaction TPO from 1.0mol% acid addition into CO₂/H₂ system over Katalco 51-8 catalyst

Post reaction TPO analysis of the catalyst revealed that carbon was present on the catalyst surface. The presence of formate groups and other methanol precursor species were likely as well as the possibility of carbon laydown from the addition of the acid. Overall the evolutions of CO₂ were reasonably small and therefore showed that little to no carbon laydown of the acid took place.

3.3.5.6 Summary

The results from the effects of varying the gas feed composition on the behaviour of the acid are shown below:

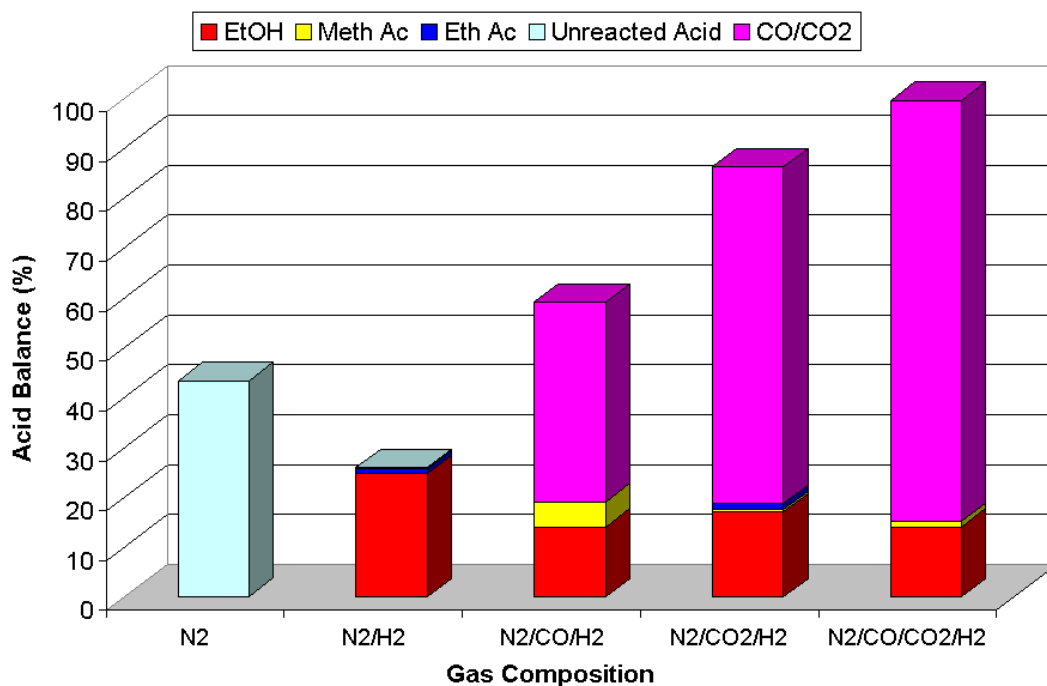


Figure 3-74 Acid balance of each system versus the feed gas composition of each system

Ethanol and esters (methyl acetate/ethyl acetate) were observed in every system in reasonable concentrations apart from the inert. The presence of these species was due to the hydrogenation of the acid (ethanol) and the reaction of the acid with an alcohol (methyl acetate/ethyl acetate).

Ethanol was produced in the highest yield in the N₂/H₂ system as was expected due to the high partial pressure of H₂. The other systems all had similar levels of ethanol.

Methyl acetate was produced in the systems where methanol was synthesised. Ethyl acetate production took place in the N₂/H₂ system (where no methanol was present) and in the CO₂/H₂ system (where the levels of methanol and ethanol in the system were approximately the same).

The only other product that was observed upon addition of the acid was CO/CO₂. As explained in previous sections, the conversion of acetic acid to CO/CO₂ was

most likely through decomposition. Decomposition of surface acetate groups on various transition metals had been shown to proceed through a decarboxylation mechanism, to yield gaseous CO_2 and an adsorbed methyl group. The methyl group had been shown to be able to decompose to yield surface carbon and gaseous hydrogen. It was postulated that the surface carbon could be oxidised to yield CO or CO_2 through either oxidation by atomic oxygen or a reverse Boudouard reaction involving CO_2 . This model was used to explain the behaviour of the acid in the classic methanol system ($\text{CO}/\text{CO}_2/\text{H}_2$), where all of the acid carbon was accounted for as products.

However, under the N_2 and N_2/H_2 feeds, CO_2 was not detected upon introduction of the acid, suggesting that decarboxylation of the acid was not occurring. Decomposition was still postulated to be taking place as a substantial amount of acid was not accounted for upon addition. Post reaction TPOs confirmed the presence of substantial deposits of carbon on the catalyst surfaces. Therefore, a different decomposition route was proceeding.

A possible explanation for the behaviour was that the decomposition of acetates on transition metal surfaces was most likely structure sensitive[97]. The literature also revealed that copper particles in methanol synthesis catalysts had been known to alter morphology, depending on the gaseous environment surrounding them [58, 59, 69]. It was therefore postulated that under the N_2 and N_2/H_2 feeds the decomposition of the acid was different to the decomposition under the classic methanol synthesis feed. Oxidation of surface carbon could not proceed either, due to the lack of atomic oxygen or CO_2 in the systems.

The lack of oxidants in the system, to lift off the surface carbon could also explain the behaviour of the acid in the CO/H_2 system. Conversion of the acetic acid to CO_2 was observed, although 40% of the carbon from the acid was deposited on the catalyst surface. If the acetic acid decomposed via decarboxylation, then gas phase CO_2 would be evolved and carbon would be deposited on the catalyst. As no CO_2 was present in the feed, and as the system was highly reducing, oxidation of the surface carbon could not take place. It was calculated that if the surface carbon had been re-oxidised, the carbon balance would have been 99% i.e all the acid would have been accounted for.

Under the CO_2/H_2 system an increase in conversion of acetic acid to CO/CO_2 was evident, suggesting that the increase in oxidation potential allowed the surface carbon to be oxidised to CO or CO_2 . It was impossible to determine if the oxidation of the carbon was due to a reverse Boudouard reaction, or the presence of atomic oxygen on the surface of the catalyst. It would have been expected if the oxidation potential of the system was crucial in oxidising surface carbon, that the CO_2/H_2 system would show the highest acid balance (as it was the most oxidising system). However the acid balance of the system was only 87%, suggesting laydown of the acid. This indicated that the oxidation potential of the system was not the only factor affecting carbon laydown, and that the morphology of the copper particles may also be important.

Finally, under the classic methanol synthesis system, all of the acid was accounted for as products, with no acid deposition on the surface of the catalyst.

Interestingly, the lowest acid balance was recorded in the N_2/H_2 system, which had the highest partial pressure of hydrogen without the presence of an oxidant (CO_2). This suggested that the presence of hydrogen enhances decomposition of the acid on the catalyst surface, whereas increasing the oxidising potential of the system results in less carbon laydown.

The results showed that the feed gas played an important part in the decomposition of the acid. As mentioned earlier, the nature of the gas feed was found by researchers to alter the morphology of the copper particles, suggesting that the decomposition of the acid was structure sensitive. This could explain why significant carbon laydown was observed in some systems, whereas in others more of the carbon was accounted for as products.

3.3.6 High Concentration / Long Term Studies

Under a classic methanol synthesis feed (CO/CO₂/H₂) the addition of acetic acid resulted in conversion of the acetic acid to CO/CO₂, ethanol and methyl acetate. None of the acid was deposited on the catalyst surface, and once the acid addition was stopped the catalyst activity returned to normal. This indicated that the effect of the acid on the catalyst was transient, and no intrinsic deactivation of the catalyst had occurred.

However, in those experiments the acid was fed over a short period of time (typically ~20-25hrs) and at very low concentrations (1.0-1.5mol%). It was therefore of interest to determine if deactivation of the catalyst occurred when acid was fed in over a prolonged period of time and also if a higher concentration of acid was introduced.

3.3.6.1 Reaction Conditions

Prior to reaction, the catalyst was reduced *in situ* in the reactor under 50ml min⁻¹ flowing hydrogen at a temperature of 523K. The catalyst was held at this temperature for 3hrs.

The experiments were performed using a classic methanol synthesis gas feed of CO/CO₂/H₂ in a 1:1:8 molar ratio. A small concentration of nitrogen was also fed in as a reference gas, for the calculation of conversion. The exact gas mix composition used was 10ml N₂ / 25ml CO / 25ml CO₂ / 190 ml H₂.

- Reaction Temperature (K) 523
- Pressure (barg) 50
- Gas Flow (ml min⁻¹) 250
- Catalyst Volume (ml) 1.36
- GHSV (hr⁻¹) ~11,000

The acid addition for the long term experiment was of 1.0mol%. The acid addition for the high concentration experiment was of 5.0mol%.

3.3.6.2 Long Term Addition

Short term additions of low levels of acetic acid were shown to have a transient effect on methanol synthesis without having an intrinsic effect on the catalyst itself. It was of interest to determine if an extended addition of acetic acid would bring about deactivation of the catalyst.

To this end, acetic acid was fed in to a classic methanol synthesis system at a molar feed rate of 1.0mol% (2.5×10^{-7} moles min^{-1}) over an extended period of time.

For the first 6hrs of the run, no acid was fed in and the system behaved as expected, with a methanol yield of ~9%.

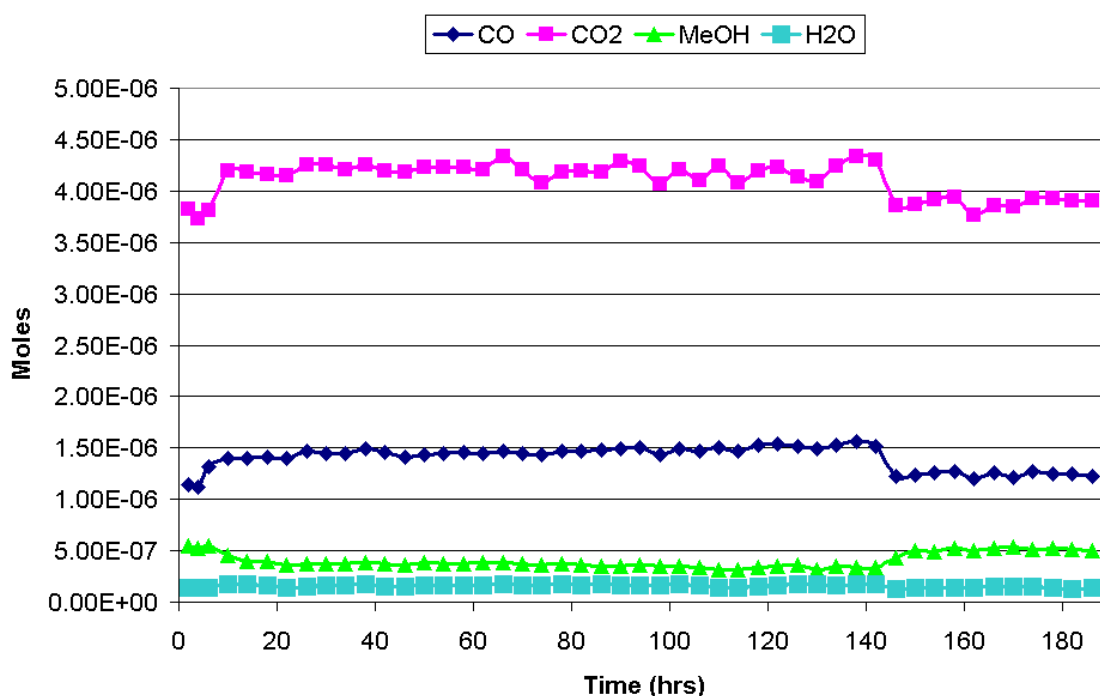


Figure 3-75 Reaction profile from 1.0mol% acid addition into CO/CO₂/H₂ system over Katalco 51-8 catalyst (acid fed in between 6 and 142hrs)

Upon addition of the acid, immediate increases in CO and CO₂ levels were apparent. Production of methyl acetate and ethanol also began as the acid was fed in, and an associated increase in water levels with the production was also observed. Methanol synthesis decreased sharply upon the introduction of the acid, as surface acetate groups blocked sites for methanol synthesis.

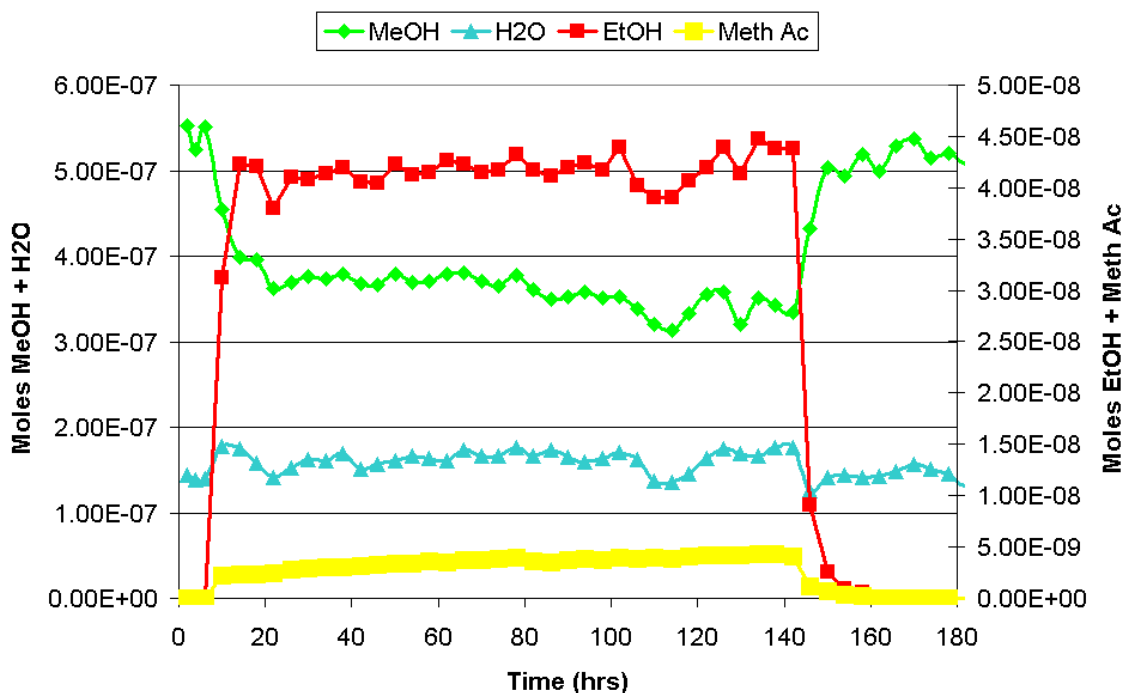


Figure 3-76 Reaction profile from 1.0mol% acid addition into CO/CO₂/H₂ system over Katalco 51-8 catalyst (acid fed in between 6 and 142hrs)

The acid was fed in to the system over 136hrs. During this period the system reached equilibrium, as the levels of all the products and reactants in the system remained at fairly constant levels.

When the acid feed was switched off at 142hrs the system returned to its original state prior to the acid addition. Ethanol and methyl acetate levels dropped to zero while CO, CO₂, water and methanol levels all returned to normal. This indicated that like the short term addition the effect of the acid at low levels was transient and even after an extended period of time the catalyst was not intrinsically affected.

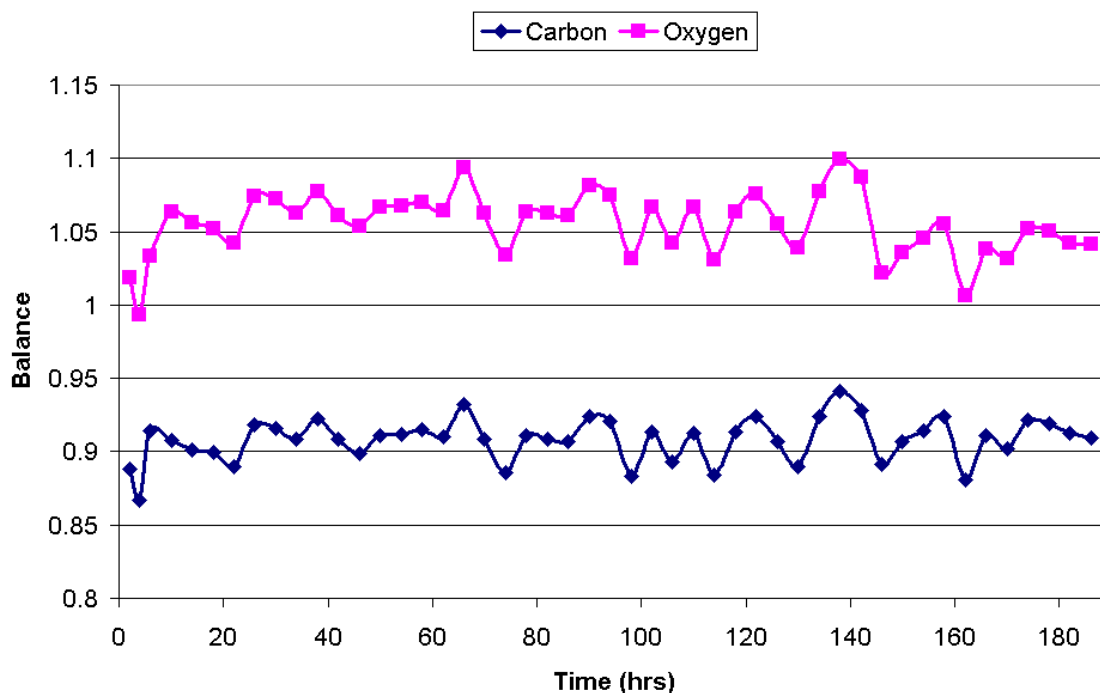


Figure 3-77 Mass balances from 1.0mol% acid addition into CO/CO₂/H₂ system over Katalco 51-8 catalyst (acid fed in between 6 and 142hrs)

Finally, the carbon and oxygen balances throughout the run remained constant, even during the acetic acid addition. This suggested that no acid was laid down on the catalyst.

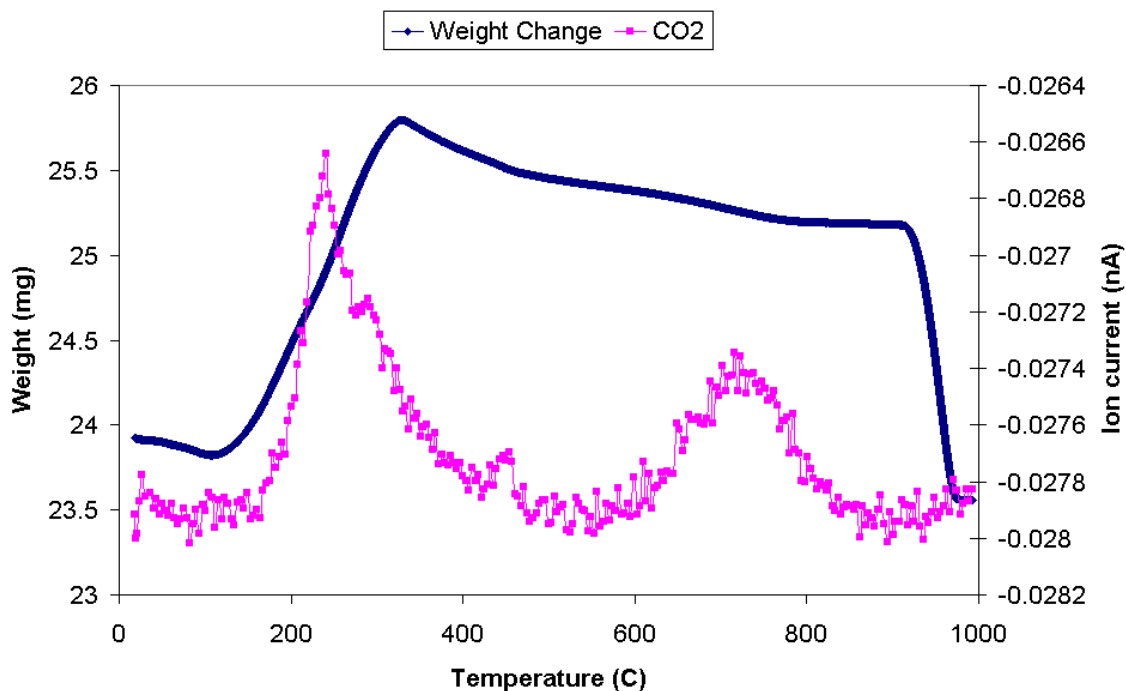
3.3.6.3 Acid Balance

Acid to Ethanol (%)	13.0
Acid to Methyl Acetate (%)	1.0
Acid to CO / CO ₂ (%)	88.0
Total (%)	102.0

Figure 3-78 Acid balance from 1.0mol% acid addition into CO/CO₂/H₂ system over Katalco 51-8 catalyst (long term addition)

The acid balance was in complete agreement with the carbon and oxygen balances of the system, showing that all the acid that was fed in could be accounted for as products. The product selectivities were very similar to the selectivities recorded for the short term addition, and well within experimental error.

3.3.6.4 Temperature Programmed Oxidation (TPO)



The post reaction TPO of the catalyst showed a small low temperature evolution of CO₂, which was most likely from the presence of formate groups on the catalyst surface, or other methanol precursor species. As the acid balance revealed that all the acid could be accounted for, it was unlikely that the evolution of CO₂ was due to surface acetate groups.

3.3.6.5 High Concentration Addition

As well as determining if long term addition of acetic acid affected the catalyst, it was also of interest to learn if a higher concentration of acetic acid would deactivate the catalyst.

To this end a run was performed where acetic acid was fed in at a molar feed rate of 5.0mol% (1.55×10^{-6} moles min⁻¹). The concentration of acid in the system was five times that of the previous experiment.

Initially for the first 4hrs of the run the system behaved as expected with a methanol yield of ~10% produced.

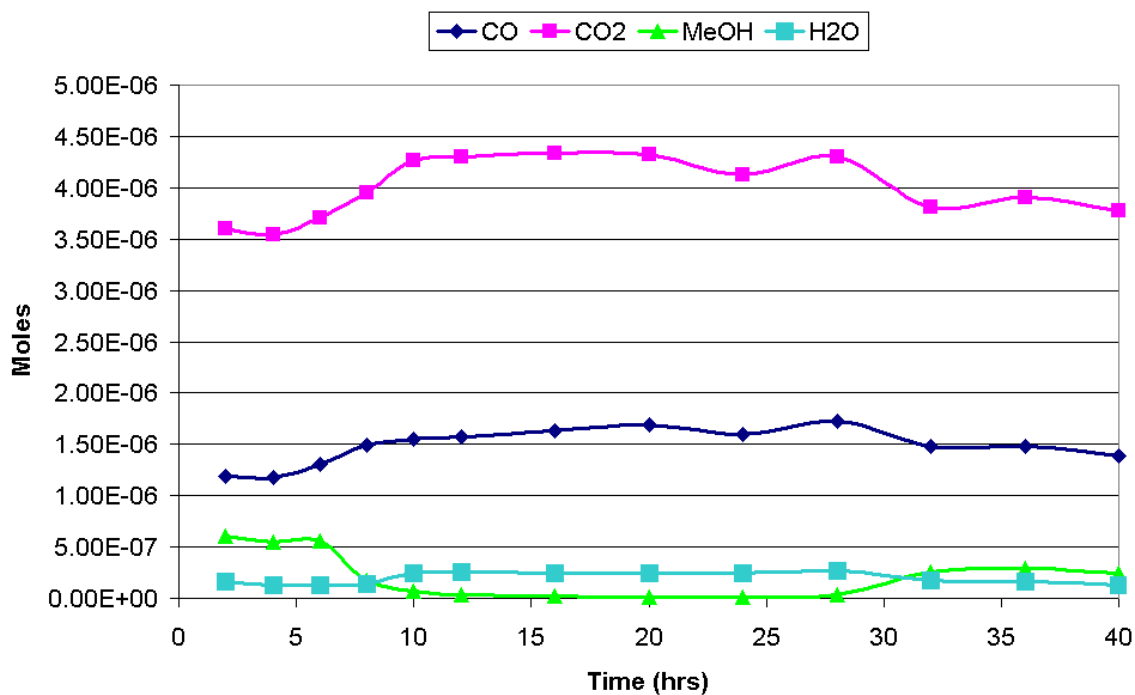


Figure 3-79 Reaction profile from 5.0mol% acid addition into CO/CO₂/H₂ system over Katalco 51-8 catalyst (acid fed in between 4 and 24hrs)

Upon addition of the acid there were instant increases in the CO and CO₂ levels, as observed in previous experiments. The methanol production decreased dramatically, from a yield of 10% to a yield of 0.13% at the lowest point. It was thought initially that this would be due to surface saturation of the catalyst with acetate groups, blocking the methanol synthesis. However it was observed later that once the acid feed was stopped the methanol production did not return to its original level as shown in previous systems. This indicated that permanent deactivation of the catalyst had occurred.

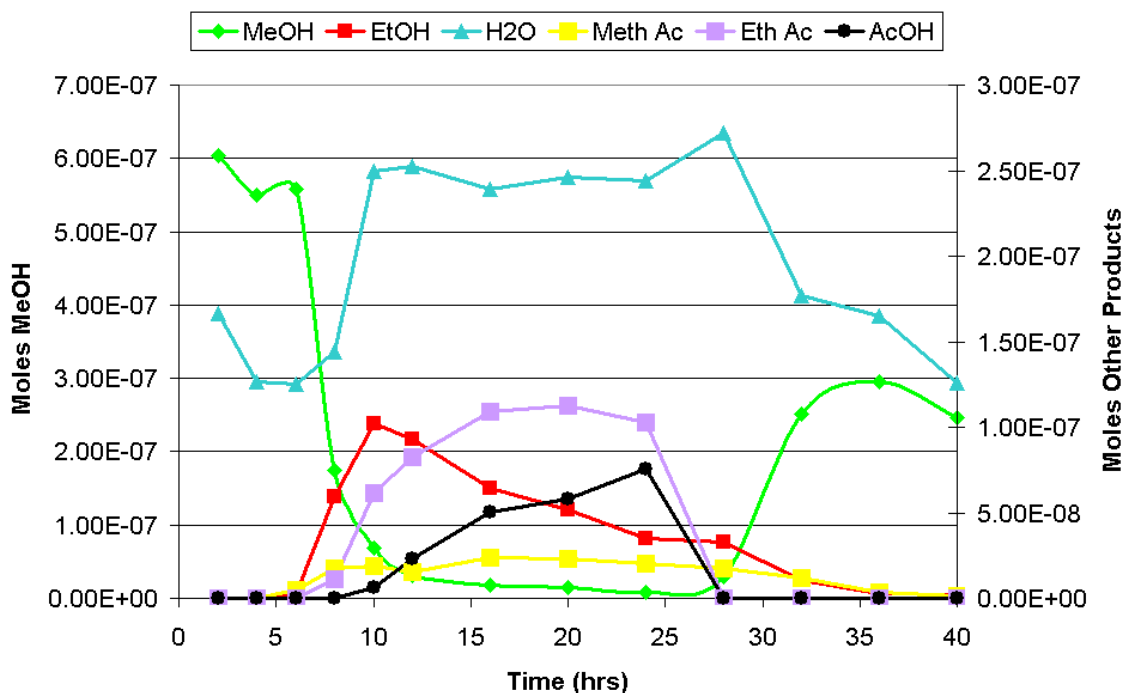


Figure 3-80 Reaction profile from 5.0mol% acid addition into CO/CO₂/H₂ system over Katalco 51-8 catalyst (acid fed in between 4 and 24hrs)

When acid was fed in to the system, initially the usual products were observed with CO and CO₂ levels increased and ethanol and methyl acetate production occurring. However the ethanol levels began to diminish as ethyl acetate production began to take over. Due to the dramatic decrease in methanol production, the most abundant alcohol in the system became ethanol and therefore a condensation reaction between ethanol and the acid took place to produce ethyl acetate. Interestingly the methyl acetate levels did not decrease significantly as the methanol levels decreased to trace levels, indicating that its production was favoured.

A few hours after the production of ethyl acetate began, unreacted acetic acid was also observed. Unreacted acetic acid was not observed in the classic methanol synthesis system when the acid was fed in at lower concentrations. This suggested that the level of acetic acid was so high that not all of it could be converted to products.

As mentioned previously, when the acid feed was switched off the system did not return back to its original state. Methanol production had dropped by 50%, and the levels of CO and CO₂ in the system were consequently higher, reflecting the lower conversion.

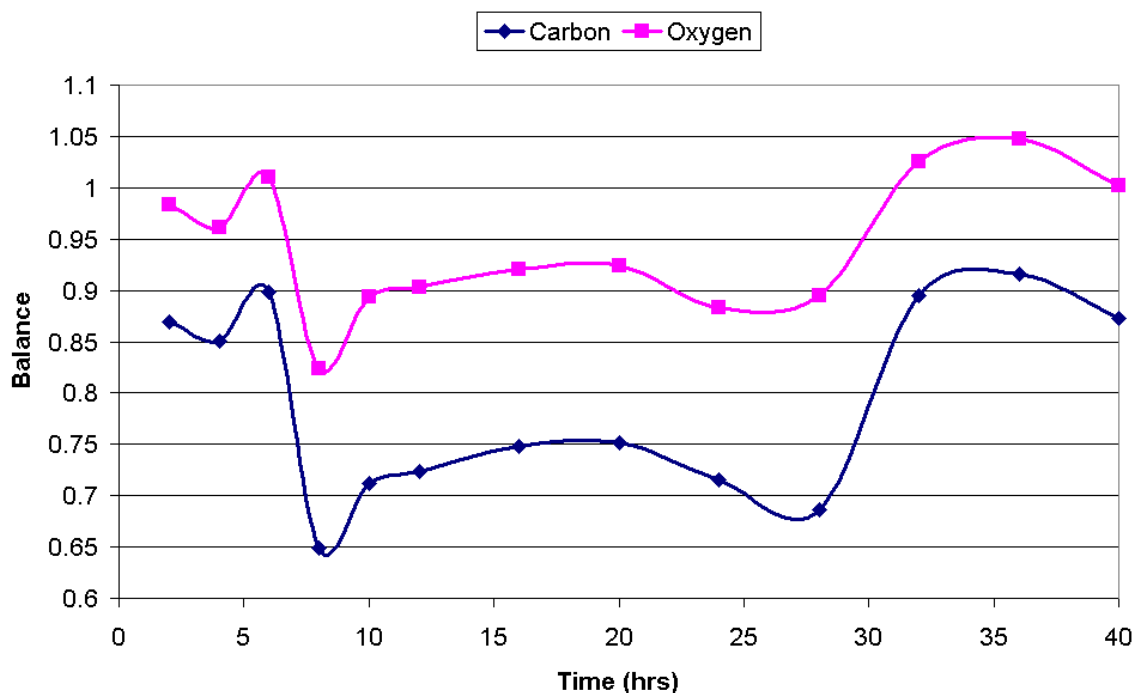


Figure 3-81 Mass balances from 5.0mol% acid addition into CO/CO₂/H₂ system over Katalco 51-8 catalyst (acid fed in between 4 and 24hrs)

The mass balances for the system showed that substantial amounts of carbon and oxygen were not accounted for during the acid addition. When a lower concentration of acid was fed in to previous classic methanol synthesis systems, the mass balances of the systems remained high, and indicated that no carbon deposition had taken place. However, in the current system, massive decreases were observed, indicating that deposition of the acid had occurred on the catalyst surface.

Post reaction when the catalyst reactor lid was removed, the inside of the reactor was covered with a brown powder. On closer inspection two of the catalyst pellets had completely lost their structure and had been degraded into powder. The remaining pellets were severely deteriorated, with cracks clearly visible. SEM images of the degraded pellets were taken, as well as images of pre-reaction pellets.

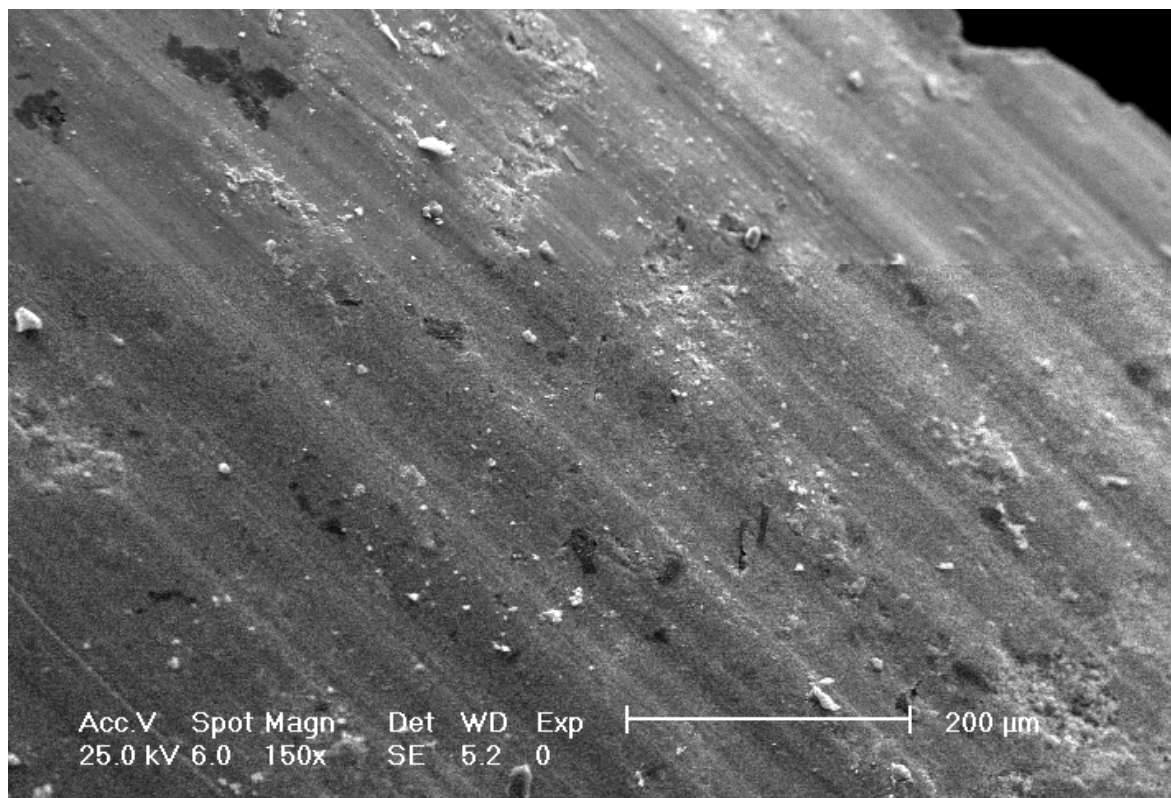


Figure 3-82 SEM image of Katalco 51-8 pellet pre acid addition

The pre-reaction pellet (fig 3-83) showed a reasonably smooth surface, with slight grooves apparent from the manufacturing process. In comparison, the SEM images taken of the post reaction catalyst pellets showed severe degradation of the catalyst pellets.

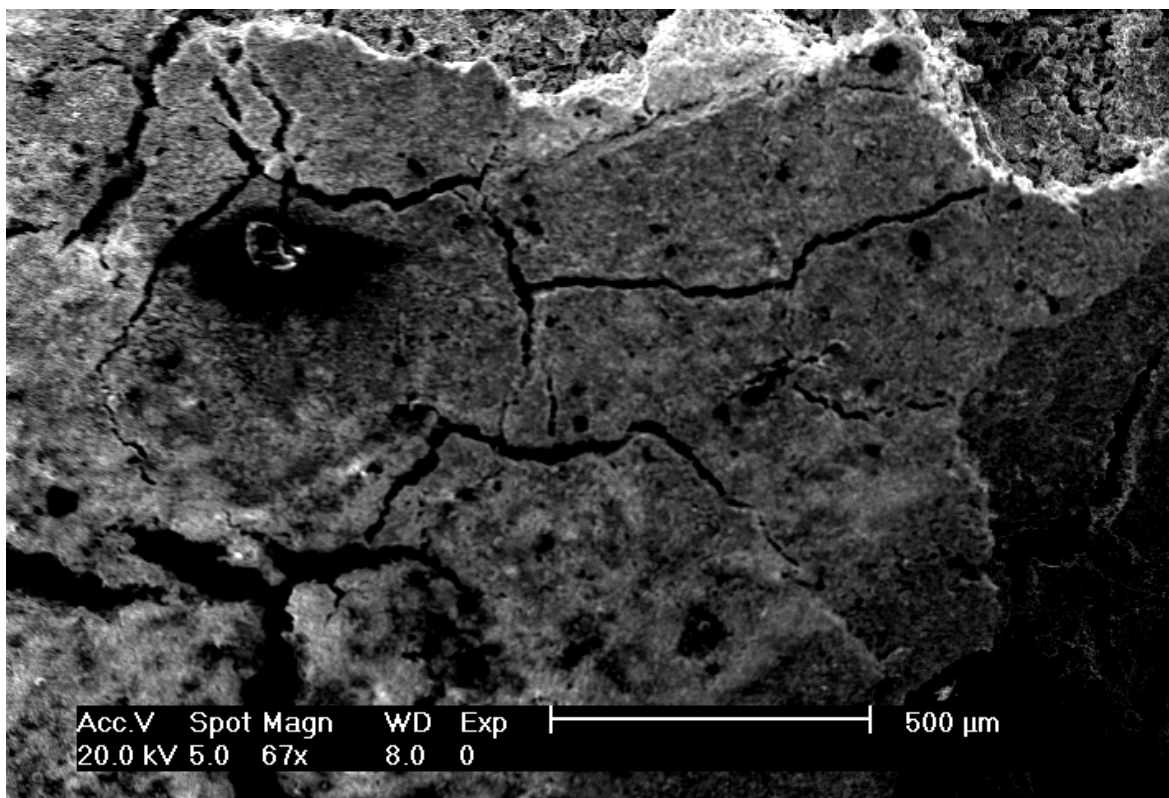


Figure 3-83 SEM image of Katalco 51-8 catalyst pellet after exposure to 5.0mol% acetic acid feed

Deep cracks were apparent on the catalyst surface, and images taken at a higher magnification showed that the inside of the catalyst had been powdered.

X-ray diffraction (XRD) analysis was used to examine the effect that the high concentration of acid had on the catalyst sample. An XRD pattern obtained from a Katalco catalyst exposed to a smaller concentration of acid under a CO/CO₂/H₂ feed was used for comparison, as well as an XRD pattern from a reduced Katalco sample.

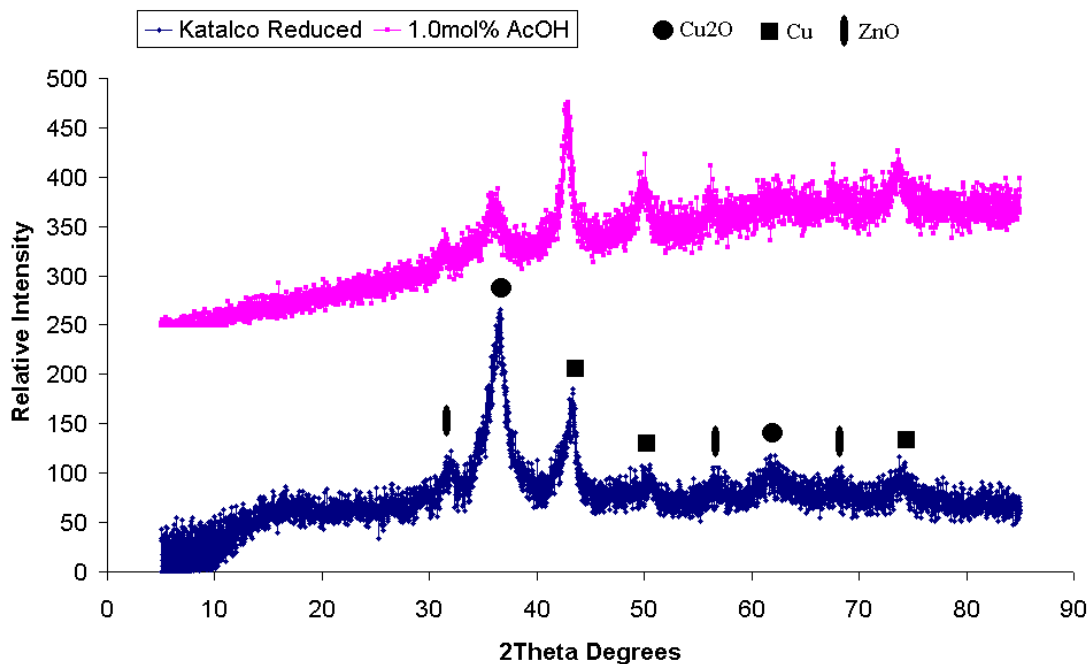


Figure 3-84 XRD patterns of a reduced Katalco catalyst and a Katalco catalyst exposed to 1.0mol% acetic acid under a CO/CO₂/H₂ feed

The XRD pattern for a reduced Katalco catalyst showed reflections relating to the presence of copper oxide (CuO), copper metal (Cu) and zinc oxide (ZnO). The presence of a zinc oxide phase was not observed previously under hot stage XRD examination, however the partial pressure of hydrogen used in the reduction was only 2%. The sample of Katalco used here was reduced in the reactor under pure hydrogen prior to XRD analysis. However, as a consequence, a significant presence of copper oxide was also observed and presumably formed upon opening of the reactor lid. Only a small reflection for copper oxide was observed in the hot stage XRD over 150°C.

When compared with the XRD pattern obtained for the 1 mol% acid addition run, an increase in crystallinity of copper metal was obtained, with a subsequent decrease in copper oxide. This indicated that growth of metallic copper particles increased during the run. As the reaction was run under predominantly reducing conditions, this was expected.

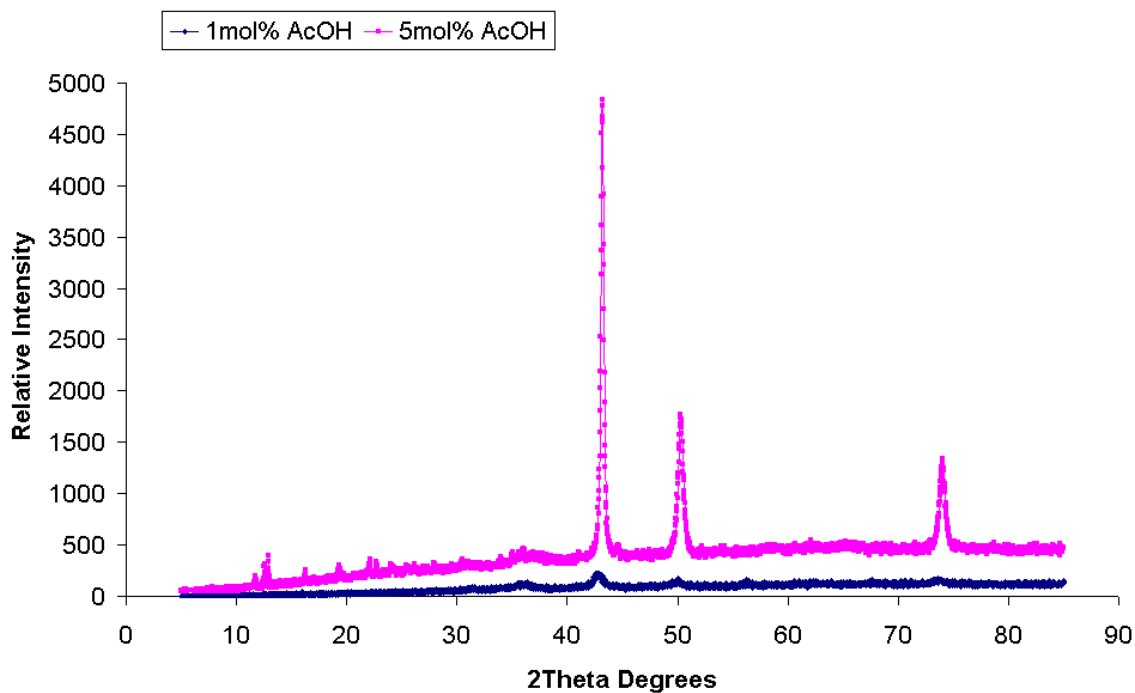


Figure 3-85 XRD patterns of Katalco catalysts exposed to 1.0mol% and 5mol% acetic acid under a CO/CO₂/H₂ feed

When the pattern for the 5mol% addition was compared with the pattern obtained for the 1mol% addition run, a huge increase in the intensity of the copper metal peaks was observed. This indicated that an increase in crystallinity of the copper had occurred. Normally, an increase in crystallinity of metals under catalytic conditions is simply due to sintering, and is accompanied by a decrease in surface area and an increase in metal crystallite size. Analysis of the XRD's using the Scherrer equation revealed an increase in copper crystallite size from 9.25nm (post reduction) to 29.5nm (post 5% acid addition). In addition, BET analysis of the catalysts confirmed that a significant loss of surface area was observed upon exposure to a high concentration of acid:

Catalyst	Surface Area (m ² / g)	Pore Diameter (Å)
Katalco 51-8 catalyst (unreduced)	89	37
Katalco 51-8 catalyst exposed to 5mol% AcOH addition	1	204

Table 3-18 Surface area comparison of fresh Katalco catalyst and Katalco catalyst exposed to 5mol% AcOH

However, as the catalyst pellets were almost completely destroyed by the addition of the acid, it was more likely that the loss of surface area was due to the complete degradation of the catalyst framework, rather than simply sintering. If this were to occur, then the observed pore diameter increase upon addition of the acid would actually be the distance between huge particles of the degraded catalyst.

The degradation of the catalyst framework was thought to possibly occur via two processes.

- Phase Change
- Extraction

Both possibilities were explored:

3.3.6.6 Phase Change

Phase changes have been shown previously to occur with a substantial loss of surface area. For example, gamma aluminas, of surface areas of around 100m² g⁻¹ have been shown to convert to alpha aluminas, with surface areas of ~1m² g⁻¹. Although the alumina present in the Katalco 51-8 catalyst was amorphous, it was possible that if the phase changed to alpha, then collapse of the catalyst structure would follow.

On closer inspection of the post reaction XRD however, no peaks relating to the presence of alpha alumina were detected, or any phase of alumina, indicating that it was still present in an amorphous state.

3.3.6.7 Extraction

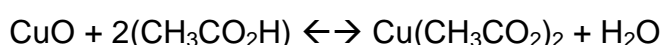
The Katalco 51-8 catalyst was prepared via a co-precipitation process, which is used to generate a homogeneous distribution of all the catalyst components. Therefore every component is critical to the catalyst structure being maintained. If one or more of the components was to be extracted from the catalyst then complete collapse of the catalyst structure would ensue.

In the Katalco catalyst it was possible that the acetic acid could extract several components. Zinc oxide and magnesium oxide are present in the Katalco catalyst to prevent sintering of the copper particles. As both components were basic in nature (amphoteric in the case of zinc oxide) it was possible that the acetic acid would display an affinity for the compounds. Conversion of both oxides to acetates would significantly increase the solubility of the metals and could be extracted into the water vapour. If this were to occur then sintering of the copper particles would occur, as well as collapse of the catalyst structure. In support of this, features relating to zinc oxide were not observed in the post reaction XRD of the catalyst, although features were present in the 1.0mol% addition catalyst and the reduced catalyst sample.

Another possibility was the reaction of copper with the acetic acid. Acetic acid has been used to leach metals such as copper in hydrometallurgical extraction. Leaching processes of metallic copper or ores containing copper in the divalent state have been the subject of many research works[149-151]

In relation to catalysis, after deactivation the components of the catalysts can be used as secondary source of metals. This is considered a more environmentally friendly and economical process than landfill depositing.

Copper (II) oxide is a basic oxide, and dissolves in acetic acid according to the following equation:



It's possible that under the classic methanol synthesis system, the presence of unreacted acid could maybe lift copper out of the catalyst matrix, and hence degradation of the pellet occurred.

Whichever process by which the acid degraded the catalyst framework, the loss of surface area explains the substantial decrease in methanol synthesis that was observed after the addition had ended.

3.3.6.8 Acid Balance

Acid to Ethanol (%)	3.3
Acid to Methyl Acetate (%)	1.5
Acid to Ethyl Acetate (%)	14.5
Acid to CO/CO ₂ (%)	41.4
Unreacted Acid (%)	3.7
Total (%)	64.4

Table 3-19 Acid balance from 5.0mol% acid addition into CO/CO₂/H₂ system over Katalco 51-8 catalyst

Overall the acid was converted to ethanol, ethyl acetate, methyl acetate and CO/CO₂, with a small percentage of the acid coming through the system unreacted. Unlike for previous acid additions into a classic methanol synthesis system, not all of the acid was accounted for as products. A significant amount of the acetic acid was missing, presumably deposited on the catalyst surface.

3.3.6.9 Temperature Programmed Oxidation (TPO)

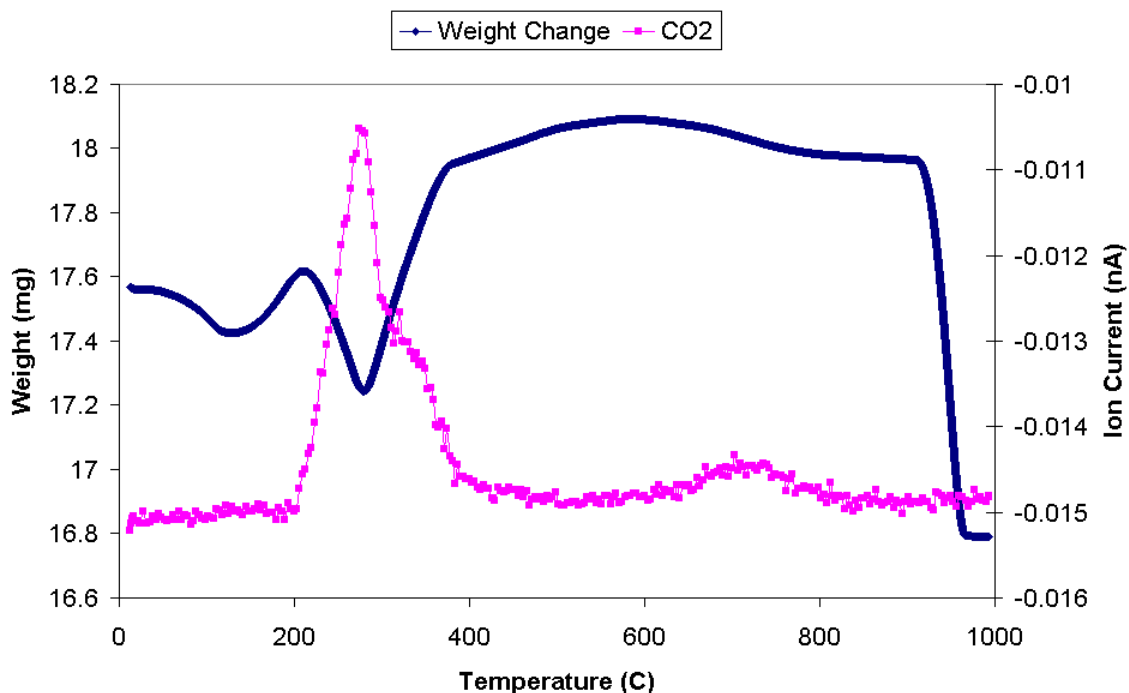


Figure 3-86 Post reaction TPO from 5.0mol% acid addition into CO/CO₂/H₂ system over Katalco 51-8 catalyst

It has become a characteristic of these catalysts under oxidising conditions that a linear weight increase of the sample is observed, due to copper metal in the sample reoxidising. In the current sample however, a significant weight decrease was observed at around 278°C and corresponded to the evolution of CO₂ from the catalyst surface. Enough carbon was removed from the surface to result in a perturbation of the linear weight increase.

The results confirmed that a substantial amount of the acetic acid that was introduced to the system was deposited on the catalyst surface.

3.3.6.10 Summary

Introduction of acetic acid at low concentrations to the classic methanol synthesis system for an extended period of time resulted in no intrinsic deactivation of the catalyst, only a transient decrease in methanol production. The same reaction profile was observed for the prolonged addition as it was for the short term addition. This suggested that at the low levels present, the catalyst was not affected and could convert all of the acid to products.

Upon introduction of a higher concentration of the acid, the catalyst was irreversibly deactivated, with two of the five catalyst pellets completely degraded. SEM pictures of the catalysts showed deep cracks in the pellet structure. Further studies using XRD and BET showed a significant decrease in surface area and suggested that the catalyst structure had collapsed. Consequently, methanol synthesis activity of the catalyst did not recover to its original levels after the acid addition had been stopped.

The mechanism of the deactivation was unclear, possibly extraction of copper from the catalyst matrix or acid attack on the basic metal oxides, followed by extraction by water vapor. The presence of unreacted acid in the system was therefore deemed to be deleterious to the copper catalyst.

3.4 Methyl Acetate Studies

Although the liquid phase Cativa process exhibits a high selectivity towards the production of acetic acid (99%), in the envisaged process by BP, gas phase carbonylation would be utilised.

In the halide free gas phase carbonylation, methyl acetate has been shown to be the major acetyl produced, although acetic acid can still be formed[93, 94].

Therefore, as well as acetic acid, it was of interest to determine if methyl acetate would deactivate the methanol synthesis catalyst, or inhibit methanol synthesis (as shown in the acetic acid studies

3.4.1 Standard Addition

As an initial experiment it was decided to introduce methyl acetate at a low concentration into a classic methanol synthesis system, to observe the effects of the ester on the catalyst. It was of interest to determine if the ester deactivated the catalyst, and if so, if the deactivation was transient or permanent. It was of further interest to determine if the ester would react to produce other species such as methanol and ethanol.

3.4.1.1 Experimental

Prior to reaction, the Katalco 51-8 catalyst was reduced *in situ* in the reactor under 50ml min⁻¹ flowing hydrogen at a temperature of 523K. The catalyst was held at this temperature for 3hrs.

The experiment was performed using a classic methanol synthesis gas feed of CO/CO₂/H₂ in a 1:1:8 molar ratio. A small concentration of nitrogen was also fed in as a reference gas, for the calculation of conversion. The exact gas mix composition used was 10ml N₂ / 25ml CO / 25ml CO₂ / 190 ml H₂.

- Reaction Temperature (K) 523
- Pressure (barg) 50
- Gas Flow (ml min⁻¹) 250
- Catalyst Volume (ml) 1.36

- GHSV (hr^{-1}) $\sim 11,000$

The methyl acetate was fed in at a molar feed rate of 1.1mol% ($3.4 \times 10^{-7} \text{ moles min}^{-1}$)

3.4.1.2 Reaction Data

For the first 6hrs of the run, no methyl acetate was introduced to the system. The catalyst performed as expected, with a methanol yield of $\sim 9.3\%$ obtained. Steady levels of all the components in the system were observed, confirming that equilibrium had been attained.

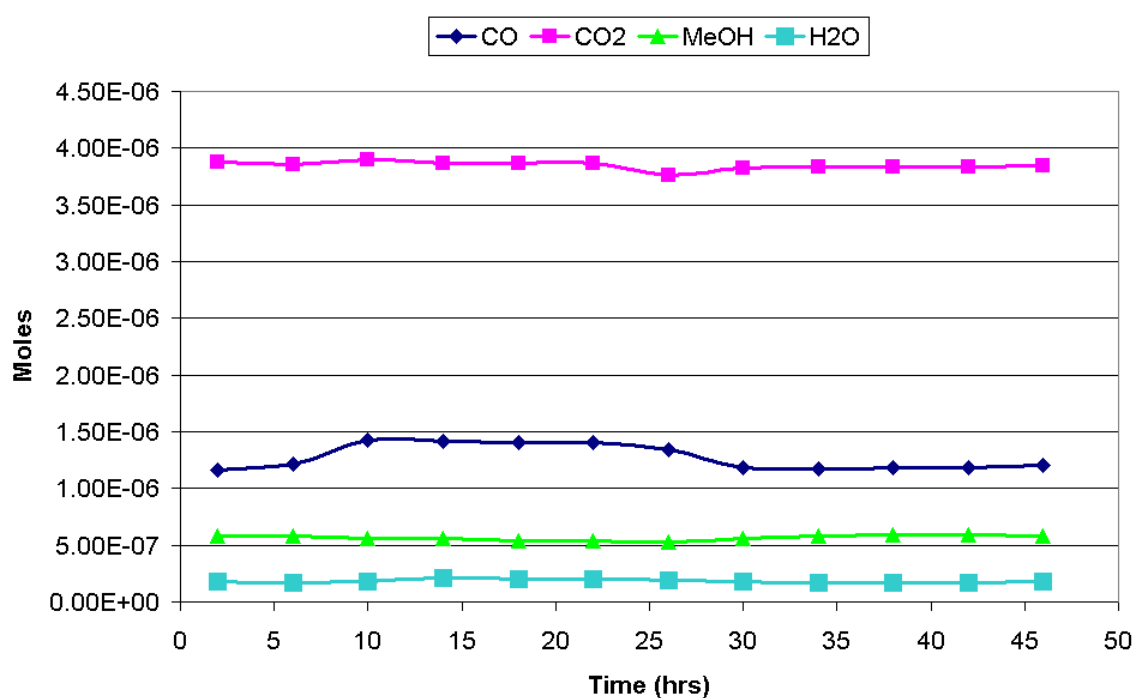
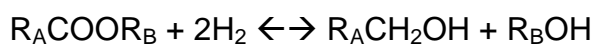


Figure 3-87 Reaction profile from 1.1mol% ester addition into CO/CO₂/H₂ system over Katalco 51-8 catalyst (ester addition between 6 and 22hrs)

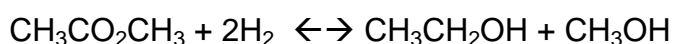
Upon addition of the ester to the system after 6hrs, a number of effects were observed. Methanol production decreased, although only slightly. This was in complete contrast to the extensive decrease observed upon addition of acetic acid. However, the decrease in methanol production was most likely attenuated by the conversion of part of the ester to methanol. It was thought that this may be occurring on the basis of the ethanol production that was observed upon addition of the ester.

The catalytic reduction of esters to alcohols encompasses reactions in which the C-O bond adjacent to the carbonyl group is cleaved according to the following stoichiometry[104, 105]:



Where R_A represents an alkyl group and R_B represents another alkyl group or hydrogen. For example the reduction of ethyl acetate over copper catalysts proceeds via the dissociative adsorption of the reagent into $\text{CH}_3\text{C}^*\text{O}$ and $\text{C}_2\text{H}_5\text{O}^*$ species in which * represents a surface site[105]. Subsequent hydrogenation of these species yields the desired alcohols.

Therefore if the reduction of methyl acetate was to proceed via the same mechanism then methanol and ethanol would be produced:



Ethanol was observed in the system upon addition of the ester and it can be assumed that methanol would also be formed in a 1:1 molar ratio. Therefore a larger inhibition effect on methanol production could be taking place upon addition of the methyl acetate, but is offset slightly by the production of methanol through hydrogenolysis.

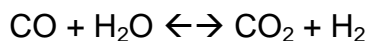
The decrease in methanol production upon addition of the ester was compared with the decrease in methanol production that was observed upon addition of the acetic acid. When acetic acid was introduced to the system, the methanol concentration decreased by $\sim 2.0 \times 10^{-7}$ moles, compared with a smaller decrease of $\sim 4.7 \times 10^{-8}$ moles upon addition of the ester. Assuming that methyl acetate is converted to ethanol and methanol in a 1:1, the decrease in methanol production upon addition of the ester increased to $\sim 9.1 \times 10^{-8}$ moles. The addition of acetic acid into the system resulted in a decrease in methanol production that was double the decrease observed for when methyl acetate was introduced. Methyl acetate therefore had much less of an effect on the methanol synthesis activity.

Another effect that was observed upon addition of the ester was a reasonable increase in CO levels and only a tiny increase in CO_2 levels. This differed to the

substantial increases in both CO and CO₂ that occurred upon addition of acid. The difference in the CO/CO₂ levels could possibly be due to the mechanism of decomposition.

In the acetic acid system it was postulated that the decomposition of the acetic acid resulted in CO₂ and adsorbed carbon. The adsorbed carbon could then be oxidised, either by reaction with surface oxygen or via a reverse Boudouard reaction involving CO₂.

If full oxidation of the surface carbon proceeded via a reaction with surface oxygen, then conversion of the acetic acid would yield CO₂. Via the WGS, An increase in CO₂ levels, coupled with the high partial pressure of hydrogen present would result in the equilibrium shifting to the left, to re-establish equilibrium.



In the case of the methyl acetate decomposition, if the methyl acetate was converted to CO rather than CO₂, the water gas shift would be limited by the relatively low water concentration. Therefore the equilibrium could not shift to the right, and the conversion of CO to CO₂ would not occur.

This could explain the reasonable increase in CO levels without an increase in CO₂ as well.

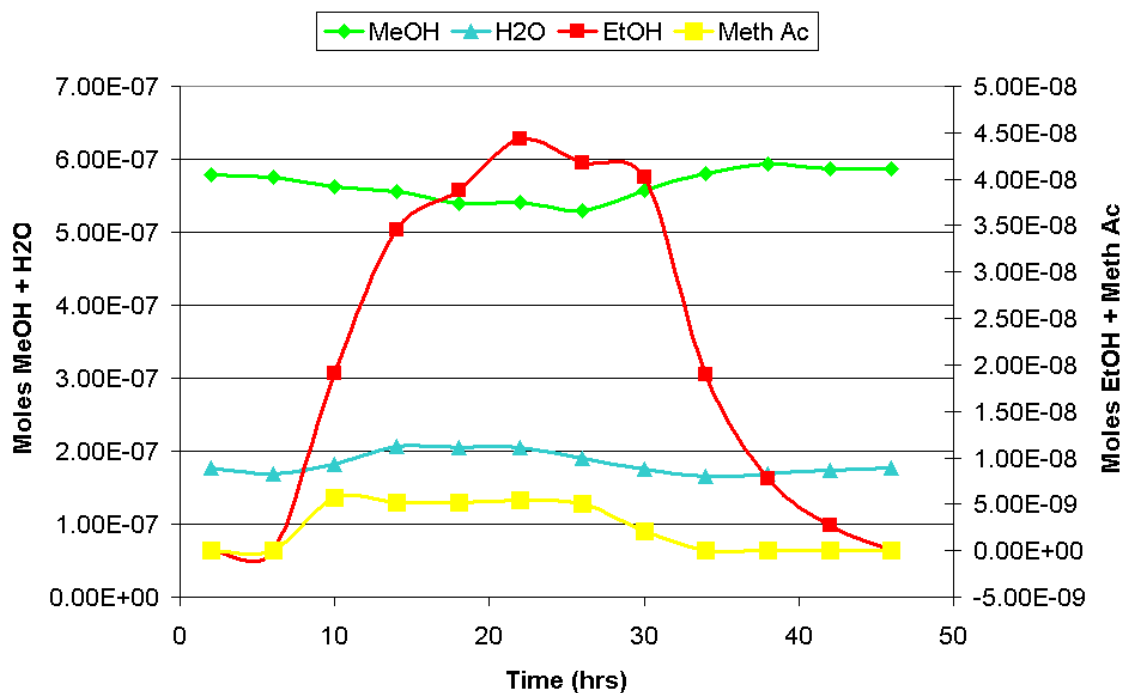


Figure 3-88 Reaction profile from 1.1mol% ester addition into CO/CO₂/H₂ system over Katalco 51-8 catalyst (ester addition between 6 and 22hrs)

Methyl acetate itself was detected in low concentrations throughout the addition. Upon cessation of the addition the system returned back to normal, indicating that the methyl acetate did not have an intrinsic effect on the catalyst itself, it was only transient.

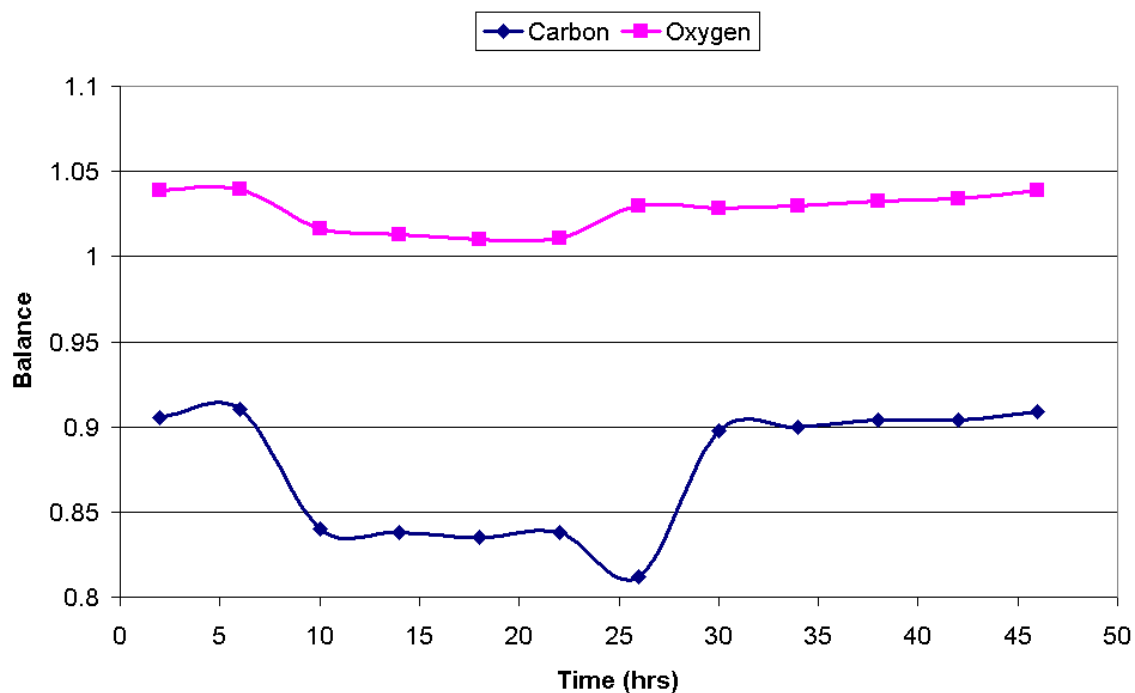


Figure 3-89 Mass balances from 1.1mol% ester addition into CO/CO₂/H₂ system over Katalco 51-8 catalyst (ester addition between 6 and 22hrs)

Unlike for the low level acetic acid additions, the carbon balance did not remain steady upon addition of the ester. The balance dropped slightly indicating that some of the methyl acetate had been potentially deposited on the catalyst surface.

3.4.1.3 Ester Balance

Ester to Ethanol (%)	9.6
Ester to Methanol (%)	4.8
Ester unreacted (%)	1.8
Ester to CO / CO ₂ (%)	21.2
Total (%)	37.6

Table 3-20 Ester balance from 1.1mol% ester addition into CO/CO₂/H₂ system over Katalco 51-8 catalyst

The table shows that the ester was converted to ethanol and methanol (presumably through the hydrogenolysis of the ester) and CO/CO₂ (possibly through the conversion of the ester to CO). Although the production of methanol

could not be observed directly as methanol was already present in the system, it was assumed that for every mole of ethanol that was produced, one mole of methanol was also produced. Finally, some of the ester was detected unreacted.

The majority of the ester however remained unaccounted for and suggested that it was deposited on the surface of the catalyst.

3.4.1.4 Temperature Programmed Oxidation (TPO)

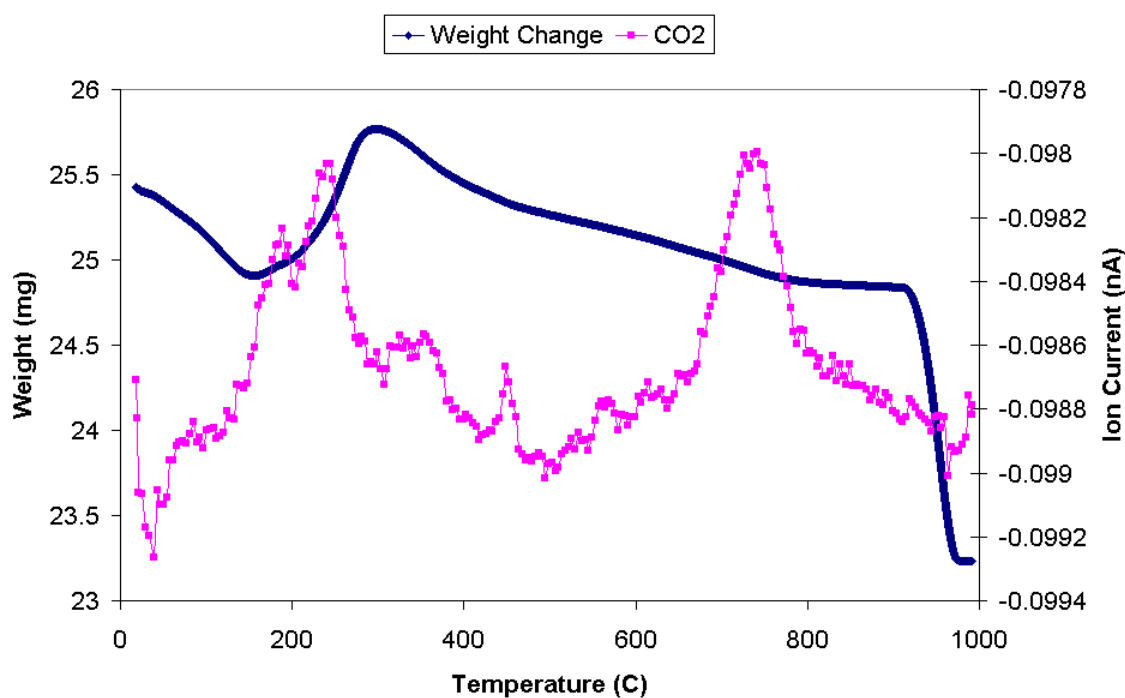


Figure 3-90 Ester balance from 1.1 mol% ester addition into CO/CO₂/H₂ system over Katalco 51-8 catalyst

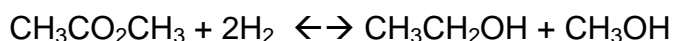
The post reaction TPO of the catalyst revealed that low temperature evolutions of CO₂ were observed at 193°C, 235°C and 275°C. The evolutions at 235°C and 275°C were at similar temperatures to those observed for catalysts exposed to acetic acid, suggesting similar species. The evolution at 193°C could possibly have been strongly adsorbed methyl acetate, possibly held in the pores of the catalyst.

The evolution at high temperatures was thought to be oxidation of the catalyst binder material, as already discussed.

3.4.1.5 Summary

In summary, the behaviour of the methyl acetate upon introduction to the classic methanol synthesis system (CO/CO₂/H₂ feed, Katalco catalyst) was significantly different to the behaviour observed for the addition of acetic acid.

Hydrogenolysis of the ester was found to occur, with the subsequent alcohols methanol and ethanol being produced:

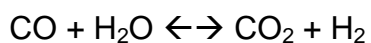


The mechanism of the hydrogenolysis of esters has appeared many times in the literature, and as there was a high partial pressure of hydrogen present in the system, the reaction was not unexpected. Although the production of methanol could not be observed directly as methanol was already present in the system, it was assumed that for every mole of ethanol that was produced, one mole of methanol was also produced. Carbon labelling, similar to the experiments performed for the acetic studies would be useful in determining if the mechanism was correct.

Methanol production decreased slightly upon the addition of the ester, in complete contrast to the significant decrease observed during addition of acetic acid. Initially it was thought that the hydrogenolysis of the ester to produce methanol could possibly have attenuated the decrease, however it would only have made a slight difference (assuming hydrogenolysis of the ester resulted in the production of methanol and ethanol in a 1:1 ratio). Therefore it was apparent that the methyl acetate had much less of a detrimental effect on methanol production than acetic acid. It was unclear as to the exact reason why.

Another interesting observation, similar to the phenomenon observed during the acetic acid additions was the conversion of the ester to CO/CO₂. However conversion of the acetic acid was found to result in similar increases in both CO and CO₂, whereas methyl acetate was found to be converted to mainly CO, with only a slight increase in CO₂. A possible explanation for the behaviour lay in the mechanism.

For the conversion of acetic acid to CO/CO₂ it was postulated that the acid decomposed on the catalyst to yield CO₂ and adsorbed carbon. The carbon could then be oxidised to CO or CO₂. If the surface carbon was fully oxidised to CO₂ then via the reverse WGS the CO₂ could be converted to CO (as hydrogen was also abundant in the system).



Therefore the decomposition of acetic acid would result in increases in both CO and CO₂ concentrations.

However, if methyl acetate was converted to CO on the surface instead of CO₂, the water gas shift mechanism would be limited by the relatively low concentration of water in the system. Studies on the decomposition pathways of methyl acetate were not found in the literature and therefore no comparisons could be made.

Finally, unlike for the addition of acetic acid, the addition of methyl acetate to the system resulted in substantial carbon laydown. Over 62% of the methyl acetate was unaccounted for as gas phase products, and had been deposited on the catalyst surface. As altering the feed gas had been shown in the acetic acid studies to alter the amount of carbon deposited on the surface of the catalyst, it was thought that this approach may also change the behaviour of the ester.

3.4.2 Gas Composition Studies

As the morphology of the copper particles had been previously shown in the literature to change depending on the feed gas environment surrounding them [57-59, 69], it was decided to carry out a programme of work investigating the effects of altering the feed gas composition on the behaviour of the ester.

Studies performed previously revealed that the behaviour of the acetic acid was directly affected by the gas feed composition, and this could be further related to the morphology of the copper. It was therefore of interest as to whether the methyl acetate would also show the same behaviour.

3.4.2.1 Experimental

Prior to reaction, the catalyst was reduced *in situ* in the reactor under 50ml min⁻¹ flowing hydrogen at a temperature of 523K. The catalyst was held at this temperature for 3hrs.

The following reaction conditions were used:

- Reaction Temperature (K) 523
- Pressure (barg) 50
- Gas Flow (ml min⁻¹) 250
- Catalyst Volume (ml) 1.36
- GHSV (hr⁻¹) ~11,000

The feed gas was varied for each experiment, to allow the effect of each gas component on the behaviour of the acid to be observed. The gas feeds used are listed below:

Gas Composition	MI min ⁻¹
N ₂	250
N ₂ / H ₂	60 / 190
N ₂ / CO / CO ₂ / H ₂	10 / 25 / 25 / 190

Table 3-21 Feed gas compositions

In all experiments N₂ was used as a reference gas, for the calculation of conversion. Methyl acetate was fed in to each system at a molar feed rate of 1.1mol% (3.4x10⁻⁷ moles min⁻¹).

3.4.2.2 Nitrogen Atmosphere (N₂)

Under an inert atmosphere unreacted methyl acetate was the main compound detected passing through the system. Aside from this, conversion of the methyl acetate took place to yield methanol, ethanol and methane.

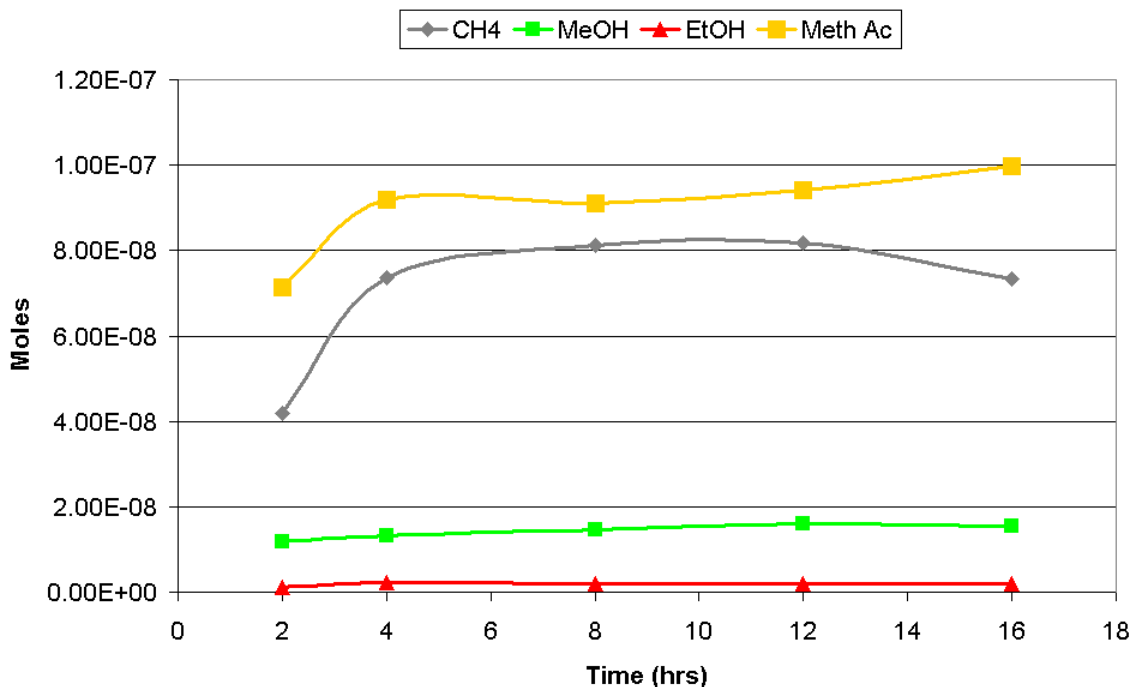


Figure 3-91 Reaction profile from 1.1mol% ester addition into N₂ system over Katalco 51-8 catalyst (ester fed in continuously from 2hrs)

The mechanism for the conversion of the ester to methanol and ethanol was through hydrogenolysis:



Although the reaction was carried out in an inert atmosphere, the catalyst was activated under flowing hydrogen. Trace amounts of hydrogen were probably left in the system, and would account for the trace levels of methanol and ethanol that were observed.

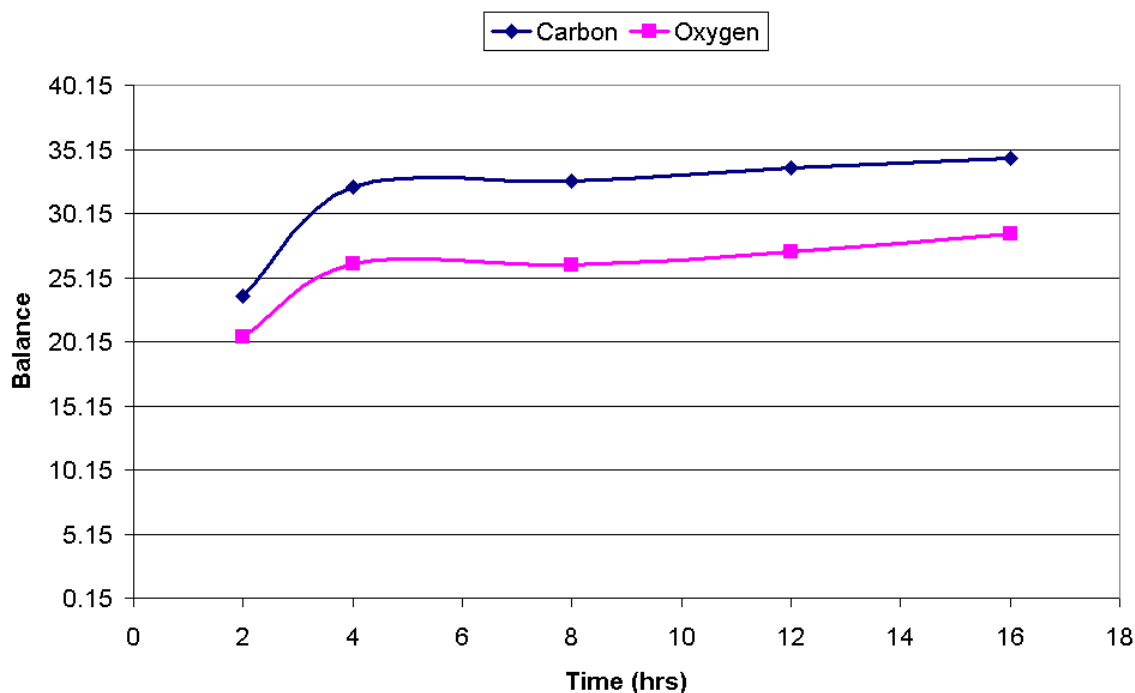


Figure 3-92 Mass balances from 1.1mol% ester addition into N₂ system over Katalco 51-8 catalyst (ester fed in continuously from 2hrs)

Methane was detected in a much higher yield than both of the alcohols and was probably formed from the complete hydrogenation of the methyl fragment of the ester. Transition metal catalysts (including copper and zinc) supported on alumina have been shown to convert esters to hydrocarbons at temperatures of ~523K, the reaction temperature employed during the run [152, 153]. Surprisingly, as methane was produced in a reasonable yield, no ethane formation was detected.

Ester to Ethanol (%)	0.4
Ester to Methanol (%)	1.3
Ester to Methane (%)	6.4
Ester unreacted (%)	26.3
Total (%)	34.4

Table 3-22 Ester balance from 1.1mol% ester addition into N₂ system over Katalco 51-8 catalyst

Although several products from the addition of the methyl acetate were observed, the majority of the ester could not be accounted for and was thought to be laid down on the catalyst surface.

Post reaction, a TPO was performed on the catalyst and revealed that a substantial amount of carbon was present on the catalyst surface. Two low temperature evolutions were observed at 276°C and 308°C, and were large enough to disrupt the weight gain profile of the catalyst (from the oxidation of reduced copper).

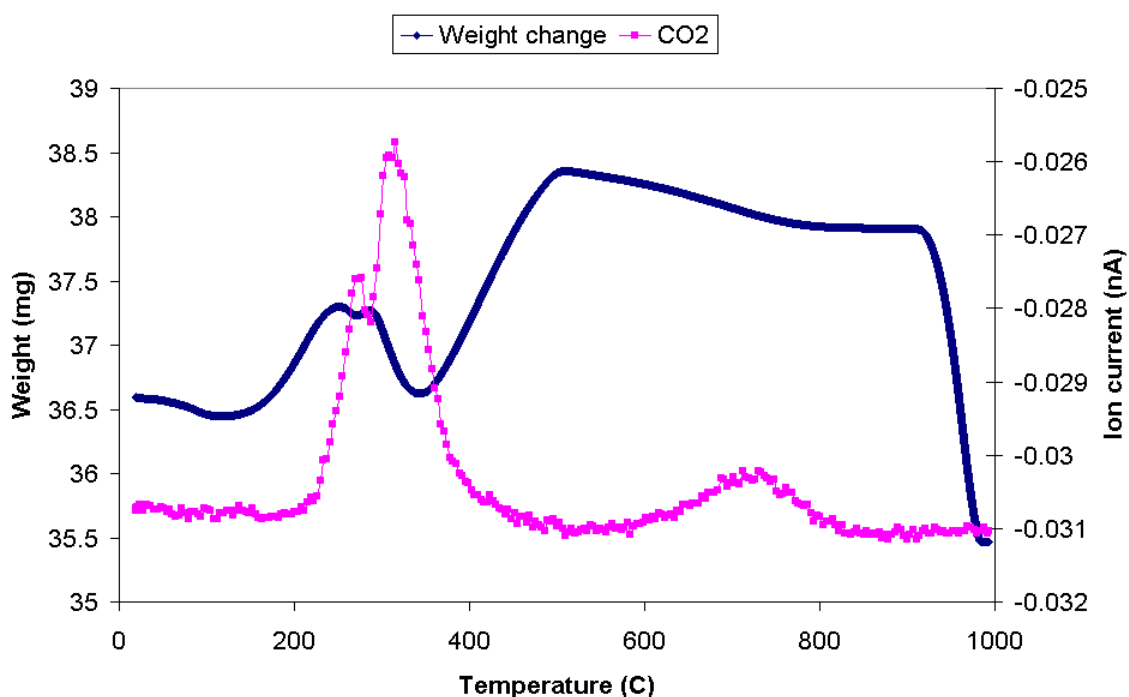


Figure 3-93 Post reaction TPO of catalyst from 1.1 mol% ester addition into N₂ system over Katalco 51-8 catalyst

As under the feed gas employed methanol was not produced, the presence of formate groups on the surface was ruled out. A DSC trace showed that the evolutions were exothermic, suggesting that it could be the burn off of carbon fragments.

A high temperature evolution of CO₂ was also observed and had been previously assigned to be oxidation of the catalyst binder.

3.4.2.3 Nitrogen / Hydrogen Atmosphere (N_2/H_2)

Under a reducing feed gas methyl acetate was introduced to the system after 6hrs. Instantly production of methane, ethane, methanol, ethanol and water took place. Methanol and ethanol were the products of hydrogenolysis due to the high partial pressure of hydrogen in the system. However straightforward hydrogenolysis would yield methanol and ethanol in a 1:1 ratio. This was not the case as the methanol:ethanol ratio recorded was 1.7:1. As mentioned for the previous experiment, methanol and ethanol can be further hydrogenated to methane and ethane. Both were detected during the run, with ethane being the major hydrocarbon.

The results suggested that the methoxy fragment of the ester was easily hydrogenated to methanol but not as easily hydrogenated to methane. In contrast the ethoxy fragment of the ester was easily hydrogenated through to ethane.

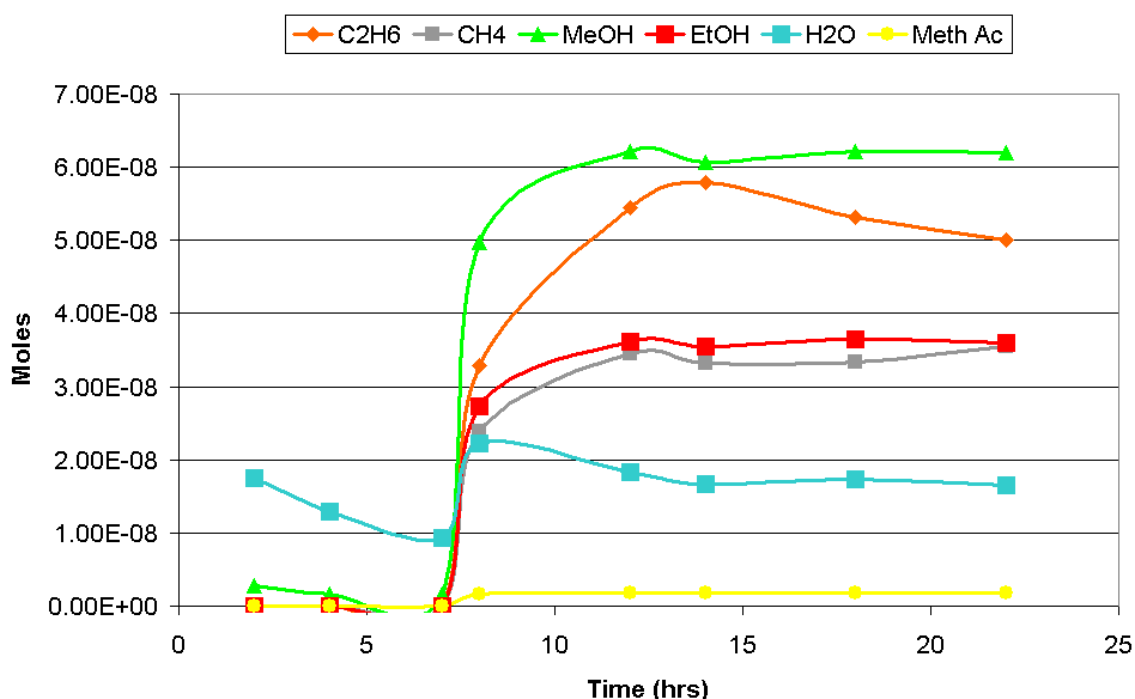


Figure 3-94 Reaction profile from 1.1mol% ester addition into N_2/H_2 system over Katalco 51-8 catalyst (ester fed in continuously from 6hrs)

Full hydrogenation of the ester fragments would also result in the formation of water and although its production was observed, the concentration was too low to account for all the hydrocarbons present. It was therefore thought that a fraction of the water would be present on the catalyst surface, most likely as hydroxyl groups.

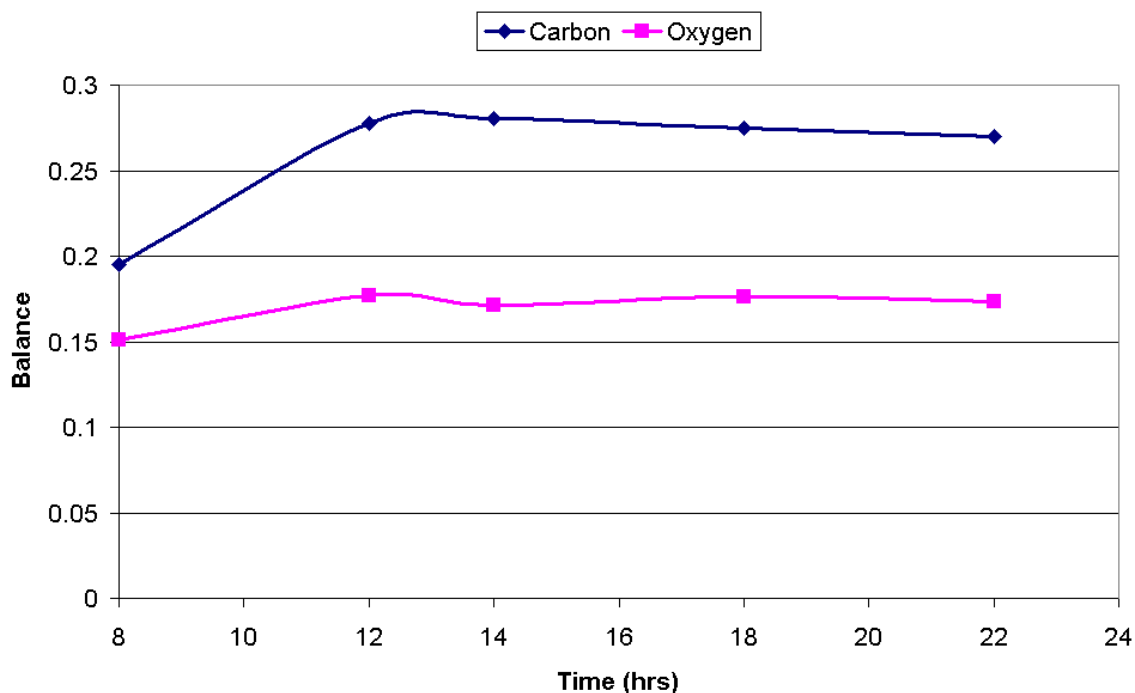


Figure 3-95 Mass balances from 1.1 mol% ester addition into N_2/H_2 system over Katalco 51-8 catalyst (ester fed in continuously from 6 hrs)

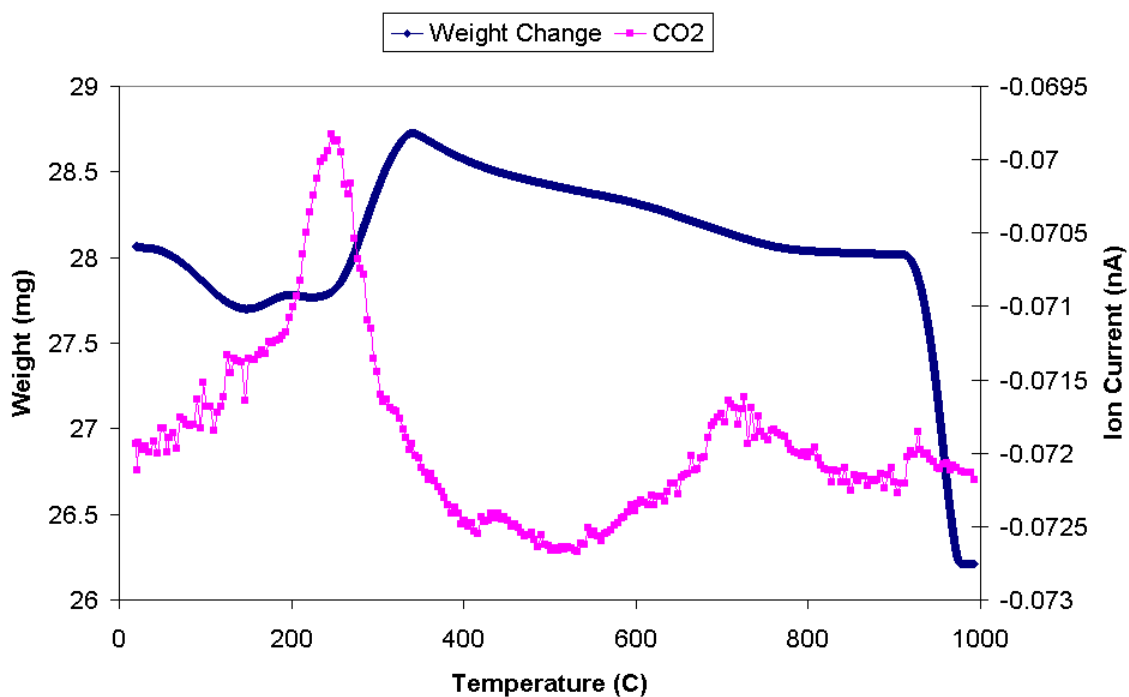
The mass balances for the system upon the addition of the ester only showed ~27% of the carbon in the ester showing up as products. Even less of the oxygen in the system was accounted for and both balances suggested that the majority of the ester had been deposited on the catalyst surface.

Ester to Ethanol (%)	7.1
Ester to Methanol (%)	6.1
Ester unreacted (%)	0.5
Ester to Methane (%)	3.5
Ester to Ethane (%)	9.8
Total (%)	27.0

Figure 3-96 Ester balance from 1.1 mol% ester addition into N_2/H_2 system over Katalco 51-8 catalyst

The acid balance of the system showed that only 27% of the carbon could be accounted for as the alcohols and the hydrocarbons.

The post reaction TPO of the catalyst showed a similar weight change profile to the one observed for the N₂ atmosphere.



Normally a linear weight gain is observed, due to the reduced copper in the sample oxidising. However, as the deposits of carbon on the sample were so large, the linear weight increase is perturbed by the evolution of the surface carbon as CO₂. The evolutions were exothermic in nature, suggesting burn off of surface carbon species.

3.4.2.4 Summary

The results from the effects of varying the gas feed composition on the behaviour of the ester are shown below:

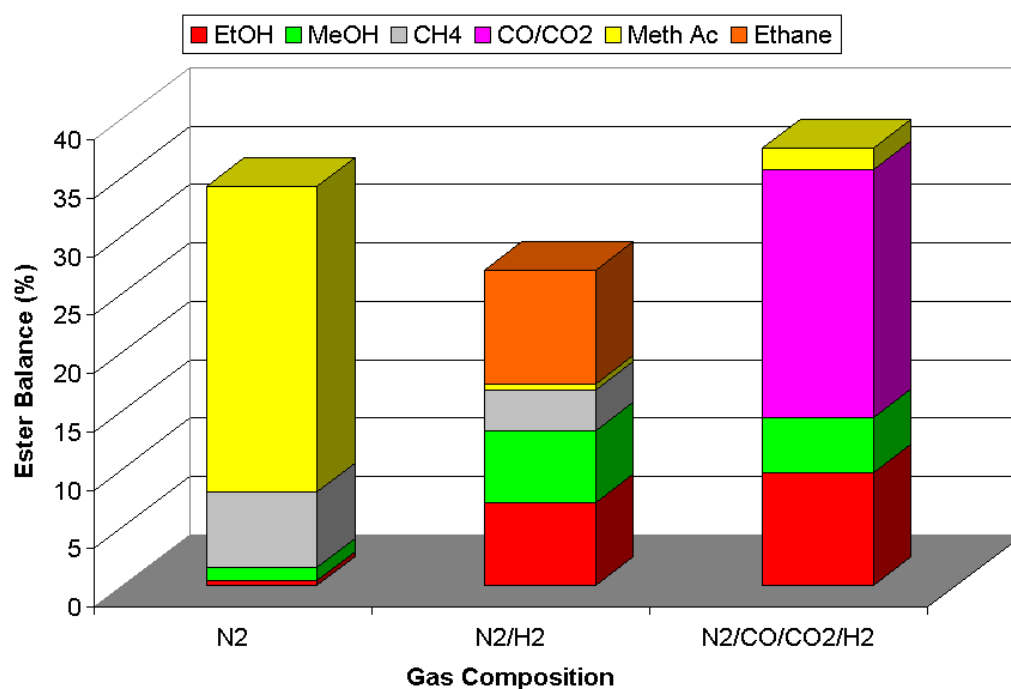


Figure 3-97 Ester balance of each system versus the feed gas composition of each system

Under an inert atmosphere methyl acetate underwent hydrogenolysis to methanol and ethanol. Methane was also formed, indicating that complete reduction of the methoxy fragment of the ester could proceed in the presence of small concentrations of hydrogen. Interestingly, no ethane was detected.

On moving to a more reducing environment, more of the ester underwent hydrogenolysis to the alcohols, as well as full reduction to hydrocarbons. Interestingly the production of methane decreased upon moving to the more reducing environment, which was unusual.

Under the reducing atmosphere, the ethoxy fragment of the ester was favourably fully hydrogenated to ethane, whereas the methoxy fragment was favourably converted to methanol. This suggested that upon moving to the classic methanol synthesis feed of CO/CO₂/H₂ (which was more oxidising) the formation of both ethanol and methane would increase. Although an increase in the formation of ethanol was observed, no methane was detected. Methanol was observed, but at

a low yield (based on the concentration of ethanol produced and assuming a 1:1 molar ratio).

Under the classic methanol synthesis system conversion of the ester to CO/CO₂ was also observed. Conversion of acetic acid to CO/CO₂ took place under the system previously, however similar amounts of both CO and CO₂ were produced. The ester yielded mostly CO with only a tiny increase in CO₂ observed. The behaviour was attributed to the differences in decomposition profiles of the acid and the ester.

Acetic acid was proposed to decompose fully to either two CO₂ molecules or CO and CO₂ in a 1:1 ratio. Conversion of the two CO₂ molecules to yield CO as well could occur via the water gas shift mechanism. Either mechanism could explain the similar increases in CO/CO₂ concentrations upon addition of the acid.

For the methyl acetate however it was proposed that if the ester decomposed to yield CO, conversion of the CO to CO₂ via the water gas shift would be limited by the small concentration of water present in the system. This would explain why an increase in CO was observed without a similar increase in CO₂.

In comparison with the gas composition studies performed for acid additions, a couple of similarities were observed. Firstly the carbon balance for the N₂/H₂ systems were the lowest for both studies, indicating that the presence of a high partial pressure of hydrogen in the system without the presence of CO₂ as an oxidant results in an enhancement of carbon deposition. Secondly, the classic methanol synthesis system yielded the highest carbon balance for both systems, indicating that the level of oxidation in the system could potentially be important. However, in the acid system all the acid carbon could be accounted for, whereas for the ester addition significant carbon laydown was observed.

Overall, the feed gas composition (and consequently the copper particle morphology) was shown to have a dramatic effect on the product distribution observed for the addition of the ester, but did not significantly alter the amount of carbon deposited on the catalyst. Although the addition of ester into the classic methanol synthesis system did not have as a pronounced effect on the methanol synthesis as the addition of acid did, substantial carbon laydown of the ester was

observed. Laydown over the course of the experiment did not deactivate the catalyst, however if the ester was present for an extended period of time the carbon would eventually build up and deactivate the catalyst.

3.4.3 High Concentration Additions

Finally several runs were performed under a CO/CO₂/H₂ system where methyl acetate was fed in to the system at a molar feed rate of 1.5mol%. Although the molar feed rate was only slightly higher than for the previous runs, an interesting effect was observed. The reactions were aborted as there were significant fluctuations in the data. The additions of methyl acetate were ceased and nitrogen purged through the reactor for several hours at temperature to completely remove the ester from the system. However, upon opening of the reactor lid after cooling, a pool of liquid had formed on the bottom of the reactor. In addition the catalyst pellets appeared wet.

A sample of the liquid found at the bottom of the reactor was taken and injected through the GC to determine the compounds present. As well as this, a soxhlet extraction was performed on the catalyst pellets using iso-propanol as the solvent. Results of both analysis revealed that methyl acetate was the compound present.

The presence of methyl acetate within the catalyst pellet indicated that condensation of the ester within the pores may have taken place. This could explain as to why the catalyst appeared wet. Upon shutting down the reactor, the drop in temperature and pressure could have caused some of the methyl acetate to “crash out” of the catalyst pellets, and would explain why a pool of methyl acetate was present on the bottom of the reactor.

Prior to the experiments, it would have been expected that if either acetic acid or methyl acetate would condense in the catalyst pores, that it would have been acetic acid. Condensation of the methyl acetate was therefore attributed to being due to an unusually strong binding on to the catalyst surface.

4 Conclusions

Throughout the project, the experimental work undertaken focussed on several main objectives. Overall, the main focus of the project was to investigate the effects that chemicals generated from a carbonylation reactor (such as methyl acetate and acetic acid) had on a methanol synthesis catalyst. The project was split into three main areas: (i) investigation of precious metal catalysts for methanol synthesis and tolerance towards acetic acid/methyl acetate, (ii) investigation of the effects of acetic acid on a commercial methanol catalyst and (iii) investigation of the effects of methyl acetate on a commercial methanol synthesis catalyst.

Studies performed on lab prepared precious metal catalysts revealed that Pd and Ir supported on silica catalysts exhibited high selectivities towards methanol from a CO/H₂ feed. In contrast, a Rh on silica catalyst catalysed the production of a wide range of compounds and this was due to the ability of Rh to adsorb CO dissociatively and non-dissociatively. Overall, the catalysts produced very low yields of methanol and this was attributed to a very low rate of reaction. As the yields were so low, it was unlikely that precious metal catalysts would be suitable for a commercial process and therefore it was decided to focus on studying the effects of acetic acid / methyl acetate over the commercial Cu/ZnO/Al₂O₃ catalyst.

Passing acetic acid at low concentrations over the commercial catalyst under standard methanol synthesis operating conditions (CO/CO₂/H₂ feed, 50 barg, 523K) resulted in a decrease in the methanol yield. This was attributed to acetate groups blocking sites for methanol synthesis by preventing adsorption of reactants. However upon switching off of the acid feed, methanol production returned to normal indicating the effect on the catalyst was transient.

The acetic acid was found to react upon entering the system, and underwent three distinct processes - (i) hydrogenation to ethanol, (ii) an esterification reaction with methanol to form methyl acetate and (iii) decomposition to CO/CO₂. These processes were confirmed by the addition of ¹³C labelled acetic acid to the system and following the responses of the relevant masses using a mass spectrometer. All of the acid carbon was accounted for and no laydown on the catalyst surface took place. Decomposition of the acid to CO/CO₂ was postulated to proceed via

decarboxylation to gas phase CO_2 and a surface methyl group. The surface methyl group was then proposed to decompose further to yield surface carbon and H_2 . Surface carbon could then be oxidised via reaction with surface oxygen, or via a reverse Boudouard process. Hydrolysis of the acid was shown not to be the route towards CO/CO_2 .

Studies performed changing the gas feed composition revealed that the decomposition of the acid could be altered. A possible reason for this was that the morphology of copper particles in methanol synthesis catalysts has been shown to alter, depending on the gas environment surrounding them. If the decomposition of acetates was structure sensitive, then this could explain the change in behaviour.

Finally low levels of acetic acid were shown not to have an intrinsic effect on the catalyst under standard methanol synthesis conditions, even when fed in for extended periods of time. However, increasing the concentration of the acid had a severe derogatory effect on the catalyst structure, and resulted in complete collapse of the catalyst pellet. Degradation was attributed to extraction of a component or components from the catalyst matrix.

The interactions of methyl acetate over the catalyst were also investigated and under methanol synthesis conditions, the ester was found to be reactive. Hydrogenolysis took place to yield methanol and ethanol, as well as decomposition to yield CO/CO_2 . Methanol synthesis was only slightly decreased, but was postulated to have been attenuated by the production of methanol from hydrogenolysis of the ester. Substantial amounts of the ester were deposited on the catalyst surface and would potentially deactivate the catalyst over time as layers of carbon would build up.

The behaviour of the ester was also found to change upon altering the gas composition, similar to the effect that was observed for the acetic acid studies. The phenomenon was attributed to the changing morphology of the copper particles.

5 Future Work

Possible future work includes:

- Inductively Coupled Plasma (ICP) analysis on the Katalco pellets exposed to higher concentrations of acetic acid could be performed. This would yield information as to which (if any) of the catalyst components were extracted from the pellet matrix
- As the morphology of the copper particles was proposed to play an important part in governing the behaviour of the acid / ester in the system, it would be of interest to perform studies on different morphologies of copper. Possible experiments could involve pulsing acid / ester vapour over various copper single crystal planes to determine if product distribution is changed
- It would be of interest to vary the CO:CO₂ ratio in the classic methanol synthesis feed, as this may alter the behaviour of the acid / methyl acetate in the system
- The effects of products from the acetic acid and methyl acetate additions (such as ethanol and ethyl acetate) must also be considered. Further experiments feeding in these products to the methanol synthesis system could show any effects
- Labelling studies could be performed for the methyl acetate additions to determine as to whether hydrolysis of the ester occurs

6 References

- [1] www.chemlink.com.au/methanol.htm.
- [2] BASF German Patents 415686, 462837. 1923.
- [3] J. Hagen, *Industrial Catalysis - A Practical Approach*. Wiley - VCH, 1999.
- [4] G. Natta, *Catalysis Vol 3*. Reinhold Publishing Corp, 1955.
- [5] P. Davies, F.F. Snowdon, G.W. Bridger, D.O. Huges, and P.W. Young. UK Patent 1010871.
- [6] J.T. Gallagher, and J.M. Kidd. UK Patent 1159035.
- [7] D. Cornthwaite. UK Patent 1296212.
- [8] K.C. Waugh, *Catalysis Today* 15 (1992) 51-75.
- [9] M. Twigg, *Catalyst Handbook*. Wolfe Publishing Ltd, 1989.
- [10] G.C. Chinchen, P.J. Denny, J.R. Jennings, M.S. Spencer, and K.C. Waugh, *Applied Catalysis* 36 (1988) 1-65.
- [11] <http://www.jmcatalysts.com/ptd/pdfs-uploaded/Methanol%20Synthesis%20KATALCO.pdf>.
- [12] R.J. Farrauto, and C.H. Bartholomew, *Fundamentals of Industrial Catalytic Processes*. Blackie Academic + Professional, 1997.
- [13] R.G. Herman, K. Klier, G.W. Simmons, B.P. Finn, J.B. Bulko, and T.P. Kobylinski, *Journal of Catalysis* 56 (1979) 407-429.
- [14] S. Mehta, G.W. Simmons, K. Klier, and R.G. Herman, *Journal of Catalysis* 57 (1979) 339-360.
- [15] K. Klier, *Applications of Surface Science* 19 (1984) 267-297.
- [16] J.B. Bulko, R.G. Herman, K. Klier, and G.W. Simmons, *The Journal of Physical Chemistry* 83 (2002) 3118-3122.
- [17] G.C. Chinchen, P.J. Denny, D.G. Parker, M.S. Spencer, and D.A. Whan, *Applied Catalysis* 30 (1987) 333-338.
- [18] Y.B. Kagan, *Doklady Akademii Nauk Sssr* 221 (1975) 1093.
- [19] Y.B. Kagan, A.Y. Rozovskii, L.G. Liberov, E.V. Slivinskii, G.I. Lin, S.M. Loktev, and A.N. Bashkirov, *Doklady Akademii Nauk Sssr* 224 (1975) 1081-1084.
- [20] C.V. Ovesen, P. Stoltze, J.K. Nørskov, and C.T. Campbell, *Journal of Catalysis* 134 (1992) 445-468.

- [21] C.V. Ovesen, B.S. Clausen, B.S. Hammershøi, G. Steffensen, T. Askgaard, I. Chorkendorff, J.K. Nørskov, P.B. Rasmussen, P. Stoltze, and P. Taylor, *Journal of Catalysis* 158 (1996) 170-180.
- [22] J. Skrzypek, M. Lachowska, M. Grzesik, J. Sloczynski, and P. Nowak, *Chemical Engineering Journal and the Biochemical Engineering Journal* 58 (1995) 101-108.
- [23] Wade, Kirk Othmer *Encyclopedia of Chemical Tehnology*. Wiley, New York, 1981.
- [24] L. Bissett, *Chemical Engineering* 84 (1971) 155.
- [25] P.J.A. Tijm, F.J. Waller, and D.M. Brown, *Applied Catalysis A: General* 221 (2001) 275-282.
- [26] C.N. Satterfield, *Heterogeneous Catalysis in Practice*, McGraw - Hill Engineering Series 1980.
- [27] W.X. Pan, R. Cao, D.L. Roberts, and G.L. Griffin, *Journal of Catalysis* 114 (1988) 440-446.
- [28] J.S. Campbell, *Industrial & Engineering Chemistry Process Design and Development* 9 (2002) 588-595.
- [29] G.C. Chinchen, P.J. Denny, D.G. Parker, G.D. Short, M.S. Spencer, K.C. Waugh, and D.A. Whan, *Preprints Am. Chem. Soc. Div. Fuel. Chem.* 29 (1984) 178.
- [30] G.C. Chinchen, K.C. Waugh, and D.A. Whan, *Applied Catalysis* 25 (1986) 101-107.
- [31] G.C. Chinchen, and K.C. Waugh, *Journal of Catalysis* 97 (1986) 280-283.
- [32] B. Denise, R.P.A. Sneeden, B. Beguin, and O. Cherifi, *Applied Catalysis* 30 (1987) 353-363.
- [33] W.R.A.M. Robinson, and J.C. Mol, *Applied Catalysis* 44 (1988) 165-177.
- [34] R. Burch, and R.J. Chappell, *Applied Catalysis* 45 (1988) 131-150.
- [35] R. Burch, R.J. Chappell, and S.E. Golunski, *Catalysis Letters* 1 (1988) 439-443.
- [36] H.H. Kung, *Catalysis Reviews-Science and Engineering* 22 (1980) 235-259.
- [37] K. Klier, H.P. D.D. Eley, and B.W. Paul, *Advances in Catalysis*, Academic Press. 243-313.
- [38] G. Liu, D. Willcox, M. Garland, and H.H. Kung, *Journal of Catalysis* 96 (1985) 251-260.
- [39] A.Y. Rozovskii, *Kinetics and Katalysis* 20 (1980) 97.
- [40] A.Y. Rozovskii, *Kinetics and Katalysis* 16 (1975).

- [41] W.R.A.M. Robinson, and J.C. Mol, *Applied Catalysis* 60 (1990) 61-72.
- [42] J.S. Lee, K.H. Lee, S.Y. Lee, and Y.G. Kim, *Journal of Catalysis* 144 (1993) 414-424.
- [43] P.B. Rasmussen, P.M. Holmblad, T. Askgaard, C.V. Ovesen, P. Stoltze, J.K. Nørskov, and I. Chorkendorff, *Catalysis Letters* 26 (1994) 373-381.
- [44] P.B. Rasmussen, M. Kazuta, and I. Chorkendorff, *Surface Science* 318 (1994) 267-380.
- [45] J. Nakamura, I. Nakamura, T. Uchijima, T. Watanabe, T. Fujitani, W.N.D.E.I. Joe W. Hightower, and T.B. Alexis, *Studies in Surface Science and Catalysis*, Elsevier. 1389-1399.
- [46] J. Yoshihara, and C.T. Campbell, *Journal of Catalysis* 161 (1996) 776-782.
- [47] B. Notori, *Proceedings of the 7th International Congress of Catalysis A* (1981) 487.
- [48] K. Kochloeff, *Proceedings of the 7th International Congress of Catalysis A* (1981) 486.
- [49] L.E.Y. Nonneman, and V. Ponc, *Catalysis Letters* 7 (1990) 213-217.
- [50] E.K. Poels, and D.S. Brands, *Applied Catalysis A: General* 191 (2000) 83-96.
- [51] D.S. Brands, E.K. Poels, T.A. Krieger, O.V. Makarova, C. Weber, S. Veer, and A. Blik, *Catalysis Letters* 36 (1996) 175-181.
- [52] T.M. Yurieva, L.M. Plyasova, O.V. Makarova, and T.A. Krieger, *Journal of Molecular Catalysis A: Chemical* 113 (1996) 455-468.
- [53] M. Muhler, E. Törnqvist, L.P. Nielsen, B.S. Clausen, and H. Topsøe, *Catalysis Letters* 25 (1994) 1-10.
- [54] C.T. Campbell, *Applied Catalysis* 32 (1987) 367-369.
- [55] I. Chorkendorff, P.B. Rasmussen, H. Christoffersen, and P.A. Taylor, *Surface Science* 287 (1993) 208-211.
- [56] G.J. Millar, C.H. Rochester, and K.C. Waugh, *Catalysis Letters* 14 (1992) 289-295.
- [57] B.S. Clausen, J. Schiøtz, L. Gråbæk, C.V. Ovesen, K.W. Jacobsen, J.K. Nørskov, and H. Topsøe, *Topics in Catalysis* 1 (1994) 367-376.
- [58] P.C.K. Vesborg, I. Chorkendorff, I. Knudsen, O. Balmes, J. Nerlov, A.M. Molenbroek, B.S. Clausen, and S. Helveg, *Journal of Catalysis* 262 (2009) 65-72.
- [59] J.D. Grunwaldt, A.M. Molenbroek, N.Y. Topsoe, H. Topsoe, and B.S. Clausen, *Journal of Catalysis* 194 (2000) 452-460.

- [60] K.C. Waugh, *Catalysis Letters* 58 (1999) 163-165.
- [61] T. Fujitani, and J. Nakamura, *Catalysis Letters* 56 (1998) 119-124.
- [62] J.C. Frost, *Nature* 334 (1988) 577-580.
- [63] K.M. Vandenbussche, and G.F. Froment, *Applied Catalysis a-General* 112 (1994) 37-55.
- [64] M. Bowker, H. Houghton, and K.C. Waugh, *Journal of the Chemical Society, Faraday Transactions 1: 77* (1981) 3023 - 3036.
- [65] P.A. Taylor, P.B. Rasmussen, C.V. Ovesen, P. Stoltze, and I. Chorkendorff, *Surface Science* 261 (1992) 191-206.
- [66] P.B. Rasmussen, M. Kazuta, and I. Chorkendorff, *Surface Science* 318 (1994) 267-280.
- [67] J. Yoshihara, S.C. Parker, A. Schafer, and C.T. Campbell, *Catalysis Letters* 31 (1995) 313-324.
- [68] T. Fujitani, I. Nakamura, T. Uchijima, and J. Nakamura, *Surface Science* 383 (1997) 285-298.
- [69] C.V. Ovesen, B.S. Clausen, J. Schiotz, P. Stoltze, H. Topsoe, and J.K. Nørskov, *Journal of Catalysis* 168 (1997) 133-142.
- [70] M.N. Berube, B. Sung, and M.A. Vannice, *Applied Catalysis* 31 (1987) 133-157.
- [71] L.R. Radovic, and M.A. Vannice, *Applied Catalysis* 29 (1987) 1-20.
- [72] M.L. Poutsma, L.F. Elek, P.A. Ibarbia, A.P. Risch, and J.A. Rabo, *Journal of Catalysis* 52 (1978) 157-168.
- [73] M. Josefina Pérez-Zurita, M. Cifarelli, M. Luisa Cubeiro, J. Alvarez, M. Goldwasser, E. Pietri, L. Garcia, A. Aboukais, and J.-F. Lamonier, *Journal of Molecular Catalysis A: Chemical* 206 (2003) 339-351.
- [74] S.H. Ali, and J.G. Goodwin, *Journal of Catalysis* 176 (1998) 3-13.
- [75] S.D. Jackson, B.J. Brandreth, and D. Winstanley, *Applied Catalysis* 27 (1986) 325-333.
- [76] J.M. Driessen, E.K. Poels, J.P. Hindermann, and V. Ponec, *Journal of Catalysis* 82 (1983) 26-34.
- [77] A. Gotti, and R. Prins, *Catalysis Letters* 37 (1996) 143-151.
- [78] L.E.Y. Nonneman, A.G.T.M. Bastein, V. Ponec, and R. Burch, *Applied Catalysis* 62 (1990) L23-L28.
- [79] W.Y. Kim, H. Hayashi, M. Kishida, H. Nagata, and K. Wakabayashi, *Applied Catalysis a-General* 169 (1998) 157-164.

- [80] W.-Y. Kim, T. Hanaoka, M. Kishida, and K. Wakabayashi, *Applied Catalysis A: General* 155 (1997) 283-289.
- [81] W.-J. Shen, Y. Ichihashi, H. Ando, M. Okumura, M. Haruta, and Y. Matsumura, *Applied Catalysis A: General* 217 (2001) 165-172.
- [82] M.M. Bhasin, W.J. Bartley, P.C. Ellgen, and T.P. Wilson, *Journal of Catalysis* 54 (1978) 120-128.
- [83] R.P. Underwood, and A.T. Bell, *Applied Catalysis* 21 (1986) 157-168.
- [84] S.D. Jackson, B.J. Brandreth, and D. Winstanley, *Journal of the Chemical Society, Faraday Transactions 1*: 84 (1988).
- [85] K.P. De Jong, J.H.E. Glezer, H.P.C.E. Kuipers, A. Knoester, and C.A. Emeis, *Journal of Catalysis* 124 (1990) 520-529.
- [86] F.G.A. van den Berg, J.H.E. Glezer, and W.M.H. Sachtler, *Journal of Catalysis* 93 (1985) 340-352.
- [87] M. Ichikawa, *CHEMTECH* 12 (1982) 674-680.
- [88] J.R. Katzer, A.W. Sleight, P. Gajardo, J.B. Michel, E.F. Gleason, and S. McMillan, *Faraday Discussions of the Chemical Society* 72 (1981) 121-133.
- [89] M. Inoue, A. Kurusu, K. Terada, and T. Inui, *Applied Catalysis* 67 (1990) 203-214.
- [90] N. Yoneda, S. Kusano, M. Yasui, P. Pujado, and S. Wilcher, *Applied Catalysis A: General* 221 (2001) 253-265.
- [91] M.J. Howard, M.D. Jones, M.S. Roberts, and S.A. Taylor, *Catalysis Today* 18 (1993) 325-354.
- [92] G.J. Sunley, and D.J. Watson, *Catalysis Today* 58 (2000) 293-307.
- [93] R.W. Wegman, *Journal of the Chemical Society, Chemical Communications* (1994) 947.
- [94] F. Peng, and X.B. Fu, *Catalysis Today* 93-95 (2004) 451-455.
- [95] M. Bowker, and Y.X. Li, *Catalysis Letters* 10 (1991) 249-258.
- [96] M. Bowker, *Catalysis Today* 15 (1992) 77-100.
- [97] N. Aas, and M. Bowker, *Journal of the Chemical Society-Faraday Transactions* 89 (1993) 1249-1255.
- [98] W. Rachmady, and M.A. Vannice, *Journal of Catalysis* 192 (2000) 322-334.
- [99] M. Kitson, and P.S. Williams. *European Patent Application* 0.285.420.A2 (1986).
- [100] M.K. Kitson, and P.S. Williams. *European Patent Application* 0.198.682.A2 (1986).

- [101] G. Pimblett, K.A. McLachlan, and P.J. Price. European Patent Application 0.372.847.A2 (1989).
- [102] J. Cressely, D. Farkhani, A. Deluzarche, and A. Kiennemann, *Materials Chemistry and Physics* 11 (1984) 413-431.
- [103] M.A. Natal-Santiago, J.M. Hill, and J.A. Dumesic, *Journal of Molecular Catalysis A: Chemical* 140 (1999) 199-214.
- [104] T. Turek, D.L. Trimm, and N.W. Cant, *Catalysis Reviews: Science and Engineering* 36 (1994) 645 - 683.
- [105] M.A.N. Santiago, M.A. Sánchez-Castillo, R.D. Cortright, and J.A. Dumesic, *Journal of Catalysis* 193 (2000) 16-28.
- [106] V. Ponec, *Catalysis Today* 12 (1992) 227-254.
- [107] B. Imelik, and J.C. Vedral, *Catalyst Characterization: Physical Techniques for Solid Materials*. New York: Plenum Press, 1994.
- [108] H. van Beklam, E.M. Flanigen, and J.C. Jansen, *Introduction to Zeolite Science and Practise*. Amsterdam: Elsevier Science Publishers B.V., 1991.
- [109] Powder Diffraction File (CD-ROM). International Centre for Diffraction Data: Newton Square, 2000.
- [110] S. Bertarione, D. Scarano, A. Zecchina, V. Johaneck, J. Hoffmann, S. Schauerer, M.M. Frank, J. Libuda, G. Rupprechter, and H.-J. Freund, *The Journal of Physical Chemistry B* 108 (2004) 3603-3613.
- [111] A.T. Bell, and E. Shustorovich, *Journal of Catalysis* 121 (1990) 1-6.
- [112] J.A. Anderson, and M.M. Khader, *Journal of Molecular Catalysis A: Chemical* 105 (1996) 175-183.
- [113] A. Coteron, and A.N. Hayhurst, *Chemical Engineering Science* 49 (1994) 209-221.
- [114] E.R.A. Matulewicz, M.S. Dekeijser, J.C. Mol, and F. Kapteijn, *Thermochimica Acta* 72 (1984) 111-116.
- [115] K. Klier, V. Chatikavanij, R.G. Herman, and G.W. Simmons, *Journal of Catalysis* 74 (1982) 343-360.
- [116] P.B. Rasmussen, P.M. Holmblad, T. Askgaard, C.V. Ovesen, P. Stoltze, J.K. Nørskov, and I. Chorkendorff, *Catalysis Letters* 26 (1994) 373-381.
- [117] K. Föttinger, R. Schlogl, and G. Rupprechter, *Chemical Communications* (2008) 320-322.
- [118] P.Z. Lin, D.B. Liang, H.Y. Luo, C.H. Xu, H.W. Zhou, S.Y. Huang, and L.W. Lin, *Applied Catalysis A: General* 131 (1995) 207-214.

- [119] D.J. Schreck, D.C. Busby, and R.W. Wegman, *Journal of Molecular Catalysis* 47 (1988) 117-121.
- [120] R.G. Schultz, and P.D. Montgomery, *Journal of Catalysis* 13 (1969) 105-106.
- [121] M.A. Ryashentseva, K.M. Minachev, and E.P. Belanova, *Russian Chemical Bulletin* 23 (1974) 1833-1835.
- [122] R. Pestman, R.M. Koster, J.A.Z. Pieterse, and V. Ponec, *Journal of Catalysis* 168 (1997) 255-264.
- [123] P. Baumann, H.P. Bonzel, G. Pirug, and J. Werner, *Chemical Physics Letters* 260 (1996) 215-222.
- [124] B.A. Sexton, *Chemical Physics Letters* 65 (1979) 469-471.
- [125] M. Bowker, and R.J. Madix, *Applications of Surface Science* 8 (1981) 299-317.
- [126] Z. Li, F. Calaza, F. Gao, and W.T. Tysoe, *Surface Science* 601 (2007) 1351-1357.
- [127] G. Hoogers, D.C. Papageorgopoulos, Q. Ge, and D.A. King, *Surface Science* 340 (1995) 23-35.
- [128] D.H.S. Ying, and R.J. Madix, *Journal of Catalysis* 60 (1979) 441-451.
- [129] R.J. Madix, J.L. Falconer, and A.M. Suszko, *Surface Science* 54 (1976) 6-20.
- [130] J.L. Falconer, and R.J. Madix, *Surface Science* 46 (1974) 473-504.
- [131] M. Neurock, *Journal of Catalysis* 216 73-88.
- [132] E. Hansen, and M. Neurock, *The Journal of Physical Chemistry B* 105 (2001) 9218-9229.
- [133] J.L. Davis, and M.A. Barteau, *Surface Science* 256 (1991) 50-66.
- [134] M.A. Barteau, M. Bowker, and R.J. Madix, *Journal of Catalysis* 67 (1981) 118-128.
- [135] M. Bowker, H. Houghton, and K.C. Waugh, *Journal of Catalysis* 79 (1983) 431-444.
- [136] A.J. Capote, A.V. Hamza, N.D.S. Canning, and R.J. Madix, *Surface Science* 175 (1986) 445-464.
- [137] T. Kakumoto, and T. Watanabe, *Catalysis Today* 36 (1997) 39-44.
- [138] J.C. Meyer, P.A. Marrone, and J.W. Tester, *Aiche Journal* 41 (1995) 2108-2121.

- [139] V.N. Gel'man, A.L. Turcheninov, G.I. Salomatin, V.S. Sobolevskii, V.I. Yakerson, and E.Z. Golosman, *Russian Chemical Bulletin* 35 (1986) 2433-2437.
- [140] M. Afzal, P.K. Butt, and H. Ahmad, *Journal of Thermal Analysis and Calorimetry* 37 (1991) 1015-1023.
- [141] M. Mohamed, S. Halawy, and M. Ebrahim, *Journal of Thermal Analysis and Calorimetry* 41 (1994) 387-404.
- [142] A. Obaid, A. Alyoubi, A. Samarkandy, S. Al-Thabaiti, S. Al-Juaid, A. El-Bellihi, and E.-H. Deifallah, *Journal of Thermal Analysis and Calorimetry* 61 (2000) 985-994.
- [143] H. Dropsch, and M. Baerns, *Applied Catalysis A: General* 158 (1997) 163-183.
- [144] G. Spoto, E.N. Gribov, G. Ricchiardi, A. Damin, D. Scarano, S. Bordiga, C. Lamberti, and A. Zecchina, *Progress in Surface Science* 76 (2004) 71-146.
- [145] Y.I. Khimchenko, V.P. Vasilenko, L.S. Radkevich, V.V. Myalkovskii, T.V. Chubar, and V.M. Chegoryan, *Powder Metallurgy and Metal Ceramics* 16 (1977) 327-332.
- [146] S. Poulston, E. Rowbotham, P. Stone, P. Parlett, and M. Bowker, *Catalysis Letters* 52 (1998) 63-67.
- [147] P. Villa, P. Forzatti, G. Buzzi-Ferraris, G. Garone, and I. Pasquon, *Industrial & Engineering Chemistry Process Design and Development* 24 (2002) 12-19.
- [148] K. Klier, V. Chatikavanij, R.G. Herman, and G.W. Simmons, *Journal of Catalysis* 74 (1982) 343-360.
- [149] T. Oishi, K. Koyama, S. Alam, M. Tanaka, and J.C. Lee, *Hydrometallurgy* 89 (2007) 82-88.
- [150] O.N. Ata, S. Çolak, Z. Ekinci, and M. Çopur, *Chemical Engineering & Technology* 24 (2001) 409-413.
- [151] N. Habbache, N. Alane, S. Djerad, and L. Tifouti, *Chemical Engineering Journal* 152 (2009) 503-508.
- [152] P. Claus, M. Lucas, B. Lücke, T. Berndt, and P. Birke, *Applied Catalysis A: General* 79 (1991) 1-18.
- [153] C. Travers, J.P. Bournonville, and G. Martino, *Journal of Molecular Catalysis* 25 (1984) 327-336.